Pontificia Universidad Católica del Perú

Escuela de Posgrado

Tesis

ASSESSMENT OF ACCUMULATION OF SELECTED METALS BY NATIVE PLANTS GROWING IN POLLUTED PERUVIAN POST-MINING AREAS

EVALUACIÓN DE LA ACUMULACIÓN DE METALES POR PLANTAS NATIVAS QUE CRECEN EN SUELOS CONTAMINADOS EN ÁREAS POST-MINERAS PERUANAS

Para obtener el grado de:

Doctor en Ingeniería

Presentado por: Cruzado Tafur, Edith Maricela

Asesores: Lisard Torró I Abat
Joanna Szpunar

Miembros del Jurado:

Bernhard Dold - Pontificia Universidad Católica del Perú
Mariella Moldovan Feier - Universidad de Oviedo, España
Stephane Mari - INRAE, Francia
Lena Ruzik - Universidad Tecnológica de Varsovia, Polonia
Joanna Szpunar - CNRS-IPREM, Francia (Asesor)
Lisard Torró I Abat - Pontificia Universidad Católica del Perú (Asesor)

Miembros invitados:

Silvia Rosas - Pontificia Universidad Católica del Perú

Mayo, 2021- Pau, Francia

THÈSE

UNIVERSITÉ DE PAU ET DES PAYS DE L'ADOUR

École doctorale sciences exactes et leurs applications ED211

Présentée et soutenue le 6 Mai 2021

par **Edith Maricela CRUZADO TAFUR**

pour obtenir le grade de docteur

de l'Université de Pau et des Pays de l'Adour et l'Université Pontificale Catholique du Pérou

Spécialité: Chimie analytique de l'environnement

ASSESSMENT OF ACCUMULATION OF SELECTED METALS BY NATIVE PLANTS GROWING IN POLLUTED PERUVIAN POST-MINING AREAS

L'EVALUATION DES MOLECULES IMPLIQUEES DANS L'ACCUMULATION DE METAUX PAR DES PLANTES POUSSANT DANS DES ZONES POST-MINIERES PERUVIENNES

MEMBRES DU JURY

RAPPORTEURS

• Mariella MOLDOVAN FEIER	Professeur / Université d'Oviedo - Espagne
• Stephane MARI	Directeur de Recherche / INRAE - France

EXAMINATEURS

• Bernhard DOLD	Professeur / Université Pontificale Catholique du Pérou
• Lena RUZIK	Professeur / Université de Technologie de Varsovie - Pologne

DIRECTEURS

• Joanna SZPUNAR	Ingénieur de Recherche / CNRS-IPREM - France
• Lisard TORRÓ	Professeur / Université Pontificale Catholique du Pérou

INVITÉS

• Silvia ROSAS	Professeur / Université Pontificale Catholique du Pérou

UNIVERSITÉ DE PAU ET DES PAYS DE L'ADOUR

ET LUX IN TENEBRIS LUCET MCMXVII

PONTIFICIA UNIVERSIDAD CATÓLICA DEL PERÚ

ET LUX IN TENEBRIS LUCET
MCMXVII

ACKNOWLEDGMENTS

« *If there is a will, there is a way* » or « *Querer es Poder* », phrases has accompanied me during the three years of my doctoral life. I always knew that the doctorate was not going to be easy but I did not doubt that it was impossible.

This research was initiated as part of a collaboration between the University of Pau and Pays de l'Adour (UPPA) and the Pontifical Catholic University of Peru (PUCP), so, this thesis has been possible thanks to the financial support of the Franco-Peruvian Doctoral School in Engineering Sciences and Geosciences (FPDSESG) through Dr. Silvia ROSAS, Coordinator of FPDSESG; and of the funding received from the project HUB MesMic at the Institute of Analytical Sciences and Physico-Chemistry for the Environment and Materials (IPREM) through Dr. Ryszard LOBINSKI, Director of IPREM.

I would hereby like to express my sincere gratitude to my PhD advisors: Dr. Joanna SZPUNAR and Dr. Lisard TORRÓ, many thanks for giving me the great opportunity to do research under her/his great scientific experience; for their dedication, guidance, continuous support, and encouragement, and even more, that have made possible the successful completion of my PhD thesis in these challenging times of pandemic. Wielkie dzięki Joanna, for your support in everything, even since before I started my doctorate, for be no only the director of the thesis, for being friendly support, for giving me security in my doubts and mistakes, for always being with me when I needed advice, for your help from the beginning of the pandemic and for trusting me. Moltes gràcies Lisard, for not hesitating to join me as my thesis director, for your help during the fieldwork, for listening to me in my doubts, for giving me a lot of advice during the development of the research, for being friendly support.

I wish to thanks Katarzyna BIERLA, a researcher at IPREM lab for providing all help me when I needed it during experimental and scientific work; many thanks for Katarzyna KINSKA, post Doctorate at IPREM for guiding and help me in the experimental part of the speciation analyzes of this work, and thanks for Ange ANGAÏTS for his technical help at IPREM lab. Many thanks to Dr. Martin TIMANÁ, researcher at PUCP, for his lessons for collecting plant samples and assistance in the taxonomic identification; I wish to thank Rodolfo LAZO DAVILA and Karem SOLANO HERRERA from Activos Mineros S.A.C (AMSAC-Peru) for the permission granted for sampling in the study area in Hualgayoc. I would also like to thanks Willem VIVEEN, researcher at PUCP for the geology advice at the beginning of my investigation and friendship; thanks to Edmundo ALFARO, researcher at PUCP for the support provided in the logistics with the external lab for the soil analysis, thanks to Rudi CRUZ, student at PUCP for helping me with the drying process of the plants. In addition, I feel grateful to all people who worked with me on my publications.

Many thanks to my dear friends at IPREM, for to be my family in Pau, for every lunch times, laughter, jokes, randonnée to the pyrenees and walks beaches: Maria Angels SUBIRANA, Rosanna MARGALEF, Silvia QUEIPO, Javier GARCIA, Mikel BERNABEU, Yago GARCIA-RODEJA, Nang HTAY, Francisco CALDERON, Celia TRUJILLO, Sebastiano GOZZO, Maríka BUSCARINO, Ntau MAFISA, Maximillien GUIBERT, Maricarmen GARCIA, Maroussia PARAILLOUX, Claudia MARCHAN and Vicmary VARGAS. Likewise, thanks to all persons who had shared offices with me at IPREM. Also, thank you to my friends around the world for give me their support, good talks, travels, and motivations during my PhD life: Clarissa RIOS, Jeroen OVERMAN, David MELENDEZ, Morita PERPERE, Federico SANJUAN, Diego MARQUEZ and Romina CERRO. Thanks to all my friends in Pau and Peru.

For last, thanks a lot to my lovely family, my mother Teresa TAFUR, my sisters Nataly CRUZADO and Liliana CRUZADO, my father Reynaldo CRUZADO, and to the new family member Simba, that despite being thousands of kilometers away, I never lacked their immense support, patience, tolerance, advices, company, and motivations for me and my work, who with the smallest detail, be it a little word or a simple smile, gave me happiness, lifted my spirits and gave me the courage to continue. Gracias totales !

Merci à tous.

« *Nothing in life is to be feared, it is only to be understood. Now is the time to understand more, so that we may fear less* ». Marie Curie

ABSTRACT

Metal mining is one of the economic pillars of the Peruvian economy. Peru is the main producer of gold, zinc, lead, and tin in Latin America and the second largest producer of copper, silver, and zinc worldwide. Despite its economic importance, mining has also left a plethora of Mining Environmental Liabilities (MEL) whose inadequate waste management represents a risk for both the environment and human health and is a common trigger of social problems. The Cajamarca region is the second region in Peru in terms of the number of MEL sites with the majority of them located in the Hualgayoc district.

The goal of the PhD project is the assessment of the environmental impact of MEL in the Peruvian Andes using as an example two post-mining sites in the Hualgayoc district. This evaluation includes the study of soils and native plant species in terms of their metal accumulation potential and the species involved in the process, in order to generate information on a possible use of Andean native plants for phytoremediation. The mineralogical composition of soils is dominated by illite, kaolinite, quartz, and jarosite. Soil analyses also reveals a high acidity, very low content of essential nutrients, and potentially toxic concentrations of Pb, Cd, As, Cu, Ag, and Zn out of the 34 analysed elements. Sequential fractionation soil analyses indicate that the highest content of the metals is in fractions with limited metal mobility. Soils are classified as extremely polluted according to several geochemical indexes, thus represent a serious risk to the local ecosystem.

The main part of the project concerns native Andean flora and contributes to their inventory with the identification of 22 plants belonging to 12 family species. The metal content in plant organs is correlated with that of the soil, in order to assess the phytoremediation potential of native plant species by establishing their metal bioaccumulation and translocation capabilities. Some plants are found to be potentially suitable for phytoremediation of Cd, Cu, and Zn but none of them for Pb, As, and Ag.

The speciation studies carried out by HPLC with parallel elemental (ICP) and molecular (ESI) mass spectrometric detection allows the identification of the chemical species responsible for the translocation of Cu and Zn. Nicotianamine complexes are the major species of copper and zinc in organs of *Arenaria digyna*, *Nicotiana thyrsiflora* and *Puya sp.*; they are accompanied by deoxymutageneic acid complexes. In addition, a novel, never reported so far, dihydroxy-nicotianamine species was identified as the most abundant Cu and Zn ligand in *Hypericum laricifolium*.

RESUMÉ

L'exploitation minière des métaux est l'un des piliers économiques de l'économie péruvienne. Le Pérou est le principal producteur d'or, de zinc, de plomb et d'étain d'Amérique latine et le deuxième producteur mondial de cuivre, d'argent et de zinc. Malgré son importance économique, l'exploitation minière a également laissé une pléthore de Responsabilités Environnementales Minières (REM) dont la gestion inadéquate des déchets représente un risque pour l'environnement et la santé humaine et est un déclencheur courant de problèmes sociaux. La région de Cajamarca est la deuxième région du Pérou en termes de nombre de sites REM, la majorité d'entre eux étant situés dans le district de Hualgayoc.

L'objectif du projet de doctorat est l'évaluation de l'impact environnemental des REM dans les Andes péruviennes en utilisant comme exemple deux sites post-miniers dans le district de Hualgayoc. Cette évaluation comprend l'étude des sols et des espèces végétales indigènes en termes de potentiel d'accumulation des métaux et des espèces impliquées dans le processus, afin de générer des informations sur une éventuelle utilisation des plantes indigènes andines pour la phytoremédiation. La composition minéralogique des sols est dominée par l'illite, la kaolinite, le quartz et la jarosite. Les analyses de sol révèlent également une acidité élevée, une très faible teneur en nutriments essentiels et des concentrations potentiellement toxiques en Pb, Cd, As, Cu, Ag et Zn sur les 34 éléments analysés. Les analyses de sol par fractionnement séquentiel indiquent que la teneur la plus élevée en métaux se situe dans les fractions pour lesquelles la mobilité métallique est limitée. Selon plusieurs indices géochimiques, les sols sont classés comme extrêmement pollués et représentent ainsi un sérieux risque pour l'écosystème local.

L'essentiel du projet concerne la flore andine indigène et contribue à leur inventaire avec l'identification de 22 plantes appartenant à 12 familles. La teneur en métaux des organes végétaux est corrélée à celle du sol, afin d'évaluer le potentiel de phytoremédiation des espèces végétales indigènes en établissant leurs capacités de bioaccumulation et de translocation des métaux. Certaines plantes se révélent être potentiellement appropriées pour la phytoremédiation du Cd, du Cu et du Zn, mais aucune d'entre elles pour le Pb, l'As et l'Ag.

Les études de spéciation réalisées par HPLC avec détection par spectrométrie de masse parallèle élémentaire (ICP) et moléculaire (ESI) permettent d'identifier les espèces chimiques responsables de la translocation de Cu et Zn. Les complexes de nicotianamine sont les principales espèces de cuivre et de zinc dans les organes d'Arenaria digyna, de *Nicotiana thyrsiflora* et de *Puya sp.*; ils sont accompagnés de complexes d'acide désoxymutagénique. En outre, une nouvelle espèce de dihydroxy-nicotianamine, jamais signalée à ce jour, est identifiée comme le ligand Cu et Zn le plus abondant dans l'*Hypericum laricifolium.*

ET LUX IN TENEBRIS LUCET
MCMXVII

RESUMEN

La minería metálica es uno de los pilares económicos de la economía peruana. Perú es el principal productor de oro, zinc, plomo y estaño de América Latina y es el segundo productor mundial de cobre, plata y zinc. A pesar de su importancia económica, la minería también ha dejado una gran cantidad de Pasivos Ambientales Mineros (PAM) cuya inadecuada gestión de residuos representa un riesgo tanto para el medio ambiente como para la salud humana y es un desencadenante habitual de problemas sociales. La región de Cajamarca es la segunda del Perú en número de PAM y la mayoría de ellos se encuentran en el distrito de Hualgayoc.

El objetivo del proyecto de doctorado es la evaluación del impacto ambiental de PAM en los Andes peruanos utilizando como ejemplo dos emplazamientos post-mineros en el distrito de Hualgayoc. Esta evaluación incluye el estudio de los suelos y de las especies vegetales nativas en cuanto a su potencial de acumulación de metales y las especies involucradas en el proceso, con el fin de generar información sobre un posible uso de las plantas nativas andinas para fitorremediación. La composición mineralógica de los suelos está dominada por illita, caolinita, cuarzo y jarosita. Los análisis del suelo también revelan una elevada acidez, un contenido muy bajo de nutrientes esenciales y concentraciones potencialmente tóxicas de Pb, Cd, As, Cu, Ag y Zn de entre los 34 elementos analizados. Los análisis de suelos por fraccionamiento secuencial indican que el mayor contenido de los metales se encuentra en las fracciones con movilidad limitada de los metales. Los suelos se clasifican como extremadamente contaminados según los índices geoquímicos, por lo que representan un grave riesgo para el ecosistema local.

La parte principal del proyecto se refiere a la flora nativa andina y contribuye a su inventario con la identificación de 22 plantas pertenecientes a 12 especies familiares. El contenido de metales en los órganos de las plantas es correlacionado con el del suelo, con el fin de evaluar el potencial de fitorremediación de las especies de plantas nativas estableciendo su capacidad de bioacumulación y translocación de metales. Algunas plantas resultan ser potencialmente adecuadas para la fitorremediación de Cd, Cu y Zn, pero ninguna de ellas para Pb, As y Ag.

Los estudios de especiación realizados por HPLC con detección elemental (ICP) y molecular (ESI) de espectrometría de masas en paralelo permiten identificar las especies químicas responsables de la translocación de Cu y Zn. Los complejos de Nicotianamina son las principales especies de cobre y zinc en órganos de *Arenaria digyna, Nicotiana thyrsiflora* y *Puya sp.*; están acompañados por complejos de ácido desoximutagénico. Además, se identifica una nueva especie de dihidroxi-nicotianamina, nunca reportada hasta ahora, como el ligando de Cu y Zn más abundante en *Hypericum laricifolium*.

ET LUX IN TENEBRIS LUCET
MCMXVII

INTRODUCTION

Inadequate waste management after the cessation of mining activities lead to the accumulation of Mining Environmental Liabilities (MEL), which represent a risk for the environment and human health and may generate social problems. The mining sector is one of the economic pillars of Peru; however, has also left a legacy of countless MEL sites (approximately 8448), most of them without an identified responsible. With 1156 catalogued MEL, the Cajamarca region is the second region with the higher number of MEL sites, of which 943 are located in the Hualgayoc district. The long mining history of Hualgayoc dates back to the Spanish colony, and metal production includes Ag-rich polymetallic mineralization. The MEL in this area are potential threats to extant flora and fauna along the Tingo-Maygasbamba, Hualgayoc-Arascorgue, and Llaucano river basins.

The goal of the PhD is to assess the environmental impact of, and the phytoremediation potential of native plants growing in, Peruvian MEL located in the Peruvian Andes from the holistic study of two post-mining sites in the Ex-Mining Unit Los Negros, located in the Hualgayoc district in the Cajamarca region.

The three main pillars in which this research has foucused are:

(i) the study of the morphological, physicochemical, mineralogical properties, and total concentrations of soils, as well as the evaluation of the soil environmental quality. Also, the inventory of native flora growing in MEL sites of potential use for phytoremediation purposes (Chapter A);

(ii) the study of the uptake and accumulation of metals present in the contaminated soils by inventoried native plants and the assessment of their phytoremediation potential through the bioconcentration and (BCF) and the translocation (TF) factors (Chapter B); and

(iii) the study of the metal speciation in native species using analytical strategies that allow the identification of the species involved in translocation of metal pollution in the studied native flora (Chapter C).

The research developed in the framework of this thesis has led to the identification of native flora with potential resistance to heavy-metal contaminated soils and therefore are a promising alternative for remediation of MEL sites in the Peruvian Andes.

Table of Contents

Figures

Tables

ET LUX IN TENEBRIS LUCET
MCMXVII

I. INTRODUCTION

ET LUX IN TENEBRIS LUCET
MCMXVII

I. INTRODUCTION

1.1. METAL MINING ACTIVITIES

Around the world there are more than 20 million mines (Aznar-Sánchez et al., 2019). Polymetallic mining refers to the operations of extract metals such as Au, Ag, Pb, and Zn from ore that is mined (NSW EPA, 2016; Sun et al., 2018). Mining agglutinates natural and anthropogenic factors as mineral deposits correspond to natural positive metal anomalies. Mining involves several methods such as surface mining, with the excavation at the earth's surface, and underground mining; the selection of one or the other method depends on the geology of the mineral deposit, physical characteristics, environmental factors, and profitability (Candeias et al., 2018).

The exploration and exploitation of minerals for thousands of years have left a rich legacy of mining and metallurgical traditions (Kaźmierczak et al., 2019). However, mining activities confront important challenges such as economic sustainability, environmental impact, and social rejection (Aznar-Sánchez et al., 2019). Mining operations cause environmental disturbance by creating open pits, waste rock dumps, tailings ponds, and other mine facilities (Kapusta and Sobczyk, 2015) which may potentially generate large amounts of waste that contain toxic elements causing soil, water, and air impact long after mining operations have ceased (Pérez-Sirvent et al., 2015). Mine development in the past was usually carried out without environmental responsibility, resulting in severe negative environmental impact (Candeias et al., 2018). Inappropriate mining exploitation causes serious heavy metal pollution problems through a range of pathways such as physical disturbance of the landscape, dust emissions, spilling of mine tailings, and generation of acidic drainage (Sun et al., 2018). The negative perception of mining activities is mostly due to the fact that they can negatively affect the terrestrial ecosystems, toxic chemicals may accumulate in the soil, or the soil begins to acidify. These potential problems may affect the fertility of the soil, cause plant toxicity and, ultimately, contaminate the food chain (Saenz and Ostos, 2020).

The environmental impact of mining activity can be analyzed by the comparison of the condition of the environment before and after the mining activity is developed (Santos-Francés et al., 2017a).

1.2. POST-MINING AREAS CONTAMINATION

After the closure of a mine, the environmental impact may continue for long periods of time and require proper environmental management measures (Manhart et al., 2019). The term post-

mining areas usually refers to lands where mining activities ceased but acceptable mine clean-up or rehabilitation was not carried out properly or was incomplete (Otamonga and Poté, 2020). Therefore, post-mining sites are areas that have been exposed to anthropogenic disturbance, as land subsidence and topsoil stripping, generating the sensitivity of environmental components such as landform, vegetation, and soil. Slopes are one of the most relevant factors since mining activities developed on steep slopes will potentially cause a greater amount of erosion than those located on the level ground (Yang et al., 2017). As a result, the abandoned mines represent a potential hazard to the environment, human health, and safety, becoming the negative legacy of environmental degradation left by past mining activities (Otamonga and Poté, 2020). Often, for ancient mines, the responsibility for their rehabilitation cannot be allocated to any company or person (Unger, 2017).

Before environmental legislation existed, land used for mining was irresponsibly abandoned without proper remediation. The number of abandoned mines around the world is estimated at over one million (Corzo and Gamboa, 2018). Inadequate mine closure processes and abandoned mine management have generated inadequate engagement with local communities in terms of cultural heritage (Unger, 2017). In this way, the residents of mining communities have been often adversely affected for long periods of time (Otamonga and Poté, 2020) and claim the return of post-mining land to safe and non-polluting landforms (Hendrychová et al., 2020).

Therefore, abandoned mine sites present a number of inherent challenges inlcuding the absence of planning for rehabilitation, degraded state of the topsoil that often bears with denuded expanses of regolith, bedrock, and tailings emplacements, presenting hostile environments for revegetation, unexpected chemical contamination, and acid soils after long-term exposure to site pollution (Venkateswarlu et al., 2016). Amongst the possibilities of mitigating negative impacts from mining activities and generating wealth for governments and communities is the regeneration of mined landscapes (Unger, 2017). Any restoration of post-mining areas needs to consider the adaption of the plant species to the local environment since the geographic distribution and the interactions of different plant species are important factors to measure the ecological restoration capacity (Dong et al., 2019). Rehabilitation of post-mining sites can significantly contribute to local biodiversity, so, the measures of the success may be investigated by plant species diversity and soil development (Klimaszewski et al., 2016).

1.3. PERU – CURRENT KNOWLEDGE PROBLEMS RELATED TO THE ENVIRONMENTAL IMPACT OF MINING

Peru has been the country with the highest mining potential in Latin American (Sánchez-Albavera and Lardé, 2006). Globally (**Figure 1**), Peru currently ranks second as a producer of copper, silver, and zinc, in lead production it ranks third, fourth in the production of tin and molybdenum, and eighth in gold production. Furthermore, at the Latin American level it stands out for being the main producer of gold, zinc, lead, and tin, as well as the second producer of copper, silver, and molybdenum (Ministerio de Energía y Minas, 2020). Mining and metals sectors represent more than half the value of the total exports of assets of Peru (Comisión Económica para América Latina y el Caribe (CEPAL), 2018). The representation in the mining industry that Peru has sustained worldwide in recent decades reflects not only the country's high geological potential (Ministerio de Energía y Minas, 2020) but also the long mining tradition dating back to pre-Inca times. During the Republican period and especially in the 20th century, mining activities intensified throughout the country, especially in the Andes, allowing the opening of many mines, of which some continue to operate and others were abandoned (Chappuis, 2019). The Peruvian Andes represent indeed a great reserve of natural resources, geological and abundant hydrological wealth allowing the progress of human and industrial activities (Corzo and Gamboa, 2018) and establishing mining as an important component of Peruvian economic growth (Aron and Molina, 2019).

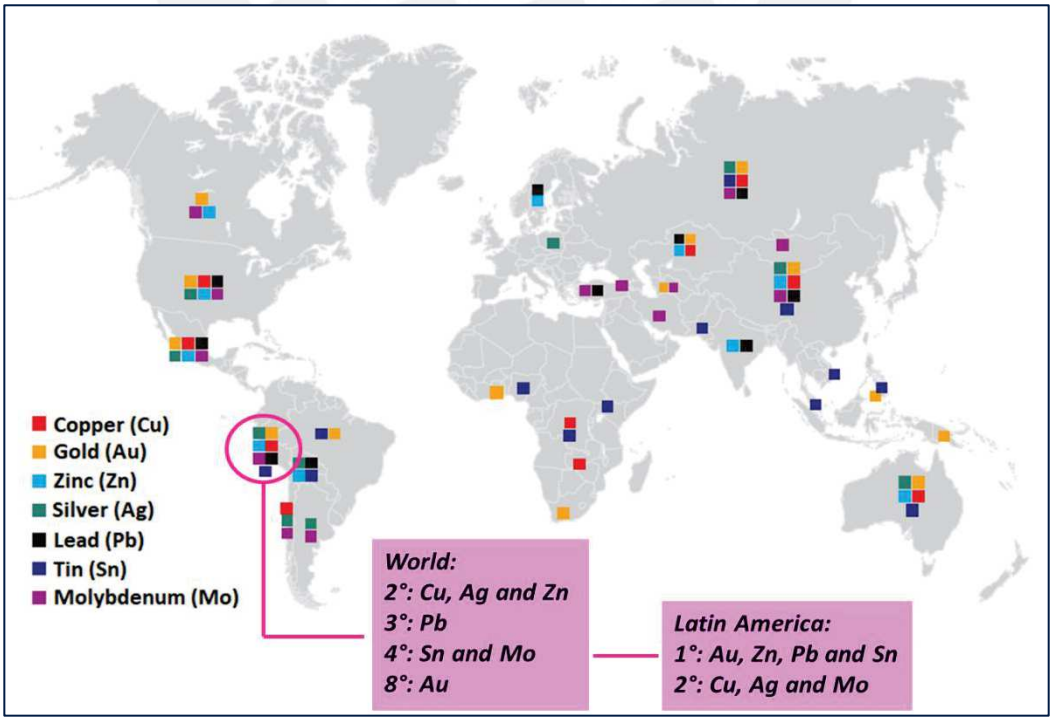

Figure 1. World production of main metals, adapted from Ministerio de Energía y Minas, (2020)

In Latin America, the environmental degradation and loss of land use because of mining activities are a hot topic of discussion (Helwege, 2015). During the past two decades, the resource extraction has generated innumerable conflicts throughout the region, principally in Peru, where the expansion of mining arrived into areas never before used for mining activity, including areas formerly devoted to agriculture and farming (F. Li et al., 2019). Many Andean mines are located at the headwaters of rivers, of which water is used for personal consumption, irrigation, and pasture (Brain, 2017). The communities in the highlands of Peru coexist with such activity (most Peruvian mining activity develops over 3500 m a.s.l.), representing an ongoing environmental threat to a highly ecosystem dependent lifestyle (Corzo and Gamboa, 2018).

In the 1990s, most of the countries in Latin American introduced substantial changes in their mining laws, granting mining rights for exploration and exploitation under concession, the most common term of which is between 20 and 25 years (Sánchez-Albavera and Lardé, 2006).

Despite the fact that mining is one of the most important activities with the greatest impact on the Peruvian economy (Chappuis, 2019), and in spite of the implementation of reforms in the mining sector and the promotion of private investment, the rapid expansion of mining in the Andean highlands has carried with it environmental contamination, mobilizations related to land rights, and demands for access to services (Gustafsson, 2018).

Mining Environmental Liabilities (MEL) refer to the environmental impact caused by abandoned mine activities with or without a responsible party identified and where a mine closure has not been carried out, regulated, and certified by the corresponding authority (Yupari, 2003). In Peru, MEL (*Pasivos Ambientales Mineros, in Spanish*) are defined as those installations, effluents, emissions, remains, or residue deposits produced by mining operations, abandoned or inactive, that constitute a permanent and potential risk to human health, environment, and patrimony (Ministerio de Energía y Minas, 2004).

Although Peru was the first Latin American country to establish a specific legal framework for MEL, these have accumulated over the long history of mining in considerable size and volume (Oblasser and Chaparro Ávila, 2008). These mines were abandoned without effective shut-down procedures causing a nuisance in the mining districts due to metal transfer to the environment (Bouzekri et al., 2019). In 2019, in the Peruvian territory, the number of MEL was at least 8448 (**Figure 2**), most of them without an identified responsible party (Ministerio de Energía y Minas, 2019); the highest number of them are located in the Ancash, Apurímac, Cajamarca, Huancavelica, Junín, Madre de Dios, and Pasco regions (Chappuis, 2019; Ministerio de Energía y Minas, 2020). Heavy metal

pollution around MEL, and associated acidic conditions and elevated toxic metal concentrations affecting the flora and fauna, is a serious and recurring problem in Peru (Chang Kee et al., 2018). The majority of conflicts in the populations close to the mining operations are the lack of trust and the fear that more MEL will arise (Chappuis, 2019). In other words, the negative public perception of mining is due to the imbalance between the economic benefit and the potential adverse environmental and social impacts (Oblasser and Chaparro Ávila, 2008).

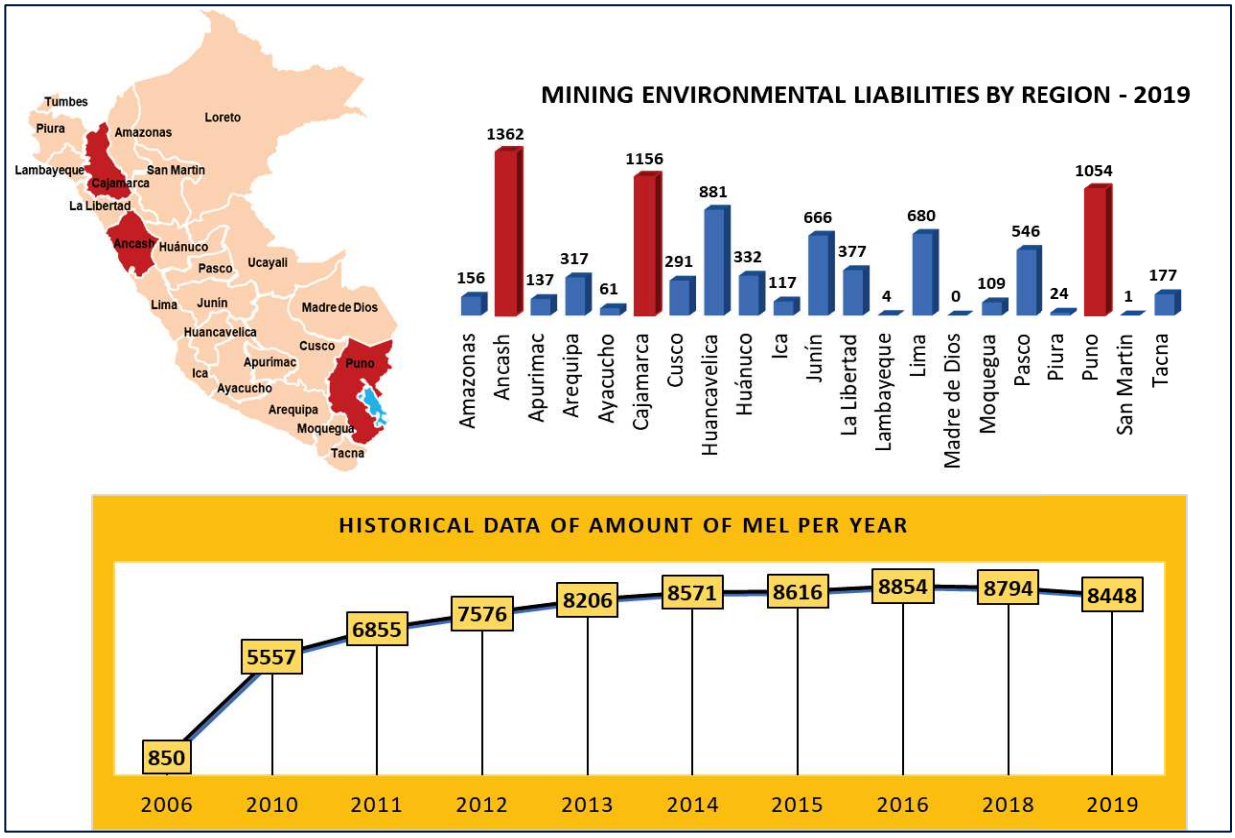

Figure 2. Peru historical data of MEL per year and per region, adapted from Ministerio de Energía y Minas, (2020)

In the framework for sustainable mining, it is relevant to remedy the environmental impacts caused by the mining on soil, water, and air (Aznar-Sánchez et al., 2019). Currently, Peruvian mining faces a series of challenges including guaranteeing society a sustainable closure of the mines and the absence of MEL, which constitute a problematic legacy for the communities and for the governmental structure (local and regional governments). To do this, it is necessary to adopt measures in order to

avoid or reduce any risk of contamination of soils or water bodies (surface and underground) (Rodríguez and Julca, 2020).

1.4. IMPACT OF MINING ACTIVITIES ON SOILS

1.4.1. Soil characterization

Soil is a natural body of mineral and organic constituents, differentiated into horizons or layers with contrasting morphology, physical structure, composition, chemical properties, and biological characteristics (Osman, 2013). Soil is an essential component of the biosphere as a natural buffer controlling the transport of substances and chemical elements to the atmosphere, hydrosphere, and biota (Kabata-Pendias, 2011). Moreover, it is a vital component of terrestrial ecosystems, being the most sensitive to human activities and difficult to reclaim when degraded (Kapusta and Sobczyk, 2015). Soil is the principal receiver of the contaminants such as heavy metals (Nouri and Haddioui, 2016), being mining activity one of the principal causes of soil pollution (Santos-Francés et al., 2017b) profoundly affecting their properties and constituents (Kodirov, 2018).

The physical properties of soil include colour, texture, consistence, and structure, which are related with types of soil particles and their arrangement (Osman, 2013). Soil colour is one of several tools evaluating the suitability of the soil; also, it is an indicator of mineral weathering, amount and distribution of organic matter, and the state of aeration. Munsell colour chart is the most widely chart used for its evaluation (Gupta et al., 2008). Soil colours vary in lightness or darkness, purity and intensity. On the other hand, soil colour classification provides relevant information about its properties and behaviour (Osman, 2013), allowing the very precise characterization and classification of individual soil profiles (IUSS Working Group WRB, 2015).

The soil properties, such as pH, electrical conductivity, carbonate and organic matter content, amount and mineral composition of fine granulometric fraction, and cation exchange capacity (CEC), play an important role in the behaviour of chemical elements (Kabata-Pendias, 2011). Soil pH is one of the most important factors of the soil component since it directly affects the metal availability. Low pH values are correlated with a higher metal mobility, whereas high pH values are related with lower mobility and availability (Kabata-Pendias, 2011; Shah and Daverey, 2020; Stefanowicz et al., 2020). Carbonates are common constituents in soils, and are easily dissolved and leached out with a high rate of percolating water. The organic matter acts as an important regulator of the mobility of trace elements in soils (Kabata-Pendias, 2011; Stefanowicz et al., 2020). Soils with low organic matter are much more susceptible to trace metal contamination, whereas high organic matter affects the metal

immobilization for the retention capacity (Shah and Daverey, 2020). Organic matter is of importance in the transportation and accumulation of cations present in soils and water as chelates and the supply of these ions to plant roots (Kabata-Pendias, 2011).

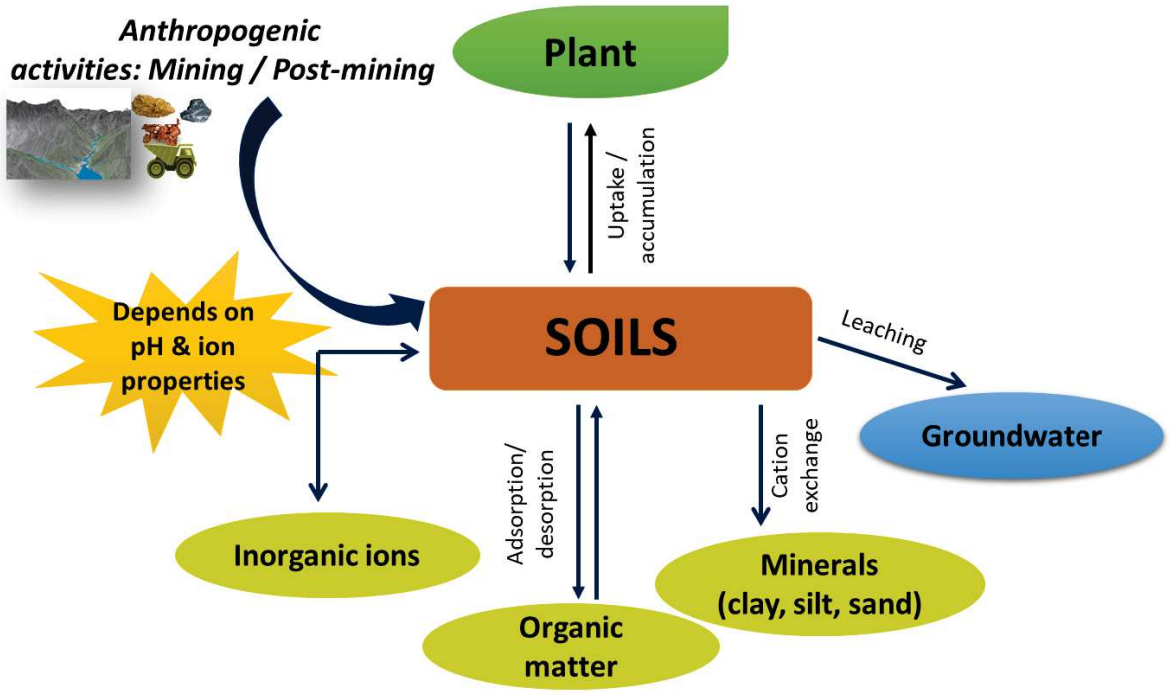

Figure 3. Soil system, adapted from Kodirov, (2018) and Kushwaha et al., (2018)

The level of the metal contamination can be also influenced by the particle size distribution. Soil particles with size < 100 μm have a higher surface area and are more reactive than coarser soil particles (Shah and Daverey, 2020).

The extent and degree of contamination around mine sites also depends upon the mineralogical characteristics of the ore, host rocks, and degree of mineralization of the tailings (Iavazzo et al., 2012). Several methods are used in the study of soil mineralogy, such as electron microscopy, infrared spectroscopy, geochemistry, isotopic analyses; however, the X-ray Diffraction (XRD) method remains the most favourable (Gupta et al., 2008).

1.4.2. Soil metal content

The presence of heavy metals in the soil is a problem of world concern and represents a potential risk to the ecological environment and human health (Z. Li et al., 2019). Metal-contaminated

soils have restrictive physical and chemical characteristics that hinder self-regenerating mechanisms (Artiola et al., 2004). It has to be underlined that the persistence of the trace metals is much longer than other contamination of soil (Kabata-Pendias, 2011).

The soil properties are essential factors for plant growth as soil provides plants nutrients, water, air, warmth, and protects them from toxins (Osman, 2013). For the ecological environment, soil heavy metals represent many potential risks since they can be transported into the ecosystem through atmosphere and precipitation (Santos-Francés et al., 2017b). It should be noted that all soils naturally contain background quantities of heavy metals, whose concentrations depend upon the composition of the parent rock material from which the soil was derived (Nouri and Haddioui, 2016). The information on these background values is essential in studies on the impact caused by human activities on the soil quality of an area (Santos-Francés et al., 2017b).

The transfer of metals from mines to soil is complex and depends on the transport process involved, the size of eroded particles, mineralogical characteristics, and soil properties (Iavazzo et al., 2012).

1.4.3. Soil pollution indices

Ecological risk parameters are used to assess the potential ecological risks and enrichment by heavy metal levels in soils (Liu et al., 2020); they include (i) geoaccumulation index (Igeo), (ii) Nemerow index (NI), (iii) Ecological risk index (Eri), and (iv) Potential ecological risk index (RI) (Santos-Francés et al., 2017b). The soil pollution characteristics and environmental risk assessments studies are important to take decisions concerning soil remediation (Liu et al., 2020). The simultaneous use of several pollution indices assesses more accurately soil quality (e.g. contamination level relative to individual metals, overall contamination of soil, use of geochemical background and potential ecological risk, etc.; Mazurek et al., 2019).

1.4.3.1. Index of geo-accumulation (Igeo)

The geo-accumulation index (I_{geo}), first introduced by Muller (1969), has been successfully applied to the assessment of soil contamination (JI et al., 2008). The Igeo is based on the ratio between the content of metals in a soil sample and the content of metals of a specific geochemical background (Różański et al., 2018). The Igeo is calculated using the following equation:

$$I_{geo} = log_2 \frac{C_i}{1.5 * B_i}$$

where C_i is the measured concentration of the i metal examined in the soil; B_i is the background level of the i metal. The I_{geo} discriminates between 7 soil groups or classes (JI et al., 2008; Różański et al., 2018): unpolluted (Igeo ≤ 0), unpolluted to moderately polluted (0 < Igeo ≤ 1), moderately polluted (1 < Igeo ≤ 2), moderately to strongly polluted (2 < Igeo ≤ 3), strongly polluted (3 < Igeo ≤ 4), strongly to very strongly polluted (4 < Igeo ≤ 5) and very strongly polluted (Igeo > 5).

1.4.3.2. Nemerow pollution index (NI) and Improve Nemerow index (INI)

The Nemerow pollution index (NI) measures levels of pollution by metals and can estimate the effects of various metals in the soil quality and the environment (Zhang et al., 2018). It is defined as:

$$I = \sqrt{\frac{Pi_{ave}{}^2 + Pi_{max}{}^2}{2}}$$

where, *Pi* is the Pollution factor, which quantifies the contamination of one individual metal, $Pi = C_i/B_i$, where C_i is the concentration of the measured contaminant and B_i is the geological background level (Santos-Francés et al., 2017b). Likewise, Pi_{ave} is the average value of single pollution indices, and Pi_{max} is the maximum value of single pollution indices. The quality of the soil environment is classified as class 0 (NI < 0.7) non-contamination, 1 (0.7 < NI < 1) slight contamination, 2 (1 < NI < 2) low contamination, 3 (2 < NI < 3) moderate contamination, and 4 (NI > 3) heavy contamination (Z. Li et al., 2019).

According to Santos-Francés et al. (2017a, 2017b) and Mazurek et al. (2019), the Improved Nemerow index (INI) reflects more accurately soil reality using other similar pollution indexes, such as the geo-accumulation index (Igeo) in substitution of the pollution factor (Pi). INI is calculated using the following equation:

$$INI = \sqrt{\frac{1}{2}\left(Igeo_{max}{}^2 + Igeo_{ave}{}^2\right)}$$

where, $Igeo_{max}$ is the maximum value of the Igeo of all metals in a sample and $Igeo_{ave}$ is the arithmetic mean of the Igeo. INI discriminate between class 0 - uncontaminated (INI < 0.5), class 1- uncontaminated to moderately contaminated (0.5 ≤ INI < 1), class 2 - moderately contaminated (1 ≤ INI < 2), class 3 - moderately to heavily contaminated (2 ≤ INI < 3), class 4 - heavily contaminated (3 ≤ INI < 4), class 5 - heavily to extremely contaminated (4 ≤ INI < 5) and Class 6 - extremely contaminated (INI > 5) soils.

1.4.3.3. Potential ecological risk (RI)

The method considers the potential impact of heavy metals on ecosystems and is used for the assessment of soil in large regional areas (Zhang et al., 2018). It is capable of assessing potential risks of one or multiple toxicological elements to the surrounding ecology (Liu et al., 2020). The Ecological Risk Index (Er) evaluates the toxicity of individual metals in soils, and the Potential Ecological Risk (RI) reflects the general situation of contamination caused by the simultaneous presence of the metals (Santos-Francés et al., 2017b). It is calculated following equations:

$$Er = Tr \cdot Pi$$

$$RI = \sum_{i=1}^{n} Er$$

where Tr is the toxicity coefficient of each metal (standard values are Pb = 5, Zn = 1, As = 10, Cu = 5, Ag = 50, and Cd = 30; Duodu et al., 2016; Santos-Francés et al., 2017a). Er classifies the situation of the contamination as low contamination risk ($Er < 40$), moderate contamination risk ($40 \leq Er < 80$), considerable contamination risk ($80 \leq Er < 160$), high contamination risk ($160 \leq Er < 320$) and extreme contamination risk ($Er > 320$). The categories for the RI are: low ecological risk of contamination ($RI < 150$), moderate ecological risk ($150 \leq RI < 300$), considerable ecological risk ($300 \leq RI < 600$) and very high ecological risk ($RI > 600$).

1.4.4. Metals fractionation in soil

Total metal concentrations are indicators of contamination but does not provide enough information on the bioavailability, distribution, and mobility of metals in soils (Gabarrón et al., 2018). From the ecological point of view, it is essential to know which part of the total concentration of a metal is available to determine its toxic effect (Głosińska et al., 2005). Metal mobility varies with the composition of the soils (Kushwaha et al., 2018) and with the variability of the metal's physicochemical characteristics because its affinity to soil components will govern its fractionation (Kabata-Pendias, 2011).

Sequential extraction procedures allow the identification of the phase associations of trace elements in soils, and the strength of metal binding to particulates, helping to understand the geochemical processes governing metal mobilization and its potential effects (Gabarrón et al., 2018).

A sequential extraction scheme employs several steps to allow differentiation between mobile and residual fractions, characterizing the different labile fractions (Alan and Kara, 2019).

Tessier et al., (1979) developed the first sequential extraction procedure, which includes five steps to obtain concentrations of elements:

1. exchangeable (F1),
2. bound to carbonates (F2),
3. associated with oxides of iron and manganese (F3),
4. bound to organic matter, and sulfides (F4), and
5. the residual fraction (F5)

The procedure relies on the use of specific extraction agents able to release metals bound to different soil components followed by the total element detemination in the leachate.

Of all fractions, the exchangeable one is considered the most mobile and bioavailable for plants uptake and adsorption (Ndubueze, 2018). The other metal fractions are more or less immobile; since the metal mobilization or transformation of mobile to immobile metal species is often a slow process (Kabata-Pendias, 2011), the metal is not readily available to plants (Ndubueze, 2018).

Also, the speciation of the soil elements is associated with the inherited chemistry from their parent materials (Kabata-Pendias, 2011). The acidic conditions of soils could advantage the heavy metal content in their mobility and availability to more mobile fractions (Arenas-Lago et al., 2014).

1.5. EFFECT OF MINING ACTIVITIES ON VEGETATION

Soil contamination by heavy metals has an important effect on the ecosystems (Madejón et al., 2018); it inhibits the growth and establishment of plants, and restricts agricultural activities (Córdova et al., 2011). Metals mainly influence the plant's physiological activities such as photosynthesis, absorption of essential elements, water transport, and reproduction rate, affecting the growth and development of the vegetation (França Afonso et al., 2020). However, some plants are adapted to metal contaminated soils, including the native plants, which are often excellent in terms of growth, reproduction, and survival to strong environmental stress (Midhat et al., 2019). These plants have developed certain external and internal mechanisms to transport and store metals in their leaves, stems, and other above-ground physiological parts (Claveria et al., 2019). The geological and seasonal factors and the plant's tolerance, will influence in the revegetation capacities on contaminated soils (Dazy et al., 2009).

1.5.1. Plant species identification

Plants play a really important role in human life, mainly by providing oxygen and food (Zhang et al., 2020). Plants regulate the climate, are essential for agricultural productivity and sustainability for the ecosystems. Therefore, in addition to studies of the known species, it is important to identify new ones and to measure their geographical extent (Cope et al., 2012).

Every plant is distinct in size, shape, and colour. Plant identification is very important because knowing the taxonomic rank to which the species belongs, permits access to the information linked to that specific name, its uses, geographic distribution, and abundance (Cope et al., 2012). The identification of plants capable of surviving and growing in contaminated areas is advantageous to potentially develop phytoremediation technologies (Dazy et al., 2009).

The initial step in the identification is plant collection in a field in order to recognize unknown specimens. It has to be underlined that the species encountered in harsh environments are often small, atypical plants with no flowering or fruiting parts; so, the whole plant should be collected, including the leaves, stems, and roots (Bowles, 2004). The taxonomy identification of plants is carried out by comparing the morphological, floral, and fruit characteristics of one plant with the characteristics of previously identified plants (El-Raouf, 2021). In this way taxonomists can identify species and assign taxonomic labels to them (Cope et al., 2012).

South America is the floristically richest region in the world with great native populations (Kvist et al., 2006), of which Peru is characterized for having rich biodiversity; it is estimated that 17144 flowering plant species exist in Peru, of which 5354 (31.3%) are endemic, while the rest are native or introduced (Guillen Quispe et al., 2017).

In the previous section, the effect of soils on the plants was disccused. However, it is important to stress that the plants and soil mutually influence each other (*e.g.,* plant roots affect the characteristics of soil, mostly its physical properties such as mechanical composition, soil mineralogical structure stability, and porosity).

1.5.2. Elemental composition of plants

The trace element content of plants is strongly related to the physiological and biochemical processes, that is, photosynthesis, growth, reproductivity, chlorophyll biosynthesis, redox reactions, and sugar metabolism (Kumar et al., 2021). Among different metals, 17 are essential for all plants,

namely Al, B, Br, Cl, Co, Cu, F, Fe, I, Mn, Mo, Ni, Rb, Si, Ti, V, and Zn (Kabata-Pendias, 2011). These trace elements in small quantities are required by plants for normal growth. For this reason, they are considered to be essential micronutrients (Hirve et al., 2020) and cannot be substituted by others in their biochemical roles (*e.g.,* uptake and transport within a plant) (Kabata-Pendias, 2011). Other elements such as Cd, As, Cr, and Pb are considered as nonessential elements, that is, not required by plants for their normal growth; the presence of these elements even at very low concentration can cause toxic effects on plants (Hirve et al., 2020). **Table 1** summarizes the estimations of approximate ranges of normal trace elements concentrations in mature leaf tissue that may be used for the comparison and evaluation of metal status in plants.

Table 1. Ranges of normal trace elements concentrations in mature leaf tissue, adapted from Kabata-Pendias, (2011)

Element	Concentration sufficient or normal (mg/kg)
Ag	0.5
As	1 - 1.7
B	10-100
Be	<1 - 7
Cd	0.05 - 0.2
Co	0.02 - 1
Cr	0.1-0.5
Cu	5-30
F	5-30
Li	3
Mn	30-300
Mo	0.2-5
Ni	0.1-5
Pb	5-10
Se	0.01-2
Sb	7-50
V	0.2-1.5
Zn	27-150

Despite essentiality and nonessentiality of trace elements (Hirve et al., 2020), the presence of excessive levels of metals in plants causes alterations in growth and metabolism, impacting their physiological and biochemical processes and consequently, the whole ecosystem (Nagajyoti et al., 2010). Accumulation of heavy metals from contaminated soil affects the whole plant body (leaves, roots, and stems) (Kumar et al., 2021). Their accumulation for long periods of time interferes with the photosynthesis and absorption of essential minerals (biochemical processes) and often modifies the morphology of components of cells and organs (e.g., anatomical alterations of roots, leaves) (Rehman

et al., 2021). Some other effects of stress caused by heavy metals are stunted plant growth, decreased nutrient uptake, and changes in enzymatic activities related to photosynthesis (Hirve et al., 2020).

Unmanaged mining waste pollutes the surrounding ecosystem, inhibiting the development of natural vegetation and affecting the diversity of vegetal species (Hosseini et al., 2018). It is so, that the habitats of the plants in metalliferous soils are very restrictive due to phytotoxicity, resulting in severe selection pressures; likewise, the evolution of metal tolerance takes place at each specific site (Baker et al., 2010). Some plants are capable to tolerate mining waste and accumulate metals from mine soils (Hosseini et al., 2018). On the other hand, the degree of tolerance of the plant to the metals depends on the bioavailable fraction of the metal in the soil and the type of mineralization, so, at extremely high soil metal concentrations (polymetallic soils) the plants are not able to evolve extreme tolerances to several heavy metals simultaneously (Baker et al., 2010). The behaviour of the trace elements influences the availability of them to plants. For: Ag, Cr, Sn, Ti, and Y, there are not easily taken up by plants and are very slightly soluble in the soil. For As, Hg, Pb, and F, they are not readily transported to above-ground parts of plants and relatively strongly sorbed by soil. For B, Co, Cu, Mn, Mo, and Ni are readily taken up by plants and mobile in the soil. Cadmium, Se, and Zn are easily bioaccumulated by plants and very mobile in soils (Kabata-Pendias, 2011).

Plants take up heavy metals from contaminated soil transporting them from roots to different over ground organs. Thus, the mechanisms of toxicity tolerance/accumulation potential of heavy metals depends on different plant and metal species (Kumar et al., 2021). Plants behaviour when dealing with metal excess is schematically presented in **Figure 4**. It allows their classification into: (i) *excluders*, in which there is no uptake and metal concentrations in plants are unaffected (to a critical level) by toxic metal concentrations in soils; (ii) *indicator* plants, which reflect the metal concentrations of the soil in both roots and the shoots; (iii) *accumulator* plants, which have the ability to concentrate metals in the aerial parts - those accumulating significantly higher levels of metals than present in soil are the referred to as *hyperaccumulators* (Bini et al., 2017). Hyperaccumulators take up elements from soil and sequester them in their leaves (Alford et al., 2010). Hyperaccumulators plants of As, Co, Cu, Cr, Ni, Pb, and Se can reach concentrations higher than 1000 mg kg^{-1}. For Mn and Zn, hyperaccumulators can reach values of 10000 mg kg^{-1}, whereas for Cd, values higher than 100 mg kg^{-1} are reported (Bech et al., 2017; Kabata-Pendias and Mukherjee, 2007).

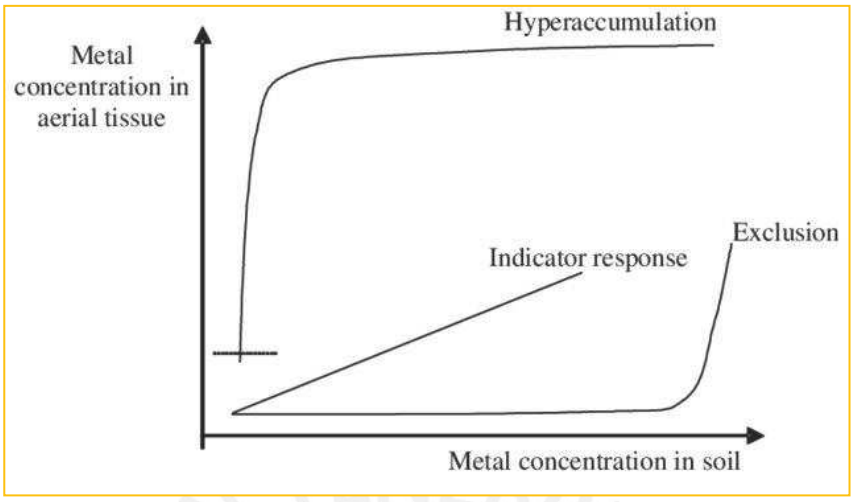

Figure 4. Conceptual responses of plants to increasing metal concentrations (Callahan et al., 2006)

The plants behave like hyperaccumulators or excluders to cope with the high level of toxic metal concentrations (Wenzel et al., 2003). The spontaneous vegetation that grows in heavily contaminated mining areas under stressful conditions is the result of strong environmental pressure on the selection of tolerance mechanisms of the plants. Several studies have demonstrated that such species show higher resistance, accumulation and tolerance to the potentially harmful concentrations (Fernández et al., 2017). More than 500 species accumulating high levels of trace metals have been identified (Hosseini et al., 2018). Likewise, the study of the native plant species on metal-rich sites allows identifying both plants with bioaccumulation factors and the ability to hyperaccumulate, tolerating potentially harmful trace elements in their shoots (Fernández et al., 2017). **Table 2,** presents examples of native plant species able to accumulate high levels of metals in Latin American contaminated post-mining areas.

Table 2. Selected exmples of native plant species growing in Latin America contaminated mining sites

Family	Native Species	Information on Publications about metals	Name of the mine	Country	Reference
Asteraceae	*Ageratina sp.*	Zn and Pb	Carolina mine - Hualgayoc	Peru	Bech et al., 2017, 2016
	Achyrocline alata	As, Cu, Pb and Zn			
	Baccharis latifolia	As, Cu, Pb and Zn			
		As, Ba, Cu, Fe, Mn, Zn and Hyperaccumulator of Pb	Carolina mine - Hualgayoc	Peru	Durán Cuevas, 2010; Oyuela Leguizamo et al., 2017
	Baccharis amdatensis	As, Cd, Cu, Pb and Zn	Bartolomé mine	Ecuador	Bech et al., 2017
	Baccharis rhomboidalis	Cu, Pb and Zn	Teniente mine	Chile	
	Baccharis dracunculifolia DC.	Cd, Cr, Pb, V, Ba	Camaquã mine	Brasil	França Afonso et al., 2020
	Baccharis trimera Less DC				
Melastomataceae	*Miconia lutescens*	As, Cu and Zn	Turmalina mine - Piura	Peru	Bech et al., 2017
Poaceae	*Cortaderia Hapalotricha*	Hyperaccumulator of Pb	Carolina Mine - Hualgayoc	Peru	
	Cortaderia nitida	As, Cd, Cu, Pb and Zn	Bartolomé mine	Ecuador	
Polygonaceae	*Muehlenbeckia hastulata*	Cu, Zn and Pb	No mine - Los Maitenes area in the Puchuncaví Valley	Chile	Córdova et al., 2011
Solanaceae	*Nicotiana*	Cr, Mn, Fe, Co, Ni, Cu, Zn, As, Sb, Hg and Pb	Wadley antimony mine district - San Luis, Potosí	Mexico	Levresse et al., 2012

Taxa in contaminated soils are classified as plants *Metallophytes, Pseudo metallophytes*, and *Accidental metallophytes* (Durán Cuevas, 2010). *Metallophytes* are plant species that have developed physiological mechanisms to resist, tolerate and survive in soils with high levels of trace elements. Therefore, they are endemic to areas with natural outcrops of metallic minerals, with a very limited geographical distribution (Becerril et al., 2007; Durán Cuevas, 2010). The *Pseudo metallophytes* species are more extensively spread; their tolerance to metals is low, but by selective pressure they are able

to survive in metalliferous soils; that is, they can be present in contaminated and uncontaminated soils in the same region (Becerril et al., 2007; Durán Cuevas, 2010). Finally, there are the *Accidental metallophytes* species that include ruderal species which appear only sporadically and show reduced vigour. Therefore, M*etallophytes* and *Pseudo metallophyte* plants have developed true heavy metal tolerance strategies, while *Accidental metallophytes* show stress effects of high concentrations of metals (Durán Cuevas, 2010).

In Latin America, only a few metal tolerant and metal hyperaccumulator plants have been reported, which represent a low proportion when compared to the high plant diversity described for the region (Baker et al., 2010). In Peru, scientific research indicates that there exists three arsenic hyperaccumulating plants (*Bidens cynapiifolia* (Asteraceae), *Paspalum racemosum* and *P. tuberosum* (Poaceae)) and one possible copper tolerant plant (*Bidens cynapiifolia*) which grow near a copper mine in the northern Peruvian Andes (Baker et al., 2010; Bech et al., 1997).

1.5.3. Metal speciation in plants

Toxic elements intervene in the physiological and biochemical processes of the plant provoking the inactivation of enzymes and proteins, disruption of the membrane integrity, and alteration of the key metabolic reactions such as respiration, photosynthesis, and fixation and assimilation of some essential nutrients (Raza et al., 2021). Metals can form ligands in plants either as complexes easily transported or strongly bound (metal ions form complexes mainly with organic ligands) controlling the mechanisms of transport of nutrients within the plant organs (Kabata-Pendias, 2011).

The chemical transformations, mobility, and reactivity of metal(oids) in the environment depend on their speciation; element species are present as high and low molecular weight species in all the organs including building blocks and plants liquids. Plant xylem and phloem contain a large variety of metal-binding ligands that form complexes in plants, either easily transported or strongly bound e.g., to cell walls (Kabata-Pendias and Mukherjee, 2007; Łobiński and Adams, 1997; Schaumlöffel et al., 2003). The metal-binding ligands most often reported in xylem and phloem are nicotianamine, histidine and organic acids (Cui et al., 2020). Phytochelatins and metallothioneins are induced following the presence of the excess of Cd, Zn, Cu, Ag, Hg (Grill et al., 1987; Schat et al., 2002). The phytochelatins that behave like chelators, also play an important role in the transport and immobilization of trace metals, whose quantity increases when the cell needs ligands to survive in presence of high concentrations of metals (Kabata-Pendias, 2011). DNA, polysaccharides, pectins,

proteins, lignins, phytoferritins are the common metal chelating agents in plants (**Figure 5**) (Kabata-Pendias, 2011; Kabata-Pendias and Mukherjee, 2007). The ligands, by forming complexes with metal ions, function to sequester, detoxify, and store high levels of metals (Cui et al., 2020).

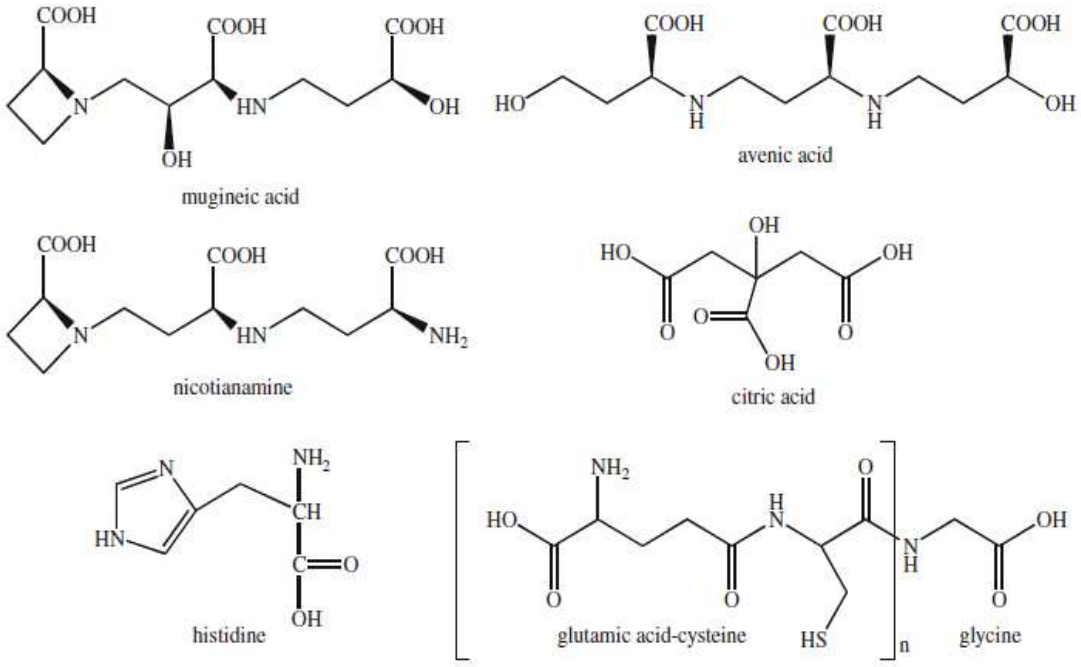

Figure 5. Examples of some metal binding ligands in plants (Callahan et al., 2006)

The term *speciation analysis* is used to describe processes of identification and/or quantification of the different forms of an element in a sample (Łobiński and Adams, 1997). The analytical procedure requires analytical techniques that produce a signal characteristic not of the total element but of a specific species allowing its detection, confirmation of its identity, and quantification (Wojcieszek et al., 2018). The techniques used often combine element selectivity of ICP-MS and a separation technique, usually liquid chromatography; HPLC-ICP-MS is used for the quantitative determination of species of interest and cartography of species of interest (Szpunar, 2000; Wojcieszek et al., 2018); electrospray MS detection is used for molecular targets in biological systems or the identification of the metabolism products (Wojcieszek et al., 2018). HPLC with the parallel ICP MS and electrospray MS detection is used for the exploratory studies and identification of novel metallomolecules in biological systems (Łobiński and Szpunar, 1999; Wojcieszek et al., 2018).

1.6. REMEDIATION TECHNOLOGIES IN SOIL POLLUTED WITH TOXIC ELEMENTS

Preservation of the agricultural and ecological functions of soil is very important for its productivity (Kabata-Pendias, 2011), and also for animal and human health due to the fact that through the food chain the toxic metals can bioaccumulate in food (Santos-Francés et al., 2017b). However, the main soil problems of pollution are its rapid degradation and serious regional pollution (Dong et al., 2019). In many active mines, as well as in the abandoned mines, the landscape is devastated and the natural soil components have lost the ability to self-regeneration having negative consequences for surrounding ecosystems (Favas et al., 2018).

Soil pollution has been intensively investigated around post-mining areas (Camizuli et al., 2020), resulting in the general realization that the abandoned mines can be reintegrated into cultural landscapes for local communities thus contributing a source of future economic opportunities (Bainton and Holcombe, 2018). As environmental issues related to mining operations which cause severe damage to land, it is sought to develop appropriate methods of management of such sites after their abandonment to counterbalance the potentially adverse effects (Kapusta and Sobczyk, 2015).

Environmental remediation focuses on the implementation of strategies geared to reverse environmental impacts (Artiola et al., 2004). The soil remediation techniques are chosen depending on the nature, concentration, and distribution of the heavy metals, the site characteristics, and the soil properties (Bini et al., 2017). The majority of the traditional remediation techniques for metal-polluted soils include removing and burying contaminated soil and use of physical and chemical measures (Dong et al., 2019) such as isolation of mine tailings, excavation and burial, stabilization, electrokinetics, leaching, and chemical compound additions (Chang Kee et al., 2018). Depending on the type of heavy metal(oids) and site characteristics, different remediation technologies could be applied (Gong et al., 2018). **Table 3** summarizes the most commonly used physical, chemical, and biological processes and their advantages, disadvantages, and in situ and ex-situ applicability.

Table 3. Remediation technologies for heavy metal-contaminated soils, adapted from Gong et al., (2018) and Liu et al., (2018)

Categories	Remediation Technique	Applicability	Description	Advantages	Disadvantages
Physical	Surface capping	-In situ -High contamination	It is the covering of the polluted site with a layer of waterproof material to form a stable, protection surface. However, this technique does not remove the heavy metal contaminants or reduce their reactivity in the soil	-Low in cost -Easy to install -High security	-Limited to specific geographic locations -Loss of land cropping function
	Vitrification	-In situ and ex situ -High contamination	Application of high temperature to melt the soil and achieve stabilize heavy metals after cooling within a glassy mass	-Good long-term effectiveness -Wide application range -Volume reduction of materials -Products with potential reuse options -High efficiency	-High cost -Off-gases can be created and should be treated -Limited to small area/volume soil -The soils losing environmental functions
	Electrokinetic	-In situ -Moderate to high contamination	Use of electricity on the electrolytic tank containing saturated contaminated soil	-Appropriate for saturated soils with low groundwater flow -Minimal soil disturbance -Low energy consumption -Complete reparation	-Low efficiency -Time-consuming -Limited treatment depth -Recommendable for fine-textured soils with low permeability
	Thermal treatment	-Ex situ -Moderate contamination	Heating of the soil polluted via steam, microwave, and infrared radiation to volatilize the contaminant without combustion of contaminants	- Simple process and safe -Effective extraction and recovery of mercury	-Elevated costs -Effectiveness only at high total soil mercury contents -Necessary control of the gas emission and particular facilities

Categories	Remediation Technique	Applicability	Description	Advantages	Disadvantages
Chemical	Chemical stabilization	-In situ -Moderate to high contamination	The addition of chemical agents to the soil polluted to decrease the bioavailability, mobility, and bioaccessibility of heavy metals in soil	-Cost effective, simple, and rapid	-Cannot remove or extract contaminants from soil -Changes the physicochemical properties of soil
	Soil washing	-Ex situ -Moderate to high contamination	Leaching of heavy metals from soils by physical and chemical processes using various reagents and extractants	-High efficiency -Rapid method -Permanent removes soil metal contaminants	-Extreme soil disturbance -Elevated cost -Rigorous working processes
	Solidification/ stabilization	-In situ and ex situ -High contamination	Solidification is to trap or immobilize pollutants in a monolithic solid of high structural integrity. Stabilization refers to the addition of reagents to the polluted soil to induce physicochemical interactions and to reduce the mobility of the toxic waste	-Low cost -Fast to implement -High resistance to biodegradation	-Higher volume of the treated material -The soils losing environmental functions -Long-term monitoring is needed
Biological	Phytoremediation	-In situ -Low to moderate contamination	Use of plants to remove heavy metals from contaminated soils	-Low cost -Non-invasive -Easy to implement -Suitable for large areas -No secondary pollution	-Limited to a metal-specific -Prolonged repairing cycle -Soil limited treatment depth
	Bioremediation	-In situ -Low to moderate contamination	The process by microorganisms (i.e., bacteria, fungi, and algae) to induce precipitation, adsorption, oxidation, and reduction of heavy metals	-Low cost -Minimal soil disturbance	-Low efficiency -Employed together with other remediation techniques

Biological methods are eco-friendly, safe, with a minimal disturbance to the natural environment or local ecological systems, least destructive, and cost-efficient (Gong et al., 2018). Compared with other remediation techniques, phytoremediation is a technology with a growing potential for remediating mining sites of large areas at shallow depths due to relatively a low cost in situ remediations, and it respects the environment (Chang Kee et al., 2018; Liu et al., 2018).

1.7. PHYTOREMEDIATION POTENTIAL

Phytoremediation is the use of plants to clean up soil, air, and water contaminated with hazardous contaminants. It usually involves the revegetation of a post-industrial (*e.g.,* post-mining) area using suitable plant species surviving in difficult ecological conditions and growing fast (Cundy et al., 2016; Venkateswarlu et al., 2016). Due to the interactions between soil and plants, the environmental quality of the site affected by contamination is improved (Moreno-Jiménez et al., 2011). Improving the topsoil quality through soil remediation reduces the land sensitivity, allowing the growth of vegetation (Yang et al., 2017). Phytoremediation is a method applicable to large areas allowing the stabilization of toxic substances (Venkateswarlu et al., 2016).

The element accumulation in plants depends on the mobilization and uptake from the soil, metal capture, and transport efficiency within the root, and the metal distribution in the aerial parts (Tack, 2010). Native plants are adapted to the high content of metal contaminants of the mining soil and can survive the low levels of essential nutrients (Cui et al., 2020).

There are five classes of phytoremediation including: (i) phytoextraction, (ii) phytostabilization, (iii) phytodegradation, (iv) phytovolatilisation, and (v) rhizofiltration (**Figure 6**) (Rizwan et al., 2019). The first step of these processes is the uptake of contaminants by the plant roots along with water and nutrients.

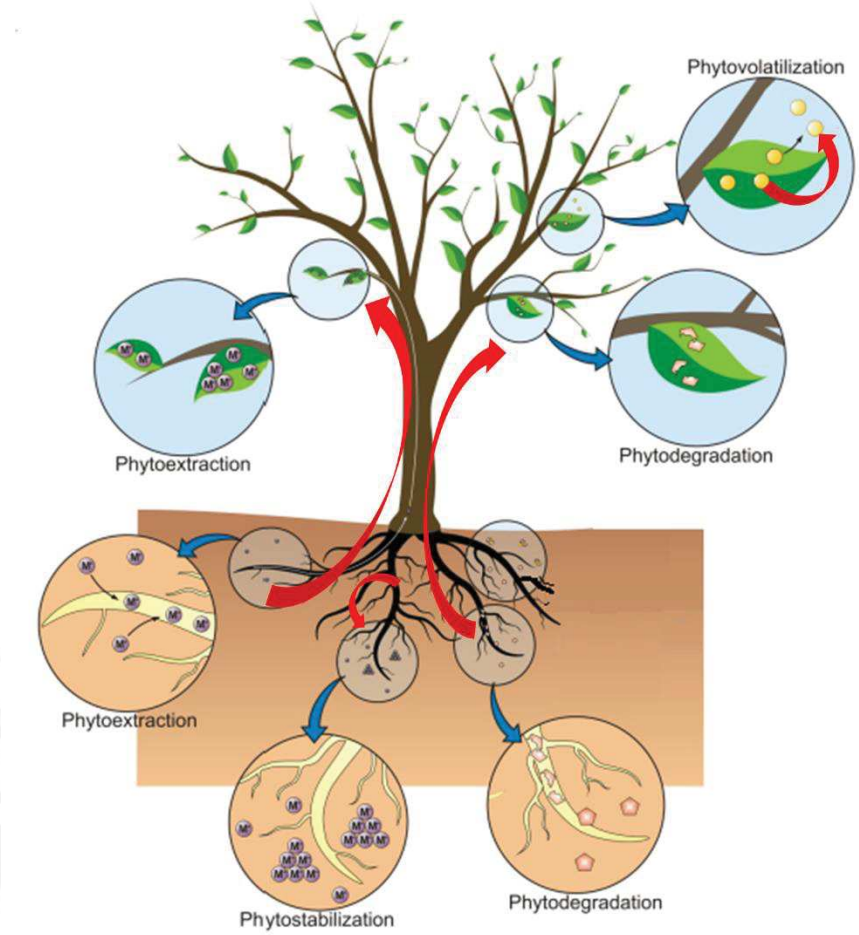

Figure 6. Schematic presentation of phytoremediation processes, adapted from Favas et al., (2014)

(i) *Phytoextraction* is an *in situ* technique that uses hyperaccumulator plants to purposely bio-concentrate high levels of metal(loid)s (Corzo Remigio et al., 2020). The metals are translocated from roots to the aerial parts of the plant (leaves, stems, shoots) (Favas et al., 2014; Shah and Daverey, 2020).

(ii) *Phytostabilization* is referred to *in situ* inactivation or immobilization of heavy metals, reducing their bioavailability and preventing their off-site transport (Shah and Daverey, 2020). Toxic metals are immobilized in the plant rhizosphere region (soil matrix), so that they avoid the entry into the food chain of the ecosystem (Gautam and Agrawal, 2019; Patra et al., 2020).

(iii) *Phytodegradation*, also knowing as *phytotransformation*, includes the use of plants to degrade or transform toxic contaminants (Cundy et al., 2016); the mineralization of the metal ions by specific enzymes takes place inside plant cells (Favas et al., 2014; Shah and Daverey, 2020).

(iv) *Phytovolatilisation* involves the translocation of metals from root to shoot system and their release into the atmosphere by a diffusion process (Patra et al., 2020). It can be applied to some elements such as Hg, Se, and As (groups IIB, VA, and VIA of the periodic table), they can be transformed into non-toxic volatile forms such asmethylated derivatives (Favas et al., 2014).

(v) *Rhizofiltration* allows for the elimination of toxic contaminants from aquatic and terrestrial ecosystems by adsorption (Patra et al., 2020) by the plant roots and associated microorganisms (Cundy et al., 2016).

Phytoremediation potential can be estimated by calculation of the bioconcentration (BCF) and translocation factors (TF). The BCF is defined as the ratio of the metal content accumulated in the plant to the content in the soil (Lago-Vila et al., 2019), as given below:

$$BCF = Cp/Cso$$

where Cp is the metal concentration in the plant (shoot) and Cso is the total metal concentration in the soil. Plants with a BCF value higher than one are considered to be suitable candidates for phytoextraction (Kamari et al., 2014; Yoon et al., 2006).

The ability of the trace metal transfer from the roots to aerial part is expressed using the translocation factor TF (Lago-Vila et al., 2019), calculated as follows:

$$TF = Cs/Cr$$

where Cs is the metal concentration of the aerial part (shoot) of the plant and Cr is the concentration in roots. Plants with TF values higher than one can be potentially used for phytoextraction (Ghazaryan et al., 2019).

I.B. ANALYTICAL TECHNIQUES USED IN THE ASSESSMENT OF ELEMENT STATUS IN SOILS AND PLANTS

The knowledge of the contents of trace, and ultra-trace elements is essential in various fields of science, industry, and technology; therefore, there is a need for accurate measurements (Bulska and Ruszczyńska, 2017; Helaluddin et al., 2016). **Table 4**, and **Figure 7** summarizes and compare the performance of GF AAS (graphite furnace atomic absorption spectroscopy), HG AAS (hydride generation atomic absorption spectroscopy), F AAS (flame atomic absorption spectroscopy), ICP-AES (inductively coupled plasma atomic emission spectroscopy), and ICP-MS (inductively coupled plasma mass spectrometry) describing their detection limit range of each technique.

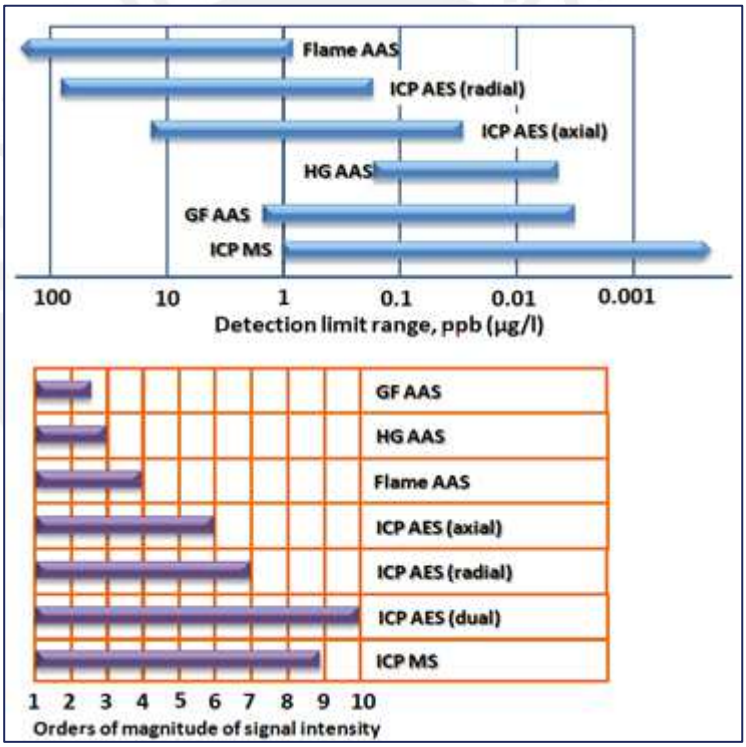

Figure 7. Typical detection limits and orders of magnitude of signal intensity for common elemental techniques

Table 4. Summary of Analytical Techniques (Helaluddin et al., 2016)

	GFAAS	HGAAS	FAAS	ICP-OES	ICP-MS
Description	The measurement is based on the fact that free atoms will absorb light at wavelengths characteristic of the element of interest			The measurement is based on the use of inductively coupled plasma	
	Samples are mixed with modifiers prior to the atomization in a graphite tube (atomizer)	Aqueous samples react with a reducing agent to generate volatile hydrides, which are then transported to the heated quartz cell (atomizer)	Samples aerosol is atomised in a flame	to produce excited atoms and ions that emit electromagnetic radiation at wavelengths characteristic of a particular element	to atomize the sample and create atomic ions (of different isotopes of the same element)
Detection limits	Very good for some elements	very good but only for hydride forming elements	Good for some elements	Very good for most elements	Excellent for most elements' ppb
Sample throughput	Slow: 5-6 mins per element	30-50 secs per element	10-15 secs per element	60 elements in < 1 minute	All elements in < 1 minute
Interferences Spectral	Few	Very few	Few	Many	Few
Chemical (matrix)	Very few	Very few	Many	Few	Some
Sample volume required	Very small (aprox. 20 µl)	Large	Large	Small	Small to medium

In comparison to the other techniques, the ICP-based ones have a lot of advantages such as multi-element detection, high sample throughput, high sensitivity, extensive linear dynamic range, and long-term stability (Kroukamp et al., 2016).

2.1. Total element analysis by ICP-based techniques

Inductively coupled plasma (ICP) is widely used as an ionization source in atomic mass spectrometry (MS) and an excitation source in optical emission spectrometry (AES) (Deng et al., 2017). ICP technology uses argon-based plasma, whose temperatures vary between 4500 to 10000 °K depending on the exact position inside the plasma; they allow efficient atomization and ionization of most of the elements (Seubert, 2001).

The ICP torch consists of three concentric quartz tubes (15–30 mm in diameter), where the outer channel is flushed with the plasma argon at a flow rate of 14 L/min, the intermediate channel (called auxiliary) transports the argon gas flow (0–2 L/min), used for the shape and the axial position of the plasma, the inner channel (called injector, flow rate 0.5-1.5 L/min) encloses the nebulizer gas stream forming the nebulizer/spray chamber combination (Makonnen and Beauchemin, 2020; Seubert, 2001). ICP torch is surrounded by an induction coil that is connected to a radiofrequency generator, operating at 27 or 40 MHz at 1-1.5 kW (**Figure 8**). The plasma energy is coupled inductively into the argon gas flow via a water-cooled copper coil (load coil) of two or three turns, that is connected to an RF generator (Fernández-Sánchez, 2018). Consequently, the plasma (the "fireball") is formed immediately after an ignition spark is applied to seed electrons and ions in the region of the induction coil (Sanz-Medel et al., 2013; Seubert, 2001). The sample is usually delivered as liquid spray via a nebulizer, small droplets entering the plasma undergo desolvation, dissociation, atomization, excitation and ionization. With the ICP at sufficiently high temperatures and sufficient residence times, the sample solvent vaporizes, and the analyte is reduced to free atoms, experiencing excitement; resulting in the emission of light at specific frequencies that it separates into discrete wavelengths for elements in the sample, which is proportional to their concentration (Bonchin et al., 2017). The advantages of ICP result from the plasma characteristics; its high electron density and temperature, high gas kinetic temperature, high excitation and capability of ionization almost all the elements (Deng et al., 2017). ICP-OES and ICP-MS are considered the most efficient techniques for total metal analysis. Each ICP-based technique has different advantages and drawbacks which depend on the number of analytes to measure, required sensibility, interferences and matrix effects (Bulska and Ruszczyńska, 2017). The ICP-MS and ICP-OES techniques use different principles; for ICP-MS the elemental separation and detection are based on the mass-to-charge ratio (m/z), while that for ICP-OES

characteristic optical emission line of an element is fundamental; likewise, the same ICP source could be shared for MS and OES simultaneously (Deng et al., 2017).

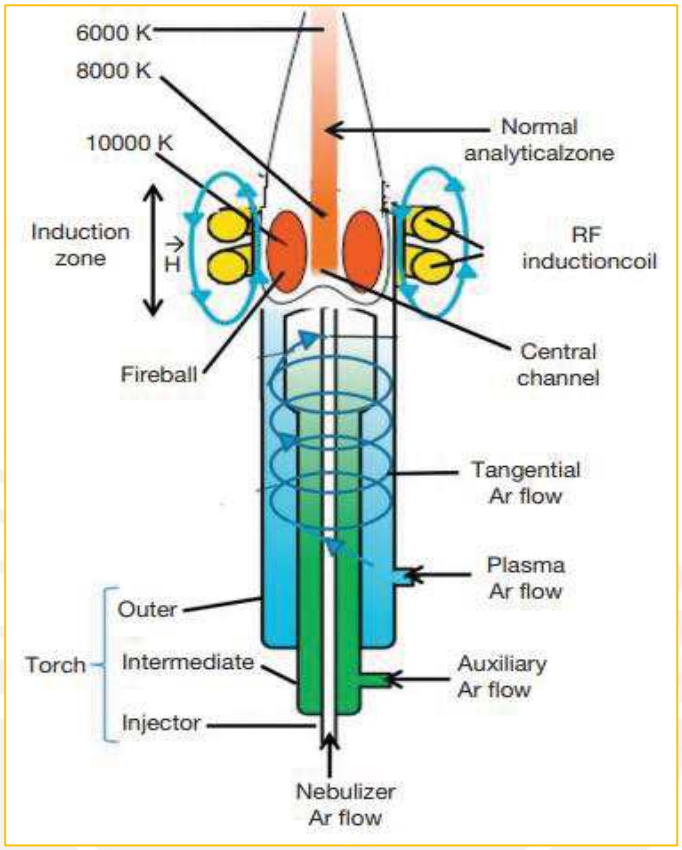

Figure 8. Inductively Coupled Plasma and torch schematic (Fernández-Sánchez, 2018)

Before the quantification analysis by ICP-MS and ICP-OES, the digestion of solid samples is necessary; it usually involves the use of concentrated mineral acids such as nitric, hydrochloric, and sulfuric, etc (Godoy et al., 2021; Narukawa and Chiba, 2013). Conventional liquid sample introduction with a nebulizer permits constant plasma-load and stable, so that, in ICP MS mass-to-charge ratios can be measured sequentially (Limbeck et al., 2016).

2.1.1. ICP-AES

Inductively coupled plasma atomic emission spectrometry (ICP-AES), also referred to as Inductively Coupled Plasma Optical Emission Spectrometry (ICP-OES), is excellent for the determination of trace elements with high sensitivity (Bulska and Ruszczyńska, 2017), but is is less

sensitive than ICP-MS, having, at the same time, a lower cost of instrumentation and maintenance (Deng et al., 2017).

ICP-OES operation involves three main steps: volatilization, sample atomization (in order to produce free atoms or ions), and atoms/ions excitation (Fernández-Sánchez, 2018). The atomic/ionic excited state species may then relax to the ground state via emission of photons (Helaluddin et al., 2016; Hou et al., 2016). The energy of these photons, for each type of atom or ion (*i.e*, element) are determined by the quantized energy level structure (Hou et al., 2016); so that, the wavelength of the photons may be used to identify the elements (Helaluddin et al., 2016). The plasma viewing optics picks up the light emitted by the atoms or ions for detection in ICP-OES (Makonnen and Beauchemin, 2020). The intensity of electromagnetic radiation is indicative of the concentration of the element within the sample and detected by a photomultiplier or a semiconductor detector (Bulska and Ruszczyńska, 2017; Helaluddin et al., 2016).

Therefore, ICP-OES (**Figure 9**) is based on the unprompted emission of photons from atoms and ions that have been excited, in a radiofrequency discharge; the argon gas, is ionized in the intense electromagnetic field and flows in a particular rotationally symmetrical pattern toward the magnetic field of the radio-frequency coil. For atomization of analyte present in a sample, the plasma work to very high temperatures (up to 10000 °K); the wavelength of the photons are used to identify the elements, due to the number of photons is directly proportional to the concentration of the element; so In addition, ICP-OES have two different photometry methods, such as radial view (using either a lateral, direction perpendicular to the plasma), and axial view (direction parallel to the plasma) (Morishige and Kimura, 2008), in both viewing modes, the plasma radiation is focused using a concave or a convex lens, in the entrance slit of the wavelength dispersive device (Makonnen and Beauchemin, 2020).

For the signal acquisition in ICP-OES, typical integration intervals of several seconds, are used generating total analysis low times, which depends on the number of measured replicates and the sensitivity required (Limbeck et al., 2016). Some ICP-OES advantages are multi-element techniques, that have a large analytical range, high sample throughput, low sample volume and simple sample preparation (Wilschefski and Baxter, 2019) ; therefore an ICP-AES suffers from a lot of interferences (Bulska and Ruszczyńska, 2017), such as (i) physical interference due to changes in viscosity, etc. of

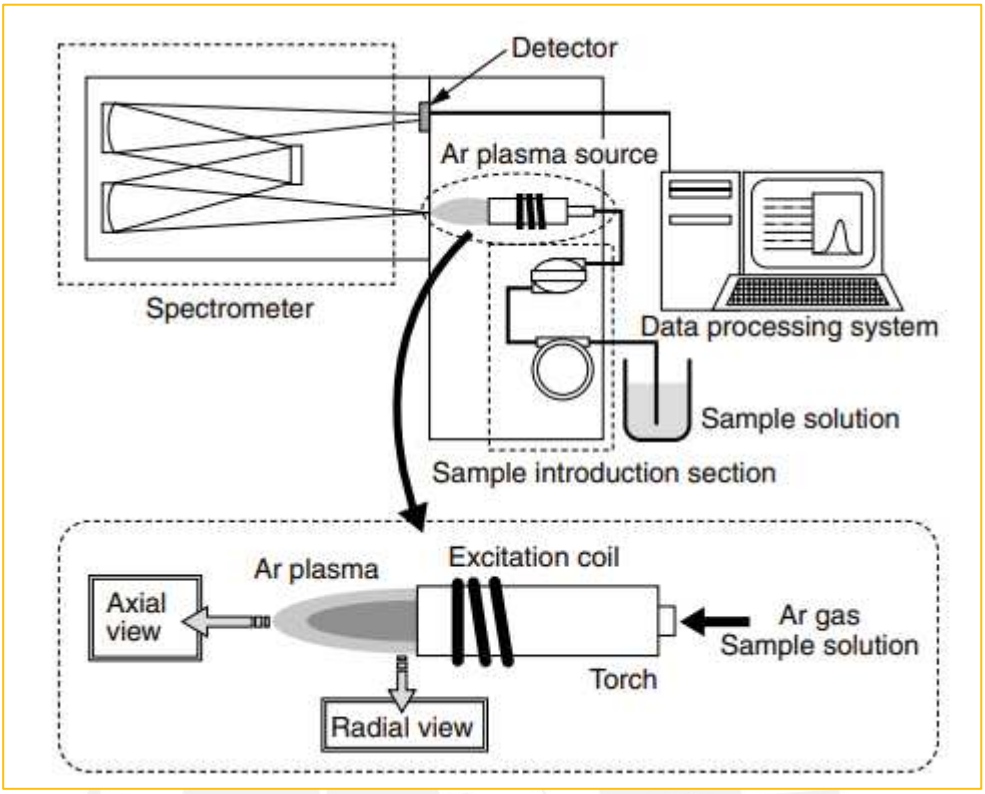

Figure 9. Schematic of typical ICP-OES equipment (Morishige and Kimura, 2008)

the sample solution; and (ii) chemical interference due to the generation of compounds that have low atomization efficiency, (iii) spectral interference due to the superposition, etc. of emission/absorption lines, and (iv) ionization interference due to changes in ionization equilibrium state (Morishige and Kimura, 2008) of which, spectral interference is usually inevitable in the ICP-OES system, due to a large number of atomic emission lines for many elements, which come from atomic emission lines, ionic emission lines, and molecular emission bands; (Deng et al., 2017). To obtain an accurate analytical result they should be eliminated before or during the determination, any possible interference, in the case of, chemical interference from a complicated sample matrix is commonly used complex sample pretreatment for pre-separation and preconcentration of analyte (Deng et al., 2017).

2.1.2. ICP MS

Inductively Coupled Plasma Mass Spectrometry (ICP-MS) is one of the most important techniques used for the multi elemental quantification (Godoy et al., 2021), standing out by the high detection power and sensitivity, especially for heavy elements (Limbeck et al., 2016), the ability for isotope dilution analysis, isotope detection capacity and broad dynamic range (Narukawa and Chiba, 2013; Wang et al., 2017). ICP-MS provides information on the total metal content of a sample, but not

about the oxidation state of the metal (Kroukamp et al., 2016). The elemental mass spectrometers cover the mass range from 6 to 254 a.m.u., thus, the detection of isotope ions of the majority of elements from the periodic table is possible (Bulska and Ruszczyńska, 2017). Advantages of ICP-MS include high precision, selectivity, and low detection limits, allowing work with low consumption of sample volume and analyse diluted samples (Godoy et al., 2021; Wang et al., 2017).

ICP-MS technique is related to the efficient generation of ions in the zone of the inductively coupled plasma and sensitivity of the ion detector (counts per second or cps), which are obtained through a series of analytical steps such as (i) conversion of the sample (usually liquid) into an aerosol (droplets) or its direct injection in gaseous form, (ii) transport of the aerosol/gas into plasma, (iii) atomization of the particles and/or droplets, followed by ionization of atoms in the hot plasma operated at atmospheric pressure, (iv) transport of the generated ions from the plasma to the mass separator (analyser, operates under high vacuum) which involves ion extraction through ion optics ICP-MS, (v) separation of the ions according to their mass to charge ratios (m/z), and (vi) detection of these separated ions, and conversion of ion flux intensity to an electronic signal (cps) (Bulska and Ruszczyńska, 2017). In **Figure 10**, is presented the principle of the analysis by ICP-MS.

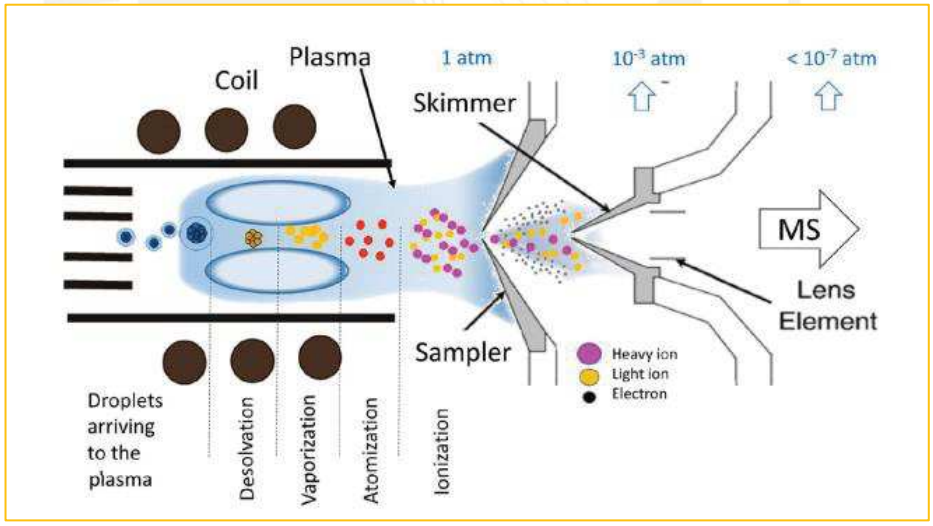

Figure 10. Principle of ICP-MS (Todolí, 2019)

The extraction of ions to atmospheric pressure from the plasma into the MS part is carried out in a multiple-stage differentially pumped interface; the first part is a cooled nickel or platinum cone (sampler) (Makonnen and Beauchemin, 2020; Seubert, 2001). A rotary pump evacuates the expansion chamber to ensure a pressure below 3 mbar behind the sampler, this pressure difference creates a

supersonic jet into the mass spectrometer, whereby, is placed a second cone with a small orifice (skimmer). The next part of the ICP-MS is the ion optic of an extraction lense for the acceleration of positively charged ions. The standard mass analyzer of ICP-MS is the quadrupole (Seubert, 2001), and an electrostatic deflector is used to push the separated ions into a electron multiplier (Makonnen and Beauchemin, 2020). The most popular, single quadrupole ICP-MS, has six fundamental parts: the sample introduction system, inductively coupled, plasma, interface, ion optics, mass analyser and detector (**Figure 11**) (Wilschefski and Baxter, 2019). The liquid sample is nebulising in the sample introduction system and then is transferred to the argon plasma, to dissociate the sample into its basic atoms or ions. The ions are released from the plasma and handed into the mass spectrometer, where they are isolated according to their mass-charge ratio (m/z) by a quadrupole, time-of-flight or magnetic sector analyser, and finally, these ions are measured at the detector (Helaluddin et al., 2016; Wilschefski and Baxter, 2019). The dwell times mass-to-charge ratios (m/z) in ICP-MS are in the order of below 10 ms to some 100 ms (Limbeck et al., 2016). Likewise, ICP-MS as a detection system allows the impurities determination up to the ultra-trace level, as well as, analysis with restricted sample amounts (e.g. single crystals, thin-film coatings, etc.), excellent depth profiling laterally resolved analysis of advanced materials (Limbeck et al., 2016).

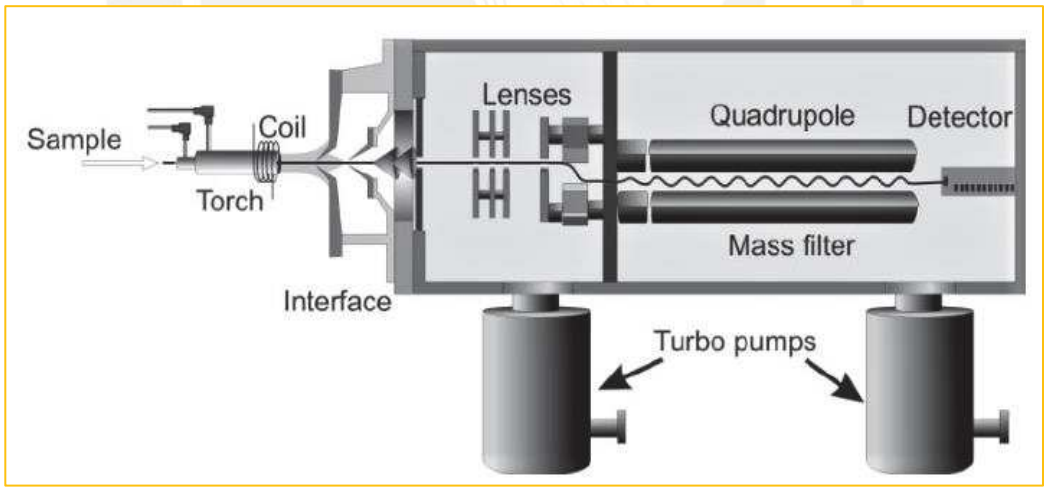

Figure 11. Cross section schematic of an ICP-MS (Wilschefski and Baxter, 2019)

Spectroscopic interferences is one of the main issues during the analysis using quadrupole-type ICP-MS. The two main types of interferences: spectroscopic and nonspectroscopic (Todolí, 2019).

Spectroscopic interferences: the isobaric interferences can appear when the interfering species have the same nominal m/z as the analyte (Sanz-Medel et al., 2013; Todolí, 2019), which is a significant issue due to each analyte has only a few alternative isotopes, if any; isobaric and polyatomic

interferences may come from atomic and polyatomic plasma species, acids of the sample preparation (digestion processes), matrix elements, the entrained atmosphere and so on (Makonnen and Beauchemin, 2020).

Matrix (non-spectroscopic) interferences : The interfering species (i.e. isotope of another element or a molecular ion) is formed by matrix components, water, plasma gas, and entrained atmospheric gases (Todolí, 2019).

In general interferences in ICP-MS analysis can be overcome by :

- Sample preparation techniques aimed at the removal of species capable of producing polyatomic interferences.
- Use of blanks to correct for polyatomics produced by reagents used in sample preparation (e.g., acid, water) and plasma gases.
- Use of high resolution sector field mass analyzers
- Making use of reaction/collision cells techniques with suitable gases such as He, H_2, NH_3, CH_4, or O_2 (Narukawa and Chiba, 2013).

Table 5 shows the elements analyzed during this study, isotopes and polyatomic interferences that may affect the signal obtained for each metal.

Table 5. Isotopes, abundance and polyatomic interferences of Ag, As, Cd, Cu, Pb and Zn (May and Wiedmeyer, 1998)

Isotope	Abundance	Interference
^{107}Ag	51.8	$^{91}Zr^{16}O^{+}$
^{109}Ag	48.2	$^{92}Zr^{16}O^{1}H^{+}$
^{75}As	100	$^{40}Ar^{35}Cl^{+}$, $^{59}Co^{16}O^{+}$, $^{36}Ar^{38}Ar^{1}H^{+}$, $^{38}Ar^{37}Cl^{+}$, $^{36}Ar^{39}K$, $^{43}Ca^{16}O_2$, $^{23}Na^{12}C^{40}Ar$, $^{12}C^{31}P^{16}O_2^{+}$
^{110}Cd	12.5	$^{39}K_2{}^{16}O^{+}$
^{111}Cd	12.8	$^{95}Mo^{16}O^{+}$, $^{94}Zr^{16}O^{1}H^{+}$, $^{39}K_2{}^{16}O_2{}^{1}H^{+}$
^{112}Cd	24.1	$^{40}Ca_2{}^{16}O_2$, $^{40}Ar_2{}^{16}O_2$, $^{96}Ru^{16}O^{+}$
^{113}Cd	12.22	$^{96}Zr^{16}O^{1}H^{+}$, $^{40}Ca_2{}^{16}O_2{}^{1}H^{+}$, $^{40}Ar_2{}^{16}O_2{}^{1}H^{+}$, $^{96}Ru^{17}O^{+}$
^{114}Cd	28.7	$^{98}Mo^{16}O^{+}$, $^{98}Ru^{16}O^{+}$
^{116}Cd	7.49	$^{100}Ru^{16}O^{+}$
^{63}Cu	69.1	$^{31}P^{16}O_2^{+}$, $^{40}Ar^{23}Na^{+}$, $^{47}Ti^{16}O^{+}$, $^{23}Na^{40}Ca^{+}$, $^{46}Ca^{16}O^{1}H^{+}$,$^{36}Ar^{12}C^{14}N^{1}H^{+}$, $^{14}N^{12}C^{37}Cl^{+}$, $^{16}O^{12}C^{35}Cl^{+}$
^{65}Cu	30.9	$^{49}Ti^{16}O^{+}$, $^{32}S^{16}O_2{}^{1}H^{+}$, $^{40}Ar^{25}Mg^{+}$, $^{40}Ca^{16}O^{1}H^{+}$, $^{36}Ar^{14}N_2{}^{1}H^{+}$, $^{32}S^{33}S^{+}$, $^{32}S^{16}O^{17}O^{+}$, $^{33}S^{16}O_2^{+}$, $^{12}C^{16}O^{37}Cl^{+}$, $^{12}C^{18}O^{35}Cl^{+}$,$^{31}P^{16}O^{18}O^{+}$
^{206}Pb	24.1	$^{190}Pt^{16}O^{+}$
^{207}Pb	22.1	$^{191}Ir^{16}O^{+}$
^{208}Pb	52.4	$^{192}Pt^{16}O^{+}$
^{64}Zn	48.89	$^{32}S^{16}O_2^{+}$, $^{48}Ti^{16}O^{+}$, $^{31}P^{16}O_2{}^{1}H^{+}$, $^{48}Ca^{16}O+$, $^{32}S_2^{+}$, $^{31}P^{16}O^{17}O^{+}$ $^{34}S^{16}O_2^{+}$, $^{36}Ar^{14}N_2^{+}$
^{66}Zn	27.81	$^{50}Ti^{16}O^{+}$, $^{34}S^{16}O_2^{+}$, $^{33}S^{16}O_2{}^{1}H^{+}$, $^{32}S^{16}O^{18}O^{+}$, $^{32}S^{17}O_2^{+}$,$^{33}S^{16}O^{17}O^{+}$, $^{32}S^{34}S^{+}$, $^{33}S_2^{+}$
^{67}Zn	4.11	$^{35}Cl^{16}O_2^{+}$, $^{33}S^{34}S^{+}$, $^{34}S^{16}O_2{}^{1}H^{+}$, $^{32}S^{16}O^{18}O^{1}H^{+}$, $^{33}S^{34}S^{+}$,$^{34}S^{16}O^{17}O^{+}$, $^{33}S^{16}O^{18}O^{+}$, $^{32}S^{17}O^{18}O^{+}$, $^{33}S^{17}O_2^{+}$,$^{35}Cl^{16}O_2^{+}$
^{68}Zn	18.57	$^{36}S^{16}O_2^{+}$, $^{34}S^{16}O^{18}O^{+}$, $^{40}Ar^{14}N_2^{+}$, $^{35}Cl^{16}O^{17}O^{+}$, $^{34}S_2^{+}$,$^{36}Ar^{32}S^{+}$, $^{34}S^{17}O_2^{+}$, $^{33}S^{17}O^{18}O^{+}$, $^{32}S^{18}O_2^{+}$, $^{32}S^{36}S^{+}$
^{70}Zn	0.62	$^{35}Cl^{35}Cl^{+}$, $^{40}Ar^{14}N^{16}O^{+}$, $^{35}Cl^{17}O^{18}O^{+}$, $^{37}Cl^{16}O^{17}O^{+}$, $^{34}S^{18}O_2^{+}$,$^{36}S^{16}O^{18}O^{+}$, $^{36}S^{17}O_2^{+}$, $^{34}S^{36}S^{+}$, $^{36}Ar^{34}S^{+}$, $^{38}Ar^{32}S^{+}$

2.2. Speciation analysis by HPLC-ICP MS/ESI MS^n

Speciation analysis has been defined by the International Union of Pure and Applied Chemistry (IUPAC) as: *"The analytical activity of identifying and/or measuring the quantities of one or more individual chemical species in a sample, which leads to distinguish that, the chemical species is the specific form of an element (i.e., isotopic composition, electronic or oxidation state, and/or complex or molecular structure); and speciation of an element is the distribution of an element amongst defined chemical species in a system"* (Templeton et al., 2000). Speciation is recognized as a major analytical field in several research fields allowing the understanding of the processes related to toxicity, and the reactivity of trace elements or biological systems, in which metals are involved; so, the most important for speciation studies is the separation and/or species identifcation (Grotti et al., 2014; Jakubowski et al., 2014).

2.2.1. Sample preparation

The choice of a sample preparation procedure, is very important for the speciation analysis due to the need of species preservation. For liquid samples, the procedure is less time-consuming than in the case of solid samples, because the stage is much simpler and in the majority of cases a sample requires only dilution and filtration (Marcinkowska and Barałkiewicz, 2016). In the analysis of plant fluids, the ideal is to carry out the speciation analysis without sample preparation which will favour xylem, phloem, or root exudates (AlChoubassi et al., 2018).

The solid sample preparation procedure by chromatography analysis requires, for solid samples, converting them into a liquid form. The difficulty lies in the necessity to use chemically mild conditions that do not provoke inter-conversion of analyzed species. The choice of the extraction procedures is fundamental, the extractant reagents in multi elemental speciation procedures more common are: water, different mixtures of water/methanol, orthophosphoric acid solutions, and enzymes (Marcinkowska and Barałkiewicz, 2016). In the case of plant tissues and roots, these can be frozen in liquid N_2, or dry to 35-50°C (Thamkaew et al., 2020), then homogenizing in a ball mill or in a mortar, centrifuged, and filtered using a 0.22-mm filter; also, is recommendable several sample preparations tested to see if consistent speciation analysis results are obtained (AlChoubassi et al., 2018).

2.2.2. Liquid chromatography separation

The role of liquid chromatography (LC) is the separation of the compounds of a sample into a string of bands during their migration along a porous bed that is percolated with a suitable solution (eluent) (Abia et al., 2010). The interaction with the liquid mobile phase causes components of a sample to move at different rates through the stationary phase and to separate from one another (Sgariglia et al., 2010). Due to the multiple interaction mechanisms between the mobile and stationary phase, LC is suitable for study a broadrange of analytes species (Zhou et al., 2019).

Liquid chromatography is an excellent separation technique due to the large choice of mobile and stationary phases used in the separation that can be modified depending on the characteistics of analytes and the sample matrix (Kroukamp et al., 2016). The different chromatographic techniques can be adapted for a particular need and can be used for the same analysis, so, choice of the hyphenated technique depends primarily on the research objective (Szpunar, 2000). The chromatographic parameters to be optimized during the development of a chromatographic method, include the type of stationary phase, the possible use and proportion of organic solvent, the nature and the concentration of salts, the pH of the mobile phase and its temperature. The applied flow-rate can be changed for decreasing run time, with the observed the pressure as the limiting factor; but this parameter has a secondary impact on HPLC separations and can be less considered. Liquid chromatography separates chemical species based on their size, hydrophobicity, charge etc. (Kroukamp et al., 2016). The liquid chromatographic techniques used in this project, namely as HILIC and SEC/UPLC SEC are discussed below.

2.2.2.1. Hydrophilic Interaction Liquid Chromatography (HILIC)

HILIC is a chromatographic technique based on the interaction between the analyte and a hydrophilic stationary phase, characterized by water which acts as a strong eluent; HILIC allows for the separation of polar analytes with no ion-pairing agent using an aqueous-organic mobile phase on polar stationary phases (Easter et al., 2010). The HILIC mobile phase uses water-miscible polar organic solvents such as methanol or acetonitrile with a small amount of water, which is similar to reversed-phase chromatography (RP-LC). **Figure 12,** describes the separation mechanism in HILIC that consist of the differential distribution of solute molecules of the analyte injected between the organic mobile phase and a water strong layer adsorbed into the hydrophilic stationary phase (Buszewski and Noga, 2012). The mobile phases used in HILIC contain from 5 to 40% water or buffer; the elution depends on the percentage of the aqueous buffer in the organic solvent. At the beginning of analysis, at high concentration of organic solvent the analytes are retained on the stationary phase, when a gradient is

applied by increasing the concentration of aqueous buffer the elution of the compounds occurs. In speciation analysis of metal complexes, the addition of organic solvent to the eluent (as the sample) can change metal speciation because of the lower solubility of some compounds potentially associated to metals. In particular, an addition of organic solvents to aqueous samples leads to the precipitation of most of the proteins (>10 kDa). Therefore, the use of HILIC is limited to studies of small (<10 kDa) metal complexes.

The solvent strengths in HILIC is as follows: acetone < isopropanol ~ propanol < acetonitrile < ethanol < dioxane < DMF ~ methanol < water. Also, to control the mobile phase pH and ion strength are used ionic additives, such as ammonium acetate and ammonium formate (Buszewski and Noga, 2012; Flis, 2013).

HILIC employs the similar polar stationary phases that normal phase chromatography (NP-LC); they are divided into different groups such as unbounded bare silica gels and bonded phases, and these ones are classified in neutral, charged, and zwitterionic phases according to functional groups (such as aminopropyl, cyanopropyl, diol) present on the surface and their charged state (Wang et al., 2019).

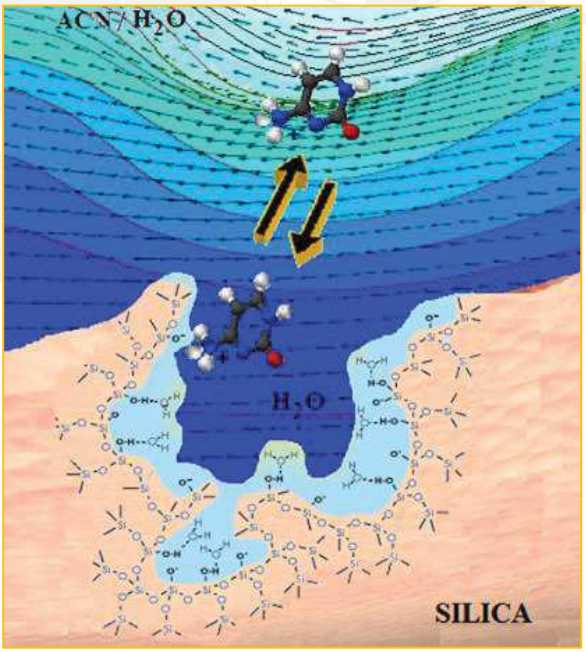

Figure 12. Separation mechanism in a HILIC system (Buszewski and Noga, 2012)

Polar chemically-bonded phases developed for specific applications by derivatization of the support surface (silica or polymer) with polar functional groups are classified in neutral, charged and zwitterionic phases on the basis of the charged state of the groups:

- Neutral stationary phases contain polar functional groups that are in neutral form in the range of pH 3–8, which retain analytes according to hydrophilic interactions. The HILIC stationary phases belonging to this category include amide, aspartamide, diol, cross-linked diol, cyano and cyclodextrin groups. These columns are used for the separation of oligosaccharides, peptides, proteins, and oligonucleotides.
- Amino phases contain an aminopropyl ligand with a primary amino group positively charged showing high affinity for anionic acid compounds.
- Zwitterionic HILIC stationary phases are considered as the HILIC all-purpose phases. Zwitterionic ligands comprise a permanent positive charged group and a permanent negative charged group. These phases can retain in relation to hydrophobicity but also in relation to ion-exchange properties and can be employed for the separation of neutral, acid and basic analytes, as well as the separation of inorganic ions.

HILIC is popular in looking for metabolites, the applications of HILIC are used to separate organic and some inorganic molecules, and some biomolecules through differences in polarity, e.g. nucleosides, nucleotides/oligonucleotides, amino acids, peptides and proteins, glycosides, saccharides, oligosaccharides, hydrophilic drugs, carbohydrates, and alkaloids. HILIC does not require ion-pair reagents; and is suitable for coupling to mass spectrometry (MS), especially in the electrospray ionization (ESI) mode (Buszewski and Noga, 2012).

2.2.2.2. Size-exclusion chromatography

Size Exclusion Chromatography (SEC) separates molecules according to their size depending on their hydrodynamic volume when a sample solution flows through a packed bed of porous packing (Kostanski et al., 2004; Lubomirsky et al., 2021); the stationary phase acts as a sieve for the molecules - it is a network of pores where molecules larger than the pore sizes are excluded, thus eluting rapidly, while that the small molecules will have more pathway options and will take longer to elute (Ponce De León et al., 2002). The differential pore permeation leads to size separation (Kostanski et al., 2004), provoking the elution at different times, achieving the fractionation (**Figure 13**). The retention time resulting is not in the function of the chemical interactions, so the mobile phase composition has a less critical role; the mobile phase just retains the conformational structure of the molecule that is similar to its native form (Ponce De León et al., 2002). The usual mobile phases in SEC are buffers with neutral

pH, the most common ones are ammonium acetate, sodium borohydride, Tris-HCl buffers, and Tris buffer with addition of NaCl (Kroukamp et al., 2016). SEC allow a calibrated according to molecular mass, therefore, allows determining molecular masses of unknown samples according to their retention time (Ponce De León et al., 2002). SEC uses two types of stationary phases: polymeric gels or modified silica particles (Flis, 2013).

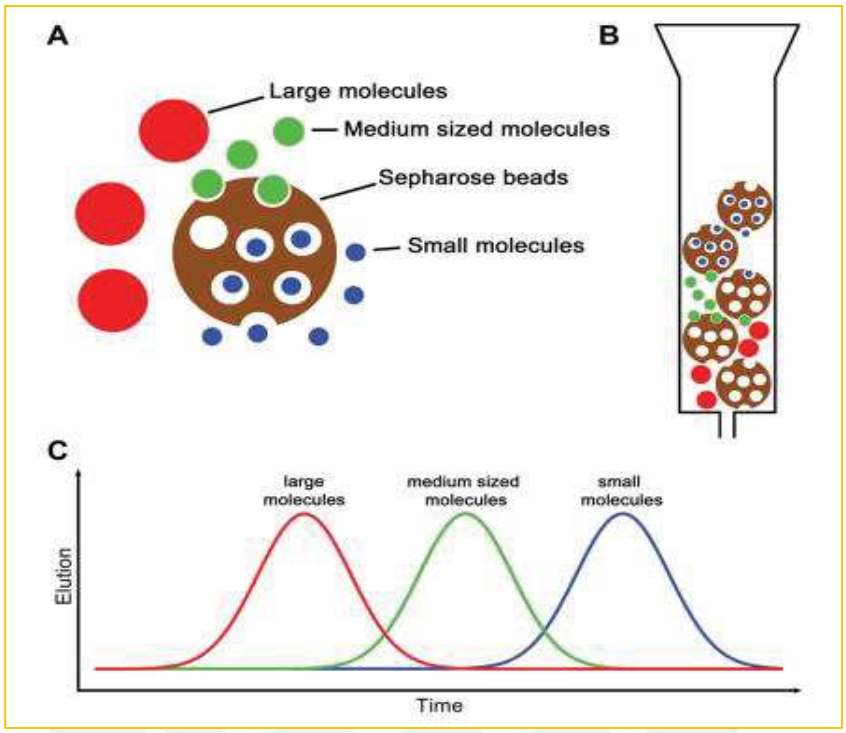

Figure 13. Size exclusion chromatography principle, A) Column bed, B) Schematic of the column, C) Time-dependent elution (Ludwig et al., 2019)

The separation by SEC is gentle and does not usually provoke high element species losses, or alterations on the column (Kroukamp et al., 2016). However, on-column dissotiation of weak metal coordination complexes can ocurr (Szpunar et al., 1999), SEC has become an important tool in speciation analysis of biological samples due to its suitability with ICP MS and has been extensively used for studies of metal complexes in samples of plant origin including lead speciation in wine (AlChoubassi et al., 2018; Szpunar et al., 1998), metal-carbohydrate complexes in fruit and vegetable (Szpunar et al., 1999), nickel speciation in *Sebertia acuminata* (Schaumlöffel et al., 2003) and metal-complexes in cocoa (Mounicou et al., 2002). However, due to the poor separation efficiency of classical SEC columns, this chromatographic technique has been considered unable to provide speciation data and is used solely for the estimation of the MW of the species present (Alchoubassi et al., 2021).

The recent introduction of novel SEC stationay phass, having the solvent stability and mechanical strength which allow their use in Ultra-High Perfomance Liquid Chromatography (UHPLC) mode, has provided significant improvements in separation efficiency and 3-4-times shortening of the analysis time (Perez-Moral et al., 2018; Uliyanchenko et al., 2011).

UPLC technology with SEC allows separations using sub-2μm particles at very high pressures (more than 40 MPa) (Perez-Moral et al., 2018), for this reason, it is known as "very high-pressure liquid chromatography" (Uliyanchenko et al., 2011). The ultra-high pressure limits allow the use of columns packed (with an internal diameter of 3 mm or less) to separate smaller particles, leading to lower theoretical plate heights at higher linear velocities, resulting in more efficient and faster separations. UHPLC may be successfully applied for the separations of small molecules and polymers (biopolymers) (Perez-Moral et al., 2018; Uliyanchenko et al., 2011). The UHPLC columns present on the market are packed with porous silica-based materials with different surface chemistries (pore sizes from 70 to 300 Å). One of the issues of the UHPLC is the generation of the heat, leading to temperature gradients across the column, which can increase the chromatographic band broadening and may jeopardize the column efficiency, requiring an increase in use of narrow-bore columns (Uliyanchenko et al., 2011).

2.2.3. HPLC-ICP MS for element selective quantitative information

High-Performance Liquid Chromatography (HPLC) coupled to an inductively coupled plasma mass spectrometry (ICP-MS) is the most accepted hyphenated technique in multi-elemental speciation analysis of environmental and biological samples (Ponce De León et al., 2002).

The versatility of the ICP-MS as a detector for HPLC enhances optimal detection conditions for analysis of almost 40 elements simultaneously, it also offers very low detection limits, excellent precision, and accuracy, as well as a wide linear dynamic range. On the other hand, the use of the chromatographic module allows separation of analytes species, differentiation them from matrix components, and considerable reduction of interfering polyatomic ionswhich can be further eliminated by the use dynamic/collision cells (Marcinkowska and Barałkiewicz, 2016). Also, ICP-MS by allowing the detection of HPLC signals in many cases down to 0.1 ng ml^{-1} of an element in the injected solution, makes it a unique analytical method for speciation analysis of endogenous elements and external tracers in a single experiment (Szpunar, 2000).

HPLC-ICPMS requires liquid samples, thus the solid samples should undergo an extraction step before the analysis. Coupling to HPLC allows the identification of individual metallic species on the basis of their retention times (Kroukamp et al., 2016). The flow rates applied in HPLC (mobile phase) separations and the liquid flow rates required for the nebulization are usually compatible, so, the

chromatographic column effluent which can be directly introduced to an ICP mss spectrometer (**Figure 14**).

The mobile phases are often prepared with organic solvents, such as methanol or acetonitrile (Caruso and Montes-Bayon, 2003) and their introduction into ICP MS negatively affects the plasma stability provoking the decrease signal intensity; also, the organic solvent present in the mobile phase may cause deposition of carbon on the torch and cones. Thus, the ICP MS instruments should be equipped with a desolvation system, a cooled spray chamber, platinum cones and work with an addition of oxygen to the plasma gas and increased RF power (Flis, 2013). Normal- flow nebulizers and micro-nebulizers have chromatographic flows from 0.1 mL min^{-1} to 1.5 mL min^{-1}.

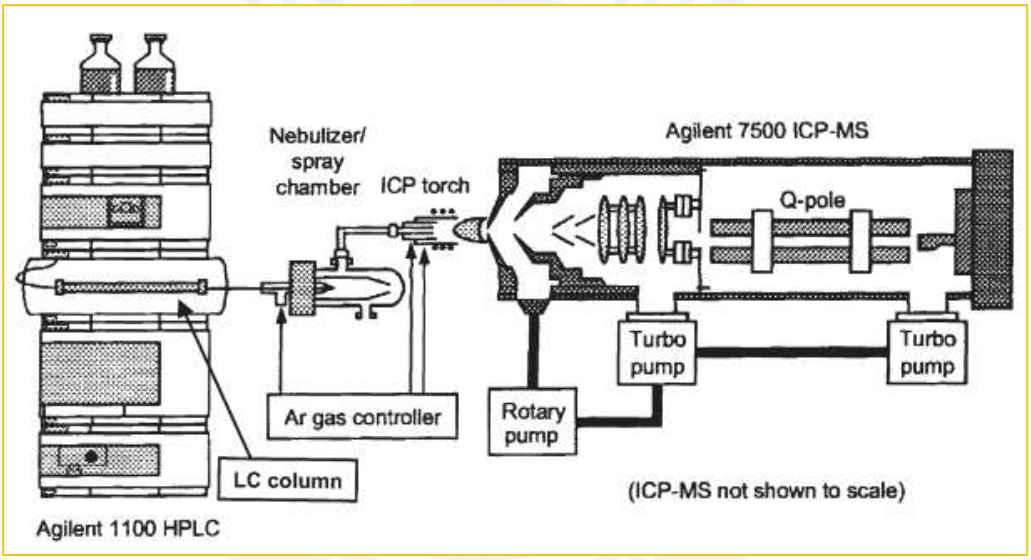

Figure 14. Schematic diagram of a HPLC/ICP-MS (Caruso and Montes-Bayon, 2003)

The optimization of the HPLC/ICP-MS should ensure (i) retention of each analyte on the chromatographic column and its elution in a reasonable analysis time (ii) complete separation and symmetrical of analytical signals; (iii) stability of the different species; (iv) elimination of interferences; and (v) low detection limits (Marcinkowska and Barałkiewicz, 2016). Quantitative speciation analysis by ICP MS assumes that only one species is present in a chromatograhic peak and requires the availability of calibration standards so is restricted to known species thus falling into the category of targeted analysis.

Marcinkowska and Barałkiewicz, (2016), describe that most speciation analysis with HPLC/ICP-MS is focused on two elements (70%), above 20% of them concern three elements, and only a few of them report to the speciation of four, five, or more elements in one analytical run (**Figure 15**) Also, the literature shows that arsenic and selenium are the elements most studied (As^{III}, As^{V}, MMA^{V} and DMA^{V} for arsenic ; and Se^{IV}, Se^{VI}, SeMet, SeCys and $(SeCys)_2$ for selenium).

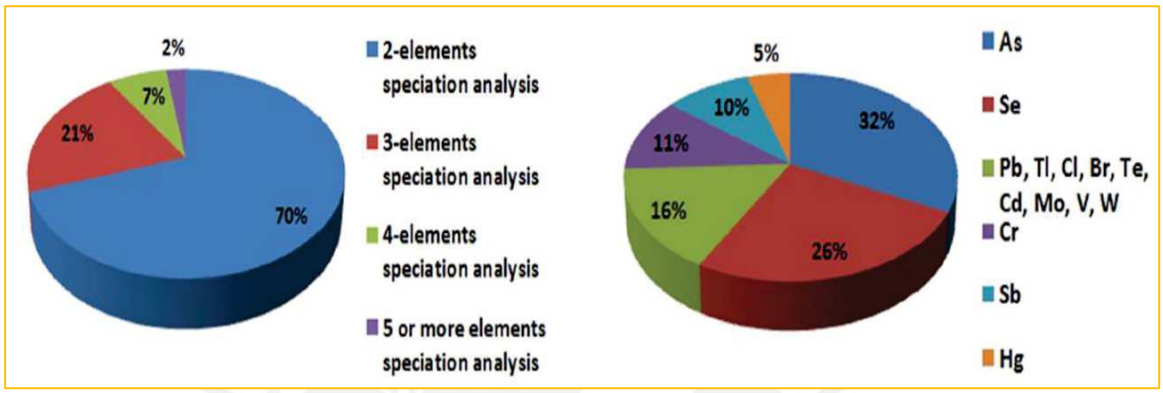

Figure 15. Number and elements determined in multielemental speciation procedures using HPLC/ICP-MS (Marcinkowska and Barałkiewicz, 2016)

Speciation analysis by HPLC-ICP MS does not give infomation on the identity of species (other than the comparison of the retention time with the standard) so in analysis of real samples containing unknown compounds, an additional step aim at the identification - meant as establishing the molecular stucture - is necessary.

2.2.4. HPLC-ESI MS for structure elucidation of elemental species

Electrospray Ionisation Mass Spectrometry (ESI-MS) technique is capable of analyzing labile species directly in a solution (Ray et al., 2004). In general, HPLC-ESI MS is capable of analyzing small and large molecules of various polarities in complex biological samples (Ho et al., 2003), ensuring that little information is lost on the original species. It is used for the identification of intact organic molecules, making it possible to induce and control their fragmentation through collisions with inert gas molecules (Kroukamp et al., 2016), leading to the structure elucidation (Rivaro et al., 2021).

Since the beginning of this century, electrospray ionization MS has been employed as a means of direct elemental speciation of organometallics and metal-containing species biological species. (Ray et al., 2004).

ESI uses electrical energy to transfer ions from the solution into the gaseous phase before their mass spectrometric analysis, so, the ionic species and neutral compounds (converted by protonation or cationisation, in ionic form in solution/or gas) present in liquid samples can be studied by ESI-MS (Ho et al., 2003). ESI involves three steps for the transfer of ionic species from solution into the gas phase, (i) dispersion of a spray of charged droplets, (ii) evaporation of the solvent, (iii) ion ejection from the highly charged droplets (Ho et al., 2003). Vaporization of solvents leads to coulombic explosions of the spray droplets, which release ions with multiple charge states z to the gas phase, ESI source is optimized to produce only ions with z = 1 (Forcisi et al., 2013). In the ESI source (**Figure 16**), a continuous stream of sample solution passes through one capillary tube (steel or quartz silica) to high voltage (e.g. 2.5 - 6.0 kV) in relation to the wall of the surrounding chamber; where a mist of highly charged droplets is generate with the same polarity as the capillary voltage, and onto the exit of the electrospray tip, the charged droplets transmit a gradient of pressure and potential toward the analyser of the mass spectrometer (Ho et al., 2003). ESI maintains an electric field of 1000V/cm (Forcisi et al., 2013).

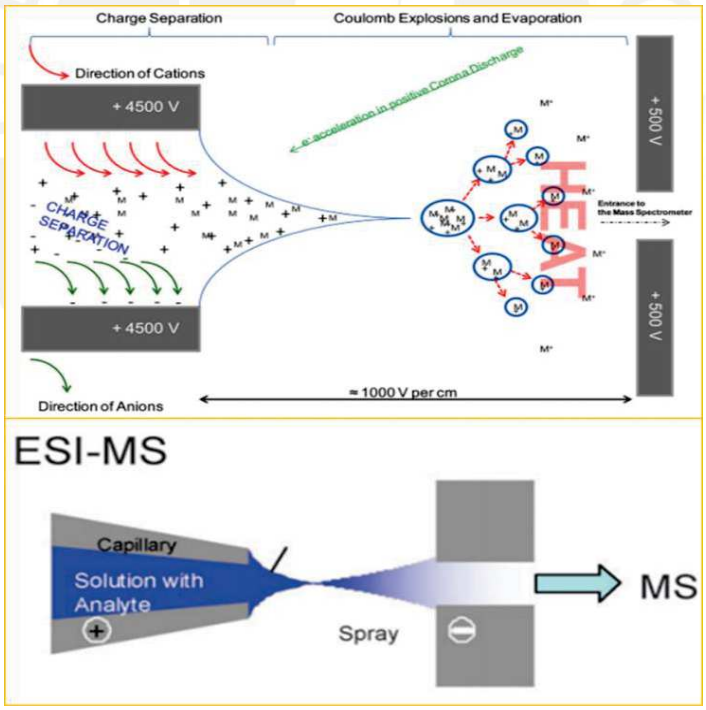

Figure 16. Principle of ESI-MS (Becker and Jakubowski, 2009; Forcisi et al., 2013)

Electrospray is the most efficient interface for injecting $[M+H]^+/[M-H]^-$ ions to mass analyzers with no or little ion fragmentation; in addition it also produces, $[M+Na]^+$ or $[M+K]^+$ ions. Cluster ions are easily generated in the gas phase, through non-covalent interactions between the neutral solvent and produced ions (Forcisi et al., 2013). Changes in pH resulting from the ESI process may modify metal-binding species and their mass spectra, likewise, several metals (as Cu, Ag, or Hg) can be

deposited directly on the ESI emitter tip by electrolytic reduction (Ray et al., 2004). ESI is a soft ionization method and has balanced ionization efficiency for various classes of chemical compounds (Forcisi et al., 2013).

ESI-MS allows the optimization of the detection conditions (e.g., positive and negative ionization mode) across a range of solvents and pH conditions. The ESI MS parameters to be optimized in order to obtain optimal detection conditions such as high sensitivity and signal stability are:

- position of the probe: to maximize the introduction of analytes into the analyzer
- capillary tension applied to Ionize the analytes: to maximize the generation of ions through the spray
- voltage applied to the different poles of ions optics: to focus the ions towards the analyzer
- temperature of transfer through capillary: to complete desolvation and help the transport of ions to the analyzer
- drying gas flow and auxiliary: to optimize desolvation (vaporization temperature can be used to facilitate desolvation) and to better focus the spray

In metal speciation analysis, ESI-MS is able to generate unique charged metal-ligand spectra, identified with relative abundance of isotopic spectra (isotopic patterns) corresponding to the metals isotopes natural abundance (**Figure 17**) (Tsednee et al., 2016).
Electrospray Ionisation Mass Spectrometry (ESI MS) is usually coupled with a high-performance liquid chromatography (HPLC) for molecular fractionation and simplification of the matrix which could othewise supress the ionization of analytes.

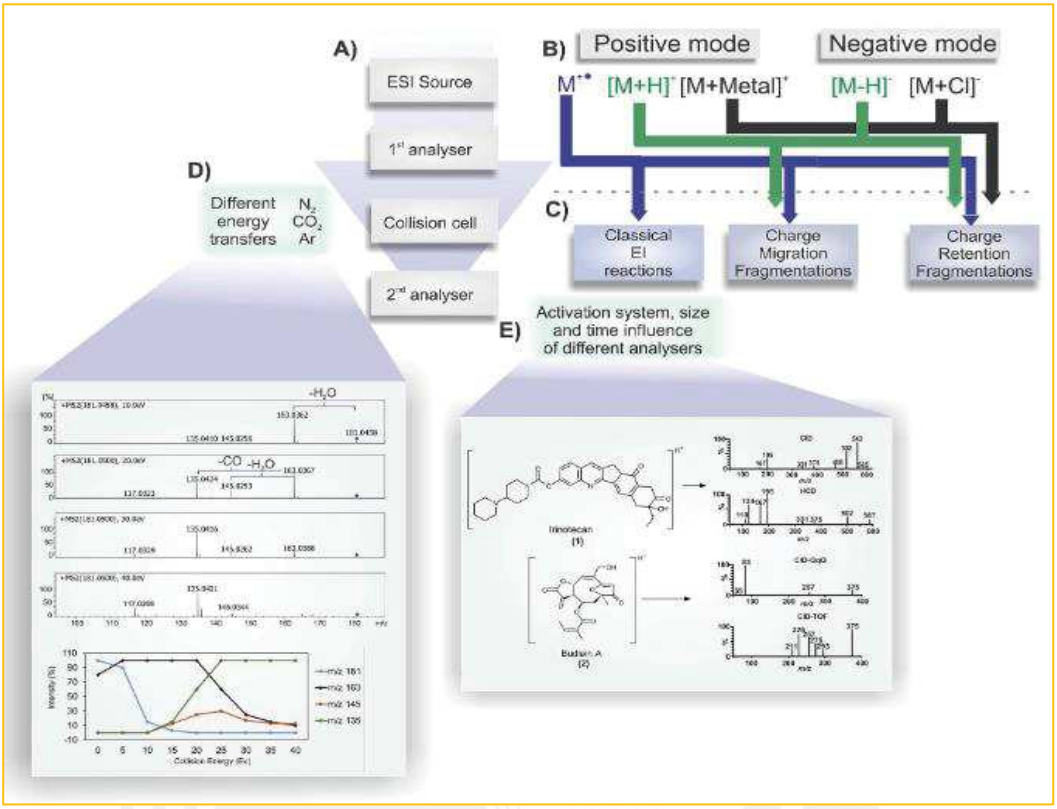

Figure 17. Fragmentation reactions using ESI MS/MS, a) representation MS structures; b) depending of the ion type, after passing for to the collision cell, charge migration fragmentations or charge retention fragmentation; c) Different collision cells; d) differe collision gases and different collision energies ; e)an example : fragmentation of 2,3 – dihydroxycinnamic acid in positive mode (Demarque et al., 2016)

The crutial role is played by a mass analyzer allowing the analyte ions of a particular mass-to charge ratio reach the detector. The mass analyzer is also responsible for filtering out all the non-analyte, interfering and matrix ions. Important parameters of the mass analyzers include: the range of masses, operating mode (continuous, pulsed), mass accuracy, analysis speed, ion permeation mode and resolution. The different mass analyzers include: quadrupole, time-of-flight (TOF), ion trap, magnetic sector, cyclotron ion resonance and Orbitrap.

The sensitivity of ESI MS depends on the analyte and its purity at the moment of its arrival at the detector, while for the ICP MS is largely not the case, thus, the comparison of both techniques is actually difficult (Bierla et al., 2018). ESI-MS is routinely used as a complementary detection method for species evaluation by HPLC/ICP-MS (Kroukamp et al., 2016). Therefore, for the simultaneous quantification and structural identification of the formed complexes, the combination of ICP-MS with ESI-MS can be deployed to one single HPLC system (AlChoubassi, 2019). The concept of the parallel

use of the elemental and molecular mass spectrometry in speciation analysis is schematially presented in **Figure 18.**

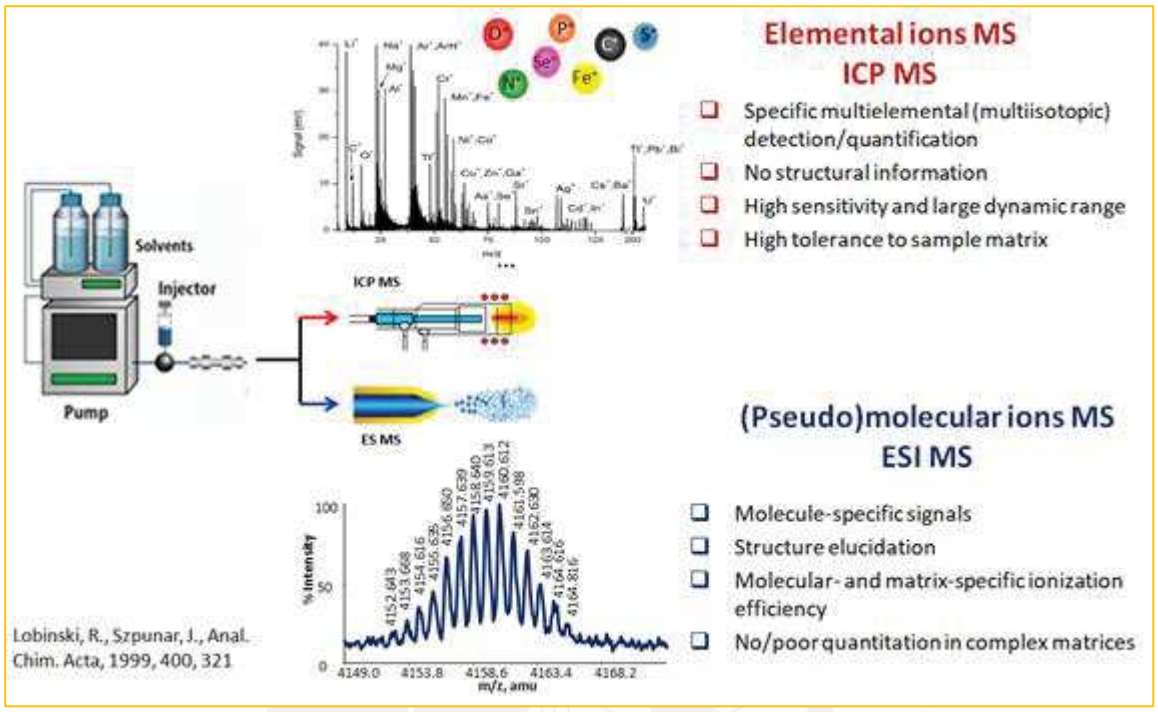

Figure 18. The concept of the parallel use of the elemental and molecular mass spectrometry in speciation analysis

2.3. Direct analysis by X-ray spectroscopy

X-ray Absorption Spectroscopy (XAS) technique is used for measuring the X-ray absorption coefficient, exciting a core-level electron into empty orbitals, bands, or out of the atom, allowing to obtain information about the chemical state and local structure analyzing the energy dependence of the absorption coefficient (Ninomiya et al., 2020). In XAS when a sample is irradiated, one part of the incident radiation is absorbed and the other part of it is transmitted, this relationship is expressed as absorption coefficient μ(E) (Subirana Manzanares, 2018). The synchrotrons are using as sources of intense X rays ; likewise, XAS shows fine structures only for one absorber element at a time (Feiters and Meyer-klaucke, 2020). The XAS spectrum contains three parts (**Figure 19**) (i) Edge, is the region of the white line, due to the incident energy, is larger than the binding energy of the electron of a chosen element, the electron is excited giving place to increase in absorption; (ii) Pre-edge, before the edge, is a region which the incident energy is not enough to excite the desired photo-electron; (iii) Post-edge, after the edge, is a region where oscillations are observed because of the scattering interactions of neighboring atoms (Subirana Manzanares, 2018). Both the absorption edge as well as the fine

structure after the edge are related by physical processes with the chemical environment of the element (Feiters and Meyer-klaucke, 2020).

X-ray absorption near-edge structure (XANES), provides detailed information about the oxidation state and geometry of the elements involved (Feiters and Meyer-klaucke, 2020), so, the absorption edge energy increases with an increase in the oxidation state, is not analyzed quantitatively (Yano and Yachandra, 2009). The extended X-ray absorption structure (EXAFS), after the edge, a region where the absorption of an X-ray provides the sufficient energy for that absorbing atom to release the electron (Yano and Yachandra, 2009); also, provide information of the surrounding ligands, type, and distance (Feiters and Meyer-klaucke, 2020).

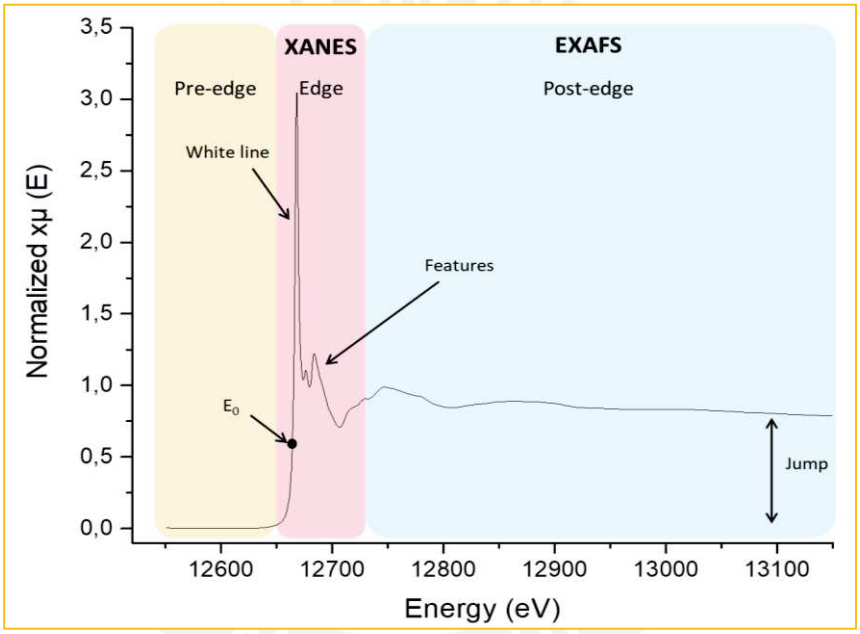

Figure 19. Schematic representation of a XAS spectrum (Subirana Manzanares, 2018)

XAS is used in the assessment of metal-uptake, tolerance and toxicity in plants, as well as, in the metal or metalloid speciation data for environmental samples providing information of the identification of the ligand in terms of oxidation state and symmetry about the target analyte (Kroukamp et al., 2016). XAS was considered for a long time as a direct technique in the elimination of the risk of changes during sample preparation and irradiation in the speciation; however, and it was discovered that grinding and analysis of pellets provoke oxidation (AlChoubassi et al., 2018). Likewise, It presented poor detection limits, problems in the integrity of the maintenance of the species, limitations quantifiable in respect to the number and variety of species, reducing its applicability; also an additional challenge is limited availability of certified reference materials (CRMs) for the analytes and species of interest (Kroukamp et al., 2016).

REFERENCES

Abia, J.A., Putnam, J., Mriziq, K., Guiochon, G.A., 2010. Design and implementation of an array of micro-electrochemical detectors for two-dimensional liquid chromatography-Proof of principle. J. Chromatogr. A 1217, 1695–1700. https://doi.org/10.1016/j.chroma.2010.01.021

Alan, M., Kara, D., 2019. Comparison of a new sequential extraction method and the BCR sequential extraction method for mobility assessment of elements around boron mines in Turkey. Talanta 194, 189–198.

AlChoubassi, G., 2019. The development of new qualitative and quantitative metal speciation approaches for low molecular weight metals complexes in plants. Université de Pau et des Pays de l'Adour.

AlChoubassi, G., Aszyk, J., Pisarek, P., Bierla, K., Ouerdane, L., Szpunar, J., Lobinski, R., 2018. Advances in mass spectrometry for iron speciation in plants. TrAC - Trends Anal. Chem. 104, 77–86. https://doi.org/10.1016/j.trac.2017.11.006

Alchoubassi, G., Kińska, K., Bierla, K., Lobinski, R., Szpunar, J., 2021. Speciation of essential nutrient trace elements in coconut water. Food Chem. 339. https://doi.org/10.1016/j.foodchem.2020.127680

Alford, É.R., Pilon-Smits, E.A.H., Paschke, M.W., 2010. Metallophytes-a view from the rhizosphere. Plant Soil 337, 33–50. https://doi.org/10.1007/s11104-010-0482-3

Arenas-Lago, D., Andrade, M.L., Lago-Vila, M., Rodríguez-Seijo, A., Vega, F.A., 2014. Sequential extraction of heavy metals in soils from a copper mine: Distribution in geochemical fractions. Geoderma 230–231, 108–118.

Aron, A.S., Molina, O., 2019. Green innovation in natural resource industries: The case of local suppliers in the Peruvian mining industry. Extr. Ind. Soc. 1–13.

Artiola, J., Pepper, I.L., Brusseau, M.L., 2004. Environmental Monitoring and Characterization. Elsevier Science & Technology books.

Aznar-Sánchez, J.A., Velasco-Muñoz, J.F., Belmonte-Ureña, L.J., Manzano-Agugliaro, F., 2019. Innovation and technology for sustainable mining activity : A worldwide research assessment. J. Clean. Prod. 221, 38–54.

Bainton, N., Holcombe, S., 2018. A critical review of the social aspects of mine closure. Resour. Policy 59, 468–478. https://doi.org/10.1016/j.resourpol.2018.08.020

Baker, A.J.M., Ernst, W.H.O., Van der Ent, A., Malaisse, F., Ginocchio, R., 2010. Metallophytes: the unique biological resource, its ecology and conservational status in Europe, central Africa and Latin America, in: Batty, L.C., Hallberg, K.B. (Eds.), Ecology of Industrial Pollution. Cambridge University Press, Cambridge, pp. 7–40. https://doi.org/10.1017/cbo9780511805561.003

Becerril, J.M., Barrutia, O., García Plazaola, J.I., Hérnandez, A., Olano, J.M., Garbisu, C., 2007. Especies nativas de suelos contaminados por metales: aspectos ecofisiológicos y su uso en fitorremediación. Ecosistemas Rev. científica y técnica Ecol. y medio Ambient. 16, 50–55.

Bech, J., Poschenrieder, C., Llugany, M., Barceló, J., Tume, P., Tobias, F.J., Barranzuela, J.L., Vásquez, E.R., 1997. Arsenic and heavy metal contamination of soil and vegetation around a copper mine in Northern Peru. Sci. Total Environ. 203, 83–91. https://doi.org/10.1016/S0048-9697(97)00136-

Bech, J., Roca, N., Tume, P., 2017. Hazardous Element Accumulation in Soils and Native Plants in Areas Affected by Mining Activities in South America, in: Assessment, Restoration and Reclamation of Mining Influenced Soils. Elsevier Inc., pp. 419–461.

Bech, J., Roca, N., Tume, P., Ramos-Miras, J., Gil, C., Boluda, R., 2016. Screening for new accumulator plants in potential hazards elements polluted soil surrounding Peruvian mine tailings. Catena 136, 66–73.

Becker, J.S., Jakubowski, N., 2009. The synergy of elemental and biomolecular mass spectrometry: New analytical strategies in life sciences. Chem. Soc. Rev. 38, 1969–1983. https://doi.org/10.1039/b618635c

Bierla, K., Godin, S., Lobinski, R., Szpunar, J., 2018. Advances in electrospray mass spectrometry for the selenium speciation: Focus on Se-rich yeast. TrAC - Trends Anal. Chem. 104, 87–94. https://doi.org/10.1016/j.trac.2017.10.008

Bini, C., Maleci, L., Wahsha, M., 2017. Mine Waste: Assessment of Environmental Contamination and Restoration, in: Assessment, Restoration and Reclamation of Mining Influenced Soils. Elsevier Inc., pp. 89–134. https://doi.org/10.1016/B978-0-12-809588-1.00004-9

Bonchin, S.L., Zoorob, G.K., Caruso, J.A., 2017. Atomic emission spectrometry | Methods and instrumentation, in: Encyclopedia of Analytical Science. pp. 177–186. https://doi.org/10.1016/B978-0-08-101983-2.00101-8

Bouzekri, S., El Hachimi, M.L., Touach, N., El Fadili, H., El Mahi, M., Lotfi, E.M., 2019. The study of metal (As, Cd, Pb, Zn and Cu) contamination in superficial stream sediments around of Zaida mine (High Moulouya-Morocco). J. African Earth Sci. 154, 49–58.

Bowles, J.M., 2004. Guide to plant collection adn identification, UWO Herbar. ed.

Brain, K.A., 2017. The impacts of mining on livelihoods in the Andes: A critical overview. Extr. Ind. Soc. 4, 410–418. https://doi.org/10.1016/j.exis.2017.03.001

Bulska, E., Ruszczyńska, A., 2017. Analytical techniques for trace element determination. Phys. Sci. Rev. 2, 1–14. https://doi.org/10.1515/psr-2017-8002

Buszewski, B., Noga, S., 2012. Hydrophilic interaction liquid chromatography (HILIC)—a powerful separation technique. Anal. Bioanal. Chem. 402, 231–247.

Callahan, D.L., Baker, A.J.M., Kolev, S.D., Wedd, A.G., 2006. Metal ion ligands in hyperaccumulating plants. J. Biol. Inorg. Chem. 11, 2–12. https://doi.org/10.1007/s00775-005-0056-7

Camizuli, E., Rossi, M., Gasquet, D., 2020. Trace metals dispersion from 1000 years of mining activity in the northern French Alps. Extr. Ind. Soc.

Candeias, C., Ávila, P., Coelho, P., Teixeira, J.P., 2018. Mining Activities : Health Impacts, 2nd ed, Encyclopedia of Environmental Health, 2nd Edition. Elsevier Inc. https://doi.org/10.1016/B978-0-12-409548-9.11056-5

Caruso, J.A., Montes-Bayon, M., 2003. Elemental speciation studies - New directions for trace metal analysis. Ecotoxicol. Environ. Saf. 56, 148–163. https://doi.org/10.1016/S0147-6513(03)00058-7

Chang Kee, J., Gonzales, M.J., Ponce, O., Ramírez, L., León, V., Torres, A., Corpus, M., Loayza-muro, R., 2018. Accumulation of heavy metals in native Andean plants: potential tools for soil

phytoremediation in Ancash (Peru). Environ. Sci. Pollut. Res.

Chappuis, M., 2019. Remediación y activación de pasivos ambientales mineros (PAM) en el Perú. Medio Ambient. y Desarro. N° 168, Com. Económica para América Lat. y el Caribe.

Claveria, R.J.R., Perez, T.R., Perez, R.E.C., Algo, J.L.C., Robles, P.Q., 2019. The identification of indigenous Cu and As metallophytes in the Lepanto Cu-Au Mine, Luzon, Philippines. Environ. Monit. Assess. 191.

Comisión Económica para América Latina y el Caribe (CEPAL), 2018. Perspectivas del comercio internacional de América Latina y el Caribe. Santiago de Chile. https://doi.org/10.18356/486d22b8-es

Cope, J.S., Corney, D., Clark, J.Y., Remagnino, P., Wilkin, P., 2012. Plant species identification using digital morphometrics : A review. Expert Syst. Appl. 39, 7562–7573. https://doi.org/10.1016/j.eswa.2012.01.073

Córdova, S., Neaman, A., González, I., Ginocchio, R., Fine, P., 2011. The effect of lime and compost amendments on the potential for the revegetation of metal-polluted, acidic soils. Geoderma 166, 135–144. https://doi.org/10.1016/j.geoderma.2011.07.022

Corzo, A., Gamboa, N., 2018. Environmental impact of mining liabilities in water resources of Parac micro-watershed, San Mateo Huanchor district, Peru. Environ. Dev. Sustain. 20, 939–961.

Corzo Remigio, A., Chaney, R.L., Baker, A.J.M., Edraki, M., Erskine, P.D., Echevarria, G., van der Ent, A., 2020. Phytoextraction of high value elements and contaminants from mining and mineral wastes: opportunities and limitations. Plant Soil 449, 11–37. https://doi.org/10.1007/s11104-020-04487-3

Cui, J., Zhao, Y., Chan, T., Zhang, L., Tsang, D.C.W., Li, X., 2020. Spatial distribution and molecular speciation of copper in indigenous plants from contaminated mine sites: Implication for phytostabilization. J. Hazard. Mater. 381, 121208.

Cundy, A.B., Bardos, R.P., Puschenreiter, M., Mench, M., Bert, V., Friesl-Hanl, W., Müller, I., Li, X.N., Weyens, N., Witters, N., Vangronsveld, J., 2016. Brownfields to green fields: Realising wider benefits from practical contaminant phytomanagement strategies. J. Environ. Manage. 184, 67–77. https://doi.org/10.1016/j.jenvman.2016.03.028

Dazy, M., Béraud, E., Cotelle, S., Grévilliot, F., Férard, J., Masfaraud, J., 2009. Changes in plant communities along soil pollution gradients : Responses of leaf antioxidant enzyme activities and phytochelatin contents. Chemosphere 77, 376–383. https://doi.org/10.1016/j.chemosphere.2009.07.021

Demarque, D.P., Crotti, A.E.M., Vessecchi, R., Lopes, J.L.C., Lopes, N.P., 2016. Fragmentation reactions using electrosprayionization mass spectrometry: an important toolfor the structural elucidation and characterizationof synthetic and natural products. R. Soc. Chem. 33, 432–455.

Deng, Y., Wu, X., Tian, Y., Zou, Z., Hou, X., Jiang, X., 2017. Sharing one ICP source for simultaneous elemental analysis by ICP-MS/OES: Some unique instrumental capabilities. Microchem. J. 132, 401–405. https://doi.org/10.1016/j.microc.2017.02.024

Dong, L., Tong, X., Li, X., Zhou, J., Wang, S., Liu, B., 2019. Some developments and new insights of environmental problems and deep mining strategy for cleaner production in mines. J. Chromatogr. A 210, 1562–1578.

Duodu, G.O., Goonetilleke, A., Ayoko, G.A., 2016. Comparison of Pollution Indices for the Assessment of Heavy Metal in Brisbane River. Environ. Pollut. 219, 1077–1091.

Durán Cuevas, P.A., 2010. Transferencia de metales de suelo a planta en áreas mineras: Ejemplos de los Andes peruanos y de la Cordillera Prelitoral Catalana.

Easter, R.N., Kröning, K.K., Caruso, J.A., Limbach, P.A., 2010. Separation and identification of oligonucleotides by hydrophilic interaction liquid chromatography (HILIC) - Inductively coupled plasma mass spectrometry (ICPMS). Analyst 135, 2560–2565. https://doi.org/10.1039/c0an00399a

El-Raouf, H.S.A., 2021. Taxonomic significance of leaves in family Aizoaceae. Saudi J. Biol. Sci. 28, 512–522.

Favas, P.J. de C., Martino, L.E., Prasad, M.N.V., 2018. Abandoned Mine Land Reclamation-Challenges and Opportunities (Holistic Approach), in: Bio-Geotechnologies for Mine Site Rehabilitation. Elsevier Inc., pp. 3–31. https://doi.org/10.1016/B978-0-12-812986-9.00001-4

Favas, P.J.C., Pratas, J., Varun, M., Souza, R.D., Paul, M.S., 2014. Phytoremediation of Soils Contaminated with Metals and Metalloids at Mining Areas : Potential of Native Flora, in: Environmental Risk Assessment of Soil Contamination. INTECH.

Fehl, C., Peters, D., Wisotzki, S., Wolff, J., 2019. Justice and Peace.Studien des Leibniz-Instituts Hessische Stiftung Friedens- und Konfliktforschung, in: Introduction: The Role of Justice in International Cooperation and Conflict. Springer VS, Wiesbaden. https://doi.org/https://doi.org/10.1007/978-3-658-25196-3_1

Feiters, M.C., Meyer-klaucke, W., 2020. X-ray absorption and emission spectroscopy in biology, in: Practical Approaches to Biological Inorganic Chemistry. Elsevier B.V., pp. 229–273.

Fernández-Sánchez, M.L., 2018. Optical Atomic Emission Spectrometry - Inductively Coupled Plasma, in: Worsfold, P., Poole, C., Townshend, A., Miró, M. (Eds.), Encyclopedia of Analytical Science. Academic Press, pp. 169–176. https://doi.org/10.1016/B978-0-12-409547-2.14542-1

Fernández, S., Poschenrieder, C., Marcenò, C., Gallego, J.R., Jiménez-Gámez, D., Bueno, A., Afif, E., 2017. Phytoremediation capability of native plant species living on Pb-Zn and Hg-As mining wastes in the Cantabrian range, north of Spain. J. Geochemical Explor. 174, 10–20.

Flis, P.M., 2013. Développement de méthodes analytiques pour une spéciation à grande échelle des composés métalliques dans les plantes. L'Université de Pau et des Pays de l'Adour.

Forcisi, S., Moritz, F., Kanawati, B., Tziotis, D., Lehmann, R., Schmitt-Kopplin, P., 2013. Liquid chromatography-mass spectrometry in metabolomics research: Mass analyzers in ultra high pressure liquid chromatography coupling. J. Chromatogr. A 1292, 51–65. https://doi.org/10.1016/j.chroma.2013.04.017

Förstner, U., 1999. Environmental impact of mining activities: Emphasis on mitigation and remedial measures. Springer-Verlag, Berlin Heidelberg, Berlin, Germany.

França Afonso, T., Faccio Demarco, C., Pieniz, S., Silveira Quadro, M., A.O. Camargo, F., Andreazza, R., 2020. Bioprospection of indigenous flora grown in copper mining tailing area for phytoremediation of metals. J. Environ. Manage. 256.

Gabarrón, M., Faz, A., Acosta, J.A., 2018. Use of multivariable and redundancy analysis to assess the behavior of metals and arsenic in urban soil and road dust affected by metallic mining as a base for risk assessment. J. Environ. Manage. 206, 192–201. https://doi.org/10.1016/j.jenvman.2017.10.034

Gautam, M., Agrawal, M., 2019. Identification of metal tolerant plant species for sustainable phytomanagement of abandoned red mud dumps. Appl. Geochemistry 104, 83–92.

https://doi.org/10.1016/j.apgeochem.2019.03.020

Ghazaryan, K., Movsesyan, H., Ghazaryan, N., Watts, B.A., 2019. Copper phytoremediation potential of wild plant species growing in the mine polluted areas of Armenia. Environ. Pollut. 249, 491–501.

Głosińska, G., Sobczyński, T., Boszke, L., Bierła, K., Siepak, J., 2005. Fractionation of some heavy metals in bottom sediments from the middle Odra River (Germany/Poland). Polish J. Environ. Stud. 14, 305–317.

Godoy, N. V., Galazzi, R.M., Chacón-Madrid, K., Arruda, M.A.Z., Mazali, I.O., 2021. Evaluating the total gold concentration in metallic nanoparticles with a high content of organic matter through microwave-assisted decomposition platform and plasma-based spectrometric techniques (ICP-MS and ICP OES). Talanta 224, 1–7. https://doi.org/10.1016/j.talanta.2020.121808

Gong, Y., Zhao, D., Wang, Q., 2018. An overview of field-scale studies on remediation of soil contaminated with heavy metals and metalloids: Technical progress over the last decade. Water Res. 147, 440–460. https://doi.org/10.1016/j.watres.2018.10.024

Grill, E., Winnacker, E.L., Zenk, M.H., 1987. Phytochelatins, a class of heavy-metal-binding peptides from plants, are functionally analogous to metallothioneins. Proc. Natl. Acad. Sci. U. S. A. 84, 439–443. https://doi.org/10.1073/pnas.84.2.439

Grotti, M., Terol, A., Todolí, J.L., 2014. Speciation analysis by small-bore HPLC coupled to ICP-MS. TrAC - Trends Anal. Chem. 61, 92–106. https://doi.org/10.1016/j.trac.2014.06.009

Guillen Quispe, Y.N., Hwan Hwang, S., Wang, Z., Sung Lim, S., 2017. Screening of Peruvian Medicinal Plants for Tyrosinase Inhibitory Properties : Identification of Tyrosinase Inhibitors in Hypericum laricifolium Juss. Molecules 22, 1–15. https://doi.org/10.3390/molecules22030402

Gupta, R.K., Abrol, I.P., Finkl, C.W., Kirkham, M.B., Camps Arbestain, M., Macías, F., Cheswort, W., 2008. Encyclopedia of Soil Science. Encyclopedia of Earth Sciences Series, Soil Science. Springer, Dordrecht. https://doi.org/10.1097/00010694-198003000-00015

Gustafsson, M.-T., 2018. Private Politics and Peasant Mobilization: Mining in Peru, Private Politics and Peasant Mobilization. Palgrave Macmillan. https://doi.org/10.1007/978-3-319-60756-6

Helaluddin, A., Khalid, R.S., Alaama, M., Abbas, S.A., 2016. Main Analytical Techniques Used for Elemental Analysis in Various Matrices. Trop. J. Pharm. Res. 15, 427–434. https://doi.org/10.4314/tjpr.v15i2.29

Helwege, A., 2015. Challenges with resolving mining conflicts in Latin America. Extr. Ind. Soc. 2, 73–84.

Hendrychová, M., Svobodova, K., Kabrna, M., 2020. Mine reclamation planning and management : Integrating natural habitats into post-mining land use. Resour. Policy 69.

Hirve, M., Jain, M., Rastogi, A., Kataria, S., 2020. Heavy metals, water deficit, and their interaction in plants: an overview, in: Plant Life Under Changing Environment. INC, pp. 175–206. https://doi.org/10.1016/b978-0-12-818204-8.00009-6

Ho, C., Lam, C., Chan, M., Cheung, R., Law, L., Lit, L., Ng, K., Suen, M., Tai, H., 2003. Electrospray Ionisation Mass Spectrometry: Principles and Clinical Applications. Clin. Biochem. Rev. 24, 3–12.

Hosseini, S.M., Rezazadeh, M., Salimi, A., Ghorbanli, M., 2018. Distribution of heavy metals and arsenic in soils and indigenous plants near an iron ore mine in northwest Iran. Acta Ecol. Sin. 38, 363–367.

Hou, X., Amais, R.S., Jones, B.T., Donati, G.L., 2016. Inductively coupled plasma optical emission

spectrometry. Encycl. Anal. Chem. 57–74. https://doi.org/10.1201/9781315118024-3

Iavazzo, P., Adamo, P., Boni, M., Hillier, S., Zampella, M., 2012. Mineralogy and chemical forms of lead and zinc in abandoned mine wastes and soils: An example from Morocco. J. Geochemical Explor. 113, 56–67. https://doi.org/10.1016/j.gexplo.2011.06.001

IUSS Working Group WRB, 2015. World Reference Base for Soil Resources 2014: International soil classification systems for naming soils and creating legends for soil maps, update 2015, World Soil Resources Reports No. 106. FAO, Rome.

Jakubowski, N., Horsky, M., Roos, P.H., Vanhaecked, F., Prohaska, T., 2014. Inductively Coupled Plasma Mass Spectrometry, in: Sector Field Mass Spectrometry for Elemental and Isotopic Analysis. Royal Society of Chemistry, pp. 208–318. https://doi.org/10.1016/B978-0-323-46140-5.00008-X

JI, Y., FENG, Y., WU, J., ZHU, T., BAI, Z., DUAN, C., 2008. Using geoaccumulation index to study source profiles of soil dust in China. J. Environ. Sci. 20, 571–578. https://doi.org/10.1016/S1001-0742(08)62096-3

Kabata-Pendias, A., 2011. Trace Elements in Soils and Plants, 4th Ed. ed. CRC Press Taylor & Francis Group, Boca Raton London New York.

Kabata-Pendias, A., Mukherjee, A.B., 2007. Part I. Biogeochemistry of the Human Environment, chapter I-5: Plants, in: Trace Elements from Soil to Human. Springer Berlin Heidelberg New York.

Kamari, A., Yusoff, S.N.M., Putra, W.P., Ishak, C.F., Hashim, N., Mohamed, A., Phillip, E., 2014. Metal uptake in water spinach grown on contaminated soil amended with chicken manure and coconut tree sawdust. Environ. Eng. Manag. J. 13, 2219–2228.

Kapusta, P., Sobczyk, Ł., 2015. Effects of heavy metal pollution from mining and smelting on enchytraeid communities under different land management and soil conditions. Sci. Total Environ. 536, 517–526.

Kaźmierczak, U., Strzałkowski, P., Lorenc, M.W., Szumska, E., Peréz Sánchez, A.A., Baker, K.A.C., 2019. Post-mining Remnants and Revitalization. Geoheritage 11, 2025–2044.

Klimaszewski, K., Pacholik, E., Snopek, A., 2016. Can we enhance amphibians' habitat restoration in the post-mining areas? Environ. Sci. Pollut. Res. 23, 16941–16945. https://doi.org/10.1007/s11356-015-5279-8

Kodirov, O., 2018. Assessment of environmental impact of tailing dumps in Chadak mining area, Uzbekistan. University of Granada.

Kostanski, L.K., Keller, D.M., Hamielec, A.E., 2004. Size-exclusion chromatography - A review of calibration methodologies. J. Biochem. Biophys. Methods 58, 159–186. https://doi.org/10.1016/j.jbbm.2003.10.001

Kroukamp, E.M., Wondimu, T., Forbes, P.B.C., 2016. Metal and metalloid speciation in plants: Overview, instrumentation, approaches and commonly assessed elements. TrAC - Trends Anal. Chem. 77, 87–99. https://doi.org/10.1016/j.trac.2015.10.007

Kumar, A., Chaturvedi, A.K., Surendran, U., Shabnam, A.A., Singh, A., Vinodakumar, S.N., Tamuly, B., Malyan, S.K., Khan, S.A., Cabral-Pinto, M.M.S., Raja, P., Yadav, K.K., 2021. Mechanistic overview of metal tolerance in edible plants: A physiological and molecular perspective, in: Handbook of Bioremediation. pp. 23–47. https://doi.org/10.1016/b978-0-12-819382-2.00003-x

Kushwaha, A., Hans, N., Kumar, S., Rani, R., 2018. A critical review on speciation , mobilization and toxicity of lead in soil- microbe-plant system and bioremediation strategies. Ecotoxicol. Environ.

Saf. 147, 1035–1045.

Kvist, L.P., Christensen, S.B., Rasmussen, H.B., Mejia, K., Gonzales, A., 2006. Identification and evaluation of Peruvian plants used to treat malaria and leishmaniasis. J. Ethnopharmacol. 106, 390–402.

Lago-Vila, M., Arenas-Lago, D., Rodríguez-Seijo, A., Andrade, M.L., Vega, F.A., 2019. Ability of Cytisus scoparius for phytoremediation of soils from a Pb/Zn mine: Assessment of metal bioavailability and bioaccumulation. J. Environ. Manage. 235, 152–160.

Lam, E.J., Cánovas, M., Gálvez, M.E., Montofré, Í.L., Keith, B.F., 2017. Evaluation of the phytoremediation potential of native plants growing on a copper mine tailing in northern Chile. J. Geochemical Explor. 182, 210–217.

Levresse, G., Lopez, G., Tritlla, J., López, E.C., Chavez, A.C., Salvador, E.M., Soler, A., Corbella, M., Sandoval, L.G.H., Corona-Esquivel, R., 2012. Phytoavailability of antimony and heavy metals in arid regions: The case of the Wadley Sb district (San Luis, Potosí, Mexico). Sci. Total Environ. 427–428, 115–125. https://doi.org/10.1016/j.scitotenv.2012.04.020

Li, F., Paola, A., Peñafiel, P., 2019. Stories of Resistance : Translating Nature , Indigeneity , and Place in Mining Activism, in: Vindal Ødegaard C., R.A.J. (Ed.), Indigenous Life Projects and Extractivism. Palgrave Macmillan, Cham, pp. 219–243. https://doi.org/10.1007/978-3-319-93435-8_9

Li, Z., Deblon, J., Zu, Y., Colinet, G., Li, B., He, Y., 2019. Geochemical baseline values determination and evaluation of heavy metal contamination in soils of lanping mining valley (Yunnan province, China). Int. J. Environ. Res. Public Health 16, 1–18. https://doi.org/10.3390/ijerph16234686

Limbeck, A., Bonta, M., Nischkauer, W., 2016. Improvements in the direct analysis of advanced materials using ICP-based measurement techniques. J. Anal. At. Spectrom. 32, 212–232. https://doi.org/10.1039/c6ja00335d

Liu, G., Shi, Y., Guo, G., Zhao, L., Niu, J., Zhang, C., 2020. Soil pollution characteristics and systemic environmental risk assessment of a large-scale arsenic slag contaminated site. J. Clean. Prod. 251. https://doi.org/10.1016/j.jclepro.2019.119721

Liu, L., Li, W., Song, W., Guo, M., 2018. Remediation techniques for heavy metal-contaminated soils: Principles and applicability. Sci. Total Environ. 633, 206–219. https://doi.org/10.1016/j.scitotenv.2018.03.161

Łobiński, R., Adams, F.C., 1997. Speciation analysis by gas chromatography with plasma source spectrometric detection. Spectrochim. Acta Part B 52, 1865–1903.

Łobiński, R., Szpunar, J., 1999. Biochemical speciation analysis by hyphenated techniques. Anal. Chim. Acta 400, 321–332.

Lubomirsky, E., Khodabandeh, A., Preis, J., Susewind, M., Hofe, T., Hilder, E.F., Arrua, R.D., 2021. Polymeric stationary phases for size exclusion chromatography: A review. Anal. Chim. Acta 1151, 338244. https://doi.org/10.1016/j.aca.2021.338244

Ludwig, N., Hong, C.S., Ludwig, S., Azambuja, J.H., Sharma, P., Theodoraki, M.N., Whiteside, T.L., 2019. Isolation and Analysis of Tumor-Derived Exosomes. Curr. Protoc. Immunol. 127. https://doi.org/10.1002/cpim.91

Madejón, P., Domínguez, M.T., Madejón, E., Cabrera, F., Marañón, T., Murillo, J.M., 2018. Soil-plant relationships and contamination by trace elements : A review of twenty years of experimentation and monitoring after the Aznalcóllar (SW Spain) mine accident. Sci. Total Environ. 625, 50–63. https://doi.org/10.1016/j.scitotenv.2017.12.277

Makonnen, Y., Beauchemin, D., 2020. The inductively coupled plasma as a source for optical emission spectrometry and mass spectrometry, in: Sample Introduction Systems in ICPMS and ICPOES. Elsevier, pp. 1–55. https://doi.org/10.1016/b978-0-444-59482-2.00001-4

Manhart, A., Vogt, R., Priester, M., Dehoust, G., Auberger, A., Blepp, M., Dolega, P., Kämper, C., Giegrich, J., Schmidt, G., Kosmol, J., 2019. The environmental criticality of primary raw materials - A new methodology to assess global environmental hazard potentials of minerals and metals from mining. Miner. Econ. 32, 91–107. https://doi.org/10.1007/s13563-018-0164-9

Marcinkowska, M., Barałkiewicz, D., 2016. Multielemental speciation analysis by advanced hyphenated technique – HPLC/ICP-MS : A review. Talanta 161, 177–204.

May, T.W., Wiedmeyer, R.H., 1998. A Table of Polyatomic Interferences in ICP-MS. At. Spectrosc. 19, 150–155.

Mazurek, R., Kowalska, J.B., Gąsiorek, M., Zadrożny, P., Wieczorek, J., 2019. Pollution indices as comprehensive tools for evaluation of the accumulation and provenance of potentially toxic elements in soils in Ojców National Park. J. Geochemical Explor. 201, 13–30. https://doi.org/10.1016/j.gexplo.2019.03.001

Midhat, L., Ouazzani, N., Hejjaj, A., Ouhammou, A., Mandi, L., 2019. Accumulation of heavy metals in metallophytes from three mining sites (Southern Centre Morocco) and evaluation of their phytoremediation potential. Ecotoxicol. Environ. Saf. 169, 150–160.

Ministerio de Energía y Minas, 2020. Anuario Minero 2019. Oficina de Imagen Institucional y Comunicaciones, Lima, Peru.

Ministerio de Energía y Minas, 2019. Ministry Resolution N° 010-2019-MEM/DM. Actualizan Inventario Inicial de Pasivos Ambientales Mineros. D. Of. El Peru.

Ministerio de Energía y Minas, 2018. Anuario Minero 2018. Oficina de Imagen Institucional y Comunicaciones, Lima, Peru.

Ministerio de Energía y Minas, 2004. Law 28271. Ley que regula los pasivos ambientales de la actividad minera. D. Of. El Peru.

Moreno-Jiménez, E., Vázquez, S., Carpena-Ruiz, R.O., Esteban, E., Peñalosa, J.M., 2011. Using Mediterranean shrubs for the phytoremediation of a soil impacted by pyritic wastes in Southern Spain: A field experiment. J. Environ. Manage. 92, 1584–1590.

Morishige, Y., Kimura, A., 2008. Ionization interference in inductively coupled plasma-optical emission spectroscopy. SEI Tech. Rev. 106–111.

Mounicou, S., Szpunar, J., Lobinski, R., Andrey, D., Blake, C.J., 2002. Bioavailability of cadmium and lead in cocoa: Comparison of extraction procedures prior to size-exclusion fast-flow liquid chromatography with inductively coupled plasma mass spectrometric detection (SEC-ICP-MS). J. Anal. At. Spectrom. 17, 880–886. https://doi.org/10.1039/b201639g

Muller, G., 1969. Index of geo-accumulation in sediments of the Rhine River. GeoJournal 2, 108–118.

Nagajyoti, P.C., Lee, K.D., Sreekanth, T.V.M., 2010. Heavy metals, occurrence and toxicity for plants: a review. Environ. Chem. Lett. 8, 199–216.

Narukawa, T., Chiba, K., 2013. Oxygenation mechanism of ions in dynamic reaction cell ICP-MS. Anal. Sci. 29, 747–752. https://doi.org/10.2116/analsci.29.747

Ndubueze, E.U., 2018. Potential of Five Plant Species for Phytoremediation of Metal- PAH-Pesticide

Contaminated Soil. The University of Western Ontario.

Ninomiya, K., Kamitani, K., Tamenori, Y., Tsuruta, K., Takata, K., Sawada, H., Kinoshita, K., Nishibori, M., 2020. Analysis of the dynamic behavior and local structure of solid-solution carbon in age-hardened low-carbon steels by soft X-ray absorption spectroscopy. Materialia 14, 4–10. https://doi.org/10.1016/j.mtla.2020.100876

Nouri, M., Haddioui, A.E.M., 2016. Assessment of Metals Contamination and Ecological Risk in Ait Ammar Abandoned Iron Mine Soil , Moroco. Ekol. Bratislava 35, 32–49. https://doi.org/10.1515/eko-2016-0003

NSW EPA, 2016. Environment compliance. Report Polymetallic mines. Environment Protection Authority.

Oblasser, A., Chaparro Ávila, E., 2008. Estudio comparativo de la gestión de los pasivos ambientales mineros en Bolivia, Chile, Perú y Estados Unidos, Recursos Naturales e Infraestructura N°131.Comisión Económica para América Latina y el Caribe (CEPAL).

Osman, K.T., 2013. Soils: Principles, Properties and Management, 1st ed. Springer Netherlands.

Otamonga, J.P., Poté, J.W., 2020. Abandoned mines and artisanal and small-scale mining in Democratic Republic of the Congo (DRC): Survey and agenda for future research. J. Geochemical Explor. 208. https://doi.org/10.1016/j.gexplo.2019.106394

Oyuela Leguizamo, M.A., Fernández Gómez, W.D., Sarmiento, M.C.G., 2017. Native herbaceous plant species with potential use in phytoremediation of heavy metals, spotlight on wetlands — A review. Chemosphere 168, 1230–1247. https://doi.org/10.1016/j.chemosphere.2016.10.075

Patra, D.K., Pradhan, C., Patra, H.K., 2020. Toxic metal decontamination by phytoremediation approach: Concept, challenges, opportunities and future perspectives. Environ. Technol. Innov. 18. https://doi.org/10.1016/j.eti.2020.100672

Perez-Moral, N., Plankeele, J.-M., Domoney, C., Warren, F.J., 2018. Ultra-high performance liquid chromatography-size exclusion chromatography (UPLC-SEC) as an efficient tool for the rapid and highly informative characterisation of biopolymers. Carbohydr. Polym. 196, 422–426.

Pérez-Sirvent, C., Hernández-Pérez, C., Martínez-Sánchez, M.J., García-Lorenzo, M.L., Bech, J., 2015. Geochemical characterisation of surface waters, topsoils and efflorescences in a historic metal-mining area in Spain. J. Soils Sediments 16, 1238–1252. https://doi.org/10.1007/s11368-015-1141-3

Ponce De León, C.A., Montes-Bayón, M., Caruso, J.A., 2002. Elemental speciation by chromatographic separation with inductively coupled plasma mass spectrometry detection. J. Chromatogr. A 974, 1–21.

Ray, S.J., Andrade, F., Gamez, G., McClenathan, D., Rogers, D., Schilling, G., Wetzel, W., Hieftje, G.M., 2004. Plasma-source mass spectrometry for speciation analysis: State-of-the-art. J. Chromatogr. A 1050, 3–34. https://doi.org/10.1016/j.chroma.2004.07.107

Raza, A., Habib, M., Charagh, S., Kakavand, S.N., 2021. Genetic engineering of plants to tolerate toxic metals and metalloids, in: Handbook of Bioremediation. pp. 411–436.

Rehman, A.U., Nazir, S., Irshad, R., Tahir, K., ur Rehman, K., Islam, R.U., Wahab, Z., 2021. Toxicity of heavy metals in plants and animals and their uptake by magnetic iron oxide nanoparticles. J. Mol. Liq. 321. https://doi.org/10.1016/j.molliq.2020.114455

Rivaro, P., Ardini, F., Grotti, M., Vivado, D., Salis, A., Damonte, G., 2021. Detection of carbohydrates in

sea ice extracellular polymeric substances via solid-phase extraction and HPLC-ESI-MS/MS. Mar. Chem. 228, 1–9. https://doi.org/10.1016/j.marchem.2020.103911

Rizwan, M., Elshamy, M.M., Abdel-aziz, H.M.M., 2019. Assessment of trace element and macronutrient accumulation capacity of two native plant species in three different Egyptian mine areas for remediation of contaminated soils. Ecol. Indic. 106, 105463. https://doi.org/10.1016/j.ecolind.2019.105463

Rodríguez, C., Julca, D., 2020. Gestión del cierre de minas en el Perú: Estudio Técnico-legal sobre el alcance de la legislación peruana en el cierre de operaciones mineras. Comisión Económica para América Latina y el Caribe (CEPAL), Santiago de Chile.

Różański, S.Ł., Kwasowski, W., Castejón, J.M.P., Hardy, A., 2018. Heavy metal content and mobility in urban soils of public playgrounds and sport facility areas, Poland. Chemosphere 212, 456–466. https://doi.org/10.1016/j.chemosphere.2018.08.109

Saenz, C., Ostos, J., 2020. Corporate Social Responsibility supports the construction of a strong social capital in the mining context : Evidence from Peru. J. Clean. Prod. 267.

Sánchez-Albavera, F., Lardé, J., 2006. Minería y competitividad Internacional en América Latina, Serie Recursos Naturales e Infraestructura N°109. Comisión Económica para América Latina y el Caribe (CEPAL). Santiago de Chile.

Santos-Francés, F., Martínez-Graña, A., Rojo, P.A., Sánchez, A.G., 2017a. Geochemical Background and Baseline Values Determination and Spatial Distribution of Heavy Metal Pollution in Soils of the Andes Mountain range (Cajamarca-Huancavelica, Peru). Int. J. Environ. Res. Public Health 14, 22.

Santos-Francés, F., Martínez-Graña, A., Zarza, C.Á., Sánchez, A.G., Rojo, P.A., 2017b. Spatial distribution of heavy metals and the environmental quality of soil in the Northern Plateau of Spain by geostatistical methods. Int. J. Environ. Res. Public Health 14. https://doi.org/10.3390/ijerph14060568

Sanz-Medel, A., Pereiro, R., Costa-Fernandez, J.M., 2013. An Overview of Atomic Spectrometric Techniques, in: Basic Chemometric Techniques in Atomic Spectroscopy, 2nd Edition. Royal Society of Chemistry, pp. 1–51. https://doi.org/10.1039/9781849739344-00001

Schat, H., Llugany, M., Vooijs, R., Hartley-Whitaker, J., Bleeker, P.M., 2002. The role of phytochelatins in constitutive and adaptive heavy metal tolerances in hyperaccumulator and non-hyperaccumulator metallophytes. J. Exp. Bot. 53, 2381–2392. https://doi.org/10.1093/jxb/erf107

Schaumlöffel, D., Ouerdane, L., Bouyssiere, B., Łobiński, R., 2003. Speciation analysis of nickel in the latex of a hyperaccumulating tree Sebertia acuminata by HPLC and CZE with ICP MS and electrospray MS-MS detection. J. Anal. At. Spectrom. 18, 120–127. https://doi.org/10.1039/b209819a

Seubert, A., 2001. On-line coupling of ion chromatography with ICP-AES and ICP-MS. TrAC - Trends Anal. Chem. 20, 274–287. https://doi.org/10.1016/S0165-9936(01)00082-6

Sgariglia, M., Soberón, J.R., Sampietro, D., Vattuone, M., 2010. Cromatografía : Conceptos Y Aplicaciones. Rev. Arakuku 1–6.

Shah, V., Daverey, A., 2020. Phytoremediation: A multidisciplinary approach to clean up heavy metal contaminated soil. Environ. Technol. Innov. 18. https://doi.org/10.1016/j.eti.2020.100774

Stefanowicz, A.M., Kapusta, P., Zubek, S., Stanek, M., Woch, M.W., 2020. Soil organic matter prevails over heavy metal pollution and vegetation as a factor shaping soil microbial communities at

historical Zn–Pb mining sites. Chemosphere 240.

Subirana Manzanares, M.A., 2018. Selenium biofortification of wheat: Distribution and spatially resolved selenium speciation by synchrotron-based techniques. Universitat Autonoma De Barcelona.

Sun, Z., Xie, X., Wang, P., Hu, Y., Cheng, H., 2018. Heavy metal pollution caused by small-scale metal ore mining activities : A case study from a polymetallic mine in South China. Sci. Total Environ. 639, 217–227.

Szpunar, J., 2000. Trace element speciation analysis of biomaterials by high-performance liquid chromatography with inductively coupled plasma mass spectrometric detection. Trends Anal. Chem. 19, 127–137.

Szpunar, J., Pellerin, P., Makarov, A., Doco, T., Williams, P., ŁObińSki, R., 1999. Speciation of metal-carbohydrate complexes in fruit and vegetable samples by size-exclusion HPLC-ICP-MS. J. Anal. At. Spectrom. 14, 639–644. https://doi.org/10.1039/a808231f

Szpunar, J., Pellerin, P., Makarov, A., Doco, T., Williams, P., Medina, B., Łobiński, R., 1998. Speciation analysis for biomolecular complexes of lead in wine by size-exclusion high-performance liquid chromatography-inductively coupled plasma mass spectrometry. J. Anal. At. Spectrom. 13, 749–754. https://doi.org/10.1039/A803038C

Tack, F.M.G., 2010. Trace elements: General Soil Chemistry, Principles and Processes, in: Trace Elements in Soils. pp. 9–37.

Templeton, D.M., Ariese, F., Cornelis, R., Danielsson, L.-G., Muntau, H., Van Leeuwen, H.P., Lobinski, R., 2000. Guidelines for terms related to chemical speciation and fractionation of elements. Definitions, structural aspects, and methodological approaches (IUPAC Recommendations 2000). Pure Appl. Chem. 72, 1453–1470.

Tessier, A., Campbell, P.G.C., Bisson, M., 1979. Sequential Extraction Procedure for the Speciation of Particulate Trace Metals. Anal. Chem. 51, 844–851.

Thamkaew, G., Sjöholm, I., Gómez Galindo, F., 2020. A review of drying methods for improving the quality of dried herbs. Crit. Rev. Food Sci. Nutr.

Todolí, J.L., 2019. Atomic mass spectrometry | inductively coupled plasma mass spectrometry. Encycl. Anal. Sci. 1, 209–217. https://doi.org/10.1016/B978-0-12-409547-2.14473-7

Tsednee, M., Huang, Y.C., Chen, Y.R., Yeh, K.C., 2016. Identification of metal species by ESI-MS/MS through release of free metals from the corresponding metal-ligand complexes. Sci. Rep. 6, 1–13. https://doi.org/10.1038/srep26785

Uliyanchenko, E., Schoenmakers, P.J., van der Wal, S., 2011. Fast and efficient size-based separations of polymers using ultra-high-pressure liquid chromatography. J. Chromatogr. A 1218, 1509–1518. https://doi.org/10.1016/j.chroma.2011.01.053

Unger, C., 2017. Legacy Issues and Abandoned Mines, in: The Political Economy of the Asia Pacific. pp. 333–369. https://doi.org/10.1007/978-3-319-61395-6

Venkateswarlu, K., Nirola, R., Kuppusamy, S., Thavamani, P., Naidu, R., Megharaj, M., 2016. Abandoned metalliferous mines: ecological impacts and potential approaches for reclamation. Environ. Sci. Biotechnol. 15, 327–354.

Wang, H., He, M., Beibei, C., Hu, B., 2017. Advances in ICP-MS based techniques for trace elements and their species analysis in cells. J. Anal. At. Spectrom. 1–26. https://doi.org/10.1039/C6JA00414H

Wang, Y., Bu, H., Wang, L., Wang, L., Guo, Y., Liang, X., Wang, S., 2019. High efficiency and simple preparation of polyacrylamide coated silica stationary phase for hydrophilic interaction liquid chromatography. J. Chromatogr. A 1605, 360357. https://doi.org/10.1016/j.chroma.2019.07.011

Wenzel, W.W., Bunkowski, M., Puschenreiter, M., Horak, O., 2003. Rhizosphere characteristics of indigenously growing nickel hyperaccumulator and excluder plants on serpentine soil. Environ. Pollut. 123, 131–138. https://doi.org/10.1016/S0269-7491(02)00341-X

Wilschefski, S.C., Baxter, M.R., 2019. Inductively Coupled Plasma Mass Spectrometry: Introduction to Analytical Aspects. Clin. Biochem. Reviwers 40, 115–133.

Wojcieszek, J., Szpunar, J., Lobinski, R., 2018. Speciation of technologically critical elements in the environment using chromatography with element and molecule speci fi c detection. Trends Anal. Chem. 104, 42–53.

Yang, Y., Ren, X., Zhang, S., Chen, F., Hou, H., 2017. Incorporating ecological vulnerability assessment into rehabilitation planning for a post-mining area. Environ. Earth Sci. 76, 1–16. https://doi.org/10.1007/s12665-017-6568-y

Yano, Y., Yachandra, V.K., 2009. X-ray absorption spectroscopy. Photosynth. Res. 102, 241–254.

Yoon, J., Cao, X., Zhou, Q., Ma, L.Q., 2006. Accumulation of Pb, Cu, and Zn in native plants growing on a contaminated Florida site. Sci. Total Environ. 368, 456–464.

Yupari, A., 2003. Pasivos ambientales mineros en Sudamérica, Informe elaborado para la CEPAL, el Instituto Federal de Geociencias y Recursos Naturales, BGR, y el Servicio Nacional de Geología y Minería, SERNAGEOMIN. CEPAL.

Zhang, H., Kuang, Z., Peng, X., He, G., Peng, J., Fan, J., 2020. Aggregating diverse deep attention networks for large-scale plant species identification. Neurocomputing 378, 283–294.

Zhang, P., Qin, C., Hong, X., Kang, G., Qin, M., Yang, D., Pang, B., Li, Y., He, J., Dick, R.P., 2018. Risk assessment and source analysis of soil heavy metal pollution from lower reaches of Yellow River irrigation in China. Sci. Total Environ. 633, 1136–1147. https://doi.org/10.1016/j.scitotenv.2018.03.228

Zhou, Z.H., Liu, Y., Zhang, B., 2019. Microfluidic Array Liquid Chromatography: A Proof of Principle Study. Chinese J. Anal. Chem. 47, 500–507. https://doi.org/10.1016/S1872-2040(19)61154-0

ET LUX IN TENEBRIS LUCET
MCMXVII

II. JUSTIFICATION AND OBJECTIVES

II. JUSTIFICATION AND OBJECTIVES

2.1. JUSTIFICATION OF THE PROJECT

Increasing contamination of soils, sediments, water, and crops with heavy metals derived from mining activities with poor ecologic management has become a worldwide concern. Phytoremediation is a sustainable technology based on the use of plants to reduce the in situ concentration of contaminants.

In this research, soils and native plants growing around two mining environmental liabilities in the Hualgayoc district, Cajamarca region (Peruvian Andes), were studied. Soils were assessed in terms of their environmental quality from a geo-ecological perspective. Native plants were assessed in terms of their ability to accumulate heavy metals. The study on metal accumulation potential, the species involved in the process, the bioaccumulation of the metals in tissues of native plants as well the translocation into over ground organs will serve to establish the potential applicability of the studied plant species for soil phytoremediation in order to enlarge the spectrum of plants potentially useful for this purpose in the Andes. The molecules involved in heavy metal uptake, transport, and storage were identified as well in order to have an insight into the processes responsible for the accumulation.

2.2. OBJECTIVES

2.1.1. General objective

The main objective of this work is to assess the environmental impact of mining environmental liabilities in soils in post-mining sites in the Peruvian Andes, to identify native plant species useful for phytoremediation strategies, and to get an insight into the metal uptake and transport between plant organs.

2.1.2. Specific objectives

- To determine the morphological and physicochemical properties and mineralogical composition of soils from two mining environmental liabilities.
- To characterize the metal contaminant concentrations in soils in post-mining areas and to assess their mobility and potential bioavailability by sequential extraction.
- To valuate the soil environmental quality in the study areas.
- To identify plants taxonomy and to establish an inventory of the native flora at the studied contaminated sites to be potentially used for phytoremediation purposes.
- To evaluate the uptake of metals present in the contaminated soils by native plants.
- To evaluate the bioaccumulation and translocation of metals by the selected native plants.
- To identify the molecules binding selected metals in studied plant species.
- To prospect the potential use of studied plants for revitalization of metal contaminated post-mining areas in the Peruvian Andes

III. RESULTS AND DISCUSSION

CHAPTER A

HEAVY METAL CONTENTS IN SOILS AND NATIVE FLORA INVENTORY AT MINING ENVIRONMENTAL LIABILITIES IN THE PERUVIAN ANDES

CHAPTER A. HEAVY METAL CONTENTS IN SOILS AND NATIVE FLORA INVENTORY AT MINING ENVIRONMENTAL LIABILITIES IN THE PERUVIAN ANDES

The initial step of the PhD project inolved the evaluation of the environmental quality of soils and the establishment of an inventory of plants that were growing in two Mining Environmental Liabilities (MEL) in the Hualgayoc district at the Cajamarca region in the Peruvian Andes.

Mining activity is one of the economic pillars of Peru; however, it has left a legacy of countless MEL sites. The Cajamarca region is the second one in terms of the number of MEL sites. The two studied sites were chosen among the 1156 MELs in the Cajamarca region and 943 in the Hualgayoc district. The MELs in this area affect the Tingo-Maygasbamba, Hualgayoc-Arascorgue, and Llaucano river basins including their flora and fauna. Also, Hualgayoc is a scene of several mining conflicts between the local communities and the mining companies. The ex-Mining Unit Los Negros, the place that was investigated in this project, posseses a high number of MEL sites and as such is representative for the evaluation of the environmental pollution in Peruvian post-mining areas.

The soils and plants were collected from the two MEL sites (site #1 located at 6°44'49" S - 78°35'36" W, 3249 m.a.s.l., and site #2- 6°44'53" S - 78°35'49", 3399 m.a.s.l.) using a carefully designed strategy taking into account the distance from the presumed contamination point and (for the determination of soil profile characteristics) - depths. The sampling of flora specimens was carried out in the same locations as for soil.

The primary goal of the study was to determine the morphological, physicochemical, and mineralogical properties as well as total metal concentrations in soil samples. For this purpose, the analyses of mineralogy, pH, electrical conductivity (CE), organic matter (OM), available phosphorus and potasium, capacity cation exchange (CEC), carbonates, and particle size were carried out. Considering the morphology and analytical data and the soil colour with Munsell Colour Charts, the studied soils were classified by horizons. Then, the concentrations of 34 metals and metalloids were determined by inductively coupled plasma emission spectrometry (ICP-OES); potentially toxic concentrations of Pb, Zn, As, Cu, Ag, and Cd were found, and the further research was focused on these six elements.

The evaluation of the soil environmental quality was carried out by:

(i) the comparison of the concentrations of the six metals (Pb, Zn, As, Cu, Ag, and Cd) with the Peruvian Environmental Quality Standards (PEQS) for agricultural soil and with the Canadian Soil Quality

Guidelines (CSQG) to know if the concentration of metals at the studied MEL sites exceeded the environmental regulations for agricultural land use

(ii) the calculation of the pollution indices including the Index of geo-accumulation (Igeo, the relationship between the content of metals in soils with the geochemical background of the sites), the Nemerow pollution index (NI) and Improved Nemerow index (INI) for the assessment of the overall soil level taking into account the content of all metals and then the Potential ecological risk (RI), to evaluate the potential impact of the heavy metals to the surrounding ecology.

The second objective in this initial part of the project was the plants taxonomy identification and establishing an inventory of the native flora growing in at the studies contaminated sites, and therefore being the potential candidates to be used for phytoremediation purposes.

Journal of South American Earth Sciences 106 (2021) 103107

Contents lists available at ScienceDirect

Journal of South American Earth Sciences

journal homepage: www.elsevier.com/locate/jsames

Heavy metal contents in soils and native flora inventory at mining environmental liabilities in the Peruvian Andes

Edith Cruzado-Tafur [a,b,*], Lisard Torró [b], Katarzyna Bierla [a], Joanna Szpunar [a], Esperança Tauler [c]

[a] Université de Pau & des Pays de l'Adour, E2S UPPA, CNRS, IPREM, Institut des Sciences Analytiques et de Physico-chimie pour l'Environnement et les Materiaux, Pau, France
[b] Geological Engineering Program, Faculty of Sciences and Engineering, Pontifical Catholic University of Peru (PUCP), Av. Universitaria 1801, San Miguel, Lima, Peru
[c] Departament de Mineralogia, Petrologia i Geologia Aplicada, Facultat de Ciències de la Terra, Universitat de Barcelona, Carrer de Martí i Franquès s/n, 08028, Barcelona, Spain

ARTICLE INFO

Keywords:
Soil pollution
Contamination indices
Ecological risk
Native plants
Cajamarca
Peruvian Andes

ABSTRACT

Inadequate waste management in Mining Environmental Liabilities (MEL) represents a risk for the environment and human health and generates social problems. The aim of this article is twofold: i) to evaluate the environmental quality of soils from a geo-ecological perspective; and ii) to inventory native flora around two MEL in the Hualgayoc district in the Peruvian Andes. Soil samples collected for topsoil (upper 30 cm; i.e., soil arable layer) and subsoil (30–60 cm) were classified as Gleyic Cambisols and showed extremely acid pH (3.50–4.19 in site #1 and 2.74–4.02 in site #2). The mineralogical composition of soils is dominated by illite, kaolinite, quartz, and jarosite. The concentrations of six potentially toxic elements (Pb, Zn, As, Cu, Ag, and Cd) were determined. High concentrations of Pb (4683 mg kg^{-1}), Zn (724.2 mg kg^{-1}), Cu (511.6 mg kg^{-1}), Ag (33.4 mg kg^{-1}), and As (3611 mg kg^{-1}) exceeded the maximum permissible limits for agricultural soils according to Peruvian and Canadian regulations. Applied geochemical indexes classified some of the soils as extremely polluted and therefore the studied MEL represent a very high ecological risk. Twenty-two species of native flora belonging to 12 family species were inventoried in such contaminated sites thus having the potential to be used for phytoremediation purposes.

1. Introduction

Mining has been one of the economic pillars of the Peruvian economy over the last decades (Figueroa et al., 2010) so that in 2018 it represented almost 10% of national GDP and about 61% of the total value of exports. Peru is the second largest producer of copper, silver and zinc, and is the first producer of gold, zinc, lead and tin in Latin America (Ministerio de Energía y Minas, 2018). Inadequate waste management during mining activity and the lack of clear regulations concerning mine closure have, however, led to the accumulation of Mining Environmental Liabilities (MEL sites) potentially causing environmental and social problems (Lam et al., 2017). MEL sites refer here to the environmental impact caused by abandoned mine activities with or without a responsible identified (Yupari, 2003). In Peru, MEL sites (*Pasivos Ambientales Mineros*, in Spanish) are defined as those installations, effluents, emissions, remains or residue deposits produced by mining operations, abandoned or inactive, that constitute a permanent and potential risk to human health, environment and patrimony (Ministerio de Energía y Minas, 2004). In 2019, the number of MEL sites in the Peruvian territory was of at least 8448, most of them without an identified responsible (Ministerio de Energía y Minas, 2019). The regions of Ancash, Apurímac, Arequipa, Cajamarca, Huancavelica, Junín, Pasco and Puno are the areas that concentrate the greatest number of MEL sites (Chappuis, 2019; Ministerio de Energía y Minas, 2019). Even though Peru was the first Latin American country to establish a legal framework for MEL sites back in 1993 (Oblasser and Chaparro Ávila, 2008), a significant number of MEL sites originated prior to this date, when mining environmental regulation and community expectation standards were much lower than those set out in the present (Unger et al., 2015).

Soil contamination with heavy metals is a major potential damage caused by MEL sites, which may seriously compromise the alternative use of abandoned mine sites (Vassilev et al., 2004; Zhang et al., 2018; Li

* Corresponding author.
E-mail address: em.cruzado-tafur@univ-pau.fr (E. Cruzado-Tafur).

https://doi.org/10.1016/j.jsames.2020.103107
Received 21 September 2020; Received in revised form 14 November 2020; Accepted 11 December 2020
Available online 16 December 2020

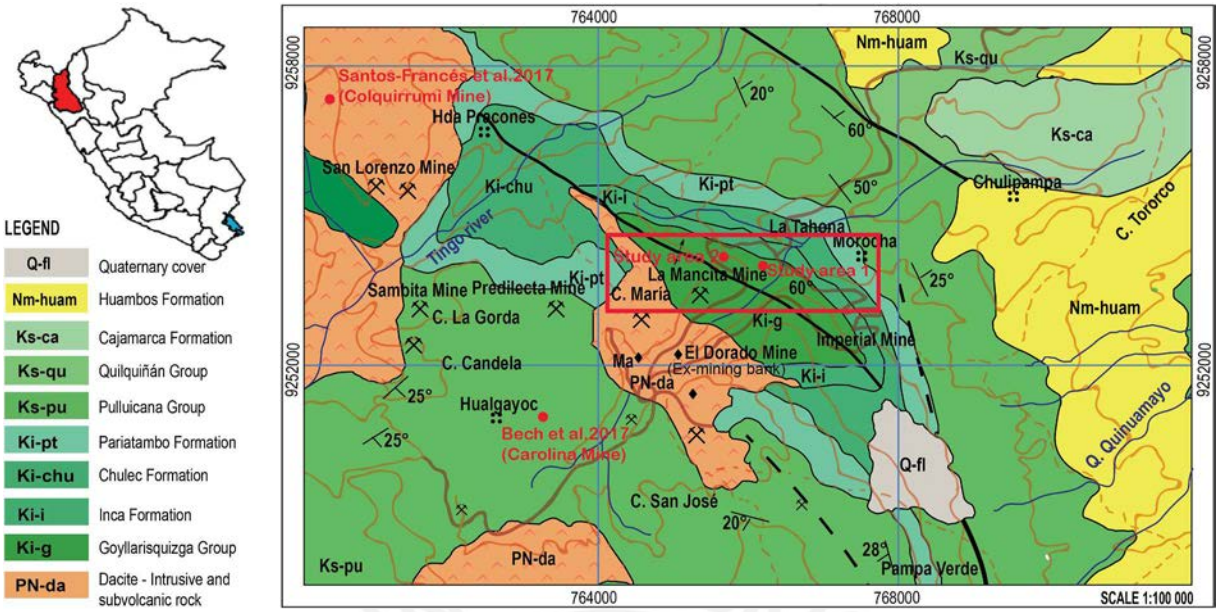

Fig. 1. Geological map of the study area in the Hualgayoc district, Cajamarca region, Peru. Adapted from INGEMMET (2017) and Padilla (2019).

et al., 2019; Liu et al., 2020; Manjate et al., 2020). Heavy metals tend to accumulate, in general, in the upper part of soil profiles (surface horizons) and subsequently migrate into deeper horizons (Mazurek et al., 2019). Elevated concentrations of heavy metals in soils can be introduced to flora, fauna or human beings through food chains thus representing direct or indirect threat to human health (Midhat et al., 2019; Zhang et al., 2018). Assessment of the degree and toxicity of soil pollution is important to control contaminated site risks, prevent further soil damage and delineate plan remedial strategies (Liu et al., 2020; Mazurek et al., 2019). Pollution indices provide a useful tool for the quantification of soil quality and the identification of pollution sources. Also, they may help during management and remediation endeavors (Mazurek et al., 2019).

For the restoration of functional ecosystems at post-mining sites, soil recovery is essential (Angst et al., 2018) and the removal of heavy metals using plants represents an often viable alternative (Chaabani et al., 2017). In contaminated areas, the use of phytoremediation with native plants provides natural rehabilitation generating, in addition, a positive visual impact. Plants, by growing roots in contaminated soil, can help immobilize pollutants (Moreno-Jiménez et al., 2011). Native species have been identified often as of high potential to withstand high concentrations of pollutants (Hauptvogl et al., 2019) with the advantage that they grow without human intervention (Gajić et al., 2018).

In the watersheds of the Cajamarca region, where our study has been developed, conspicuous pollution problems derive from the leaching of heavy metals from alteration zones and MEL sites at high altitude. The Andes mountain range is affected by erosive processes leading to soil dragging to agricultural valleys and rivers during the rainy season (Santos-Francés et al., 2017a). Hualgayoc is a mining district of the Cajamarca region with a long mining history that dates back to the times of the Spanish Colony. Metal production includes chiefly Ag and to a lesser extent, polymetallic ore (Zn, Pb and Cu; Canchaya, 1990). Because of the long mining history, the Hualgayoc district embraces a large number of MEL sites (Ministerio de Energía y Minas, 2019) potentially affecting the Tingo-Maygasbamba, Hualgayoc-Arascorgue and Llaucano river basins, their flora, fauna, and human beings (Pinto Herrera, 2014) and is a source of socio-environmental conflict (Chappuis, 2019).

The main objective of the present study is to evaluate the environmental quality of the soil in and next to MEL sites in the Hualgayoc district in the Peruvian Andes by assessing the environmental risk of heavy metal pollution. To do so, various pollution indices have been used in order to determine the correlation of physicochemical properties of soils and calculate the average content of metals. In addition, we offer an inventory of native flora that grows in such contaminated sites and that, therefore, has potential to be used for phytoremediation purposes.

2. Materials and methods

2.1. Description of the study site

The Hualgayoc district is located between the Chugur and Bambamarca districts, to the west of the Hualgayoc province, in the Cajamarca department in the Andes of northern Peru (Fig. 1), and has an extension of 226 km^2 (Padilla, 2019). The Hualgayoc city is located at an altitude of 3502 m above the sea level (m.a.s.l.), at 866 km N of Lima. The area of study is located between 6°44′46″ S - 78°35′49.7″ W and 6°44′46.2″ S - 78°35′33.2″ W. Apart from mining, the population of Hualgayoc has an agricultural tradition dedicated to the cultivation of corn, beans, potatoes, peas, oca, and olluco (Padilla, 2019).

Basement geology in the study area is largely composed of Cretaceous platform sedimentary rocks that were intruded during several magmatic episodes (Fig. 1; Canchaya, 1990; Macfarlane et al., 1994; Macfarlane and Petersen, 1990). The oldest sedimentary rocks belong to the lower Albian – Turonian Goyllarisquizga Group, which crops out in the core of a northwest–trending anticline. Rocks of the Goyllarisquizga Group comprises mostly quartzites and lesser amounts of interbedded shales and are conformably overlain by a thick carbonate sequence of lower Albian – Turonian age. Bottom to top, carbonate rocks include massive calcareous siltstones and shales of the Inca Formation, grey fossiliferous limestones and shales of the Chulec Formation and dark grey to black bituminous limestones of the Pariatambo Formation. Volcanic rocks cropping out in the Hualgayoc district are of Late Cretaceous and Miocene ages, basic to intermediate in composition and calc-alkaline in affinity according to Canchaya (1990). Dacites from the so-called Hualgayoc intrusion were dated at 14.5 ± 0.5 Ma, sills in the Hualgayoc river canyon at 10 ± 0.5 Ma, and dacite extrusive rocks in the Hualgayoc hill at 7.2 ± 0.4 Ma (Borredon, 1982). Geologically, the studied MEL sites are located on the north-western limb of a regional anticline and deposited on quartzites of the Goyllarisquizga Group (Fig. 1).

The main mineralized structures in the Hualgayoc district are mantos and veins hosted largely in the upper Goyllarisquizga Group, the Inca

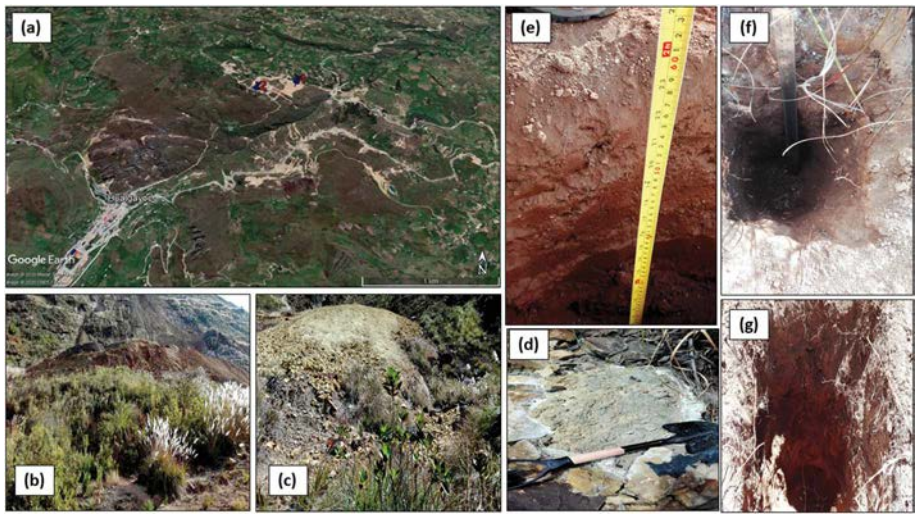

Fig. 2. (a) Localization of the study area in the Hualgayoc district, Cajamarca region, Peru. (b) Site 1- Leach pad and (c) Site 2 - Mine dump Mining Environmental Liabilities. (d) Lixiviate sample from site 1. (e), (f), and (g) soil profiles.

Formation and lower Chulec Formation rocks (Canchaya, 1990; Macfarlane et al., 1994; Macfarlane and Petersen, 1990). The ore mineralogy of both mantos and veins is composed mostly of pyrite, sphalerite, and galena and lesser amounts of arsenopyrite, chalcopyrite, marcasite, pyrrhotite, fahlore, and a wealth of Cu–Ag–Pb sulfosalts. The main gangue minerals in both types of mineralization are quartz, barite and Ca–Mg–Fe–Mn carbonates (Canchaya, 1990; Macfarlane et al., 1994; Macfarlane and Petersen, 1990).

There are 943 cataloged MEL sites in the Hualgayoc district, most of them without an identified responsible (Ministerio de Energía y Minas, 2019). In the present investigation, soils and flora from two MEL sites belonging to the Ex-Mining Unit Los Negros have been sampled. Sampling site #1 corresponds to a leach pad, which is located on top of a mine waste deposit and has no drainage. Sampling site #2 corresponds to a mine dump without stabilization, drainage or human-driven revegetation. Both studied MEL sites lie in the flank of the Llaucano river valley. The Mansita, El Dorado, and Morocha mines are located around the studied MEL sites (Padilla, 2019).

2.2. Sampling

Soils and plants were collected around sampling sites #1 (6°44′49″ S - 78°35′36″ W, 3249 m.a.s.l.) and #2 (6°44′53″ S - 78°35′49″, 3399 m.a.s.l.) in July 2018 (dry season; Fig. 2) following a criteria based on the distance from the point of contamination, wind direction, slope, vegetation cover and soil texture (Bech et al., 2002). The location of the points for soil sampling in both sites was fixed at 0, 15, 30, 45, and 60 m away from the point of contamination, along a downhill slope. For the determination of soil profile characteristics, samples were taken at four depths between 0 and 60 cm at 15 cm intervals. Following this scheme, a total of 40 soil samples of the topsoil (upper 30 cm; a.k.a. soil arable layer) and of the subsoil (30–60 cm downhole) were collected between the two sites. Soil colour was determined in situ with Munsell Colour Charts.

The sampling of flora specimens was carried out in the same locations as for soil sampling. Around each soil sampling point, an area of 4 m^2 was delimited for flora sampling. Flora samples were carefully placed inside a sheet of paper without damaging the main characteristics of the plant. A total of 29 plants in the sampling site #1 and 19 plants in the sampling site #2 were collected. It should be noted that some specimens represented biological replicates and that five species were found in common in both studied areas, thus resulting in a total of 22 species of native flora.

2.3. Chemical analysis of soils samples

Soil samples were analysed at the Soil, Plant, Water and Fertilizer Analysis Laboratory of the Universidad Nacional Agraria La Molina in Lima, Peru. Soil pH was measured using a suspension of soil in deionized water at a 1:1 ratio. The organic matter content was determined by means of the Walkley and Black method (i.e., oxidation of organic carbon with potassium dichromate) (Walkley and Black, 1934). Calcium carbonate content was determined by gas-volumetric method using a calcimeter. The electrical conductivity was measured in aqueous extract of soil in the water at a 1:1 ratio. The texture of soil samples was determined using the Bouyoucos Hydrometer method (i.e., mechanical analysis of soils by means of the suspension of solids for the quantification of the content of sand, silt, and clay in percentage; Bouyoucos, 1936). The soil available phosphorus was determined by the Olsen method (modified extraction with $NaHCO_3$ 0.5N, determination of available potassium content with NH_4OAc 1N extraction by atomic absorption spectrophotometry). The capacity cation exchange was determined using the saturation method of the clay-humic complex with ammonium acetate at pH 7, and nitrogen distillation by Kjeldahl (Sparks, 1996).

The concentration of metals in soils was analysed at the SGS Geochemical Assays Laboratory in Lima, Peru. Approximately 0.20 g of soil with particle size below 106 μm were analysed by digestion in two steps in a Hot Block (Environmental Express). The first digestion step was developed at a temperature of 90 °C for 30 min after the addition of 1 ml of concentrated nitric acid; the second digestion step was developed at a temperature of 90 °C for 1 h after the addition of 3 ml of concentrated hydrochloric acid. Once it cooled to room temperature, 2 ml of concentrated hydrochloric acid was added and diluted with ultrapure water (18.2 MΩ cm) to 20 ml (variation from EPA 3050-B method). The concentrations of metals were determined by inductively coupled plasma emission spectrometer (ICP-OES) using a Perkin Elmer Model Optima 8300 DV equipment. The concentration of the following 34 metals and metalloids was determined (detection limits, in ppm, are given in parentheses): Ag (0.2), Al(0.01), As (3), B (10), Ba (1), Be (0.5), Bi (5), Cd (0.4), Co (1), Cr (1), Cu (0.5), Fe (0.01), Hg (1), K (0.01), La (0.5), Li (1), Mg (0.01), Mn (2), Mo (1), Ni (1), P (0.01), Pb (2), S(0.01), Sb (5), Sc (0.5), Se (10), Sn (10), Sr (0.5), Te (10), V (2), W (10), Y (0.5), Zn (0.5), and Zr (0.5) (Supplementary table 1). The certified soil reference materials OREAS 906, OREAS 907, and OREAS 522 were used for quality control.

Table 1
Properties of soil samples from sites #1 and #2 in the Hualgayoc district, Cajamarca region, Peru.

Distance (m)	Depth (cm)	Munsell Colour	pH	EC (dS m^{-1})	O.M (%)	P (mg kg^{-1})	K (mg kg^{-1})	CEC (cmol.kg^{-1})	Exchangeable cations (cmol.kg^{-1})					Particle-size (%)		
									Ca^{2+}	Mg^{2+}	K^{+}	Na^{+}	$Al^{3+} + H^{+}$	Sand	Silt	Clay
Site 1																
0	0–15	2.5 YR 3/3 (dark reddish brown)	4.02	0.08	7.59	3.4	101	20.32	1.11	0.33	0.27	0.14	5.00	66	22	12
	15–30	2.5 YR 3/3 (dark reddish brown)	3.97	0.09	4.26	2.7	88	19.20	0.90	0.32	0.27	0.17	3.50	50	24	26
	30–45	2.5 YR 3/4 (dark reddish brown)	4.02	0.1	3.13	2.2	78	14.40	0.78	0.30	0.29	0.18	2.30	54	24	22
	45–60	2.5 YR 4/4 (reddish brown)	3.93	0.07	2.34	1.8	60	13.76	0.74	0.28	0.18	0.12	2.50	50	22	28
15	0–15	10 YR 5/6 (yellowish brown)	4.19	0.05	4.39	3	106	12.80	0.89	0.33	0.35	0.13	2.70	52	26	22
	15–30	10 YR 6/8 (brownish yellow)	3.89	0.07	2.48	2.6	87	14.08	0.90	0.32	0.27	0.10	3.30	42	22	36
	30–45	10 YR 5/6 (yellowish brown)	3.5	0.12	1.38	2.1	72	12.80	0.84	0.30	0.25	0.11	3.40	42	20	38
	45–60	10 YR 4/6 (dark yellowish brown)	3.51	0.39	1.02	1.9	75	13.12	1.45	0.30	0.23	0.17	4.80	50	18	32
30	0–15	10 YR 3/6 (dark yellowish brown)	3.63	0.13	3.45	3.6	62	15.20	0.64	0.27	0.20	0.16	3.00	52	24	24
	15–30	10 YR 3/6 (dark yellowish brown)	3.84	0.15	3.76	4.6	66	16.00	0.63	0.25	0.19	0.13	2.10	54	28	18
	30–45	10 YR 4/6 (dark yellowish brown)	3.76	0.12	2.87	4.9	59	16.96	0.59	0.23	0.17	0.12	1.70	50	30	20
	45–60	10 YR 4/6 (dark yellowish brown)	3.59	0.13	1.95	3.6	36	17.60	0.54	0.25	0.14	0.15	1.90	70	18	12
45	0–15	10 YR 5/8 (yellowish brown)	3.63	0.08	5.72	4.1	78	18.88	0.86	0.30	0.24	0.15	4.30	66	18	16
	15–30	10 YR 6/6 (brownish yellow)	3.67	0.08	1.79	2.2	40	10.88	0.63	0.28	0.15	0.17	2.50	52	22	26
	30–45	10 YR 6/6 (brownish yellow)	3.68	0.08	1.26	1.9	39	8.00	0.63	0.28	0.14	0.14	1.60	46	24	30
	45–60	10 YR 7/8 (yellow)	3.63	0.08	1.1	1.9	40	7.52	0.61	0.27	0.16	0.12	2.00	50	22	28
60	0–15	10 YR 6/8 (brownish yellow)	3.76	0.05	4.21	3.8	84	15.20	0.58	0.23	0.22	0.11	3.80	54	28	18
	15–30	10 YR 3/6 (dark yellowish brown)	3.59	0.09	4.51	2.6	81	19.20	0.66	0.28	0.24	0.14	4.40	50	24	26
	30–45	10 YR 3/6 (dark yellowish brown)	3.68	0.07	3.51	2.7	57	16.64	0.54	0.23	0.18	0.11	3.30	58	22	20
	45–60	10 YR 3/6 (dark yellowish brown)	3.8	0.08	3.16	2.2	54	16.32	0.58	0.27	0.17	0.14	2.60	46	24	30
Site 2																
0	0–15	7.5 YR 4/4 (brown)	3.42	0.08	10.57	3.6	92	22.08	0.63	0.30	0.24	0.13	6.90	60	22	18
	15–30	7.5 YR 4/3 (brown)	3.37	0.11	4.98	3.2	65	18.72	0.57	0.27	0.20	0.13	6.50	56	24	20
	30–45	7.5 YR 4/3 (brown)	3.67	0.06	3.31	2.7	61	12.80	0.61	0.28	0.16	0.12	4.60	58	20	22
	45–60	7.5 YR 4/3 (brown)	3.72	0.06	2.43	1.8	56	11.68	0.60	0.27	0.09	0.16	3.20	52	18	30
15	0–15	10 YR 4/4 (dark yellowish brown)	4.02	0.02	4.36	4	85	14.40	0.83	0.32	0.25	0.13	3.00	54	20	26
	15–30	10 YR 4/4 (dark yellowish brown)	3.89	0.02	4.37	3.4	78	16.32	0.63	0.28	1.03	0.12	2.80	62	20	18
	30–45	10 YR 4/4 (dark yellowish brown)	3.76	0.04	5.22	3.3	75	17.92	0.62	0.30	0.22	0.11	4.40	54	22	24
	45–60	10 YR 4/4 (dark yellowish brown)	3.72	0.04	6.09	2.7	77	17.60	0.64	0.28	0.22	0.12	4.60	60	22	18
30	0–15	7.5 YR 5/4 (brown)	3.37	0.14	2.48	3.2	83	16.48	0.67	0.25	0.24	0.11	6.00	52	18	30
	15–30	7.5 YR 3/3 (dark brown)	3.46	0.14	2.88	2.2	71	17.60	0.66	0.28	0.25	0.12	4.50	54	18	28
	30–45	7.5 YR 4/4 (brown)	3.5	0.22	3.13	1.8	68	16.00	0.61	0.28	0.21	0.13	4.00	54	20	26
	45–60	7.5 YR 3/3 (dark brown)	3.03	0.61	4.62	1.8	70	20.00	0.55	0.27	0.19	0.12	7.50	52	22	26
45	0–15	7.5 YR 4/4 (brown)	3.85	0.05	4.92	3.9	134	19.20	0.78	0.30	0.37	0.12	5.70	56	22	22
	15–30	7.5 YR 4/4 (brown)	3.72	0.05	3.28	3	91	16.48	0.65	0.28	0.29	0.17	5.10	58	22	20
	30–45	7.5 YR 4/4 (brown)	3.46	0.08	2.87	2.6	75	15.36	0.63	0.28	0.24	0.13	4.80	54	24	22
	45–60	7.5 YR 4/4 (brown)	2.9	0.4	1.99	2.7	50	15.52	0.60	0.25	0.16	0.10	4.50	50	22	28
60	0–15	7.5 YR 5/4 (brown)	2.94	0.32	2.15	4	53	16.00	0.57	0.27	0.16	0.13	4.20	54	24	22
	15–30	7.5 YR 5/4 (brown)	2.77	0.57	1.71	3.4	40	14.08	0.66	0.32	0.13	0.15	4.60	54	20	26
	30–45	7.5 YR 4/4 (brown)	2.74	0.61	1.88	3	37	16.32	0.59	0.23	0.12	0.12	4.40	56	18	26
	45–60	7.5 YR 4/4 (brown)	2.82	0.56	2.1	2.9	40	16.64	0.54	0.30	0.15	0.17	6.00	56	20	24

EC: Electrical Conductivity, OM: Organic Matter, CEC: Cation Exchange Capacity.

2.4. X-ray diffraction

Mineralogy of 2 soil samples was determined by means X-ray diffraction (XRD). A portion of about 50 g of soil after homogenization was selected for each sample. The clay fraction of soils was analysed as oriented mounts (Moore and Reynolds, 1997). XRD data were collected with a Bruker D8 Discover diffractometer in Bragg-Brentano θ/2θ geometry of 240 mm of radius, nickel filtered Cu Kα radiation (k = 1.5418 Å), and 40 kV–40 mA at the Centro de Caracterización de Materiales of the Pontifical Catholic University of Peru (CAM-PUCP). The patterns of samples on oriented mounts were collected as follows: (i) air dry, scanning from 2 to 80° (2θ); (ii) on samples saturated with ethylene glycol and scanning from 2 to 30° (2θ), (iii) by heating the sample up to 550 °C and scanning from 2 to 30° (2θ), and (iv) by heating the sample up to 550 °C and scanning from 2 to 30° (2θ) at a step size of 0.017° and a scan time of 50 s.

2.5. Electron probe microanalysis (EPMA)

The chemical composition of sphalerite grains from one ore sample picked up in the leach pad belonging to the Ex-Mining Unit Los Negros was analysed by means of EPMA with a particular interest in the concentration of Cd (i.e., sphalerite is the main Cd-bearing mineral in polymetallic hydrothermal mineralizations). Analyses were performed on a polished thick section using a five-channel JEOL JXA-8230 electron microprobe equipment (Jeol Ltd., Tokyo, Japan) available at Centres Científics i Tecnològics of the Univeristy of Barcelona (CCiT-UB), operated at 20 kV acceleration voltage, 20 nA beam current and with a beam diameter of 5 μm. Analytical standards and lines used for analyses were: sphalerite (Zn, Kα), chalcopyrite (Cu, Kα), FeS_2 (Fe and S, Kα), Ag (Ag, Lα), Sb (Sb, Lα), CdS (Cd, Lβ), PbS (Pb, Mα), GaAs (As, Lα), Sn (Sn, Lα), InSb (In, Lα) and Ge (Ge, Lα).

2.6. Pollution indices

2.6.1. Index of geo-accumulation (Igeo)

The geo-accumulation index (Igeo), first introduced by Muller (1969), has been successfully applied to the measurement of soil contamination (JI et al., 2008). The Igeo allows the assessment of the soil contamination based on the ratio between the content of metals in a soil sample and the content of metals of a specific geochemical background (Różański et al., 2018). The Igeo is calculated using the following equation:

$$I_{geo} = log_2 \frac{C_i}{1.5{*}B_i}$$

where C_i is the measured concentration of the *i* metal examined in the soil; B_i is the background level of the *i* metal. The Igeo discriminates between 7 soil groups or classes (JI et al., 2008; Różański et al., 2018): unpolluted (Igeo ≤ 0), unpolluted to moderately polluted (0 < Igeo ≤ 1), moderately polluted (1 < Igeo ≤ 2), moderately to strongly polluted (2 < Igeo ≤ 3), strongly polluted (3 < Igeo ≤ 4), strongly to very strongly polluted (<Igeo ≤ 5) and very strongly polluted (Igeo > 5).

2.6.2. Nemerow pollution index (NI) and improve Nemerow index (INI)

The Nemerow pollution index (NI) measures levels of pollution by metals and can estimate the effects of various metals in the soil quality and the environment (Zhang et al., 2018). It is defined as:

$$I = \sqrt{\frac{Pi_{\ ave}{}^2 + Pi_{\ max}{}^2}{2}}$$

where, *Pi* is *the Pollution factor*, which quantifies the contamination of one individual metal, $Pi = C_i/B_i$, where C_i is the concentration of the measured contaminant and B_i is the geological background level (Santos-Francés et al., 2017b). Likewise, Pi_{ave} is the average value of single pollution indices, and Pi_{max} is the maximum value of single pollution indices. The quality of the soil environment is classified as class 0 (NI < 0.7) non-contamination, 1 (0.7 < NI < 1) slight contamination, 2 (1 < NI < 2) low contamination, 3 (2 < NI < 3) moderate contamination, and 4 (NI > 3) heavy contamination (Li et al., 2019).

According to Santos-Francés et al. (2017a, 2017b) and Mazurek et al. (2019) the Improved Nemerow index (INI) reflects more accurately soil reality using other similar pollution indexes, such as the geo-accumulation index (Igeo) in substitution of the pollution factor (*Pi*). INI is calculated using the following equation:

$$INI = \sqrt{\frac{1}{2}\left(Igeo_{\ max}{}^2 + Igeo_{\ ave}{}^2 \right)}$$

where, $Igeo_{max}$ is the maximum value of the Igeo of all metals in a sample and $Igeo_{ave}$ is the arithmetic mean of the Igeo. INI discriminate between class 0 - uncontaminated (INI < 0.5), class 1- uncontaminated to moderately contaminated (0.5 ≤ INI < 1), class 2 - moderately contaminated (1 ≤ INI < 2), class 3 - moderately to heavily contaminated (2 ≤ INI < 3), class 4 - heavily contaminated (3 ≤ INI < 4), class 5 - heavily to extremely contaminated (4 ≤ INI < 5) and Class 6 - extremely contaminated (INI > 5) soils.

2.6.3. Potential ecological risk (RI)

The method considers the potential impact of heavy metals on ecosystems and is used for the assessment of soil in large regional areas (Zhang et al., 2018). It is capable of assessing potential risks of one or multiple toxicological elements to the surrounding ecology (Liu et al., 2020). The Ecological Risk Index (Er) evaluates the toxicity of individual metals in soils, and the Potential Ecological Risk (RI) reflects the general situation of contamination caused by the simultaneous presence of the metals (Santos-Francés et al., 2017b). It is calculated following equations:

$$Er = Tr{\cdot}Pi$$

$$RI = \sum_{i=1}^{n} Er$$

where Tr is the toxicity coefficient of each metal (standard values are Pb = 5, Zn = 1, As = 10, Cu = 5, Ag = 50, and Cd = 30; Duodu et al., 2016; Santos-Francés et al., 2017a). Er classifies the situation of the contamination as low contamination risk (Er < 40), moderate contamination risk (40 ≤ Er < 80), considerable contamination risk (80 ≤ Er < 160), high contamination risk (160 ≤ Er < 320) and extreme contamination risk (Er > 320). The categories for the RI are: low ecological risk of contamination (RI < 150), moderate ecological risk (150 ≤ RI < 300), considerable ecological risk (300 ≤ RI < 600) and very high ecological risk (RI > 600).

2.7. Identification of plant species

Herbarium samples were taxonomically identified in the Laboratory of Floristics of the Herbarium of the Natural History Museum of the Universidad Nacional Mayor de San Marcos in Lima, Peru. The procedure was carried out by comparing specimens of unknown plants with reference botanical samples of the local flora.

3. Results and discussion

3.1. Soil properties

Morphological and physicochemical properties of studied soils are shown in Table 1. Soil profiles of the two sampling sites are complex and characterized by the presence of several horizons with contrasting colour, structure, particle size, compactness, and mottling. The colour of soils in site #1 ranged from dark reddish brown (2.5 YR 3/3) to

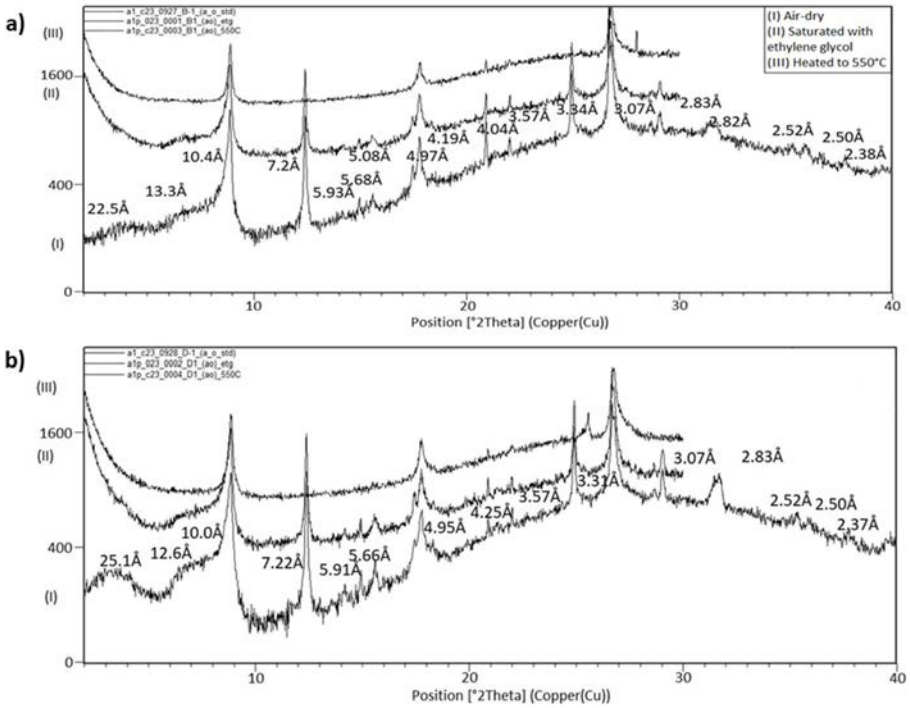

Fig. 3. Diffractogram of soil samples B-1 and D-1 in the site #1 and #2 in the Hualgayoc district, Cajamarca region, Peru.

brownish yellow (10 YR 6/8), while in site#2 ranged from brown (7.5 YR 4/3) to dark yellowish brown (10 YR 4/4). As for soil texture, the sand fraction was prevailing. In site #1, particle-size distribution classifies the studied soils as sandy clay loam (e.g., 50% sand and 32% silt) to clay loam (e.g., 42% sand, 38% clay), akin to soils in site # 2 (60% sand and 22% silt to 54% sand, 28% clay). Soils from both sampled sites yielded extreme acidity with similar pH values between 3.50 and 4.19 in site #1 and 2.74–4.02 in site #2. The soils were identified as non-saline yielding low electrical conductivity (EC) with an average value of 0.11 dSm^{-1} in site #1 and 0.21 dSm^{-1} in site #2. The organic matter (OM) content was moderate to high, between 1.1 and 7.59% in site #1, and between 1.71 and 10.57% in site #2, showing higher values in the topsoil. Available P was relatively low, in the range between 1.8 and 4.9 mg kg^{-1} in site #1 and between 1.8 and 3.9 mg kg^{-1} in site #2. Available K was low, in the range from 36 to 106 mg kg^{-1} in site#1, and 36–134 mg kg^{-1} in site #2. Both topsoils and subsoils had low capacity cation exchange (CEC) with mean values of 14.94 cmol kg^{-1} in Site#1 and 16.56 cmol kg^{-1} in Site#2. The cations of Ca^{2+}, Mg^{2+}, Na^{+} and K^{+} have been practically removed from the soil (Table 1) and no carbonate was found ($CaCO_3$ is systematically 0).

According to the moderate to high organic matter content, brown to dark yellowish-brown colour and extreme acidity, most studied soils showed Andic properties (IUSS Working Group WRB, 2015). Considering the morphology and analytical data (taxonomy of the World Reference Base; IUSS Working Group WRB, 2015), and the soil colour with Munsell Colour Charts, the studied soils are classified as Gleyic Cambisols. In the study performed by Santos-Francés et al. (2017a, 2017b), in the Colquirrumi mine and in the mining project of the Zanja in the Cajamarca region, soils were classified as Haplic Umbrisols, and Umbric Andosols; in addition, these authors also identified Dystric Regosols and Gleyic Cambisols.

The limited availability of P and K in the studied soils can be attributed to the low pH and associated low CEC (Claveria et al., 2019). The soil particle-size, though variable, is relatively coarse (sandy clay loam and clay loam), a fact that is commonly observed in mining waste environments (Delplace et al., 2020). Soils are very poor in essential nutrients when the cations of calcium, magnesium, sodium, and potassium are released and replaced by hydrogen and aluminum instead (Gardi et al., 2015). Our results show that low clay content is directly correlated with decreasing CEC, which has been also described by Kodirov et al. (2018). The bioavailability of nutrients could have been affected by low pH in soils (Claveria et al., 2019) and the unbalanced content of macronutrients points to poor soil management (Egerić et al., 2019). Mining-affected soils show low fertility and low ability to hold cations thus facilitating metal lixiviation, which is further accelerated by the acidic character of soils (Delplace et al., 2020) pointing out the need to introduce corrective measures.

Soils at the Carolina mine, located 4 km SW of the study area (Fig. 1) and studied by Bech et al. (2017) showed basic pH values (up to 8.0) and high calcium carbonate levels, moderate organic carbon contents and silt loam texture. Soils studied by Santos-Francés et al. (2017a, 2017b) at the Colquirrumi mine, located 6 km NW of our study area were acid (pH = 4.6), had low organic matter content (5.04%), moderate CEC (31.7 cmol.Kg^{-1}) and silt sand texture (41.5 silt, 30.8% clay, and 29.5% sand). It is noteworthy that soils at the Carolina mine are on a substrate of carbonate rocks with intercalation of black shales (Pulluicana Group; Fig. 1) that may have exerted an important role in the neutralization of acidity and increased carbonate levels in soils (Crozier and Hardy, 2003; Webb and Sasowsky, 1994). In contrast, the studied soils at Hualgayoc and Colquirrumi are on quartzite and dacite substrates, respectively, which are much less reactive.

3.2. Soil mineralogy

Identification of minerals in B-1 and D-1 samples was achieved by comparison of XRD diffractogram with ICDD database (2007 release) using Diffrac plus Evaluation software. The following minerals were identified: illite, kaolinite, quartz, and jarosite; in addition, a maximum of X-ray diffraction at 4.3 Å was detected, which coincides with the most intense diffraction peak of cristobalite; however, the presence of this mineral in not expected in the studied soils (Fig. 3). Two very wide and low-intensity diffraction maximum were observed for B-1 at 22.5 Å and 13.3. Å, and for D-1, at 25.1 Å and 12.6 Å, which were identified as interstratified minerals from the clays group possibly as an illite-

Table 2
Concentration of Pb, Zn, As, Cu, Ag and Cd (mg kg^{-1}) in soil samples from sites #1 and #2 picked at distances between 0 and 60 m from the contamination points and at depths of 0–15, 15–30, 30–45 and 45–60 cm in the Hualgayoc district, Cajamarca region, Peru.

Distance (m)	Depth (cm)	Pb	Zn	As	Cu	Ag	Cd
			Site 1				
0	0–15	2523	287.2	287	273.8	14.9	1.143
	15–30	2370	290.8	305	267.5	7.7	1.072
	30–45	1944	529	85	183.9	2.3	1.79
	45–60	3278	432.8	400	271.5	6.7	1.472
15	0–15	2322	724.2	395	462.1	13.3	1.759
	15–30	1951	243.9	274	246.9	4.2	0.949
	30–45	1504	241.5	255	230.6	3	1.075
	45–60	1328	167.8	234	202.1	4.2	0.799
30	0–15	1949	375.9	390	333.7	9.2	1.743
	15–30	1506	287.6	343	317.3	4.2	1.284
	30–45	1517	240	1123	369.2	4.1	2.306
	45–60	1493	214.8	3611	302.2	2.2	5.017
45	0–15	1607	353.2	385	369.7	20.7	1.895
	15–30	1129	523.2	252	511.6	4.1	1.64
	30–45	1912	216	168	353.4	0.4	1.054
	45–60	2205	212.3	155	361.1	2.5	1.234
60	0–15	4683	696.3	401	351.9	33.4	4.703
	15–30	3061	368.8	321	307.3	16.3	2.298
	30–45	1535	300.2	336	361.5	4.9	1.909
	45–60	1482	358	346	329.2	3.2	2.05
			Site 2				
0	0–15	2367	277.2	295	277.1	20.4	1.584
	15–30	969	304.6	197	241	3.7	1.116
	30–45	884	122.6	171	168.4	3	0.859
	45–60	814	122	184	166	2.7	0.914
15	0–15	670	230.1	119	117.5	2.7	0.989
	15–30	932	198.1	165	131.3	4.2	0.873
	30–45	1007	239.8	183	156.6	7.2	1.056
	45–60	988	215.5	159	150.2	6.5	0.972
30	0–15	1025	193.7	226	252.7	4.2	0.754
	15–30	934	198.6	213	283	4	0.856
	30–45	906	233.4	216	314.4	3.6	0.952
	45–60	960	201.7	165	247.9	3.5	0.893
45	0–15	1327	145.8	343	255.4	9.7	0.985
	15–30	1086	120.7	292	189.4	11.5	0.761
	30–45	1135	96.7	253	238.3	13.9	0.79
	45–60	1138	73.8	200	237.3	8.4	0.698
60	0–15	1772	120.4	728	149	7.5	0.788
	15–30	1919	138.2	736	146.7	6.5	0.898
	30–45	1155	113.3	846	154	3.8	0.832
	45–60	1086	100.9	924	151.7	7.5	0.808

smectite interstratified. The B-1 sample showed greater abundance of the interstratified clay relative to the sample D-1. The weight proportions of the minerals were difficult to determine due to the presence of amorphous material, identified by the high background (see Fig. 3). In both samples, the diffractograms obtained in the oriented mounts with the treatments showed and confirmed the presence of illite, due to the fact that this mineral did not show any change in the 00l spacings with the ethylene glycol (ETG) and 550 °C treatments (Moore and Reynolds, 1997). Also, the presence of kaolinite was confirmed since the diffraction maximum disappeared when the sample was heated to 550 °C. On the other hand, the diffraction maximum identified as illite-smectite interstratified disappeared when the sample was heated and no clear displacement of the diffraction maximum was observed when the sample was treated with ETG, which made its identification unclear. Semi-quantitative analysis from the RIR (Davis et al., 1990) of the minerals identified in the studied samples showed that illite was very abundant in B-1 (71 wt %), other phases occurring in minor amounts (kaolinite, 21 wt %; quartz, 6 wt %; jarosite and cristobalite (<2 wt %) akin to sample D-1 (illite/sericite, 55 wt %; kaolinite, 27 wt %; quartz, 9 wt %; jarosite, 7 wt %; cristobalite, 3 wt %; Fig. 3a and b). It is worth noting that studied soils lack detectable amounts of carbonate minerals, which agree with the nil calcium carbonate contents according to the calcimetry assay (Table 2).

3.3. Soil elemental composition

Potentially toxic concentrations of Pb, Zn, As, Cu, Ag and Cd were found out of a total of 34 elements analysed. Metal and metalloid concentrations in soils from site #1 are provided in Table 2 and graphically shown in Supplementary Fig. S1. Concentrations are relatively highly variable among the studied samples. In general terms, Pb was the metal showing the highest concentrations, which were in the range between 1129 and 4683 mg kg^{-1}. Although the distribution pattern of Pb is rather erratic, it is maximum in the topsoil with the exception of the soil profile sampled at 0 m from the contamination point, in which the concentration of Pb is maximum at a depth of 45–60 cm. There is also a

Table 4
Geo-accumulation index (Igeo) for soils sampled at five distances from the contamination points and at four depths (topsoil: 0–15 and 15–30 cm; subsoil: 30–45 and 45–60 cm) in sampling sites #1 and #2 in the Hualgayoc district, Cajamarca region, Peru.

Metals	Pb	Zn	As	Cu	Ag	Cd
Geochemical baseline values in a natural region - From the mining project La Zanja (2006) [a]	44.87	47.42	27.5	22.2	–	4.36
Abundances of Chemical Elements in the Earth's Crust[b]	16	83	1.7	47	0.07	0.13
Geo-accumulation index (Igeo)						
Site 1						
Minimum (Min)	4.07	1.24	1.04	2.47	1.93	−3.03
Maximum (Max)	6.12	3.35	6.45	3.94	8.31	−0.38
Average	5.09	2.29	3.75	3.20	5.12	−1.71
Site 2						
Minimum (Min)	3.32	0.05	1.53	1.82	4.68	−3.23
Maximum (Max)	5.14	2.10	4.49	3.24	7.60	−2.05
Average	4.23	1.08	3.01	2.53	6.14	−2.64

[a] Santos-Francés et al. (2017a).
[b] Yaroshevsky (2006).

Table 3
Representative analyses of sphalerite in the sampling sites from the Hualgayoc district with chemical composition in wt. % (EPMA data).

	Sample	2018-HUALGA-A	2018-HUALGA-A	2018-HUALGA-A	2018-HUALGA-A	2018-HUALGA-A	2018-HUALGA-A
d.l.	Analysis no.	Circle E-sl	Circle D-sl-001	Circle D-sl-002	Circle C-sl-001	Circle B-sl-001	Circle A-sl-001
0.07	S	32.87	32.89	32.58	32.57	32.79	32.66
0.18	Pb	0.19	<d.l.	0.26	0.22	<d.l.	<d.l.
0.07	Zn	66.38	66.48	66.84	66.96	67.10	66.12
0.05	Fe	1.06	0.94	0.68	0.80	0.54	1.02
0.06	Cd	0.46	0.29	0.30	0.28	0.38	0.63
	Total	100.95	100.60	100.65	100.83	100.82	100.43

Sb, In, As, Ga, Ge, Cu, Ag, Sn < d.l.: below detection limit.

Table 5
Nemerow Pollution Index (NI) and Improved Nemerow Index (INI) calculated for soils sampled at five distances from the contamination points and at four depths in the sampling sites #1 and #2 in the Hualgayoc district, Cajamarca region, Peru.

Samples	*Pi*						NI	INI (based in Igeo values)
	Pb	Zn	As	Cu	Ag	Cd		
Site 1								
Minimum (Min)	25.16	3.54	3.09	8.28	5.71	0.18	31.41	3.66
Maximum (Max)	104.37	15.27	131.31	23.05	477.14	1.15	345.41	6.52
Average	46.02	7.45	18.30	14.43	115.36	0.43	188.41	5.09
Site 2								
Minimum (Min)	14.93	1.56	4.33	5.29	38.57	0.16	28.43	3.53
Maximum (Max)	52.75	6.42	33.60	14.16	291.43	0.36	210.72	5.80
Average	25.71	3.63	12.03	9.07	96.07	0.21	119.58	4.67

Table 6
Individual ecological risk index (Er) and Potential Ecological Risk Index (RI) calculated for the studied soils from the Hualgayoc district, Cajamarca region, Peru.

Samples	Er						RI
	Pb	Zn	As	Cu	Ag	Cd	
Site 1							
Minimum (Min)	125.81	3.54	30.91	41.42	285.71	5.50	651.27
Maximum (Max)	521.84	15.27	408.36	115.23	23857.14	34.52	24651.10
Average	323.82	9.41	219.64	78.32	12071.43	20.01	12651.18
Site 2							
Minimum (Min)	74.66	1.56	43.27	26.46	1928.57	4.80	2084.63
Maximum (Max)	263.76	6.42	336.00	70.81	14571.43	10.90	15021.62
Average	169.21	3.99	189.64	48.64	8250.00	7.85	8553.12

Table 7
Native flora with their family name in the sampling site #1 in the Hualgayoc district, Cajamarca region, Peru.

N°	Family name	Scientific name	biological replicates
1	Asteraceae	*Achyrocline alata*	2
2		*Ageratina fastigiate*	3
3		*Ageratina glechonophylla*	2
4		*Baccharis alnifolia*	1
5	Bromeliaceae	*Puya sp*	1
6	Caryophyllaceae	*Arenaria digyna*	1
7	Ericaceae	*Bejaria sp.*	1
8		*Pernettya prostrata*	1
9	Hypericaceae	*Hypericum laricifolium*	4
10	Iridaceae	*Orthrosanthus chimboracensis*	1
11	Melastomalaceae	*Brachyotum radula*	2
12	Poaceae	*Calamagrostis recta*	2
13		*Chusquea scandens*	2
14		*Cortaderia bifida*	5
15	Solanaceae	*Nicotiana thyrsiflora*	1

Table 8
Native flora with their family name in the sampling site #2 in the Hualgayoc district, Cajamarca region, Peru.

N°	Family name	Scientific name	biological replicates
1	Asteraceae	*Achyrocline alata*	1
2	Calceolariaceae	*Calceolaria tetragona*	2
3	Ericaceae	*Gaultheria glomerata*	1
4		*Pernettya prostrata*	2
5		*Vaccinium floribundum*	1
6	Hypericaceae	*Hypericum laricifolium*	1
7	Melastomalaceae	*Brachyotum radula*	2
8		*Miconia vaccinioides*	1
9	Poaceae	*Cortaderia bifida*	5
10		*Festuca sp*	1
11	Polygonaceae	*Muehlenbeckia tamnifolia*	1
12	Scrophulariaceae	*Buddleja interrupta*	1

general enrichment trend in Pb with decreasing distances to the contamination point, with the notable exception of the soil profile sampled at 60 m from the contamination source, which registers indeed the highest Pb concentration. Zinc concentrations were in the range between 167.8 and 724.2 mg kg^{-1}, with the highest values recorded in topsoil samples located at a distance of 15 and 60 m from the contamination point (724.2 and 696.3 mg kg^{-1}, respectively) and general enrichment on the topsoil. Exceptionally, the sample collected at the contamination point (0 m) at a depth of 45–60 cm yields a higher concentration of Zn regarding upper soil layers. The concentration of As was in the range from 85 to 3611 mg kg^{-1} and is normally higher in the topsoil regarding the subsoil. Nevertheless, soil sampled at 30 m of distance to the contamination point yields extremely high As concentrations (1123–3611 mg kg^{-1}) in the subsoil. Copper concentrations varied between 183.9 and 511.6 mg kg-1, showing a slight increase in topsoil samples at distances of 15 and 45 m from the contamination point (462.1 and 511.6 mg kg-1). Copper concentrations remain relatively constant in the other studied soil samples regardless their location and depth of sampling. Silver contents were relatively low, between 0.4 and 33.4 mg kg^{-1}, and Cd presented the lowest concentrations in the range between 1 and 5 mg kg^{-1}.

In soils from sampling site #2, Pb was the most concentrated metal with values between 670 and 2367 mg kg^{-1}. The highest concentration was found in the upper soil layer located adjacent to the contamination point. In the soil sampled at 15 m from the contamination point, however, samples in the subsoil yielded higher Pb concentrations than samples in the topsoil. The values of Zn varied in the range between 73.8 and 304.6 mg kg^{-1}. Akin to Pb, Zn concentration was maximum in soil sampled adjacent to the contamination point and its concentration in the topsoil steadily decreases at increasing distances from the contamination point. The concentrations of As were in the range between 119 and 924 mg kg^{-1}, and in general, increased progressively at increasing distances from the contamination point, so that, the highest concentrations were obtained at 60 m of distance. Copper contents in studied soils were in the range between 117.5 and 314.4 mg kg^{-1}. Soils sampled at 0 and 45 m from the contamination point had higher Cu concentrations in the

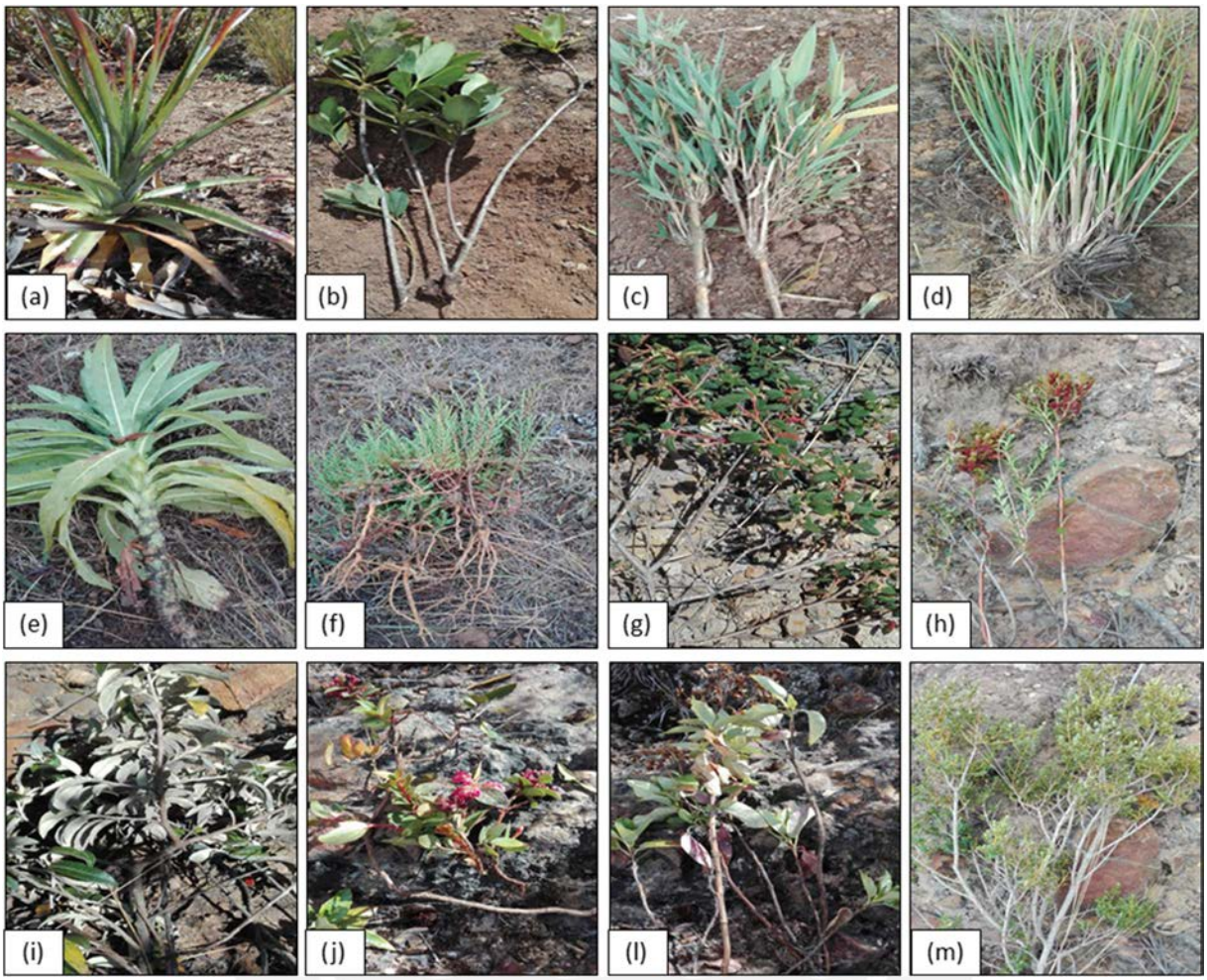

Fig. 4. Native flora from sampling sites: (a) *Puya sp*, (b) *Bejaria sp*, (c) *Chusquea scandens*, (d) *Cortaderia bifida*, (e) *Nicotiana thyrsiflora*, (f) *Hypericum laricifolium*, (g) *Brachyotum radula*, (h) *Pernettya prostrata*, (i) *Buddleja interrupta*, (j) *Gaultheria glomerata*, (l) *Calceolaria tetragona*, (m) *Miconia vaccinioides.*

Table 9
Native plant species studied in terms of Phytoremediation in Latin America.

Family	Native Species	Information on Publications about metals	Soils pH values	Name of the mine	Country	Reference
Asteraceae	*Ageratina sp.*	Phytoextraction of Zn Hyperaccumulator of Pb	6.8–8 (basic)	Carolina mine - Hualgayoc	Peru	Bech et al., 2017, 2016
	Achyrocline alata	As, Cu, Pb and Zn Phytoextraction of Zn				
	Baccharis latifolia	As, Cu, Pb and Zn				
		As, Ba, Cu, Fe, Mn, Zn and Hyperaccumulator of Pb	7,4 ± 0,5 (neutro)			Durán Cuevas (2010); Oyuela Leguizamo et al. (2017)
	Baccharis amdatensis	As, Cd, Cu, Pb and Zn	<4 (acid)	Bartolomé mine	Ecuador	Bech et al. (2017)
	Baccharis rhomboidalis	Cu, Pb and Zn	3.9 (acid)	Teniente mine	Chile	
	Baccharis dracunculifolia DC. Baccharis trimera Less DC	Cd, Cr, Pb, V, Ba	6.2 (basic)	Camaquã mine	Brasil	França Afonso et al. (2020)
Melastomataceae	*Miconia lutescens*	As, Cu and Zn	4.8 (acid)	Turmalina mine - Piura	Peru	Bech et al. (2017)
Poaceae	*Cortaderia Hapalotricha*	Hyperaccumulator of Pb	6.8–8 (basic)	Carolina Mine - Hualgayoc	Peru	
	Cortaderia nitida	As, Cd, Cu, Pb and Zn	<4 (acid)	Bartolomé mine	Ecuador	
Polygonaceae	*Muehlenbeckia hastulata*	Cu, Zn and Pb	5.4 (acid)	No mine - Los Maitenes area in the Puchuncaví Valley	Chile	Córdova et al. (2011)
Solanaceae	*Nicotiana*	Cr, Mn, Fe, Co, Ni, Cu, Zn, As, Sb, Hg and Pb	Acid	Wadley antimony mine district - San Luis, Potosí	Mexico	Levresse et al. (2012)

topsoil regarding samples from deeper sampling levels; in contrast, soils sampled at 15, 30 and 60 m from the contamination point showed the opposite trend. The Ag concentrations varied between 2.7 and 20.4 mg kg^{-1} and Cd concentrations were systematically very low and rather constant for all samples with an average concentration of 0.9 mg kg^{-1}.

The heavy metals concentrated in the studied soils are in close linkage with the ore mineralogy of the Ex Mining unit Los Negros in the Hualgayoc district, which includes abundant iron sulphides (mostly pyrite, but also marcasite, and pyrrhotite), galena, sphalerite and arsenopyrite. EPMA analyses on sphalerite grains, in addition, show moderate concentrations of Cd in the range between 0.28 and 0.63 wt % (Table 3).

According to the Peruvian Environmental Quality Standards (PEQS) for agricultural soil, the maximum allowed contents of Pb, As, and Cd are of 70, 50, and 1.4 mg kg^{-1}, respectively (Ministerio del Ambiente, 2017), tantamount to Canadian Soil Quality Guidelines (CSQG; Canadian Council of Ministers of the Environment, 2007) for Pb and Cd. The CSQG, however, establishes a maximum allowed value of 12 mg kg^{-1} for As. In sampling sites #1 and #2, measured concentrations of Pb and As exceeded the maximum allowed values by environmental regulations. Cadmium concentrations were mostly below maximum allowed concentrations in both sites. PEQS does not establish maximum concentrations for Ag, Cu, and Zn whereas CSQG contemplates maximum values of 20, 250, and 63 mg kg^{-1}, respectively (Canadian Council of Ministers of the Environment, 2018, 2007). According to Canadian standards, Zn concentrations exceeded the maximum allowed values in samples from site #1, mainly in the topsoil and in samples from site #2 at 0 m in the topsoil. Copper concentrations in both sites considerably exceeded the maximum values allowed according to CSQG, and the maximum allowed content of Ag was only exceeded at 45–60 m from the contamination point for site#1 and at 0m from the contamination point for site #2. High concentrations of heavy metals largely exceeding maximum allowed concentrations according to both PEQS and CSQG are reported in soils from neighbouring Colquirrumi (Pb = 2068.76 mg kg^{-1}, Zn = 1893.06 mg kg^{-1}, As = 428.32 mg kg^{-1}, Cu = 197.70 mg kg^{-1}, Cd = 13.03 mg kg^{-1}; Santos-Francés et al., 2017a) and Carolina (Pb = 3992–16,060 mg kg^{-1}, Zn = 11550-28059 mg kg^{-1}, As = 256–2070 mg kg^{-1}, Cu = 280–1030 mg kg^{-1}; Bech et al., 2017) mining areas (Fig. 1).

3.4. Indices of soil pollution

3.4.1. The geoaccumulation index, the Nemerow Pollution index and Improved Nemerow Index

Geochemical baselines for Pb, Zn, As, Cu, and Cd were established in soils from the La Zanja mining project, which is located 30 km SW of our sampling sites, in 2006 (i.e., before its exploitation; Santos-Francés et al., 2017a). For Ag, we considered the natural abundance in the Earth's crust (Yaroshevsky, 2006). All indices were calculated for topsoil and subsoil portions (Tables 4 and 5). The Igeo values revealed that the level of soil pollution ranged from unpolluted to extremely polluted in both sampling sites (Table 4). Considering the Igeo, studied soils were unpolluted with Cd, but moderately to highly polluted (site#1), and moderately polluted (site #2) with Zn. Regarding Cu, soils were highly polluted in site#1 and moderately to highly polluted in site#2, and regarding As, soils were highly polluted in both sampling sites. Studied soils are extremely polluted in site #1 and highly to extremely polluted in site #2 with Pb, and extremely polluted with Ag in both sites. Calculated Igeo values here are mostly equivalent to other studied mining soils in the region. Bech et al. (2016) reported Igeo values for soils in the Carolina mine (Fig. 1) pointing to extreme contamination with Pb and Zn, and slight to moderate contamination with As and Cu. Santos-Francés et al. (2017a, 2017b) stated that soils in the Colquirrumi mining area (Fig. 1) ranged from uncontaminated to extremely contaminated.

NI values of trace metals in soils were relatively high, ranging in sampled soils from site #1 between 31.41 and 345.41, and in soils from site #2, between 28.43 and 210.72 (Table 5) corresponding to heavy contamination (NI > 3); however, the high NI figures could be due to used background values. INI values were of 5.09 (class 6: extremely contaminated) in soils from site #1 and of 4.67 (class 5: heavily to extremely contaminated) in soils from site #2. It should be noticed that INI is considered much more accurate in assessing the environmental risks of the contamination compared with NI (Li et al., 2019). In short, the presented heavy metal analyses in mining soils from both studied sites indicate high indices of contamination and the need for effective contamination control and remediation (Li et al., 2018).

3.4.2. Ecological risk assessment

Soils contaminated with heavy metals may cause severe ecological risks and negatively impact human health though different forms of interaction (agriculture, cattle breeding, etc.) since highly toxic metals can get introduced into the food chain (Li et al., 2019). Therefore, the potential ecological risk for Pb, Zn, As, Cu, Ag, and Cd in soils were evaluated (Table 6).

According to the Er index, levels of metal contamination in the subsoil and topsoil were similar in both studied sites and varied from low to extreme ecological risk. Cadmium and Zn represented a low contamination risk (Er < 40), Cu represented a moderate risk of contamination (40 ≤ Er < 80), As represented a considerable contamination risk (80 ≤ Er < 160), and Pb and Ag represented an extreme contamination risk (Er > 320). The impact of the metals coincides with Igeo impact (Table 4). On the other hand, considering the RI for all the studied metals and metalloids, there is a very high ecological risk (RI ≥ 600). The observed extreme accumulation of metals and metalloids in the soils (chiefly Pb and As) can impact ecosystems, affect the quality and safety of food, and increase the risk of serious diseases (cancer, kidney, liver damage, etc.; Li et al., 2019).

3.5. Inventory of native flora

The results of the ecological risk assessment revealed conspicuous soil contamination with heavy metals (Nouri and Haddioui, 2016), which may have a big impact on ecosystems (Swartjes et al., 2011). Native plants colonizing polluted sites must be evaluated as chief candidates for phytoremediation, because i) they are able to perform better than other species in terms of survival, growth, and reproduction as they are already adapted to the local climate; and ii) they have intrinsically demonstrated the capability of growing in soils contaminated with heavy metals (Marchiol et al., 2013).

In this study, an inventory of the native plants that grew at the contaminated sampling sites was conducted. A total of 15 species were inventoried in site #1 (Table 7) and a total of 12 species were inventoried in site#2 totaling 22 plants of native flora belonging to 12 family species (Table 8). Fig. 4 shows pictures of some of the species identified. The following 5 species were found in both studied sites: *Achyrocline alata*, *Pernettya prostrata*, *Hypericum laricifolium*, *Brachyotum radula*, and *Cortaderia bifida*.

Bech et al. (2017) reported that in the Carolina mining area (Fig. 1), some native plants growing up in soils affected by mining activity accumulated considerable amounts of metals in their tissues. Of these plants, *Achyrocline alata*, common specie with our study, accumulated high concentrations of Zn and was considered as a promising species for phytoextraction of Zn. Table 9 contains native species of botanical families that coincide with those at our study and that have been described to grow in soils (either acidic or alkaline) with presence of toxic metals derived from active and abandoned mines in Latin America; native species in this table, in addition, have demonstrated ability to transport potential hazardous elements from roots to shoots, and are therefore considered suitable candidates for the phytoremediation.

Also noteworthy is the fact that some of the inventoried species in the studied sites are used in traditional Peruvian medicine, such as

Hypericum laricifolium (Vidal Ccana-Ccapatinta and Lino von Poser, 2015). In addition, Andean berries or wild berry of *Vaccinium floribundum* (known locally as "mortiño") are consumed as fruits, in juice and jam (Vizuete et al., 2016). This research through the identification of specific flora at MEL sites in the Andes is a first step to the identification of native plant species for phytoremediation in heavily contaminated soils.

4. Conclusions

Soil samples collected around two mining environmental liabilities (MEL sites) from the Hualgayoc district in the Peruvian Andes showed extremely acid pH values (3.50–4.19 in site #1 and 2.74–4.02 in site #2). Most soils showed Andean properties and classified as Gleyic Cambisol. Soil mineralogy was dominated by illite, kaolinite, quartz, and jarosite, and carbonates were systematically absent. The concentrations of Pb, Zn, As, Cu, and Ag (up to 4683, 724.2, 3611, 511.6, and 33.4 mg kg^{-1}, respectively) exceeded the maximum allowable values for agricultural soils according to the Peruvian and Canadian regulations. The geo-accumulation (Igeo), Nemerow Pollution (NI), Improved Nemerow (INI), and Potential Ecological Risk (RI) indexes were used to assess soil pollution. According to the Igeo index, studied soils are unpolluted to extremely polluted (increasing indexes are Cd < Zn < Cu < As < Pb < Ag). The Nemerow Pollution Index (NI) indicates heavy contamination, and the Improved Nemerow Index (INI), heavy to extreme contaminations. The RI points to a very high ecological risk reflecting serious impact caused by MEL sites and potential affectation to the ecosystems and the local communities. On the other hand, this research contributes with an inventory of native flora - 22 plants of native flora belonging to 12 family species - that grow up around the studied MEL sites and that, therefore, have potential to be used for phytoremediation purposes.

Author statement

Edith Cruzado-Tafur: Conceptualization, Methodology, Investigation, Writing – original draft preparation; Lisard Torró; : Conceptualization, Methodology, Writing- Reviewing and Editing, Supervision; Katarzyna Bierla: Methodology, Visualization; Joanna Szpunar: Conceptualization, Methodology, Supervision; Esperança Tauler: Methodology, Investigation.

Declaration of competing interest

The authors declare that they have no known competing financial interests or personal relationships that could have appeared to influence the work reported in this paper.

Acknowledgments

We thank Dr. Manuel Timaná, Director of the Centro de Geografia Aplicada (CIGA) of the Pontifical Catholic University of Peru (Peru) and Mg. Paul Gonzales Arce, Laboratory of Floristics of the Herbarium of the Natural History Museum of the Universidad Nacional Mayor de San Marcos (Peru) for their assistance in the taxonomic identification. The authors express deep gratitude to Dr. Marcial Blondet, former Director of the Ph.D. program in Engineering at the Pontifical Catholic University of Peru for the economic support. We wish to thank Rodolfo Lazo Dávila and Karem Solano Herrera from Activos Mineros S.A.C (AMSAC-Peru) for the permission granted for sampling in the study area in Hualgayoc. We appreciate the technical support by Xavier Llovet (Centres Científics i Tecnològics, Universidad de Barcelona, CCiT-UB) and Mg. Diego Benites during the acquisition of EPMA data. We are grateful to two anonymous reviewers for their constructive comments which significantly improved the manuscript.

Appendix A. Supplementary data

Supplementary data to this article can be found online at https://doi.org/10.1016/j.jsames.2020.103107.

References

Angst, G., Mueller, C.W., Angst, S., Pivokonský, M., Franklin, J., Stahl, P.D., Frouz, J., 2018. Fast accrual of C and N in soil organic matter fractions following post-mining reclamation. across the USA 209, 216–226. https://doi.org/10.1016/j.jenvman.2017.12.050.

Bech, J., Poschenrieder, C., Barceló, J., Lansac, A., 2002. Plants from mine spoils in the South American Area as potential sources of germplasm for phytorenmediation technologies. Acta Biotechnol. 22, 5–11.

Bech, J., Roca, N., Tume, P., 2017. Hazardous element accumulation in soils and native plants in areas affected by mining activities in South America. In: Assessment, Restoration and Reclamation of Mining Influenced Soils. Elsevier Inc., pp. 419–461

Bech, J., Roca, N., Tume, P., Ramos-Miras, J., Gil, C., Boluda, R., 2016. Screening for new accumulator plants in potential hazards elements polluted soil surrounding Peruvian mine tailings. Catena 136, 66–73.

Borredon, R., 1982. Etude geologique et metallogenique du district minier de Hualgayoc (Perou septentrional) aplomb-zinc-cuivre argent. Université de Paris VI.

Bouyoucos, G.J., 1936. Directions for making mechanical analyses of soils by the hydrometer method. Soil Sci. 42 (3), 225–230.

Canadian Council of Ministers of the Environment, 2018. Canadian Soil Quality Guidelines for the Protection of Environmental and Human Health: Zinc 2018, Canadian Environmental Quality Guidelines, 1999. Winnineg, Canada.

Canadian Council of Ministers of the Environment, 2007. Canadian Soil Quality Guidelines for the Protection of Environmental and Human Health: Summary Tables. Update September 2007, Canadian Environmental Quality Guidelines, 1999. Winnineg, Canada.

Canchaya, S., 1990. Stratabound ore deposits of Hualgayoc, Cajamarca, Perú. In: Fontboté, L., Amstutz, C., Cardozo, M., Cedillo, E., Frutos, J. (Eds.), Stratabound Ore Deposits in the Andes. Springer–Verlag, Berlin Heidelberg-New York, pp. 569–582.

Chaabani, S., Abdelmalek-Babbou, C., Ben Ahmed, H., Chaabani, A., Sebei, A., 2017. Phytoremediation assessment of native plants growing on Pb–Zn mine site in Northern Tunisia. Environ. Earth Sci. 76, 1–15.

Chappuis, M., 2019. Remediación y activación de pasivos ambientales mineros (PAM) en el Perú. Medio Ambient. y Desarro. N° 168, Com. Económica para América Lat. y el Caribe.

Claveria, R.J.R., Perez, T.R., Perez, R.E.C., Algo, J.L.C., Robles, P.Q., 2019. The identification of indigenous Cu and as metallophytes in the Lepanto Cu-Au Mine, Luzon, Philippines. Environ. Monit. Assess. 191.

Córdova, S., Neaman, A., González, I., Ginocchio, R., Fine, P., 2011. The effect of lime and compost amendments on the potential for the revegetation of metal-polluted, acidic soils. Geoderma 166, 135–144. https://doi.org/10.1016/j.geoderma.2011.07.022.

Crozier, C.R., Hardy, D.H., 2003. Soil Facts: Soil Acidity and Liming: Basic Information for Farmers and Gardeners. North Carolina Coop. Ext. AG, pp. 439–451.

Davis, B.L., Kath, R., Spilde, M., 1990. The reference intensity ratio: its measurement and significance. Powder Diffr. 5, 76–78. https://doi.org/10.1017/S0885715600015372.

Delplace, G., Schreck, E., Pokrovsky, O.S., Zouiten, C., Blondet, I., Darrozes, J., Viers, J., 2020. Accumulation of heavy metals in phytoliths from reeds growing on mining environments in Southern Europe. Sci. Total Environ. 712.

Duodu, G.O., Goonetilleke, A., Ayoko, G.A., 2016. Comparison of pollution indices for the assessment of heavy metal in Brisbane river. Environ. Pollut. 219, 1077–1091.

Durán Cuevas, P.A., 2010. Transferencia de metales de suelo a planta en áreas mineras: Ejemplos de los Andes peruanos y de la Cordillera Prelitoral Catalana.

Egerić, M., Smičiklas, I., Dojčinović, B., Sikirić, B., Jović, M., 2019. Geoderma Interactions of acidic soil near copper mining and smelting complex and waste-derived alkaline additives. Geoderma 352, 241–250.

Figueroa, B.E., Orihuela, R.C., Calfucura, T.E., 2010. Green accounting and sustainability of the Peruvian metal mining sector. Resour. Policy 35, 156–167.

França Afonso, T., Faccio Demarco, C., Pieniz, S., Silveira Quadro, M., Camargo, F.A.O., Andreazza, R., 2020. Bioprospection of indigenous flora grown in copper mining tailing area for phytoremediation of metals. J. Environ. Manag. 256.

Gajić, G., Djurdjević, L., Kostić, O., Jarić, S., Mitrović, M., Pavlović, P., 2018. Ecological potential of plants for phytoremediation and ecorestoration of fly ash deposits and mine wastes. Front. Environ. Sci. 6, 1–24. https://doi.org/10.3389/fenvs.2018.00124.

Gardi, C., Angelini, M., Barceló, S., Comerma, J., Cruz Gaistardo, C., Encina Rojas, A., Jones, A., Krasilnikov, P., Mendonça Santos Brefin, M.L., Montanarella, L., Muñiz Ugarte, O., Schad, P., Vara Rodríguez, M.I., Vargas, R., Ravina da Silva, M., 2015. Soil Atlas of Latin America and the Caribbean. European Commission, Publications Office of the European Union. https://doi.org/10.1002/9781118556115.ch38. L-2995 Luxembourg.

Hauptvogl, M., Kotrla, M., Prčík, M., Pauková, Ž., Kováčik, M., Lošák, T., 2019. Phytoremediation potential of fast-growing energy plants: challenges and perspectives – a review. Pol. J. Environ. Stud. 29, 505–516. https://doi.org/10.15244/pjoes/101621.

INGEMMET, I.G.M. y M., 2017. Mapa geológico del cuadrángulo de Chota 14f (1157). Serie A: Carta geológica Nacional. Escala 1, 100 000.

IUSS Working Group WRB, 2015. World Reference Base for Soil Resources 2014: International Soil Classification Systems for Naming Soils and Creating Legends for Soil Maps, Update 2015, World Soil Resources Reports No. 106. FAO, Rome.
JI, Y., FENG, Y., WU, J., ZHU, T., BAI, Z., DUAN, C., 2008. Using geoaccumulation index to study source profiles of soil dust in China. J. Environ. Sci. 20, 571–578. https://doi.org/10.1016/S1001-0742(08)62096-3.
Kodirov, O., Kersten, M., Shukurov, N., Martín Peinado, F.J., 2018. Trace metal(loid) mobility in waste deposits and soils around Chadak mining area. Uzbekistan. Sci. Total Environ. 622–623, 1658–1667.
Lam, E.J., Cánovas, M., Gálvez, M.E., Montofré, Í.L., Keith, B.F., 2017. Evaluation of the phytoremediation potential of native plants growing on a copper mine tailing in northern Chile. J. Geochem. Explor. 182, 210–217.
Levresse, G., Lopez, G., Tritlla, J., López, E.C., Chavez, A.C., Salvador, E.M., Soler, A., Corbella, M., Sandoval, L.G.H., Corona-Esquivel, R., 2012. Phytoavailability of antimony and heavy metals in arid regions: the case of the Wadley Sb district (San Luis, Potosí, Mexico). Sci. Total Environ. 427–428, 115–125. https://doi.org/10.1016/j.scitotenv.2012.04.020.
Li, L., Wu, J., Lu, J., Min, X., Xu, J., Yang, L., 2018. Distribution, pollution, bioaccumulation, and ecological risks of trace elements in soils of the northeastern Qinghai-Tibet Plateau. Ecotoxicol. Environ. Saf. 166, 345–353. https://doi.org/10.1016/j.ecoenv.2005.12.006.
Li, Z., Deblon, J., Zu, Y., Colinet, G., Li, B., He, Y., 2019. Geochemical baseline values determination and evaluation of heavy metal contamination in soils of lanping mining valley (Yunnan province, China). Int. J. Environ. Res. Publ. Health 16, 1–18. https://doi.org/10.3390/ijerph16234686.
Liu, G., Shi, Y., Guo, G., Zhao, L., Niu, J., Zhang, C., 2020. Soil pollution characteristics and systemic environmental risk assessment of a large-scale arsenic slag contaminated site. J. Clean. Prod. 251 https://doi.org/10.1016/j.jclepro.2019.119721.
Macfarlane, A.W., Petersen, U., 1990. Pb isotopes of the Hualgayoc area, northern Peru: implications for metal provenance and genesis of a Cordilleran polymetallic mining district. Econ. Geol. 85, 1303–1327.
Macfarlane, A.W., Prol-Ledesma, R.M., Conrad, M.E., 1994. Isotope and fluid inclusion studies of geological and hydrothermal processes, northern Peru. Int. Geol. Rev. 36, 645–677.
Marchiol, L., Fellet, G., Boscutti, F., Montella, C., Mozzi, R., Guarino, C., 2013. Gentle remediation at the former "Pertusola Sud" zinc smelter: evaluation of native species for phytoremediation purposes. Ecol. Eng. 53, 343–353. https://doi.org/10.1016/j.ecoleng.2012.12.072.
Mazurek, R., Kowalska, J.B., Gąsiorek, M., Zadrożny, P., Wieczorek, J., 2019. Pollution indices as comprehensive tools for evaluation of the accumulation and provenance of potentially toxic elements in soils in Ojców National Park. J. Geochem. Explor. 201, 13–30. https://doi.org/10.1016/j.gexplo.2019.03.001.
Midhat, L., Ouazzani, N., Hejjaj, A., Ouhammou, A., Mandi, L., 2019. Accumulation of heavy metals in metallophytes from three mining sites (Southern Centre Morocco) and evaluation of their phytoremediation potential. Ecotoxicol. Environ. Saf. 169, 150–160.
Ministerio de Energía y Minas, 2019. Ministry Resolution N° 010-2019-MEM/DM. Actualizan Inventario Inicial de Pasivos Ambientales Mineros. D. Of. El Peru.
Ministerio de Energía y Minas, 2018. Anuario Minero 2018, pp. 1–99.
Ministerio de Energía y Minas, 2004. Law 28271. Ley que regula los pasivos ambientales de la actividad minera. D. Of. El Peru.
Ministerio del Ambiente, 2017. Supreme Decree N° 011-2017-MINAM. Aprueban Estándares de Calidad Ambiental (ECA) para suelo, 4. D. Of. El Peru.
Moore, D.M., Reynolds, R.C.J., 1997. X-Ray Diffraction and the Identification and Analysis of Clay Minerals, Second. Oxford University Press, Oxford.
Moreno-Jiménez, E., Vázquez, S., Carpena-Ruiz, R.O., Esteban, E., Peñalosa, J.M., 2011. Using Mediterranean shrubs for the phytoremediation of a soil impacted by pyritic wastes in Southern Spain: a field experiment. J. Environ. Manag. 92, 1584–1590.
Muller, G., 1969. Index of geo-accumulation in sediments of the rhine river. GeoJournal 2, 108–118.
Nouri, M., Haddioui, A.E.M., 2016. Assessment of metals contamination and ecological risk in ait ammar abandoned iron mine soil. Moroco. Ekol. Bratislava 35, 32–49. https://doi.org/10.1515/eko-2016-0003.
Oblasser, A., Chaparro Ávila, E., 2008. Estudio comparativo de la gestión de los pasivos ambientales mineros en Bolivia, Chile, Perú y Estados Unidos. Recur. Nat. e Infraestruct. N°131.Comisión Económica para América Lat. y el Caribe 1–79.
Oyuela Leguizamo, M.A., Fernández Gómez, W.D., Sarmiento, M.C.G., 2017. Native herbaceous plant species with potential use in phytoremediation of heavy metals, spotlight on wetlands — a review. Chemosphere 168, 1230–1247. https://doi.org/10.1016/j.chemosphere.2016.10.075.
Padilla, W.G., 2019. Hualgayoc, Riqueza Y Tradición. Asociación Cultural ArteSano, Cajamarca, Peru.
Pinto Herrera, H., 2014. Los pasivos mineros ambientales y los conflictos sociales en Hualgayoc. Investig. Soc. 17, 265–277. https://doi.org/10.15381/is.v17i30.8033.
Różański, S.Ł., Kwasowski, W., Castejón, J.M.P., Hardy, A., 2018. Heavy metal content and mobility in urban soils of public playgrounds and sport facility areas, Poland. Chemosphere 212, 456–466. https://doi.org/10.1016/j.chemosphere.2018.08.109.
Santos-Francés, F., Martínez-Graña, A., Rojo, P.A., Sánchez, A.G., 2017a. Geochemical background and baseline values determination and spatial distribution of heavy metal pollution in soils of the Andes mountain range (Cajamarca-Huancavelica, Peru). Int. J. Environ. Res. Publ. Health 14, 22.
Santos-Francés, F., Martínez-Graña, A., Zarza, C.Á., Sánchez, A.G., Rojo, P.A., 2017b. Spatial distribution of heavy metals and the environmental quality of soil in the Northern Plateau of Spain by geostatistical methods. Int. J. Environ. Res. Publ. Health 14. https://doi.org/10.3390/ijerph14060568.
Sparks, D.L., 1996. Chemical methods. In: Methods of Soil Analysis. Soil Science Society of America, Inc. American Society of Agronomy, Inc., Madison, Wisconsin, USA.
Swartjes, F.A., Breure, A.M., Beaulieu, M., 2011. Introduction to ecological risk assessment. In: Dealing with Contaminated Sites. Springer Science Business Media B. V., pp. 573–619. https://doi.org/10.1007/978-90-481-9757-6
Unger, C.J., Lechner, A.M., Kenway, J., Glenn, V., Walton, A., 2015. A jurisdictional maturity model for risk management, accountability and continual improvement of abandoned mine remediation programs. Resour. Policy 43, 1–10. https://doi.org/10.1016/j.resourpol.2014.10.008.
Vidal Ccana-Ccapatinta, G., Lino von Poser, G., 2015. Phytochemistry letters acylphloroglucinol derivatives from Hypericum laricifolium Juss. Phytochem. Lett. 12, 63–68.
Vizuete, K.S., Kumar, B., Vaca, A.V., Debut, A., Cumbal, L., 2016. Mortiño (Vaccinium floribundum Kunth) berry assisted green synthesis and photocatalytic performance of Silver-Graphene nanocomposite. J. Photochem. Photobiol. A Chem. 329, 273–279. https://doi.org/10.1016/j.jphotochem.2016.06.030.
Walkley, A., Black, I.A., 1934. Estimation of soil organic carbon by the chromic acid titration method. Soil Sci. 37, 29–38. https://doi.org/10.1097/00010694-193401000-00003.
Webb, J.A., Sasowsky, I.D., 1994. The interaction of acid mine drainage with a carbonate terrane: evidence from the Obey River, north-central Tennessee. J. Hydrol. 1694, 327–346.
Yaroshevsky, A.A., 2006. Abundances of chemical elements in the Earth's crust. Geochem. Int. 44, 48–55.
Yupari, A., 2003. Pasivos ambientales mineros en Sudamérica, Informe elaborado para la CEPAL, el Instituto Federal de Geociencias y Recursos Naturales, BGR, y el Servicio Nacional de Geología y Minería, SERNAGEOMIN. CEPAL.
Zhang, P., Qin, C., Hong, X., Kang, G., Qin, M., Yang, D., Pang, B., Li, Y., He, J., Dick, R. P., 2018. Risk assessment and source analysis of soil heavy metal pollution from lower reaches of Yellow River irrigation in China. Sci. Total Environ. 633, 1136–1147. https://doi.org/10.1016/j.scitotenv.2018.03.228.

CHAPTER B

ACCUMULATION OF AS, AG, CD, CU, PB AND ZN BY NATIVE PLANTS GROWING IN SOILS CONTAMINATED BY MINING ENVIRONMENTAL LIABILITIES IN THE PERUVIAN ANDES

CHAPTER B. ACCUMULATION OF AS, AG, CD, CU, PB AND ZN BY NATIVE PLANTS GROWING IN SOILS CONTAMINATED BY MINING ENVIRONMENTAL LIABILITIES IN THE PERUVIAN ANDES

The second part of the project was devoted to studies of the uptake of metals present in the contaminated soils by native plants growing naturally in the post-mining environments. Based on the infomation gathered in the intial step of this project, 21 native plants together with corresponding soil samples were selected from the two MEL sites.

The physicochemical properties including: pH, electrical conductivity (EC), carbonates, organic matter (OM), and texture as well as metals composition of soil samples were established. Based on the initial screening of 34 elements, As, Ag, Cd, Cu, Pb, and Zn were found to be of the highest interest because of their high contents and potential toxicity. As from the ecological point of view, the total content of metals in soils does not fully reflect their potential environmental risk; the samples were subjected to sequential extraction using the modified Tessier approach consisting of four steps and identifying the following metal/metalloid fractions: (i) exchangeable, (ii) bound to hydrated iron and manganese oxides, (iii) bound to organic matter, and (iv) mineral fraction; the metals present in the individual fractions were quantified by ICP mass spectrometry (ICP-MS).

This informaton was correlated with the investigation of metal content in plant organs. In order to assess the the phytoremediation potential of the studied plants the bioconcentration and (BCF), and the translocation (TF) factors were calculated.

plants

MDPI

Article

Accumulation of As, Ag, Cd, Cu, Pb, and Zn by Native Plants Growing in Soils Contaminated by Mining Environmental Liabilities in the Peruvian Andes

Edith Cruzado-Tafur [1,2], Katarzyna Bierla [1], Lisard Torró [2] and Joanna Szpunar [1,*]

[1] Université de Pau et des Pays de l'Adour, E2S UPPA, CNRS, IPREM UMR 5254, Hélioparc, 64053 Pau, France; em.cruzado-tafur@univ-pau.fr (E.C.-T.); katarzyna.bierla@univ-pau.fr (K.B.)
[2] Geological Engineering Program, Faculty of Sciences and Engineering, Pontifical Catholic University of Peru (PUCP), Av. Universitaria 1801, San Miguel, Lima 15088, Peru; ltorro@pucp.edu.pe
* Correspondence: joanna.szpunar@univ-pau.fr

Abstract: The capability of native plant species grown in polluted post-mining soils to accumulate metals was evaluated in view of their possible suitability for phytoremediation. The study areas included two environmental liabilities in the Cajamarca region in the Peruvian Andes. The content of As, Ag, Cd, Cu, Pb, and Zn was determined in individual plant organs and correlated with soil characteristics. The degree of the pollution depended on the metal with results ranging from uncontaminated (Cd) to moderately (Zn), strongly (As, Cu), and extremely contaminated (Pb, Ag) soils. The metals were mainly present in the fractions with limited metal mobility. The bioaccumulation of the metals in plants as well the translocation into overground organs was determined. Out of the 21 plants evaluated, *Pernettya prostrata* and *Gaultheria glomerate* were suitable for Zn, and *Gaultheria glomerata* and *Festuca* sp. for Cd, phytostabilization. The native species applicable for Cd phytoremediation were *Ageratina glechonophylla*, *Bejaria* sp., whereas *Pernettya prostrata Achyrocline alata*, *Ageratina fastigiate*, *Baccharis alnifolia*, *Calceolaria tetragona*, *Arenaria digyna*, *Hypericum laricifolium*, *Brachyotum radula*, and *Nicotiana thyrsiflora* were suitable for both Cd and Zn. None of the studied plants appeared to be suitable for phytoremediation of Pb, Cu, As and Ag.

Keywords: mining environmental liabilities; native plants; metals; translocation factor; bioconcentration factor; phytoremediation

Citation: Cruzado-Tafur, E.; Bierla, K.; Torró, L.; Szpunar, J. Accumulation of As, Ag, Cd, Cu, Pb, and Zn by Native Plants Growing in Soils Contaminated by Mining Environmental Liabilities in the Peruvian Andes. *Plants* **2021**, *10*, 241. https://doi.org/10.3390/plants10020241

Academic Editors: Domenico Morabito, Sylvain Bourgerie and Manhattan Lebrun
Received: 16 December 2020
Accepted: 22 January 2021
Published: 27 January 2021

1. Introduction

Mining has been around since ancient times and has been essential for economic and industrial development of societies [1]. The extraction of natural resources has generated an economic surge in Latin America [2]. During the recent decades, the mining sector has been one of the main economic pillars of Peru [3], making it the main producer of gold, zinc, lead, and tin in Latin America and the second largest producer of copper, silver, and zinc worldwide [4].

Nevertheless, mining operations are also responsible for significant environmental damage by producing a large amount and diversity of residues, affecting the quality of water, soil, and air [5], of which soil pollution is one of the most crucial environmental problems [6]. Likewise, the abandoned mines without effective shut-down procedures are causing a nuisance in the mining districts due to metal transfer to the environment [7], being one principal reason for the emergence of conflicts in Peru [8]. Metals are persistent in the environment and, being nonbiodegradable [9], cause serious harm bioaccumulating in flora and fauna [6,10]. The installations, effluents, emissions, remains, or deposits of residues from abandoned or inactive mines constituting a permanent and potential risk for health, the surrounding ecosystem, and property are defined as mining environmental liabilities (MELs) [11,12]. The lack of adequate legislation has caused MELs to increase

in number and magnitude resulting in significant environmental damage [5], generating problems to local farmers and peasants [13] and provoking resistance and opposition from local communities [2]. In 2019 in the Peruvian territory, approximately 8448 MELs [14] were identified with the highest number of them located in Ancash, Apurímac, Arequipa, Cajamarca, Huancavelica, Junín, Pasco, and Puno regions [14,15]. Although Peru has embarked on a process of regulation and institutional changes aimed at achieving adequate protection of the environment [8], these efforts are insufficient, thus increasing the demand for innovative and sustainable solutions [16].

Phytoremediation is considered to have many advantages over other methods, such as low cost, in situ remediation, respect for the environment, and landscape improvements [17]. Phytoremediation, including phytostabilization and phytoextraction, has shown satisfactory results and is a promising alternative relying on the natural ability of plants to recover metals from soil [9,17–20]. The uptake, translocation, and phytoaccumulation of metals from the soil depends specifically on plant species [18]. Native plant species are preferred because they are adapted to the local climatic conditions and, by growing in contaminated places, they have already proven their resistance to an excess of metals [1,21].

The study areas included two environmental liabilities in the Hualgayoc district, Cajamarca region in the Peruvian Andes. The principal problems of metal contamination in the watersheds in the Cajamarca region derive from the mining operations located at high altitudes so that in the rainy season, the mining waste goes directly to the lower agricultural valleys [22]. Within the region of Cajamarca, Hualgayoc is a complex mining district that since Spanish colonial times has been known for Ag-rich polymetallic mineralization; in addition to Zn, Pb, and Cu [23,24]. Currently, this region is one of the most affected by the presence of mining environmental liabilities [25]. The Hualgayoc district has a mostly rural population dedicated to agriculture; the mining sector represents a great possibility of economic development for this area, however, fears persist regarding an increase in environmental pollution [25]. In this context, the main objective of this research was to evaluate the capacity of bioaccumulation of As, Ag, Cd, Cu, Pb, and Zn in tissues of native plants as well the translocation into over-ground organs from polluted post-mining soils. The purpose was to establish the potential of different plants species for phytoremediation in post-mining sites.

2. Materials and Methods

2.1. Study Area and Sampling

The sampling sites were located in the Andes of northern Peru, in the Hualgayoc district, in the west of the province of Hualgayoc, between the districts of Chugur and Bambamarca in the department of Cajamarca.

Hualgayoc district is located in the west of the province of Hualgayoc in the department of Cajamarca in the Andes of Northern Peru. It is ca. 45 km away, as the bird flies, from Cajamarca city and 865 km by road from Lima city [25]. Since Spanish colonial times, Hualgayoc has been famous for Ag-rich polymetallic mineralization, in addition to Zn, Pb, and Cu [23,24,26]. The main mineralized structures in the Hualgayoc district are mantos and veins hosted largely in the upper Goyllarisquizga Group, the Inca Formation and lower Chulec Formation rocks [23,24,26]. The Hualgayoc district has 943 MELs [14], two of them belonging to the ex-mining unit Los Negros have been studied here; they are found on the left bank and downstream from the Hualgayoc river creek in the flak of the Llaucano river valley. The identity of the liable parties of the generation of these MELs have not been identified yet [14]. In order to evaluate the environmental impact of the abandoned mines the two chosen sampling sites included a leach pad (S1) located on top of a mine waste deposit and a mine dump (S2) made up of clay gravel with sand.

Sampling area #1 leach pad (a latitude 6°44′49″ S, longitude 78°35′36″ W, and altitude of 3249 m above sea level) was located on top of a mine waste deposit and had no drainage. Sampling area #2 mine dump (latitude 6°44′53″ S, longitude 78°35′49″, and altitude of

3399 m above sea level) had granular material made up of clay gravel with sand, no stabilization work was observed and there was no revegetation nor drainage (Figure 1).

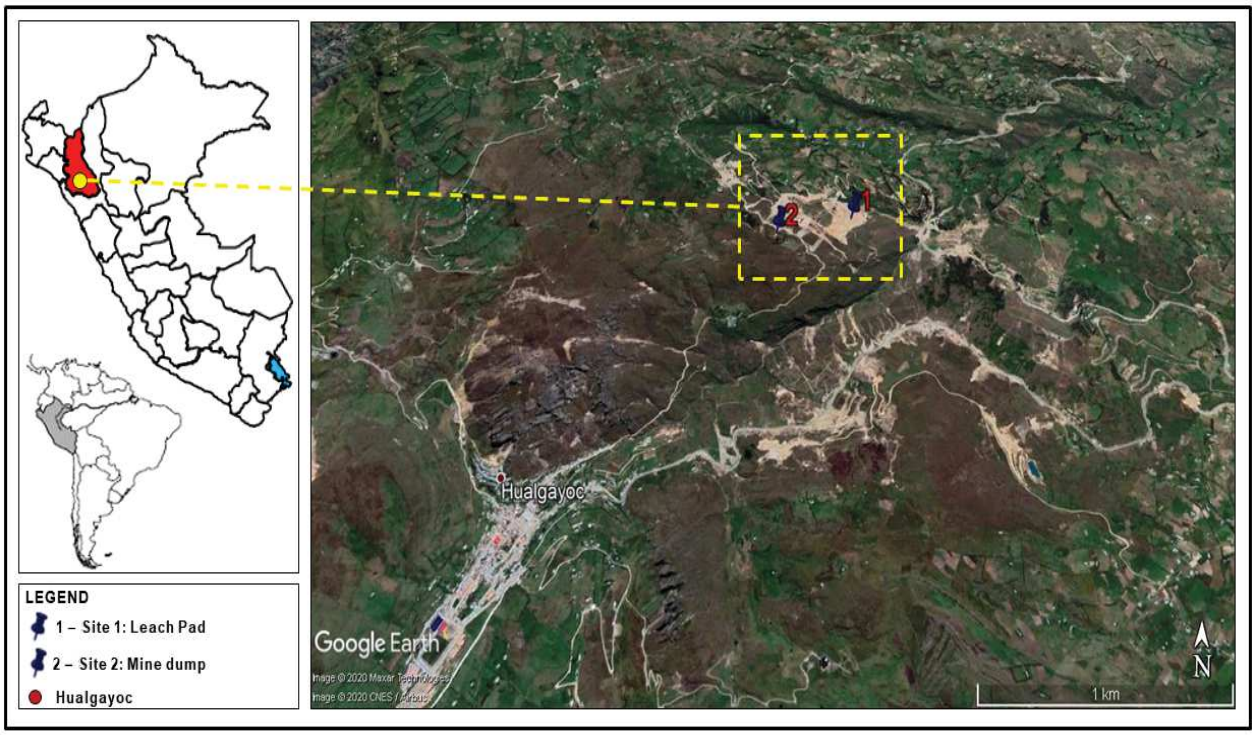

Figure 1. Localization of the mining environmental liabilities (site #1—leach pad, site #2—mine dump) of the ex-mining unit Los Negros in Hualgayoc district, Cajamarca region, Peru.

Soil and plant samples were taken following the criteria based on the distance from the point of contamination, wind direction, slope and inclination, vegetation cover, and soil texture [27]. The location of the points for soil sampling in both sites was fixed at 0, 15, 30, 45 and 60 m away from the point of contamination, forwards downhill slide. For the determination of soil profile characteristics, samples were taken at two depths between 0–15 and 15–30 cm intervals. Following this pattern, a total of 20 soil samples were collected from the two sites. Plants and soil samples were collected in July 2018 (dry season). Sampling of flora specimens was carried out in the same locations as for soil sampling. To do so, an area of 4 m^2 around each soil sampling point was delimited. Each plant was stored in polyethylene bags before being carried to the laboratory. A total of 47 plant samples (from 1 to 5 replicates) were collected from the two sampling sites, including 29 samples from site #1, and 18 samples from #2. Five species were found in both areas so a total of 21 unique species of native flora have been identified. The taxonomic identification of the collected plants was carried out by Dr. Manuel Timaná (the Pontifical Catholic University of Peru, Peru) and Mg. Paul Gonzales Arce (the Laboratory of Floristics of the Herbarium of the Natural History Museum of the Universidad Nacional Mayor de San Marcos, Peru).

2.2. Chemical Analysis of Soils

The soil samples were analyzed for pH, electrical conductivity, organic matter and texture at the Soil, Plant, Water and Fertilizer Analysis Laboratory of the Universidad Nacional Agraria La Molina in Lima (Peru). pH was measured using a suspension of soil in deionized water at a ratio 1:1 using a Consort pH-meter (Turnhout, Belgium) and electrical conductivity was measured in aqueous extract of soil in water at a ratio 1:1. Organic matter content was determined using the Walkley and Black method [28] based on the oxidation of organic carbon with potassium dichromate, sulfuric acid, and concentrated phosphoric acid.

Texture evaluation was conducted using the classical Bouyoucos Hydrometer method—the mechanical analysis of soils utilising the suspension of solids for the quantification of the content of sand, silt, and clay in percentage [29].

Metal content in soils was analyzed at the SGS Geochemical Assays Laboratory, Lima, Peru. Approximately 0.20 g of soil with particle size below 106 µm was digested in two steps in Hot Blocks (Environmental Express, Charleston, SC, USA). For the first digestion step (at 90 °C for 30 min), 1 mL of concentrated nitric acid was added; for the second one (at 90 °C for 1 h), 3 mL of concentrated hydrochloric acid was added. Once the digest cooled to room temperature, 2 mL of concentrated hydrochloric acid was added and the mixture was diluted with ultrapure water (18.2 MΩ·cm) up to 20 mL. The concentration of metals was determined by an inductively coupled plasma emission spectrometer (ICP-OES) using a Perkin Elmer Model Optima 8300 DV instrument. The certified soil reference materials OREAS 906, OREAS 907, and OREAS 522 (from ORE Research & Exploration Pty Ltd., Bayswater North, Victoria, Australia) were used for quality control.

2.3. Calculation of the Geo-Accumulation Index (I_{geo})

The geo-accumulation index (I_{geo}) was introduced by Muller [30] for the evaluation accumulation of metals in river sediments. Since then it has been adopted by many researchers in order to classify sediments and soils from the point of view of metal pollution level. The values necessary to calculate I_{geo} are concentration of metal in given soil and the background level concentrations. In our study, baseline values obtained by Santos-Francés et al. [22] from La Zanja region at ca. 30 km from the sampling place are used for calculation purposes, except for silver, for which the natural abundance in the Earth's crust was used [31]. The values used for calculations are given in Supplementary Information (Table S1).

The I_{geo} was calculated according to the equation:

$$I_{geo} = log_2 \frac{C_i}{1.5 * B_i} \quad (1)$$

where C_i is the measured concentration of the i metal examined in the soil and B_i is the background level of this metal. The factor 1.5 is used to correct possible variations in the background values of a particular metal in the environment.

Depending on the value of the I_{geo}, the soils are classified into seven groups [32]: unpolluted ($I_{geo} < 0$), unpolluted to moderately polluted ($0 \leq I_{geo} < 1$), moderately polluted ($1 \leq I_{geo} < 2$), moderately to strongly polluted ($2 \leq I_{geo} < 3$), strongly polluted ($3 \leq I_{geo} < 4$), strongly to very strongly polluted ($4 \leq I_{geo} < 5$), and very strongly polluted ($I_{geo} \geq 5$).

2.4. Sequential Extraction Procedure

In order to identify how the metals are distributed among the soil components, the soil samples were subjected to sequential extraction based on the Tessier approach [33], using the modified method [34] adapted to the soil parameters consisting of the four following steps:

1. Exchangeable (loosely bound) metals fraction: 15 mL 1 M CH_3COONH_4, pH 7 (shaking time 1 h at room temperature) followed by the addition of 30 mL 1 M CH_3COONa by acidification with CH_3COOH to pH 5 (shaking time 5 h at room temperature).
2. Metal bound with hydrated iron and manganese oxides: 30 mL 0.04 M $NH_2OH{\cdot}HCl$ in 25% (v/v) CH_3COOH (shaking time 5 h at 95 °C).
3. Metals bound with organic matter: 7.5 mL 0.02 M HNO_3 + 7.5 mL 30% H_2O, pH 2 (shaking time 2 h at 85 °C), then 7.5 mL 30% H_2O_2, pH 2 was added (shaking time 3 h at 85 °C) and finally, 15 mL 3.2 M CH_3COONH_4 in 20% (v/v) HNO_3 was added (shaking time 0.5 h at room temperature).
4. Metals bound to mineral fraction: 4.5 mL 10M HNO_3 + 3 × 3 mL H_2O_2 time 1 h, then 15 mL H_2O (shaking time 0.5 h at 95 °C) was added.

All samples were centrifuged at 400 rpm for 10 min and filtered (0.45 µm). Metals present in the supernatants were quantified by ICP mass spectrometry (ICP-MS) using the reaction cell mode pressurized with He and H_2 gas. The dilutions performed allowed work in the calibration range of 0.01–10 ppb; an 8-point calibration curve was used. The isotopes monitored were ^{107}Ag, ^{109}Ag; ^{75}As; ^{111}Cd, ^{112}Cd, ^{114}Cd; ^{63}Cu, ^{65}Cu; ^{206}Pb, ^{207}Pb, ^{208}Pb; ^{64}Zn, ^{66}Zn, and ^{68}Zn. Analytical blanks were run in parallel.

2.5. Chemical Analysis of Plants

The vegetal material was washed with tap water (for the disposal of soil remains) and then with distilled water. All the plant samples were separated into leaves, stems, and roots, which were dried at 30–40 °C. Foliar samples were crushed and ground, and 0.10 g subsamples were digested in the heat block (SCP Science, Courtaboeuf, France) in triplicate. The digestion was carried out in two steps: the first one using 2 mL of nitric acid (70%) at 85 °C for 4 h 30 min and the second one using 0.75 mL of hydrogen peroxide (30%) at 85 °C for 4 h 30 min. The digest was diluted to 50 mL with ultrapure water (18.2 MΩ·cm). The elemental composition was analyzed by ICP mass spectrometry (ICP-MS) using an Agilent 7500 (Agilent, Tokyo, Japan) instrument equipped with a reaction cell pressurized with He and H_2 gas. The dilutions performed allowed work in the calibration range of 0.1–10 ppb. A 7-point calibration curve was used. The isotopes monitored were ^{107}Ag, ^{109}Ag; ^{75}As; ^{111}Cd, ^{112}Cd, ^{114}Cd; ^{63}Cu, ^{65}Cu; ^{206}Pb, ^{207}Pb, ^{208}Pb; ^{64}Zn, ^{66}Zn, and ^{68}Zn. Analytical blanks were analyzed in parallel. The Standard Reference Material 1573a Tomato Leaves of the NIST (Gaithersburg, MD 20899, USA) was used for quality control.

2.6. Calculation of the Translocation Factor (TF) and the Bioconcentration Factor (BCF)

The translocation factor (TF) and the bioconcentration factor (BCF) were calculated to assess the phytoremediation potential of the studied plants. The BCF is defined as the ratio of the metal content accumulated in the plant to the content in the soil [35], as given below:

$$BCF = C_p / C_{so} \quad (2)$$

where C_p is the metal concentration in the plant (shoot) and C_{so} is the total metal concentration in the soil. Plants with a BCF value higher than one are considered to be suitable candidates for phytoextraction [36,37].

The ability of the trace metal transfer from the roots to the aerial part is expressed using the translocation factor TF [38], calculated as follows:

$$TF = C_s / C_r \quad (3)$$

where C_s is the metal concentration the aerial part (shoot) of the plant and C_r is the concentration in roots. Plants with TF values higher than one can be potentially used for phytoextraction [38].

2.7. Statistics

The measurements were carried out in triplicates and the results with relative standard deviation higher than 10% were discarded and the measurements repeated. Values are reported as mean ± standard deviation (SD) of three replications.

In order to assess the differences in I_{geo} values for the studied elements between the soil samples at each site, we first performed a normal test to determine whether the data was normally distributed. We found that the null hypothesis of normal distribution could not be rejected for any of the samples. Therefore, we decided to apply a *t*-test in order test for differences between each pair of elements. We applied the Bonferroni correction for multiple testing, which resulted in a significance threshold of alpha = 0.01/n, where n = 15 was the number of possible pairs of elements.

3. Results and Discussion

3.1. Soil Physicochemical Characterization

Physicochemical properties of the soils are given in Table 1. The two sites had similar extremely acidic pH values in the range of 3.59–4.19 in site #1 and 2.77–4.02 in site #2. As a result, no carbonates and low organic matter contents were present. Soil was non-saline and had low electrical conductivity (EC) with an average value of 0.08 dSm^{-1} in site #1 and of 0.15 dSm^{-1} in site #2. In the texture of soils, the sand fraction dominated at 42–66% in site #1 and at 52–62% in site #2, varying from sandy clay loam to clay loam textures in the different layers. The mineralogical composition of soils was dominated by illite/sericite, kaolinite, quartz, and jarosite [39]. The most important factor affecting trace metals availability is soil pH [1], which usually increases the mobility and bioavailability of the metal with lower pH values, with the content of organic matter and clay minerals [10,40]. On the other hand, soils rich in organic matter can bind metals efficiently in acidic conditions, however, bonding capacity depends on the metal [10]. The samples had fine granulometry due to the major presence of sandy fraction; the fine soil particles can be easily transported by wind and water erosion to the nearby environment [41]. The acidity of the soil and their unbalanced properties pointed to the poor soil management [42].

Table 1. Properties of soil samples from Hualgayoc district, Cajamarca region, Peru.

Distance (m)	Depth (cm)	pH	EC (dS m^{-1})	Carbonates (%)	Organic Matter (%)	Soil Texture (%)		
		R: <5.5–>8.8	R: <2–>8			Sand	Silt	Clay
Sampling area #1								
0	0–15	4.02	0.08	0	7.6	66	22	12
	15–30	3.97	0.09	0	4.3	50	24	26
15	0–15	4.19	0.05	0	4.4	52	26	22
	15–30	3.89	0.07	0	2.5	42	22	36
30	0–15	3.63	0.13	0	3.5	52	24	24
	15–30	3.84	0.15	0	3.8	54	28	18
45	0–15	3.63	0.08	0	5.7	66	18	16
	15–30	3.67	0.08	0	1.8	52	22	26
60	0–15	3.76	0.05	0	4.2	54	28	18
	15–30	3.59	0.09	0	4.5	50	24	26
Sampling area #2								
0	0–15	3.42	0.08	0	10.6	60	22	18
	15–30	3.37	0.11	0	5.0	56	24	20
15	0–15	4.02	0.02	0	4.4	54	20	26
	15–30	3.89	0.02	0	4.4	62	20	18
30	0–15	3.37	0.14	0	2.5	52	18	30
	15–30	3.46	0.14	0	2.9	54	18	28
45	0–15	3.85	0.05	0	4.9	56	22	22
	15–30	3.72	0.05	0	3.3	58	22	20
60	0–15	2.94	0.32	0	2.2	54	24	22
	15–30	2.77	0.57	0	1.7	54	20	26

EC: Electrical Conductivity/R: Range.

Santos-Francés et al. [22] at Colquirrumi mine, located 6 km NW of our study area, reported acid soils (pH = 4.6), low organic matter content (5.04%), and silt sand texture (29.5% sand, 41.5 silt, and 30.8% clay); also, soils Colquirrumi are on quartzite and dacite substrates, which are much less reactive [39]. These results show significant differences in comparison with the study reported by Bech et al. [43] for the Carolina Mine, located 4 km SW of the study area, which reported basic pH of soil (i.e., pH = 6.8–8.0), high calcium carbonates levels, slight electrical conductivity (0.1–0.8 dSm^{-1}), and silt loam texture.

3.2. Soil Metal Composition

Following the initial screening of 34 elements [39], the study of Pb, Zn, As, Cu, Ag, and Cd was found of the highest interest because of their extremely high contents and potential toxicity. The results obtained for these elements for 15, 30, 45, and 60 m distances from the points of contamination at two different depths (0–15 and 15–30 cm) are presented in Figure 2a,b for sampling sites #1 and #2, respectively. In view of the findings, it can be concluded that the whole studied area was characterized by relatively uniform pollution. Moreover, the analysis results (not shown) of soil from two presumably uncontaminated sites in the vicinity of the sampling areas still showed high concentrations of the studied elements.

In general, neither significant differences nor a particular trend in the concentration levels for any of the studied elements for the soils from sampling site #1 (Figure 2a) was observed, except for Ag, whose concentrations in the upper soil layer (0–15 cm) were regularly higher than in the lower (15–30 cm) one. In one particular sample (the upper layer of the soil taken at 60 m from the leach pad, the presumed contamination source), significantly higher (twice as high as the next highest value) concentrations of Pb, Ag, and Cd suggested the presence of a grain of rock enriched in these three elements. Among the elements studied, the most abundant metal was Pb, found at the average level of 2050 mg kg^{-1}. Zinc concentration was in the range between 287 and 724 mg kg^{-1}, and was at the same level as that observed for Cu concentration in the range between 245 and 512 mg kg^{-1}, and As concentration was in the range between 252 and 401 mg kg^{-1}. Much lower was the concentration of Ag, in the range between 4.1 and 20.7 mg kg^{-1}, and of Cd, with an average concentration of 1.5 mg kg^{-1}.

Concerning the results obtained for sampling site #2 (Figure 2b), a point with unusually high contents of Pb, Ag, and Cd was recorded in the upper layer of the mine dump (the presumed contamination source). Apart from this observation, no other clear trend in the measured concentrations was observed. In addition, for this sampling area (#2), lead was the metal yielding the highest concentrations with values between 934 and 2367 mg kg^{-1}. The levels of Zn, Cu, and As remained comparable with the concentrations of Zn ranging from 120 to 305 mg kg^{-1}, Cu from 131 to 283 mg kg^{-1}, and As from 119 to 343 mg kg^{-1}. Nevertheless, two exceptionally high values of ca. 730 mg kg^{-1} were recorded for As for both layers of the soil sample located farthest from the point of contamination. The average values for these three elements were significantly lower than in the case of sampling area #1. The total Ag concentration was in a range of several mg kg^{-1}, and that of Cd was in general below 1 mg kg^{-1}.

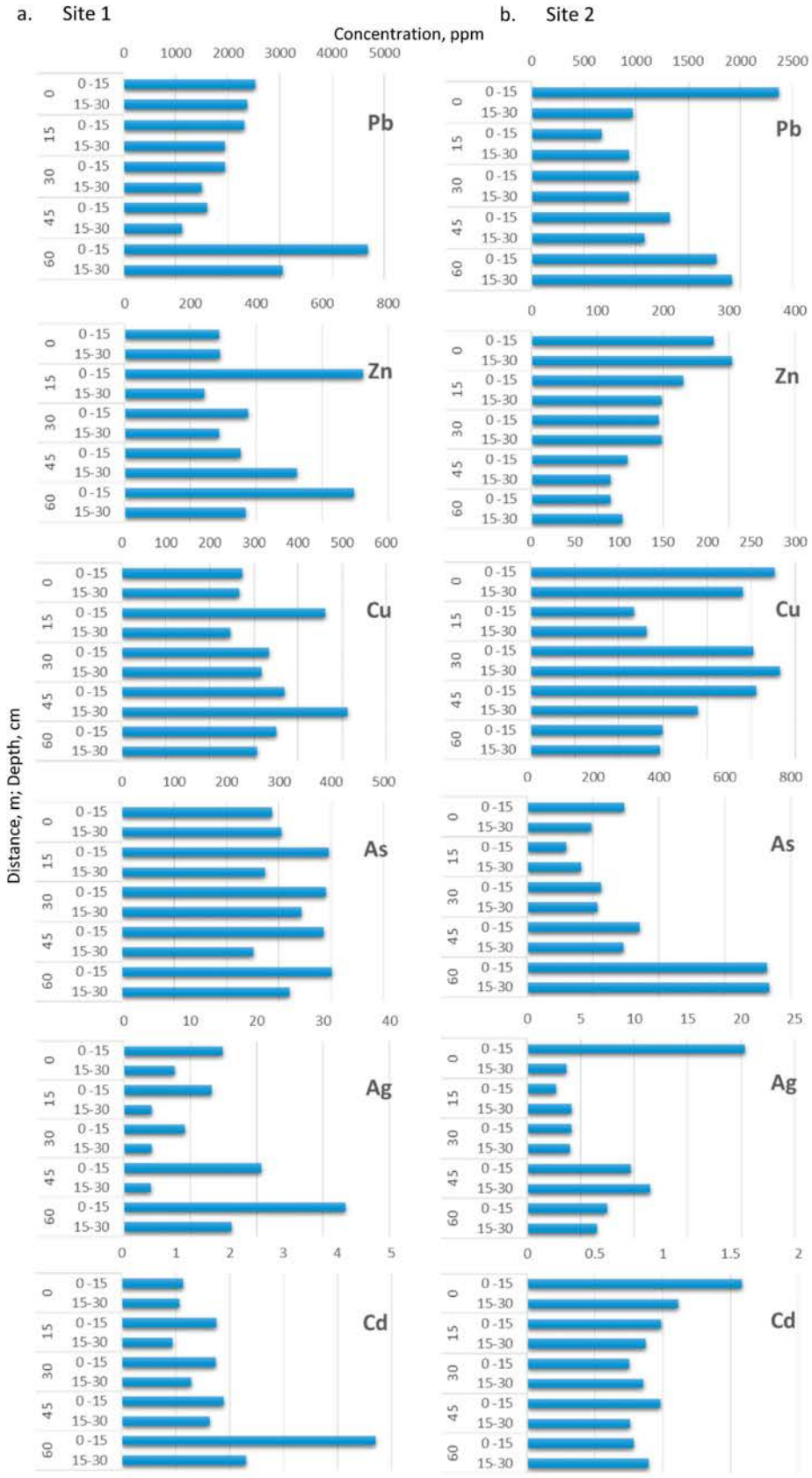

Figure 2. Soil Pb, Zn, As, Cu, Ag, and Cd concentration (mg kg^{-1}) for five distances (0–60 m) ant two depths (0–15 and 15–30 cm) in site#1 and site #2 from Hualgayoc district, Cajamarca region, Peru.

The Peruvian Environmental Quality Standards (PEQS) for soil set the maximum concentration permitted for Pb, As, and Cd in dried soils for agricultural uses at 70, 50, and 1.4 mg kg^{-1}, respectively [44], which coincides with the Pb and Cd values described in the Canadian Soil Quality Guidelines (CSQG), being stricter for As with 12 mg kg^{-1} [45]. In sampling sites #1 and #2, lead was the metal with the highest concentrations considerably exceeding the maximum values allowed by soil regulations; likewise, As content also showed great excess. However, most Cd concentrations recorded low values, except in site #1 at the furthest distances from the point of contamination (45 and 60 m), where Cd values slightly exceeded the permitted standards. The PEQS do not contemplate maximum values for Zn, Cu, and Ag, unlike the Canadian soil standards, which set permitted values at 250, 63 and 20 mg kg^{-1}, respectively [45,46]. According to Canadian standards, Zn exceeded the maximum allowed values in sampling site #1, whereas at sampling site #2 the concentration of Zn was above the legal threshold only at 0, 30, and 45 m away in the upper soil layer (0–15 cm). Copper concentrations significantly exceeded the maximum values allowed in both studied sites, and Ag was above the Canadian legal threshold only in samples from site #1 located furthest from the point of contamination (45 to 60 m). On the other hand, the Colquirrumi mine reported high content of heavy metals largely exceeding maximum allowed concentrations according to both PEQS and CSQG (Pb = 2069 mg kg^{-1}, Zn = 1893 mg kg^{-1}, Cu = 198 mg kg^{-1}, As = 428 mg kg^{-1}, and Cd = 13 mg kg^{-1}) [22,39]. In addition, the Carolina mine, when it was an active mine in the same Hualgayoc district, reported high concentrations of Pb, Zn, Cu, and As (3992–16,060, 11,550–28,059, 256–2070, and 280–1030 mg kg^{-1}, respectively) [47]. In addition, Table 2 shows concentration levels of Pb, Zn, Cu, As, Ag, and Cd found reported recently in other abandoned mines in Latin America, the majority of which are with acid soils.

Table 2. Concentrations of Pb, Zn, Cu, As, Ag, and Cd (mg kg^{-1}) reported in the literature for soil of mining sites in Peru and other South American countries.

Pb.	Zn	Cu	As	Ag	Cd	pH	pH Values	Name of the Mine	Status of the Mine	Country	Reference
3992–16,060	11,550–28,059	256–2070	280–1030	-	-	acid basic	6.8–8	Caroline mine-Hualgayoc	not active	Peru	[47]
87–341	56–772	69–5270	143–7670	-	8.9–499	acid	4.8	Turmaline mine-Piura	abandoned		
5.1–39.8	42–96	264- 977	-	-	-	acid	3.9	El teniente mine	active	Chile	
59–4890	58–18610	3–189	8.4–2240	1.6–178	2.9–342	acid	<4	San Bartolomé mine	abandoned	Ecuador	
-	-	1180–6310	-	-	-	acid	5.1–6.2	Petra verde mine	abandoned	Brazil	[48]
-	-	-	36–64	-	-	acid	4.5–5	Virgen Del Rosario and the Rayo Rojo cooperative mines	active artisanal	Bolivia	[49]
327–1754	448–505	149–459	183–14,660	-	45–308	acid basic	2.1–8.3	La Negra mine	abandoned	Mexico	[50]
780–43,700	380–>10,000	71.8–1320	19–11,800	9.5–74.2	1.0–780	acid	2.3–2.9	El Fraile mine	active	Mexico	[51]
670–4683	120–724	117–512	119–736	2.7–20.7	0.7–4.7	acid	2.8–4.9	Hualgayoc	abandoned	Peru	This work

Lead, As, Ag, Cd, as well as excess of Zn and Cu are toxic, nonbiodegradable and persist for long periods in the environment [6,21]. In strongly acidic conditions, as observed in our study case, these metals are released and cause potential hazards constituting

a serious source of pollution to the surrounding areas [52], affecting directly or indirectly soil, water, flora, fauna, and human health [21]. The concentrations of Pb, Zn, As, Cu, Ag, and Cd studied in the mining environmental liabilities exceeded Peruvian and Canadian soil standards, suggesting a potential risk of the contamination. Thus, there is a vital need to implement sustainable techniques for the remediation of these mining sites [21].

3.3. Index of Geoaccumulation

The degree of soil pollution in the studied areas was assessed using the index of geo-accumulation (I_{geo}). I_{geo} values for the studied metals are summarized in Figure 3. In general, the degree of pollution was similar in the two areas with results ranging from uncontaminated to extremely contaminated, depending on the metal. Considering Cd, the soils could be considered as unpolluted ($I_{geo} \leq 0$), whereas pollution with Zn was in the range from moderate to strong. Similarly, although higher pollution levels were observed for As and Cu. The highest I_{geo} values were obtained for Pb (from strongly to very strongly contaminated) and for Ag (very strongly polluted). Finally, after the statistical analysis (detailed in Section 2.7) the calculated geo-accumulation index showed the following order of contamination levels for both examined areas: Cd < Zn < As ≅ Cu < Pb < Ag.

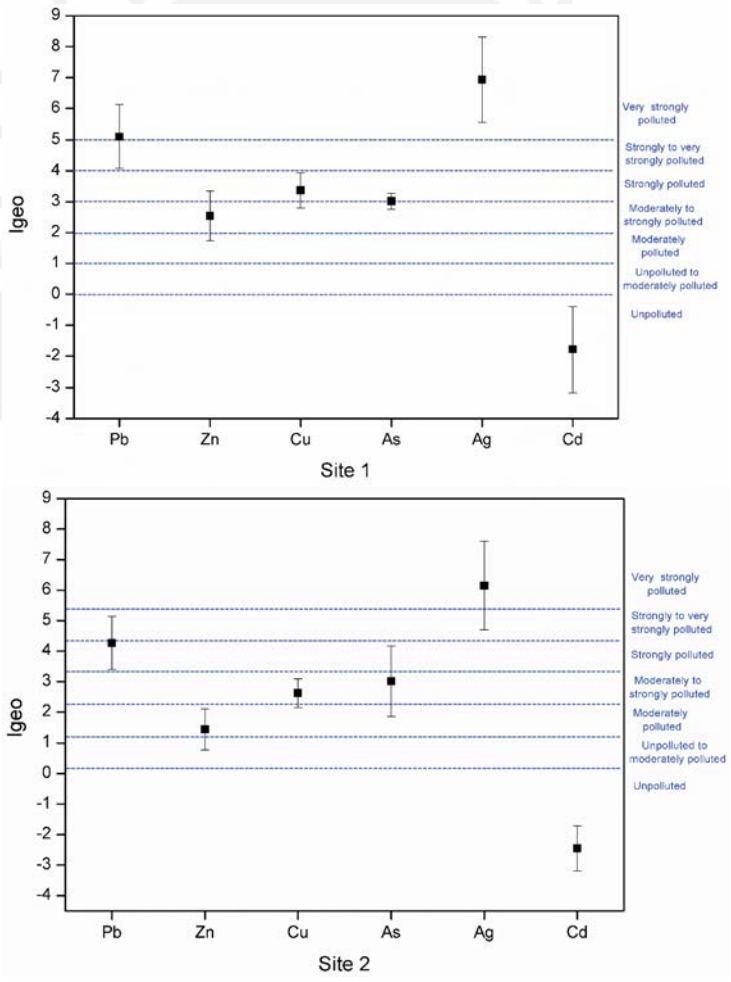

Figure 3. Geo-accumulation index (I_{geo}) for Pb, Zn, Cu, As, Ag, and Cd at the sampling sites.

3.4. Sequential Extraction Study from the Soil

The total content of metals in soils does not fully reflect their potential environmental risk; from the ecological point of view, it is important to know which part of the total concentration of a metal is available to determine its toxic effect [33,34]. The proportions of metal fractions that determine the availability and mobility of trace elements in the soil

and within the ecosystem, vary depending on the mineralogical composition of soils and other factors such as pH, organic matter content, and charge characteristics [53].

In our study, Pb, Zn, Cu, As, Ag, and Cd present in soil samples were separated into four fractions, providing a closer insight into their potential bioavailability. The fractions included (*i*) exchangeable metals forms, followed by metals bound to (*ii*) hydrated iron and manganese oxides, (*iii*) organic matter and, finally, (*iv*) mineral metal fraction. The partitioning of metals from the sampling areas #1 and #2 are presented in Figure 4a,b, respectively.

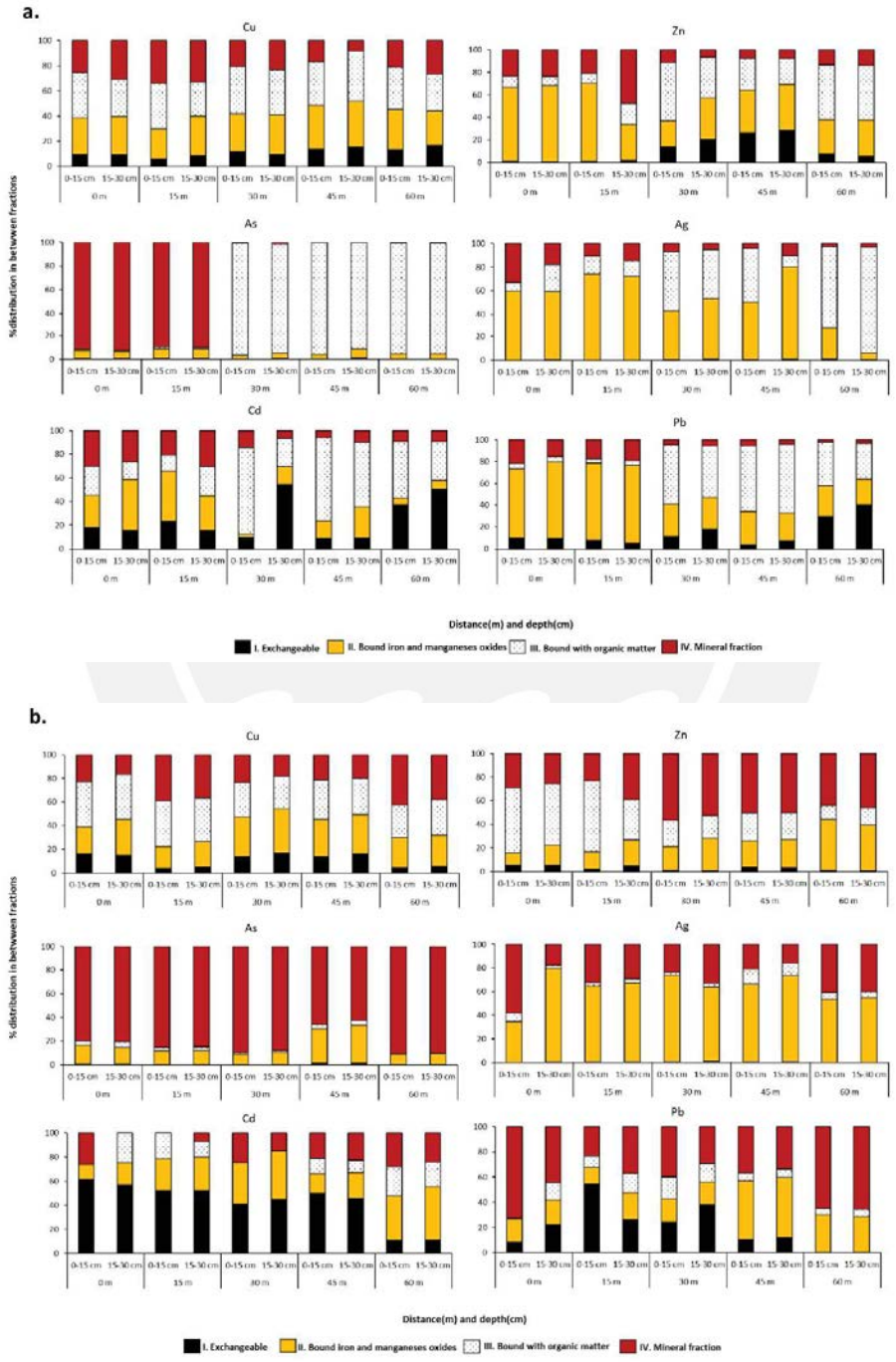

Figure 4. Percentage distribution of elements in four fractions by sequential extraction for five distances (0–60 m) and two depths (0–15 et 15–30 cm) from sampling area #1 (**a**) and #2 (**b**) in Hualgayoc district.

In general, no significant differences were found in the fractionation of Pb, Zn, Cu, As, Ag, and Cd between the upper (0–15 cm) and lower (15–30 cm) layers of soil. Out of 60 paired samples, only 6 (site #1: Zn—15 m, Ag—45 m and Cd—30 m and in site #2: Ag—0 m, Cd—0 m, Pb—0 m) displayed differences higher than +10% in the contributions of individual fractions into the total element content. The study of the distribution of elements in the soil showed the dominant presence of the fractions with limited metal mobility.

In sampling site #1, except for Cu, samples collected at 0 and 15 m from the leach pad presented notable differences from the three remaining ones collected at 30, 45, and 60 m. Copper was almost uniformly distributed among the mineral fraction and bound to organic matter and hydrated iron and manganese oxides; the remaining several percent of this metal was an exchangeable fraction. The two locations close to the presumed contamination source were characterized by the highest fraction of hydrated iron and manganese oxides-bound Pb, Ag, and Zn, whereas As was almost exclusively contained in the mineral fraction. Samples taken at 30, 45, and 60 m from the leach pad were characterized by a significant proportion of Pb, Ag, Zn, and As bound to organic matter, for which As reached more than 90% of its total content. The distribution of Cd was very variable with its total content distributed among all four fractions. The exchangeable fraction was absent for Ag, As, and Zn at 0 and 15 m from the leach pad.

The fractionation of elements from sampling site #2 is shown in Figure 4b. In general, the distribution of elements among the fractions did not vary with the distance from the contamination source. Cadmium was the only of the studied metals for which the exchangeable fraction was present at significant proportions (between 20 and 60%). Most of As (70–90%) was contained in the mineral fraction, whereas the majority of Ag was bound to hydrated iron and manganese oxides. Zinc was distributed among three main fractions including mineral, organic matter, and hydrated iron and manganese oxides, similar as in the case of copper where, additionally, 5–20% of the exchangeable fraction was present. In this area, the distribution of Pb was complex and completely different than in area #1, with a significant portion represented by mineral forms.

The first exchangeable metal fraction is considered to contain the most mobile metal species and usually those that bestow surge to toxicity problems, being available as ions [53]. Indeed, our study indicates low exchange capacity of the studied soils. The potentially high bioavailability can be also expected for metal forms contained in organic matter [54]. Metal bound with oxides Fe-Mn represents one of the dominant fractions; it indicates the role of Fe or Mn oxides in the immobilization of metals similar to that in the residual fraction, which implies the binding of metals in minerals [55]. According to the available literature on contaminated soils, the phase distribution of trace metals is the highest in Fe-Mn oxide or in the residual fractions [40], from which metals are mostly unavailable to plants [54]. Despite the highest metals content being found in the fractions with limited mobility, the acidic conditions of the soils could favor their mobility and availability [53].

3.5. Trace Elements in Native Plants

Metals transport and distribution in plant tissues are impacted by the level of metal available and by the plant species [21]. In order to evaluate whether the native plants that grow in the two mining environmental liabilities could be indicators of potential metal mobility, metal concentration was evaluated in individual plant organs (leaves, stem, and roots). The results of the trace elements determination in organs of plants studied are given in Tables S1 and S2. Different plants have different abilities in the absorption of minerals, and the species that survive naturally in metalliferous soils are often only restricted to this type of area [56]. Metal availability can also be modified by plant roots through pH regulation affecting plant metal uptake [57,58]. Among the 21 plants collected, half of them were single specimens growing in one particular location, whereas for the other half, two to five individual specimens were found at different locations.

Zinc: The highest foliar Zn concentrations were found in the leaves of *Baccharis alnifolia* (172 mg kg^{-1}—S1), *Achyrocline alata* (267 mg kg^{-1}—S1 and 198 mg kg^{-1}—S2), *Chusquea*

scandens (153 mg kg^{-1}—S1), and *Nicotiana thyrsiflora* (635 mg kg^{-1}—S1). These values exceeded the threshold concentrations of 150 mg kg^{-1} [40]. The rest of the species yielded Zn concentrations within the normal values for the aerial parts of plants. However, ten species, *Hypericum laricifolium* (S1 and S2), *Pernettya prostrata* (S1 and S2), *Ageratina glechonophylla* (S1), *Cortaderia bifida* (S1 and S2), *Calceolaria tetragona* (S2), *Gaultheria glomerate* (S2), *Festuca* sp. (S2), *Calamagrostis recta* (S1), and *Arenaria digyna* (S1) had higher Zn concentrations in the roots. Plants growing in the Carolina mine area, geographically close to the two studied sites, accumulated higher quantities of Zn in their shoots (1424–16,192 mg kg^{-1}) and roots (234–10,209 mg kg^{-1}) irrespective of the species, of which, *Achyrocline alata*, one of the species in common with our study, accumulated in their shoots significant values (1423–6694 mg kg^{-1}) [47]. This difference can be attributed to the different metal concentrations and the physicochemical characteristics of the soil, particularly pH, which was basic in soils studied by Bech et al. [47] in the Carolina mine, contrary to the highly acidic conditions in our case. In addition, other investigations in different shoot tissues reported 178–2008 mg kg^{-1} in Ecuador, 303–517 mg kg^{-1} in Chile, 11–144 mg kg^{-1} in Brazil, and 15–3414 mg kg^{-1} in Spain [47,56,59]. In our research between the two studied sites, four of the collected plant species—*Baccharis alnifolia, Achyrocline alata, Chusquea scandens*, and *Nicotiana thyrsiflora*—presented significant metal concentrations in their tissues, showing the ability to tolerate and accumulate toxic levels of Zn.

Copper: The concentrations of Cu in the majority of the native plants were the highest in the roots, of which, *Ageratina glechonophylla* (40 mg kg^{-1}—S1), *Calamagrostis recta* (55 mg kg^{-1}—S1), and *Arenaria digyna* (72 mg kg^{-1}—S1) presented the most elevated values. On the other hand, species having a higher concentration of metal in the leaves than in the roots were *Achyrocline alata* (16 mg kg^{-1}—S1 and 10 mg kg^{-1}—S2) and *Hypericum laricifolium* (11 mg kg^{-1}—S2). The only plant where the concentration in the aerial parts was higher than the normal range of 5–30 mg kg^{-1} [40] was *Nicotiana thyrsiflora* (49 mg kg^{-1}—S1). Another study carried out close to our sampling area, at the Carolina mine, also reported high values in different plant species studied (38–542 mg kg^{-1} in shoots and 43–396 mg kg^{-1} in roots); moreover, the values reported for the shoots of *Achyrocline alata* (38–130 mg kg^{-1}) [47] were higher, exceeding the range for aerial parts (30 mg kg^{-1}). Studies in countries bordering Peru, such as Ecuador, Chile, and Brazil, showed Cu concentrations in shoots at 1–85, 77–988, and 32–137 mg kg^{-1}, respectively [47,56]; likewise, other concentrations found were 40–243 mg kg^{-1} in Armenia (elevated) [38], and 20–29 mg kg^{-1} [60] in China. The results showed low Cu concentration in leaves, which may be due to low Cu translocation from roots to aerial parts, where it could interfere with photosynthesis and other essential processes [47].

Lead: In the present study, all species showed the highest Pb concentrations in the roots and the maximum value was found in *Arenaria digyna* (1658 mg kg^{-1}–S1). In this species, Pb concentration in leaves (288 mg kg^{-1}) exceeded the threshold value of 10 mg kg^{-1} for aerial parts [40]. Likewise, the concentrations in leaves of *Cortaderia bifida* (S1 and S2), *Calceolaria tetragona* (S2), *Ageratina fastigiate* (S1), *Hypericum laricifolium* (S1), *Achyrocline alata* (S1), *Puya* sp. (S1), *Orthrosanthus chimboracensis* (S1), *Nicotiana thyrsiflora* (S1), and *Ageratina glechonophylla* (S1) also exceeded the threshold value for aerial parts. Regardless of the plant species found in the Carolina mine, Pb concentrations were higher than in our study both in the roots (48–4841 mg kg^{-1}) and in the shoots (346–6886 mg kg^{-1}) [47]; also, the species common in both works, *Achyrocline alata*, showed higher concentration in shoots (1352–1650 mg kg^{-1}) than roots (1319–1138 mg kg^{-1}), presenting a different behavior than that found in our research, where most of the plants concentrate Pb in the roots and only some of them translocate it to aerial parts [61]. Previously, other studies reported the concentrations of Pb in shoots at the level of 11–614, 235–266, 0.12–341, and 7–9328 mg kg^{-1}, respectively, in Ecuador, Chile, Spain, and Turkey [6,47,59].

Cadmium: In our study, Cd concentration in soil and also in the plants was relatively low, exceeding, however, the threshold value in aerial parts of 0.2 mg kg^{-1} [40]. In this group, some plants showed higher concentrations in leaves than in the roots: *Chusquea*

scandens (0.39 mg kg^{-1}—S1), *Orthrosanthus chimboracensis* (0.76 mg kg^{-1}—S1), *Ageratina fastigiate* (1.40 mg kg^{-1}—S1), *Baccharis alnifolia* (1.70 mg kg^{-1}—S1), *Hypericum laricifolium* (1.88 mg kg^{-1}—S1 and 2.53 mg kg^{-1}—S2), *Achyrocline alata* (3.04 mg kg^{-1}—S1), and *Nicotiana thyrsiflora* (21.62 mg kg^{-1}—S1), the latter presenting an exceptionally high value. In addition, *Festuca* sp. (S2), *Gaultheria glomerate* (S2), *Calamagrostis recta* (S1), *Calceolaria tetragona* (S2), *Achyrocline alata* (S2), and *Arenaria digyna* (S1) also exceeded the normal concentration of Cd in aerial parts despite having the majority of Cd in their roots. Studies in Ecuador reported Cd content between 3–52 mg kg^{-1} in native plants [47]. Efficient inadvertent root absorption of Cd from contaminated soil was reported at mining sites in southern Morocco [21].

Arsenic: Arsenic levels in the majority of the studied species were higher in roots than in leaves. Three plants—*Puya* sp. (S1), *Calamagrostis recta* (S1), and *Arenaria digyna* (S1)—showed the highest concentrations (27, 42, and 53 mg kg^{-1}, respectively). Several species, despite having a higher concentration of As in the roots, presented significant values in leaves, such as: *Hypericum laricifolium* (2.01 mg kg^{-1}—S1), *Achyrocline alata* (3.82 mg kg^{-1}—S1), *Arenaria digyna* (3.93 mg kg^{-1}—S1), *Calamagrostis recta* (3.99 mg kg^{-1}—S1), *Puya* sp. (5.12 mg kg^{-1}—S1), *Ageratina glechonophylla* (6.44 mg kg^{-1}—S1), and *Chusquea scandens* (4.76 mg kg^{-1}—S1), exceeding the normal range of As (1.7 mg kg^{-1}) for the aerial parts [40]. Low concentrations of As in shoots and roots in these native species differed from that reported in the Carolina mine, which were 21.3–298 mg kg^{-1} for shoots and 26–246 mg kg^{-1} for roots [47]. Also, *Achyrocline alata* (a species common with this study) had far higher values of 79–126 mg kg^{-1} in shoots and 64–74 mg kg^{-1} in roots, showing more As content in shoots than in roots. Other studies also reported high values in shoots: 22–343 mg kg^{-1} in Ecuador, 0.1–40 mg kg^{-1} in Spain, and 42–15,942 mg kg^{-1} in Turkey [6,47,59]. Lower concentrations of As in the native species observed in our study are most probably related to the virtual absence of the soil fractions allowing for the higher bioavailability, i.e., the exchangeable and carbonates-bound fractions [55].

Silver: Silver concentrations in all the studied native flora species were low, with roots showing higher contents than aerial parts. Nonetheless, some species exceeded the normal threshold of 0.5 mg kg^{-1} in their leaves [40], including *Ageratina glechonophylla* (0.75 mg kg^{-1}—S1), *Brachyotum radula* (1.11 mg kg^{-1}—S1), *Arenaria digyna* (2.28 mg kg^{-1}—S1), and *Nicotiana thyrsiflora* (2.97 mg kg^{-1}—S1). Previous studies showed Ag contents between 0.22–80 mg kg^{-1} [6]. The amount of Ag absorbed by plants is related to the concentration of soils; in many cases, Ag can be concentrated by plants to attain toxic levels [40]. Our study reported low Ag concentration in soil, and low percentage distribution of soil in the exchangeable and carbonate-bound fractions, thus the low concentration in the studied plants.

Trace elements concentrations in the investigated plants were very variable. In order to resist the toxic effects of metals, many plants developed a specific tolerance mechanism, such as restriction of metal translocation from roots into shoots [21]. High concentrations of As, Cd, Cu, Zn, and Pb were observed in shoots of plants from two botanical families: Poaceae (*Cortaderia Hapalotricha* and *Cortaderia nitida*), and Asteraceae (*Ageratina sp*, *Baccharis latifolia*, *Baccharis rhomboidalis*, *Baccharis amdatensis*) in Peru (the Carolina and Turmalina mines), Ecuador, and Chile by Bech et al. [47] where, however, metal concentrations were higher than in this study. It is interesting to mention that some studied plants, such as, e.g., *Hypericum laricifolium*, are used in traditional Peruvian medicine [62].

Some of the plant species were found at different sampling locations and, if the differences in soil metal content are not very high, can be considered as biological (quasi-) replicates. Indeed, these plants presented values reasonably close to each other (The relative standard deviation (RSD) for the large majority lower than 70%). The results are given in the Supplementary Information Table S3.

3.6. Bioconcentration (BCF) and Translocation Factor (TF) of the Native Plants

Native plants of this study grow naturally around the mining environmental liabilities polluted with trace elements, demonstrating their good adaptation and tolerance to contam-

inated soil. The BCF and TF values reflected their metal accumulation and translocation. The BCF and TF values for the native Peruvian plants analyzed in this study are presented in Figures 5a–f and 6a–f, respectively. The capacity of a plant to accumulate trace metals indicates its potential applicability for phytoextraction or phytostabilization process [38]. Phytoextraction requires the translocation of metals from soil to plant roots, whereas phytostabilization is the capacity to reduce metal translocation from roots to shoots [63]. A plant's potential for phytoremediation can be estimated by the bioconcentration (BCF) and the translocation factor (TF) [37]; plants with these two indicators with values higher than one have potential to be used in phytoremediation. TF higher than one indicates a capacity to transport metal from roots to shoots, probably due to efficient metal transport systems and to the retention of metals in leaf vacuoles; low TF values show that more metals remain in the roots after plant uptake [20].

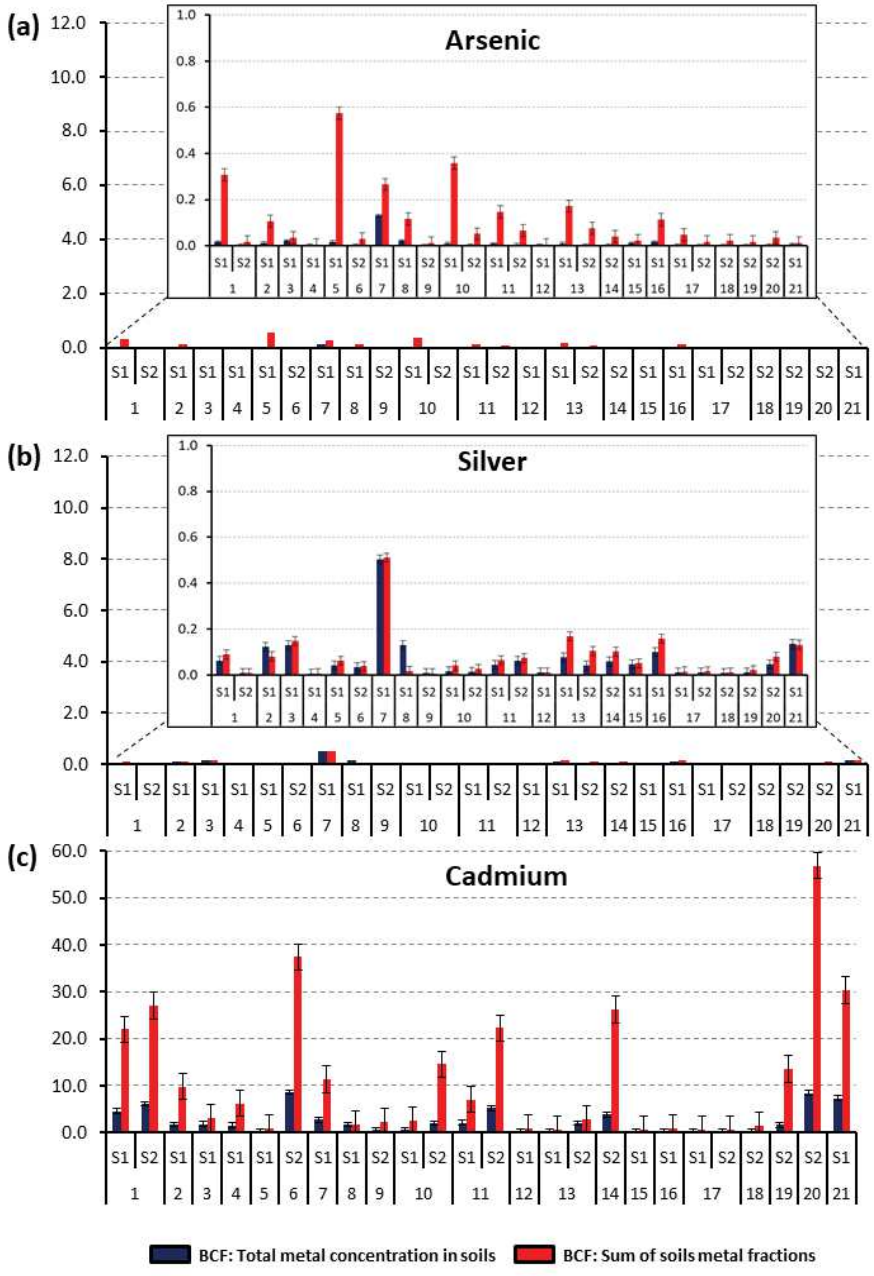

Figure 5. *Cont.*

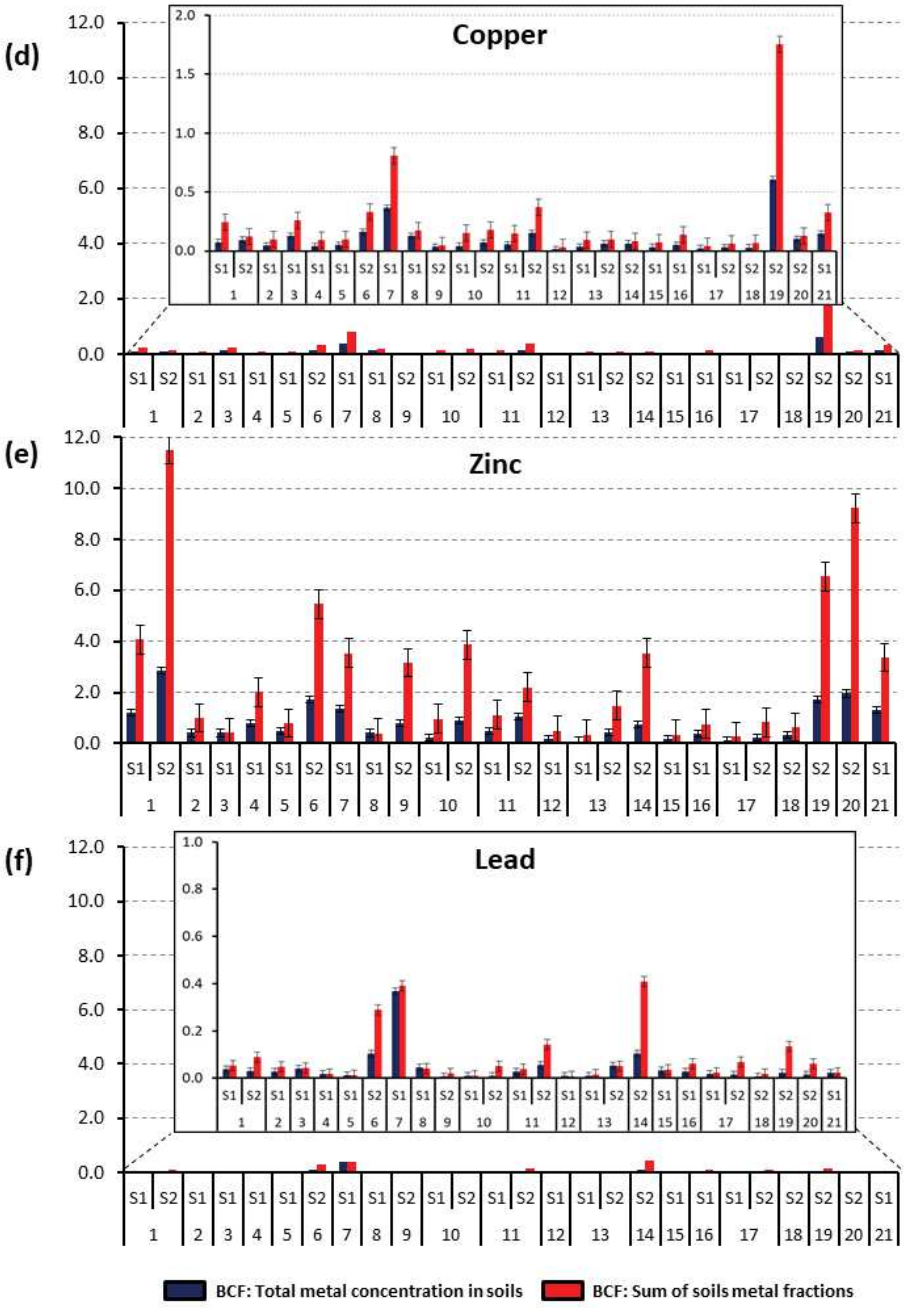

Figure 5. Bioconcentration factor (BCF) values of native species collected from two study areas (S1 and S2) in the Hualgayoc district. (**a**–**f**): 1—*Achyrocline alata*, 2—*Ageratina fastigiate*, 3—*Ageratina glechonophylla*, 4—*Baccharis alnifolia*, 5—*Puya sp*, 6—*Calceolaria tetragona*, 7—*Arenaria digyna*, 8—*Bejaria sp*, 9—*Gaultheria glomerata*, 10—*Pernettya prostrata*, 11—*Hypericum laricifolium*, 12—*Orthrosanthus chimboracensis*, 13—*Brachyotum radula*, 14—*Miconia vaccinioides*, 15—*Calamagrostis recta*, 16—*Chusquea scandens*, 17—*Cortaderia bifida*, 18—*Festuca sp*, 19—*Muehlenbeckia tamnifolia*, 20—*Buddleja interrupta*, 21—*Nicotiana thyrsiflora*.

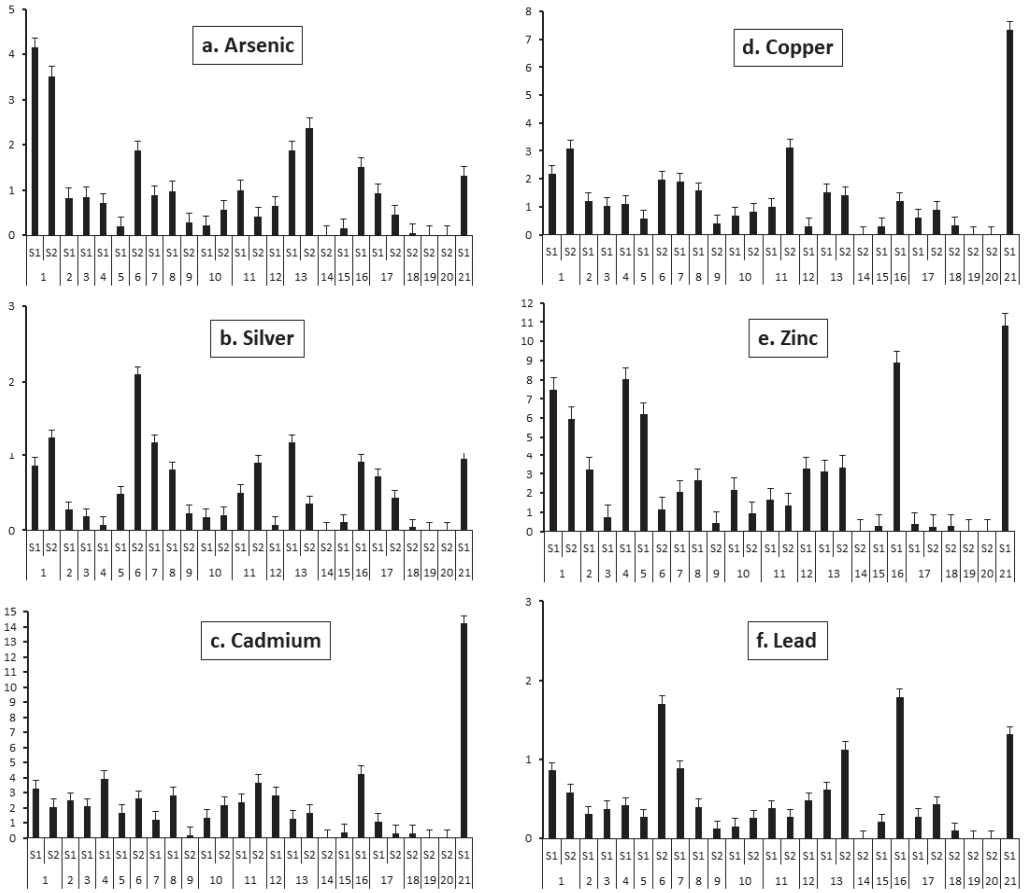

Figure 6. Translocation factor (TF) values of native species collected from two study areas (S1 and S2) in the Hualgayoc district. (**a**–**f**): 1—*Achyrocline alata*, 2—*Ageratina fastigiate*, 3—*Ageratina glechonophylla*, 4—*Baccharis alnifolia*, 5—*Puya sp*, 6—*Calceolaria tetragona*, 7—*Arenaria digyna*, 8—*Bejaria sp*, 9—*Gaultheria glomerata*, 10—*Pernettya prostrata*, 11—*Hypericum laricifolium*, 12—*Orthrosanthus chimboracensis*, 13—*Brachyotum radula*, 14—*Miconia vaccinioides*, 15—*Calamagrostis recta*, 16—*Chusquea scandens*, 17—*Cortaderia bifida*, 18—*Festuca sp*, 19—*Muehlenbeckia tamnifolia*, 20—*Buddleja interrupta*, 21—*Nicotiana thyrsiflora.*

The BCF values were calculated with respect to the total metal concentration in soils (blue bars) and the sum of soils metal fractions with potential bioavailability (i.e., exchangeable and bound to carbonates, iron-manganese oxides, and organic matter; red bars). The part contained in the mineral fraction was considered as unavailable and, as such, not harmful from the point of view of environmental pollution. For As, Ag, Cu, and Pb for all the studied plants, the BCF values were <1 with the only exception of *Muehlenbeckia tamnifolia*, which was able to accumulate almost twice (1.76) the amount of bioavailable Cu. The factors influencing Cu uptake from contaminated soils and distribution in roots have been discussed in detail by Cui et al. [60]. Results of Cu translocation (Figure 5d) showed that in roughly half of the studied species, including *Hypericum laricifolium* (S1 and S2), *Ageratina glechonophylla* (S1), *Baccharis alnifolia* (S1), *Ageratina fastigiate* (S1), *Chusquea scandens* (S1), *Brachyotum radula* (S1 and S2), *Bejaria* sp. (S1), *Arenaria digyna* (S1), *Calceolaria tetragona* (S2), *Achyrocline alata* (S1 and S2), and *Nicotiana thyrsiflora* (S1), the TF index values were higher than one. No notable similarities in BCF values were observed for plants belonging to the same families: Asteraceae, Ericaceae, Hypericaceae, and Poaceae, for which several samples were available. This fact, however, can be due to the decisive role of individual variability of the plant specimens. Indeed, the role of the plant species seems to be important, which is demonstrated by significant variability in bioaccumulation capacities of plants growing in the same locations.

For Ag, TF values (Figure 6b) higher than one were obtained for *Brachyotum radula* (S1), *Arenaria digyna* (S1), *Calceolaria tetragona* (S2), and *Achyrocline alata* (S2). For the other plants, TF was lower than one. However, in all tested samples the BCF was <1, thus, no species was considered viable for Ag phytoremediation.

The translocation factor values for Pb were >1 (Figure 6f) in *Brachyotum radula* (S2), *Calceolaria tetragona* (S2), *Chusquea scandens* (S1), and *Nicotiana thyrsiflora* (S1), indicating that these four species can translocate metals from roots to the aerial part. These results are similar with previous studies, in which it was observed that the roots can absorb Pb from soils in a passive mode, where the rate of uptake is reduced by liming and low temperature, so that Pb translocation from roots to shoots is greatly limited [40] and, in consequence, Pb is not generally bioavailable in contaminated soil [63].

The BCF values for Zn were higher than one for the following plants species: *Muehlenbeckia tamnifolia* (S2), *Buddleja interrupta* (S2), *Nicotiana thyrsiflora* (S1), *Calceolaria tetragona* (S2), *Arenaria digyna* (S1), *Achyrocline alata* (S1 and S2), *Hypericum laricifolium* (S2). Zn TF > 1 was also observed for *Calceolaria tetragona* (S2), *Hypericum laricifolium* (S1 and S2), *Arenaria digyna* (S1), *Pernettya prostrata* (S1), *Bejaria* sp. (S1), *Brachyotum radula* (S1 and S2), *Ageratina fastigiate* (S1), *Orthrosanthus chimboracensis* (S1), *Achyrocline alata* (S1 and S2), *Puya* sp. (S1), *Baccharis alnifolia* (S1), *Chusquea scandens* (S1), and *Nicotiana thyrsiflora* (S1) (Figure 5e). It is noteworthy that plants such as *Baccharis alnifolia*, *Chusquea scandens*, and *Puya* sp. yielded very low BCF values despite having the highest TF, indicating that these species had difficulties in mobilizing this metal into roots [64].

The Cd BCF values were the highest out of all the metals studied; it has to be noted that according to the I_{geo} index, the studied area cannot be considered as contaminated by this element, so the enrichment led to relatively low concentrations in plant organs (in several plants, especially in the sampling area #2, the concentrations in aerial parts were lower than the threshold value of 0.2 mg kg^{-1} [40]). The majority of the species, including *Achyrocline alata* (S1 and S2), *Ageratina fastigiate* (S1), *Ageratina glechonophylla* (S1), *Baccharis alnifolia* (S1), *Arenaria digyna* (S1), *Calceolaria tetragona* (S2), *Bejaria* sp. (S1), *Hypericum laricifolium* (S1 and S2), *Brachyotum radula* (S2), *Muehlenbeckia tamnifolia* (S2), *Buddleja interrupta* (S2), *Nicotiana thyrsiflora* (S1), *Festuca* sp. (S2), *Pernettya prostrata* (S2), and *Miconia vaccinioides* (S2) presented BCF values higher than one. Cadmium TF value was higher than one for the majority (15 out of 21) of the species (Figure 6c): *Arenaria digyna* (S1), *Brachyotum radula* (S1 and S2), *Pernettya prostrata* (S1 and S2), *Puya* sp. (S1), *Achyrocline alata* (S1 and S2), *Ageratina glechonophylla* (S1), *Hypericum laricifolium* (S1 and S2), *Ageratina fastigiate* (S1), *Calceolaria tetragona* (S2), *Orthrosanthus chimboracensis* (S1), *Bejaria* sp. (S1), *Cortaderia bifida* (S1), *Baccharis alnifolia* (S1), *Chusquea scandens* (S1), and *Nicotiana thyrsiflora* (S1). Therefore, the species *Gaultheria glomerata* and *Festuca* sp., by having TF < 1 and BCF > 1, are considered good candidates for Cd phytostabilization. *Achyrocline alata* (S1 and S2), *Ageratina fastigiate* (S1), *Ageratina glechonophylla* (S1), *Baccharis alnifolia* (S1), *Arenaria digyna* (S1), *Calceolaria tetragona* (S2), *Bejaria* sp. (S1), *Pernettya prostrata* (S2), *Hypericum laricifolium* (S1 and S2), *Brachyotum radula* (S2), and *Nicotiana thyrsiflora* (S1), with TF >1 and BCF >1, can be considered adequate candidates for Cd phytoextraction.

For As, *Hypericum laricifolium* (S1), *Nicotiana thyrsiflora* (S1), *Chusquea scandens* (S1), *Calceolaria tetragona* (S2), *Brachyotum radula* (S1 and S2), and *Achyrocline alata* (S1 and S2), showed a TF index higher than one. However, for all the plant species, the BCF values were lower than one, so the studied plants can be considered as excluders [5], hence unsuitable for phytoremediation.

Among the plants studied, *Pernettya prostrata* and *Gaultheria glomerate* can be considered suitable for Zn phytostabilization, and *Achyrocline alata*, *Ageratina fastigiate*, *Baccharis alnifolia*, *Calceolaria tetragona*, *Arenaria digyna*, *Hypericum laricifolium*, *Brachyotum radula* and *Nicotiana thyrsiflora* for Zn phytoremediation. *Gaultheria glomerata* and *Festuca* sp. are also suitable for Cd phytostabilization, and *Achyrocline alata*, *Ageratina fastigiate*, *Ageratina glechonophylla*, *Baccharis*

alnifolia, *Calceolaria tetragona*, *Arenaria digyna*, *Bejaria* sp., *Pernettya prostrata*, *Hypericum laricifolium*, *Brachyotum radula*, and *Nicotiana thyrsiflora* for Cd phytoremediation.

Bech et al. [47] reported in the Carolina mine at Hualgayoc (Cajamarca, Peru) that *Achyrocline alata* (common plant with this study) registered translocation factor values higher than one for Zn, Cu, Pb, and As metals; likewise, through shoot accumulation factor (SAF) this species was not considered as a good candidate for remediation purposes [43,47]. This research reported that for *A. alata*, TF index values were higher than one for Zn, Cu, Ag, Cd, and As, but not for Pb. Additionally, the BCF showed values <1 for Zn, Cu, Ag, As, and Pb, and >1 for Cd, so the authors considered *A. alata* as a good candidate for Cd phytoextraction. Additionally, in the Carolina mine plants from two botanical families such as Asteraceae (*Ageratina* sp. and *Baccharis latifolia*) and Poaceae (*Cortaderia Hapalotricha*) showed TF > 1 for As, Cu, Pb, and Zn, and were considered good candidates for remediation proposes for Pb and Zn [43,47,65]. However, although our study for the same botanical families—Asteraceae (*Ageratina fastigiate*, *Ageratina glechonophylla*, and *Baccharis alnifolia*) and Poaceae (*Cortaderia bifida*)—showed TF > 1 for Zn, Cu, and Cd (*A. fastigiate*), Cu and Cd (*A. glechonophylla*), Zn, Cu, and Cd (*B. alnifolia*), and Cd (*C. bifida*), none of the species had BCF > 1. Accordingly, these plants cannot be considered suitable for phytoremediation.

It has to be underlined, that the study of Bech et al. [47] concerned soils with basic pH, so despite the geographical proximity, the same plant species presented different behavior. In fact, the use of inorganic and organic amendments to acidic soil is recommended to improve metal removal efficiency by phytoremediation [66,67].

Plants with high TF and BCF values are able to extract metals from soils and transport them to the aerial parts. Plants with these characteristics could be considered as candidates for soil phytoremediation. If the BCF is high and the TF low, a plant can be used for phytostabilization [68]. Among the studied plants, *Festuca sp*, *Cortaderia bifida*, and *Gaultheria glomerate* can be considered suitable for Zn phytostabilization, and *Calceolaria tetragona* for Zn phytoremediation. *Gaultheria glomerata* and *Festuca* sp. are also suitable for Cd phytostabilization, and *Achyrocline alata*, *Arenaria digyna, Calceolaria tetragona*, and *Hypericum laricifolium* for Cd phytoremediation.

As for the BCF, no correlation could be found between the plants belonging to the same families: Asteraceae, Ericaceae, Hypericaceae, and Poaceae and their translocation capacity. However, for the same plant species, even growing at different locations (such as *Permettya prostrata*, *Hypericum laricifolium*, *Cortaderia bifida*, and *Brachyotum radula*), similar values were obtained. The plants showed similar behavior towards Pb and Ag and towards Cd, Cu, and Zn which, for the latter, is probably linked to the chemical proximity of these elements.

4. Conclusions

Native flora around two mining environmental liabilities from the Hualgayoc district in the Peruvian Andes was evaluated to assess their potential to accumulate metals in view of their possible use for the phytoremediation of post-mining sites. Soil samples collected at the two sampling sites showed the presence of high concentrations of Pb, Zn, Cu, As, Ag exceeding the levels of the Peruvian and Canadian regulations for agricultural soils, whereas the soils were not considered to be contaminated with Cd. On the other hand, the distribution of metals in the soil was studied, showing the dominant presence of fractions with limited metal mobility even if the acidic pH (observed in the studied area) is expected to increase the bioavailability of metals.

The studied native plants appeared to be well-adapted to prosper in contaminated soils. Out of the 21 plants species evaluated, *Pernettya prostrata* and *Gaultheria glomerate* were suitable for Zn phytostabilization, and *Gaultheria glomerata* and *Festuca* sp. for Cd phytostabilization. It should be noted that the species *Gaultheria glomerata* is suitable for the phytostabilization of both Zn and Cd. *Cortaderia bifida* was the most abundant plant found at the two sampling areas. In addition, the native species applicable for Cd phytoremedia-

tion were *Achyrocline alata*, *Ageratina fastigiate*, *Ageratina glechonophylla*, *Baccharis alnifolia*, *Calceolaria tetragona*, *Arenaria digyna*, *Bejaria* sp., *Pernettya prostrata*, *Hypericum laricifolium*, *Brachyotum radula*, and *Nicotiana thyrsiflora*; and for that of Zn—*Achyrocline alata*, *Ageratina fastigiate*, *Baccharis alnifolia*, *Calceolaria tetragona*, *Arenaria digyna*, *Hypericum laricifolium*, *Brachyotum radula*, and *Nicotiana thyrsiflora*. It is noteworthy that all plant species found suitable for Zn phytoremediation could also be used for Cd phytoremediation. These plants have potential resistance to contaminated soils despite their limitations for growth and are, in consequence, a promising alternative for remediating contaminated soils in highlands.

Supplementary Materials: The following are available online at https://www.mdpi.com/2223-7747/10/2/241/s1, Table S1. Chemical elements in the Earth's Crust and geochemical baseline values near at the sampling sites. Table S2. Trace elements concentrations (mg kg^{-1}) (mean ± SD) of As, Ag, Cd, Cu, Pb and Zn in different organs of the native plants from two study areas (S1 and S2) in the Hualgayoc district, Cajamarca region, Peru. Table S3. Average concentrations of trace elements in organs for the same plant species found in the same sampling area (S1 or S2).

Author Contributions: Conceptualization, E.C.-T., K.B., J.S. and L.T.; methodology, E.C.-T., K.B., J.S. and L.T.; investigation, E.C.-T., K.B. and J.S.; writing—original draft preparation, E.C.-T.; writing—review and editing, K.B. and J.S.; supervision, J.S. and L.T. All authors have read and agreed to the published version of the manuscript.

Funding: This research received no external funding.

Institutional Review Board Statement: Not applicable.

Informed Consent Statement: Not applicable.

Acknowledgments: E.C.-T. acknowledges the support of the Franco-Peruvian Doctoral School in Engineering Sciences and Geosciences. The authors thank Rodolfo Lazo Dávila and Karem Solano Herrera from Activos Mineros S.A.C (AMSAC-Peru) for granting a permission for sampling in the study areas in Hualgayoc district. We thank Manuel Timaná, Director of the Centro de Geografia Aplicada (CIGA) of the Pontifical Catholic University of Peru (Peru) and Mg. Paul Gonzales Arce, Laboratory of Floristics of the Herbarium of the Natural History Museum of the Universidad Nacional Mayor de San Marcos (Peru), for their assistance in the taxonomic identification. The technical help of Ange Angaïts (IPREM, France) in the plant analysis is appreciated.

Conflicts of Interest: The authors declare no conflict of interests.

References

1. Ozturk, M.; Altay, V.; Kucuk, M.; Ertuğrul Yalçın, I. Trace Elements in the Soil-Plant Systems of Copper Mine Areas-A Case Study from Murgul Copper Mine from the Black Sea Region of Turkey. *Phyton Int. J. Exp. Bot.* **2019**, *88*, 223–238. [CrossRef]
2. Paredes, M. The Glocalization of Mining Conflict: Cases from Peru. *Extr. Ind. Soc.* **2016**, *3*, 1046–1057. [CrossRef]
3. Figueroa, B.E.; Orihuela, R.C.; Calfucura, T.E. Green Accounting and Sustainability of the Peruvian Metal Mining Sector. *Resour. Policy* **2010**, *35*, 156–167. [CrossRef]
4. Ministerio de Energía y Minas. *Anuario Minero 2018*; Oficina de Imagen Institucional y Comunicaciones: Lima, Peru, 2018.
5. Lam, E.J.; Cánovas, M.; Gálvez, M.E.; Montofré, Í.L.; Keith, B.F. Evaluation of the Phytoremediation Potential of Native Plants Growing on a Copper Mine Tailing in Northern Chile. *J. Geochem. Explor.* **2017**, *182*, 210–217. [CrossRef]
6. Yildirim, D.; Sasmaz, A. Phytoremediation of As, Ag, and Pb in Contaminated Soils Using Terrestrial Plants Grown on Gumuskoy Mining Area (Kutahya Turkey). *J. Geochem. Explor.* **2017**, *182*, 228–234. [CrossRef]
7. Bouzekri, S.; El Hachimi, M.L.; Touach, N.; El Fadili, H.; El Mahi, M.; Lotfi, E.M. The Study of Metal (As, Cd, Pb, Zn and Cu) Contamination in Superficial Stream Sediments around of Zaida Mine (High Moulouya-Morocco). *J. Afr. Earth Sci.* **2019**, *154*, 49–58. [CrossRef]
8. Aron, A.S.; Molina, O. Green Innovation in Natural Resource Industries: The Case of Local Suppliers in the Peruvian Mining Industry. *Extr. Ind. Soc.* **2020**, *7*, 353–365. [CrossRef]
9. Manjate, E.; Ramos, S.; Almeida, C.M.R. Potential Interferences of Microplastics in the Phytoremediation of Cd and Cu by the Salt Marsh Plant Phragmites Australis. *J. Environ. Chem. Eng.* **2020**, *8*, 103658. [CrossRef]
10. Stefanowicz, A.M.; Kapusta, P.; Zubek, S.; Stanek, M.; Woch, M.W. Soil Organic Matter Prevails over Heavy Metal Pollution and Vegetation as a Factor Shaping Soil Microbial Communities at Historical Zn-Pb Mining Sites. *Chemosphere* **2020**, *240*, 124922. [CrossRef]
11. Ministerio de Energía y Minas Law 28271. Ley Que Regula Los Pasivos Ambientales de La Actividad Minera. In *Diario Oficial El Peruano*; Editora Peru: Cercado de Lima, Peru, 2004.

12. Yupari, A. *Pasivos Ambientales Mineros En Sudamérica*; CEPAL: Santiago, Chile, 2003.
13. Makhmudova, G.; Matsui, K. The Remediation Policy after Mining Works in the Kyrgyz Republic. *Resour. Policy* **2019**, *61*, 304–310. [CrossRef]
14. Ministerio de Energía y Minas Ministry Resolution N° 010-2019-MEM/DM. Actualizan Inventario Inicial de Pasivos Ambientales Mineros. In *Diario Oficial El Peruano*; Editora Peru: Cercado de Lima, Peru, 2019.
15. Chappuis, M. Remediación y Activación de Pasivos Ambientales Mineros (PAM) En El Perú. In *Medio Ambiente y Desarrollo N° 168*; Comisión Económica para América Latina y el Caribe (CEPAL): Santiago, Chile, 2019.
16. Pietrobelli, C.; Marin, A.; Olivari, J. Innovation in Mining Value Chains: New Evidence from Latin America. *Resour. Policy* **2018**, *58*, 1–10. [CrossRef]
17. Bian, F.; Zhong, Z.; Zhang, X.; Yang, C.; Gai, X. Bamboo—An Untapped Plant Resource for the Phytoremediation of Heavy Metal Contaminated Soils. *Chemosphere* **2020**, *246*, 125750. [CrossRef] [PubMed]
18. Moreno-Jiménez, E.; Vázquez, S.; Carpena-Ruiz, R.O.; Esteban, E.; Peñalosa, J.M. Using Mediterranean Shrubs for the Phytoremediation of a Soil Impacted by Pyritic Wastes in Southern Spain: A Field Experiment. *J. Environ. Manag.* **2011**, *92*, 1584–1590. [CrossRef] [PubMed]
19. Favas, P.J.C.; Pratas, J.; Varun, M.; Souza, R.D.; Paul, M.S. Phytoremediation of Soils Contaminated with Metals and Metalloids at Mining Areas: Potential of Native Flora. In *Environmental Risk Assessment of Soil Contamination*; IntechOpen: London, UK, 2014.
20. Chaabani, S.; Abdelmalek-Babbou, C.; Ben Ahmed, H.; Chaabani, A.; Sebei, A. Phytoremediation Assessment of Native Plants Growing on Pb-Zn Mine Site in Northern Tunisia. *Environ. Earth Sci.* **2017**, *76*, 1–15. [CrossRef]
21. Midhat, L.; Ouazzani, N.; Hejjaj, A.; Ouhammou, A.; Mandi, L. Accumulation of Heavy Metals in Metallophytes from Three Mining Sites (Southern Centre Morocco) and Evaluation of Their Phytoremediation Potential. *Ecotoxicol. Environ. Saf.* **2019**, *169*, 150–160. [CrossRef]
22. Santos-Francés, F.; Martínez-Graña, A.; Rojo, P.A.; Sánchez, A.G. Geochemical Background and Baseline Values Determination and Spatial Distribution of Heavy Metal Pollution in Soils of the Andes Mountain Range (Cajamarca-Huancavelica, Peru). *Int. J. Environ. Res. Public Health* **2017**, *14*, 859. [CrossRef]
23. Canchaya, S. Stratabound ore deposits of Hualgayoc, Cajamarca, Perú. In *Stratabound Ore Deposits in the Andes*; Fontboté, L., Amstutz, C., Cardozo, M., Cedillo, E., Frutos, J., Eds.; Springer: Berlin/Heidelberg, Germany, 1990; pp. 569–582. ISBN 9783642882845.
24. Macfarlane, A.W.; Prol-Ledesma, R.M.; Conrad, M.E. Isotope and Fluid Inclusion Studies of Geological and Hydrothermal Processes, Northern Peru. *Int. Geol. Rev.* **1994**, *36*, 645–677. [CrossRef]
25. Padilla, W.G. *Hualgayoc, Riqueza y Tradición*; Asociación Cultural ArteSano: Cajamarca, Peru, 2019; ISBN 978-612-47933-0-1.
26. Macfarlane, A.W.; Petersen, U. Pb Isotopes of the Hualgayoc Area, Northern Peru: Implications for Metal Provenance and Genesis of a Cordilleran Polymetallic Mining District. *Econ. Geol.* **1990**, *85*, 1303–1327. [CrossRef]
27. Bech, J.; Poschenrieder, C.; Barceló, J.; Lansac, A. Plants from Mine Spoils in the South American Area as Potential Sources of Germplasm for Phytorenmediation Technologies. *Acta Biotechnol.* **2002**, *22*, 5–11. [CrossRef]
28. Walkley, A.; Black, I.A. Estimation of Soil Organic Carbon by the Chromic Acid Titration Method. *Soil Sci.* **1934**, *37*, 29–38. [CrossRef]
29. Bouyoucos, G.J. Directions for Making Mechanical Analyses of Soils by the Hydrometer Method. *Soil Sci.* **1936**, *42*, 225–229. [CrossRef]
30. Muller, G. Index of Geo-Accumulation in Sediments of the Rhine River. *Geojournal* **1969**, *2*, 108–118.
31. Yaroshevsky, A.A. Abundances of Chemical Elements in the Earth's Crust. *Geochem. Int.* **2006**, *44*, 48–55. [CrossRef]
32. Okedeyi, O.O.; Dube, S.; Awofolu, O.R.; Nindi, M.M. Assessing the Enrichment of Heavy Metals in Surface Soil and Plant (Digitaria Eriantha) around Coal-Fired Power Plants in South Africa. *Environ. Sci. Pollut. Res.* **2014**, *21*, 4686–4696. [CrossRef] [PubMed]
33. Tessier, A.; Campbell, P.G.C.; Bisson, M. Sequential Extraction Procedure for the Speciation of Particulate Trace Metals. *Anal. Chem.* **1979**, *51*, 844–851. [CrossRef]
34. Głosińska, G.; Sobczyński, T.; Boszke, L.; Bierła, K.; Siepak, J. Fractionation of Some Heavy Metals in Bottom Sediments from the Middle Odra River (Germany/Poland). *Pol. J. Environ. Stud.* **2005**, *14*, 305–317.
35. Lago-Vila, M.; Arenas-Lago, D.; Rodríguez-Seijo, A.; Andrade, M.L.; Vega, F.A. Ability of Cytisus Scoparius for Phytoremediation of Soils from a Pb/Zn Mine: Assessment of Metal Bioavailability and Bioaccumulation. *J. Environ. Manag.* **2019**, *235*, 152–160. [CrossRef]
36. Kamari, A.; Yusoff, S.N.M.; Putra, W.P.; Ishak, C.F.; Hashim, N.; Mohamed, A.; Phillip, E. Metal Uptake in Water Spinach Grown on Contaminated Soil Amended with Chicken Manure and Coconut Tree Sawdust. *Environ. Eng. Manag. J.* **2014**, *13*, 2219–2228. [CrossRef]
37. Yoon, J.; Cao, X.; Zhou, Q.; Ma, L.Q. Accumulation of Pb, Cu, and Zn in Native Plants Growing on a Contaminated Florida Site. *Sci. Total Environ.* **2006**, *368*, 456–464. [CrossRef]
38. Ghazaryan, K.; Movsesyan, H.; Ghazaryan, N.; Watts, B.A. Copper Phytoremediation Potential of Wild Plant Species Growing in the Mine Polluted Areas of Armenia. *Environ. Pollut.* **2019**, *249*, 491–501. [CrossRef]
39. Cruzado-Tafur, E.; Torró, L.; Bierla, K.; Szpunar, J.; Tauler, E. Heavy Metal Contents in Soils and Native Flora Inventory at Mining Environmental Liabilities in the Peruvian Andes. *J. S. Am. Earth Sci.* **2021**, *106*, 1–12. [CrossRef]
40. Kabata-Pendias, A. *Trace Elements in Soils and Plants*, 4th ed.; CRC Press: Boca Raton, FL, USA, 2011; Volume 53, ISBN 9781420093681.

41. Tuo, D.; Xu, M.; Zhao, Y.; Gao, L. Interactions between Wind and Water Erosion Change Sediment Yield and Particle Distribution under Simulated Conditions. *J. Arid Land* **2015**, *7*, 590–598. [CrossRef]
42. Egerić, M.; Smičiklas, I.; Dojčinović, B.; Sikirić, B.; Jović, M. Geoderma Interactions of Acidic Soil near Copper Mining and Smelting Complex and Waste-Derived Alkaline Additives. *Geoderma* **2019**, *352*, 241–250. [CrossRef]
43. Bech, J.; Roca, N.; Tume, P.; Ramos-Miras, J.; Gil, C.; Boluda, R. Screening for New Accumulator Plants in Potential Hazards Elements Polluted Soil Surrounding Peruvian Mine Tailings. *Catena* **2016**, *136*, 66–73. [CrossRef]
44. Ministerio del Ambiente Supreme Decree N° 011-2017-MINAM. Aprueban Estándares de Calidad Ambiental (ECA) Para Suelo. In *Diario Oficial El Peruano*; Editora Peru: Cercado de Lima, Peru, 2017.
45. Canadian Council of Ministers of the Environment. *Canadian Soil Quality Guidelines for the Protection of Environmental and Human Health: Summary Tables*; Canadian Council of Ministers of the Environment: Winnineg, MB, Canada, 2007.
46. Canadian Council of Ministers of the Environment. *Canadian Soil Quality Guidelines for the Protection of Environmental and Human Health: Zinc 2018*; Canadian Council of Ministers of the Environment: Winnineg, MB, Canada, 2018.
47. Bech, J.; Roca, N.; Tume, P. Hazardous Element Accumulation in Soils and Native Plants in Areas Affected by Mining Activities in South America. In *Assessment, Restoration and Reclamation of Mining Influenced Soils*; Elsevier Inc.: Amsterdam, The Netherlands, 2017; pp. 419–461. ISBN 9780128095881.
48. Perlatti, F.; Osório Ferreira, T.; Espíndola Romero, R.; Gomes Costa, M.C.; Otero, X.L. Copper Accumulation and Changes in Soil Physical-Chemical Properties Promoted by Native Plants in an Abandoned Mine Site in Northeastern Brazil: Implications for Restoration of Mine Sites. *Ecol. Eng.* **2015**, *82*, 103–111. [CrossRef]
49. Acosta, J.A.; Arocena, J.M.; Faz, A. Chemosphere Speciation of Arsenic in Bulk and Rhizosphere Soils from Artisanal Cooperative Mines in Bolivia. *Chemosphere* **2015**, *138*, 1014–1020. [CrossRef] [PubMed]
50. Santos-Jallath, J.; Castro-Rodríguez, A.; Huezo-Casillas, J.; Torres-Bustillos, L. Arsenic and Heavy Metals in Native Plants at Tailings Impoundments in Queretaro, Mexico. *Phys. Chem. Earth* **2012**, *37*, 10–17. [CrossRef]
51. Herrera-Quiterio, A.; Toledo-Hernández, E.; Aguirre-Noyola, J.L.; Romero, Y.; Ramos, J.; Palemón-Alberto, F.; Toribio-Jiménez, J. Antagonic and Plant Growth-Promoting Effects of Bacteria Isolated from Mine Tailings at El Fraile, Mexico. *Revista Argentina de Microbiología* **2020**, *52*, 231–239. [CrossRef]
52. Yang, S.X.; Liao, B.; Yang, Z.H.; Chai, L.Y.; Li, J.T. Revegetation of Extremely Acid Mine Soils Based on Aided Phytostabilization: A Case Study from Southern China. *Sci. Total Environ.* **2016**, *562*, 427–434. [CrossRef]
53. Arenas-Lago, D.; Andrade, M.L.; Lago-Vila, M.; Rodríguez-Seijo, A.; Vega, F.A. Sequential Extraction of Heavy Metals in Soils from a Copper Mine: Distribution in Geochemical Fractions. *Geoderma* **2014**, *230*, 108–118. [CrossRef]
54. He, Z.L.; Yang, X.E.; Stoffella, P.J. Trace Elements in Agroecosystems and Impacts on the Environment. *J. Trace Elem. Med. Biol.* **2005**, *19*, 125–140. [CrossRef] [PubMed]
55. Ha, N.T.H.; Ha, N.T.; Nga, T.T.H.; Minh, N.N.; Anh, B.T.K.; Hang, N.T.A.; Duc, N.A.; Nhuan, M.T.; Kim, K.W. Applied Geochemistry Uptake of Arsenic and Heavy Metals by Native Plants Growing near Nui Phao Multi-Metal Mine, Northern Vietnam. *Appl. Geochem.* **2019**, *108*, 104368. [CrossRef]
56. França Afonso, T.; Faccio Demarco, C.; Pieniz, S.; Silveira Quadro, M.; Camargo, F.A.; Andreazza, R. Bioprospection of Indigenous Flora Grown in Copper Mining Tailing Area for Phytoremediation of Metals. *J. Environ. Manag.* **2020**, *256*, 109953. [CrossRef] [PubMed]
57. Claveria, R.J.R.; Perez, T.R.; Perez, R.E.C.; Algo, J.L.C.; Robles, P.Q. The Identification of Indigenous Cu and As Metallophytes in the Lepanto Cu-Au Mine, Luzon, Philippines. *Environ. Monit. Assess.* **2019**, *191*, 185. [CrossRef]
58. Huang, R.; Dong, M.; Mao, P.; Zhuang, P.; Paz-Ferreiro, J.; Li, Y.; Li, Y.; Hu, X.; Netherway, P.; Li, Z. Evaluation of Phytoremediation Potential of Five Cd (Hyper)Accumulators in Two Cd Contaminated Soils. *Sci. Total Environ.* **2020**, *51*, 137581. [CrossRef]
59. Fernández, S.; Poschenrieder, C.; Marcenò, C.; Gallego, J.R.; Jiménez-Gámez, D.; Bueno, A.; Afif, E. Phytoremediation Capability of Native Plant Species Living on Pb-Zn and Hg-As Mining Wastes in the Cantabrian Range, North of Spain. *J. Geochem. Explor.* **2017**, *174*, 10–20. [CrossRef]
60. Cui, J.; Zhao, Y.; Chan, T.; Zhang, L.; Tsang, D.C.W.; Li, X. Spatial Distribution and Molecular Speciation of Copper in Indigenous Plants from Contaminated Mine Sites: Implication for Phytostabilization. *J. Hazard. Mater.* **2020**, *381*, 121208. [CrossRef]
61. Hosseini, S.M.; Rezazadeh, M.; Salimi, A.; Ghorbanli, M. Distribution of Heavy Metals and Arsenic in Soils and Indigenous Plants near an Iron Ore Mine in Northwest Iran. *Acta Ecol. Sin.* **2018**, *38*, 363–367. [CrossRef]
62. Vidal Ccana-Ccapatinta, G.; Lino von Poser, G. Phytochemistry Letters Acylphloroglucinol Derivatives from Hypericum Laricifolium Juss. *Phytochem. Lett.* **2015**, *12*, 63–68. [CrossRef]
63. Drozdova, I.; Alekseeva-Popova, N.; Dorofeyev, V.; Bech, J.; Belyaeva, A.; Roca, N. A Comparative Study of the Accumulation of Trace Elements in Brassicaceae Plant Species with Phytoremediation Potential. *Appl. Geochem.* **2019**, *108*, 104377. [CrossRef]
64. Chandra, R.; Kumar, V.; Tripathi, S.; Sharma, P. Heavy Metal Phytoextraction Potential of Native Weeds and Grasses from Endocrine-Disrupting Chemicals Rich Complex Distillery Sludge and Their Histological Observations during in-Situ Phytoremediation. *Ecol. Eng.* **2018**, *111*, 143–156. [CrossRef]
65. Bech, J.; Duran, P.; Roca, N.; Poma, W.; Sánchez, I.; Barceló, J.; Boluda, R.; Roca-Pérez, L.; Poschenrieder, C. Shoot Accumulation of Several Trace Elements in Native Plant Species from Contaminated Soils in the Peruvian Andes. *J. Geochem. Explor.* **2012**, *113*, 106–111. [CrossRef]

66. Pedron, F.; Petruzzelli, G.; Barbafieri, M.; Tassi, E. Strategies to Use Phytoextraction in Very Acidic Soil Contaminated by Heavy Metals. *Chemosphere* **2009**, *75*, 808–814. [CrossRef] [PubMed]
67. Nagy, A.; Magyar, T.; Juhász, C.; Tamás, J. Phytoremediation of Acid Mine Drainage Using By-Product of Lysine Fermentation. *Water Sci. Technol.* **2020**, 1507–1517. [CrossRef]
68. Xiao, R.; Shen, F.; Du, J.; Li, R.; Lahori, A.H.; Zhang, Z. Screening of Native Plants from Wasteland Surrounding a Zn Smelter in Feng County China, for Phytoremediation. *Ecotoxicol. Environ. Saf.* **2018**, *162*, 178–183. [CrossRef]

CHAPTER C

SPECIES INVOLVED IN TRANSLOCATION OF METAL CONTAMINANTS IN INDIGENIOUS PLANTS FROM POST-MINING AREAS IN PERU

CHAPTER C. SPECIES INVOLVED IN TRANSLOCATION OF METAL CONTAMINANTS IN INDIGENIOUS PLANTS FROM POST-MINING AREAS IN PERU

The third part of the project was devoted to the characterization of the metal speciation in four native plant species of four indigenious hypertolerant plant species, *Arenaria digyna, Puya sp, Hypericum laricifolium* and *Nicotiana thyrsiflora* growing in the studied contaminated post-mining area. The goal was to gain an insight into the elemental species involved in the metal uptake and transport in these plants which is the key to understand the processes allowing certain species to adapt to life in extreme conditions and to grow in heavily contaminated environments.

The state-of-the-art approach consisting of the use of hyphenated techniques combining the chromatographic fractionation of the metal species with mass spectrometric detection - elemental (ICP MS) in order to quantify metals and molecular (ESI MS) - to confirm the species identity, was used. Two liquid chromatography separation mechanisms: fast size-exclusion (SEC) and hydrophilic interaction (HILIC) were tested, each of the methods having its advantages and limitations., were applied to provide validated data on the metal species present in water soluble fraction of roots, stem and leaves of studied plants.

Species involved in translocation of metal contaminants in indigenious plants from post-mining areas in Peru

(manuscript in preparation)

Abstract

Ag, As, Cu, Pb and Zn were found to be the principal contaminants of post-mining area of Peru (Hualgayoc, Cajamarca). Study of metal distribution of metal amongst roots, stems and leaves of four indigenious hypertolerant plant species, *Arenaria digyna, Puya sp, Hypericum laricifolium, Nicotiana thyrsiflora* indicated translocation of Zn and Cu into over ground plant organs. The water soluble As, Ag, Cu, Pb and Zn species present in plant organs (roots, stems and leaves) were fractionated by ultra-performance size-exclusion chromatography (UPSEC) and detected by ICP MS. The separations were achieved within 10 min. The UPSEC separation conditions were re-optimized to allow a direct coupling with ESI Orbitrap MS analysis of Cu and Zn species. Direct coupling of UPSEC to ESI MS was validated by a comparison with HILIC-ESI MS results and can be considered as a new fast and efficient method for analysis of metal-containing biomolecules in complex natural samples. Both targeted and exploratory approaches (based on the characteristic metal isotopic patterns) were used for the search for metal species in high-resolution high-accuracy mass spectra of samples extracts. Elucidation of the structure of particular complexes was completed by fragmentation studies using tandem MS. The presence of nicotianamine and deoxymutageneic acid copper and zinc complexes was demonstrated in organs of *Arenaria digyna, Nicotiana thyrsiflora* and *Puya sp.* A novel, never reported so far, dihydroxy-nicotianamine species was identified as the most abundant Cu and Zn ligand in *Hypericum laricifolium*.

Introduction

Mining has been essential for the economic and industrial development of Peru and remains one of its economic pillars (*1*); Peru is the main producer of gold, zinc, lead, and tin in Latin America and the second largest producer of copper, silver, and zinc worldwide (*2*). However, these developments are accompanied by an environmental cost leaving behind post-mining areas characterized by extreme soil conditions; very often very acidic with high metal contents and frequently bare with no vegetation. For this reason, a special interest is focused on native plants able to grow in such heavily polluted environments; these species are the most probable candidates for the recultivation of soils and their clean up using environment friendly phytoremediation methods. Knowledge about the species involved in metal uptake and transport in plants is the key to understand the processes allowing certain plants to adapt to life in extreme conditions and to grow in heavily contaminated post-mining areas.

The plants which are naturally adapted to tolerate extremely high concentrations of metals in their environment use two distinct strategies (i) “excluders” avoid the built up of metals in the organs, whereas (ii) “hyper-accumulators” promote the storage of metals in above-

ground organs (*3*). Hyperaccumulation of Ni, Zn, Cd, As, Cu, Co, Mn, Pb, Se, Tl and rare earth elements (REE) has been reported (*3, 4*).

Although many studies have reported the total, sometimes very high, concentrations of metals in plants growing in post-mining areas, the speciation information is scarce. In addition, the majority of studies report data for model plants grown in hydroponic conditions (*5*) (more refs) which, while providing important findings, do not mirror the full complexity of the natural circumstances. Moreover, most of the studies are usually carried out by synchrotron techniques and thus restricted to the information about the coordination environments of metal ions without revealing the molecular structure of the species (*6*) (*7, 8*) (*9, 10*). The alternative approach consists of the use of hyphenated techniques combining the chromatographic fractionation of the metal species with mass spectrometric detection - elemental (ICP MS) in order to quantify metals and molecular (ESI MS) - to confirm the species identity. This approach proved successful in the identification of a number of species of Ni in hyperaccumulating plants *Sebertia acuminata* (*11*) and *Thlaspi caerulescens* (*12*), Al (*13*), Fe (*14*) Zn and Fe in rice phloem (*5*) and establishing an inventory of metal complexes circulating in plant fluids (*15*).

Experimental

Samples

Four native Andean plants growing in a post-mining metal contaminated area were studied. They included: *Arenaria digyna, Puya sp, Hypericum laricifolium* and *Nicotiana thyrsiflora.* The taxonomic identification was carried out by Dr. Manuel Timaná (the Pontifical Catholic University of Peru, Peru) and Mg. Paul Gonzales Arce (the Laboratory of Floristics of the Herbarium of the Natural History Museum of the Universidad Nacional Mayor de San Marcos, Peru). The plants were sampled in the Andes of northern Peru, in Hualgayoc district in the west of the province of Hualgayoc, between the districts of Chugur and Bambamarca in the department of Cajamarca in the vicinity of a leach pad (a latitude 6°44'49" S, longitude 78°35'36" W and altitude of 3412 m above sea level) located on top of a mine waste deposit that has no drainage. The sampling points of *Puya sp.* and *Arenaria digyna, Hypericum laricifolium* and *Nicotiana thyrsiflora* were at a 60-m distance; the soil parameters are given in **Table 1**.

Table 1. Characteristic parameters of the soil at the plants sampling points.

Plants sampled	pH	EC (dS m^{-1})	O.M (%)	P, ppm	K , ppm	Soil Texture (%) Sand-Silt-Clay	NO_3^- (ppm)	SO_4^{2-} (ppm)
Puya sp.	4.00	0.09	5.93	3.05	94.5	58-23-19	6.49	196.2
Nicotiana thyrsiflora *Hypericum laricifolium* *Arenaria digyna*	3.68	0.07	4.36	3.20	82.5	52-26-22	5.52	152.5

Reagents

The reagents used for digestions, dilutions, and the preparation of HPLC mobile phases were obtained from Sigma-Aldrich, St. Louis, MO unless stated otherwise. They were: ammonium acetate (≥98% for molecular biology), nitric acid (70%, Fisher Chemical, Loughborough, UK), acetonitrile (≥99.9%) and hydrogen peroxide (30%). Standard solutions (1000 ppm) of Pb, Ag, Cu, Zn, As, Rh, Sc were used for the preparation of calibration curves and as internal standards (Sc and Rh). Milli-Q® Type 1 Ultrapure Water Systems (Millipore, Bedford, MA) deionized water (18.2 MΩ.cm) was used throughout.

Sample preparation

Initial sample preparation. The plants were washed with tap water (for the disposal of soil remains) and then with distilled water. All the plant samples were separated into leaves, stems, and roots; and these were dried at 30-40 °C. Afterwards, all plant organs were crushed and ground to obtain a fine powder.

Elemental speciation. 2.5 mL of 25 mM ammonium acetate pH 7 was added to 0.050 g of leaf, stem, and root samples (in triplicate) and extracted for 1 h by shaking at 400 rpm. After extraction, the samples were centrifuged for 5 min at 13 200 rpm. The supernatants were separated from the plant residue and stored at 4 degrees or analyzed after proper preparation.

Elemental analysis. The extraction residues were dried and then mineralized to determine the water-insoluble fraction of metal species. Samples were digested in DigiPrep heated-block digester (SCP Science, Courtaboeuf, France) using the following two-step program: (1) 1 ml of 70 % nitric acid at 85 °C for 4 h 30 min, after leaving the sample with acid overnight, (2) 0.5 ml of 30 % hydrogen peroxide at 85 °C for 4 h 30 min; the digest was diluted to 5 ml with ultrapure water. Before the analysis, all samples were diluted based on the preliminary results of total metal concentration in plants.

The water-soluble fraction was calculated from supernatants (250 µL) after their digestion with 1 mL of 70 % nitric acid and 0.5 mL of 30 % hydrogen peroxide in DigiPrep block (one-step program: 85 °C for 4 h 30 min); the digests were diluted to 15 ml with ultrapure water and analyze without further preparation.

Instumentation

The ICP MS spectrometers were ICP-MS 7500 (Agilent, Tokyo, Japan) equipped with an integrated autosampler (I-AS) used for the total analysis and Agilent 7700x (Agilent, Tokyo, Japan) used for coupling with HPLC pumps. Electrospray ionization mass spectrometer was LUMOS (Thermo Scientific, Bremen, Germany). The chromatographic systems used for the separation of the analytes were: Agilent 1200 Series (Agilent, Tokyo, Japan) and Dionex Ultimate 3000 RS (Thermo Scientific, Bremen, Germany. Samples were centrifuged using a MiniSpin and 5415 R centrifuges (Eppendorf, Hamburg, Germany).

Determination of the total metal content:

The elemental composition was analyzed by ICP mass spectrometry (ICP-MS) using the reaction cell pressurized with He and H_2 gas. The isotopes monitored were ^{107}Ag, ^{109}Ag; ^{75}As; ^{111}Cd, ^{112}Cd, ^{114}Cd; ^{63}Cu, ^{65}Cu; ^{206}Pb, ^{207}Pb, ^{208}Pb; ^{64}Zn, ^{66}Zn and ^{68}Zn. Analytical blanks were analyzed in parallel. Quantification was performed in the calibration range of 0.2-100 ppb for Zn and 0.1-20 ppb for the other elements; an 8-point calibration curve was used. The measurements were carried out in triplicates and the results with relative standard deviation higher than 10% were discarded and the measurements repeated. Values are reported as mean ± standard deviation (SD) of three replications.

Speciation of elemental species by HPLC coupled to ICP MS and ESI MS^n

The chromatographic conditions used are detailed in **Table 2**.

Table 2. The chromatographic conditions used.

separation mechanism	fast size–exclusion chromatography (fast-SEC)	hydrophilic interactions liquid chromatography (HILIC)	
column	ACQUITY UPLC BEH 125 SEC (1.7 µm 4.6 x 150 mm); 1–80kDa	TSKgel Amide-80 (2.0 µm, 2.0 x 150 mm)	
mobile phase	ammonium acetate 25 mM, pH=7	A: ammonium acetate 10 mM pH=7 B: ACN	
injection volume, µL	5	10	
flow rate, mL/min	0.3	0.1	0.2
elution	isocratic	0 min –80 % B 2.5 min - 80 % B 22.5 min -50 % B 25 min –50 % B 26 min –80 % B 35 min –80 % B	0 min –80 % B 2.0 min - 80 % B 3.0 min – 65% B 4.5 min – 65% B 9.0 min – 60% B 12 min – 60% B 13.8 min -50 % B 16.8 min –50 % B 17.8 min –80 % B 25 min –80 % B

Fast SEC. Before injection onto a size exclusion column, supernatants obtained from water extraction were mixed in ratio 1:1 with eluent or ACN and centrifuged. Effluents from chromatographic column were analyzed directly or after post-column ACN addition (0.3 mL/min); ACN was delivered with Agilent 1200 Series system. For the ICP MS detection, the exit of the column was directly connected to an Agilent 7700x ICP mass spectrometer equipped with a collision cell. When working with ACN as one of the eluents, O_2 was used as an optional gas (5%). Ni or Pt cones were used depending on whether organic solvent was used

HILIC. Before injection onto a HILIC column, supernatants obtained from water extraction were mixed in ratio 1: 4 with ACN, to get the same ACN percentage as w for the gradient

initial conditions. Addition of ACN may create a small amount of precipitate, containing less than 5% of the metals of interest, so all samples were centrifuged for 5 min at 13 200 rpm. The exit of the column was directly connected to an Agilent 7700x ICP MS equipped with a collision cell. Due to the use of organic solvents, platinum ICP MS cones and O_2 as an optional gas (5%) were applied.

The samples have been subsequently analyzed by ESI MS^n using both chromatographic separation modes – Fast-SEC and HILIC (*cf.* Table 2). The MS analyses were performed in positive ionization mode with ion source conditions set as default, according to the current LC flow – 0.6 mL/min and 0.1-0.2 mL/min for Fast-SEC and HILIC, respectively, including post-column ACN addition for Fast-SEC. Data were acquired at resolution 240 000 in a scan range of 150-1000 m/z with a maximum injection time of 502ms, $5e^5$ AGC target and 30% RF lens. MS/MS was performed in a targeted analysis mode, based on the results from the FullScan mode (Full MS/dd-MS^2). The inclusion mass list was prepared based on the already known metal-containing compounds as well as compounds with metal characteristic isotopic patters. To ascertain those compounds Thermo Scientific™ Compound Discoverer™ with Pattern Scoring Node was applied. Full MS/dd-MS^2 was performed as follows: 1) FullScan MS: orbitrap resolution = 240K; scan range = 150-1000m/z; maximum injection time = 300ms; AGC target = 80000; RF lens = 30%; 2) MS^2 of targeted ions was performed in the HCD cell with a collision energy of 30%; orbitrap resolution = 60K; maximum injection time = 118ms; AGC target = 75000 with the first mass of 100m/z.

Results and discussion

The elements studied

The concentrations of 14 elements were studied in the soil where the plants were collected (*16*). They were compared with the baseline values for uncontaminated soils. The choice of the elements to study was made on the basis of the soils contamination which was assessed by using the Index of Geoaccumulation (Igeo) (*17*). It was calculated on the basis of the element soil content at the plants sampling locations (**Table SI-1**) (*16*) and their abundances in the Earth's crust (*18*) and geochemical baseline values near at the sampling sites (*19*) (**Table SI-2**). The degree of the pollution (*20*) depended on the elements with results ranging from extremely contaminated (Pb, Ag, $I_{geo} \geq 4$), strongly (As, Cu, Zn $2 \leq$ Igeo < 4), moderately (Cr, Mo, Tl $1 \leq I_{geo} < 2$) to uncontaminated (Cd, Co, Mn, Ni, V, W, $I_{geo} < 1$) soils (**Figure 1**). The five elements, Ag, As, Cu, Pb and Zn for which the contamination was the highest, were selected for investigation. These elements were mainly present in soil fractions with limited metal mobility (*21*).

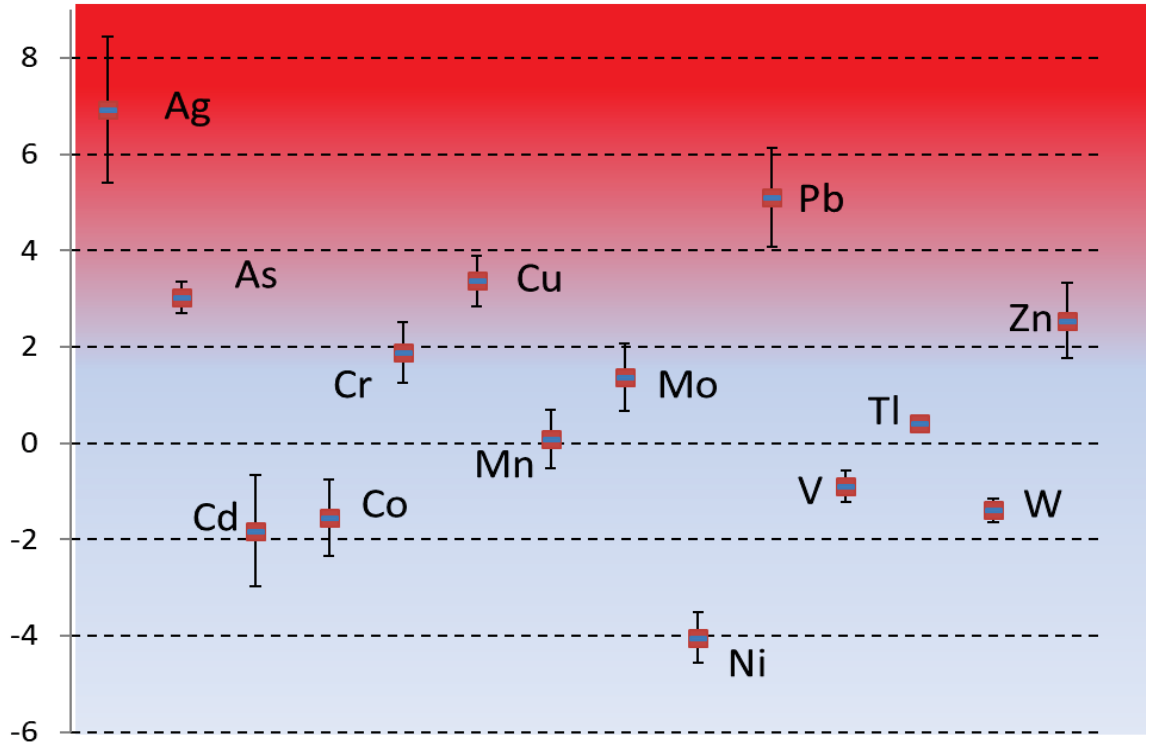

Figure 1. Index of Geoaccumulation (Igeo) for selected elements present in the soil in the contaminated post-mining site.

The choice of the plants

Four native Andean plants: *Arenaria digyna, Puya sp, Hypericum laricifolium* and *Nicotiana thyrsiflora* growing in post-mining contaminated metal areas were studied. All of them are ubiquitous in South America and can be found in growing in Andean mountain areas.

Nicotiana thyrsiflora belongs to *Nicotianas* which are important in traditional medicine in both South America and Australia, and *N. tabacum* is one of the most widely used drug plants in the world. *Nicotiana* is one of the most comprehensively studied flowering plant genera with numerous studies having accumulated a large body of information concerning evolution, cytology, taxonomy and biogeography (*22*). *Nicotiana thyrsiflora*, after evolving in southern South America east of the Andes, later dispersed to Africa, Australia, and southwestern North America (*23*). *Nicotiana thyrsiflora* has been included into a study of the propagation of native cloud forest and high Andean herbaceous and shrub species in the Cajamarca mountain range (Peru) with the aim of propagating them for environmental restoration activities, thus creating a buffer zone and conservation (*24*). The alkaloid composition of the *Nicotiana* plants was investigated, nornicotine was the dominating species in *Nicotiana thyrsiflora* in both greenhouse- and field grown plants (*25*).

Hypericum laricifolium (*Hypericaceae*) is distributed from western Venezuela along the cordilleras of Colombia and Ecuador to central Peru (*26*). The infusion of its aerial parts is

used in traditional medicine (*27*). Investigations of the aerial parts of *H. laricifolium* revealed the presence of phenolic acids, flavonoids, triterpenoids (*28*), xanthones (*29*), and dimeric acylphloroglucinol derivatives (*30*). Additionally, the essential oil composition of a *H. laricifolium* (*31*) and the identification of a group of acylphloroglucinol derivatives found in its n-hexane extract (*32*) were reported.

Puya sp. belongs to the botanical terrestrial family of *Bromeliaceae* plants and are native to the Andes Mountains of South and Southern Central America. It forms clumps of small 8-10 inch wide rosettes of very narrow powdery blue-gray leaves and has no stem. The high Andean species of Puya provide an important nutritious resource for hummingbirds, especially for those of high altitudes where the diversity of plants diminishes (*33*) (*34*). *Puya sp* tea infusions are known for antioxidant and aldose reductase inhibitory activity (*35*) The heart of the inflorescence of Puya sp. known as "aguarongo" is cooked and eaten In Ecuador (*36*).

Arenaria dygina belongs to *Caryophyllaceae;* several species of the family are used by ethnic communities as traditional medicine (*37*). *Arenaria dygina* is one of indicator species for high altitude bofedales (*38*).

Total element concentration in plant organs

The total concentration of Ag, As, Cu, Pb and Zn in individual plant organs are given in **Table 3**. Threshold criteria for the concentration in foliar tissues (dry weight basis) have been defined for various elements for plants growing in their natural habitat (**Table SI-3**); they allow the discrimination between uncontaminated and contaminated plant species. For the investigated elements they are: 10 mg kg^{-1} for Pb, 30 mg kg^{-1} for Cu, 150 mg kg^{-1} for Zn, 0.5 mg kg^{-1} for Ag, and 1.7 mg kg^{-1} for As (*39*).

All the studied plants species showed As, Pb and Zn zinc concentrations higher than the approximate generalized values reported for mature leaf tissue for various species in uncontaminated conditions (*39*). In the case of copper and silver, these values (*39*) were exceeded for two plants: *Nicotiana thyrsiflora* and *Arenaria digyna*.

Table 3. Total metal concentrations (mg kg^{-1}) (mean ± SD) of Ag, As, Cu, Pb and Zn in different organs of the native plants the Hualgayoc district, Cajamarca region, Peru

Native species	Organs	Ag			As			Cu			Pb			Zn		
Puya sp	L	0.44	±	0.06	8.33	±	0.14	13.30	±	0.82	38.19	±	1.60	145.00	±	2.57
	R	1.51	±	0.20	45.35	±	0.93	22.60	±	0.41	120.82	±	1.18	23.40	±	2.06
Nicotiana thyrsiflora	L	4.07	±	0.09	2.41	±	0.05	77.60	±	0.55	64.79	±	0.70	390.00	±	8.60
	S	0.69	±	0.06	0.50	±	0.01	123.00	±	1.18	82.13	±	5.23	447.00	±	8.80
	R	8.41	±	1.78	3.37	±	0.13	132.00	±	12.40	82.94	±	2.98	590.00	±	12.40
Hypericum laricifolium	L	1.38	±	0.13	3.77	±	0.08	9.71	±	0.74	158.76	±	3.66	305.00	±	4.73
	S	0.68	±	0.05	1.07	±	0.04	9.12	±	0.95	137.44	±	1.41	164.00	±	3.46
	R	7.84	±	0.90	7.66	±	0.36	21.53	±	3.37	407.98	±	20.22	153.00	±	14.60
Arenaria digyna	L	3.43	±	0.08	8.29	±	0.11	48.50	±	0.57	373.76	±	5.83	1051.00	±	20.60
	S	13.01	±	0.42	110.34	±	1.07	6.30	±	0.34	2245.10	±	29.03	546.00	±	30.20
	R	17.10	±	0.51	140.61	±	39.54	7.47	±	0.09	2505.49	±	280.12	105.00	±	3.78

L: leaf, S: Stem, R: Root

The data on the total element concentration in plant organs allowed the calculation of the bioaccumulation *(BCF)* and translocation factors *(TF)* in order to assess the ability of plants to mobilize elements from the soil (BCF) and translocate (TF) them from roots to aerial parts (**Table 4**) (*40*). In three out of four plants, the zinc content was the highest in leaves demonstrating efficient translocation of Zn from roots to over ground organs. None of the studied plants fulfils the criteria necessary to be to classified as hyperaccumulators; according to (*3*) they are: the shoot/root ratio of metal concentration higher than 1; (ii) metal total content in the shoots divided by total metal in the soil greater than 1 and, (iii) metal content must be 10 – 500 times higher than found in uncontaminated plants.

Table 4. Bioconcentration Factor (BCF) and Translocation Factor (TF) values of native species selected

Family	Species	Bioaccumulation factor*					Translocation factor**				
		Ag	As	Cu	Pb	Zn	Ag	As	Cu	Pb	Zn
Bromeliaceae	*Puya sp*	0.04	0.03	0.05	0.02	0.50	0.30	0.18	0.59	0.32	**6.20**
Solanaceae	*Nicotiana thyrsiflora*	0.16	0.01	0.24	0.02	0.73	0.48	0.71	0.59	0.78	0.66
Hypericaceae	*Hypericum laricifolium*	0.06	0.01	0.03	0.04	0.57	0.18	0.49	0.45	0.39	**1.99**
Caryophyllaceae	*Arenaria digyna*	0.14	0.02	0.15	0.10	1.97	0.20	0.06	**6.49**	0.15	**10.01**

* BF= C_p/C_{so} (where C_p is the metal concentration in the plant leaves and C_{so} - in the soil)
** TF = C_s/C_r (where C_s is the metal concentration the leaves and C_r - in roots)

Elemental speciation of water soluble element species

The first step to have an insight into the nature of elemental species in plant was their fractionation into water soluble and insoluble fraction, their contents in individual plant organs are presented in **Figure 2**. Lead, arsenic and silver are mostly present in insoluble form and the percentage of water species in does not exceed 8% (Pb), 23% (As), 11%(Ag).

The percentage of water soluble species was the highest for Zn and Cu reaching up to 40% and 50%, respectively, in *Nicotiana thyrsiflora* over ground organs.

The next part of the study involved the development of liquid chromatography with parallel elemental (ICP) and molecular (ESI) mass spectrometric detection for the separation of the elemental species present. Two liquid chromatography separation mechanisms: size-exclusion (SEC) and hydrophilic interaction (HILIC) were tested, each of the methods having its advantages and limitations.

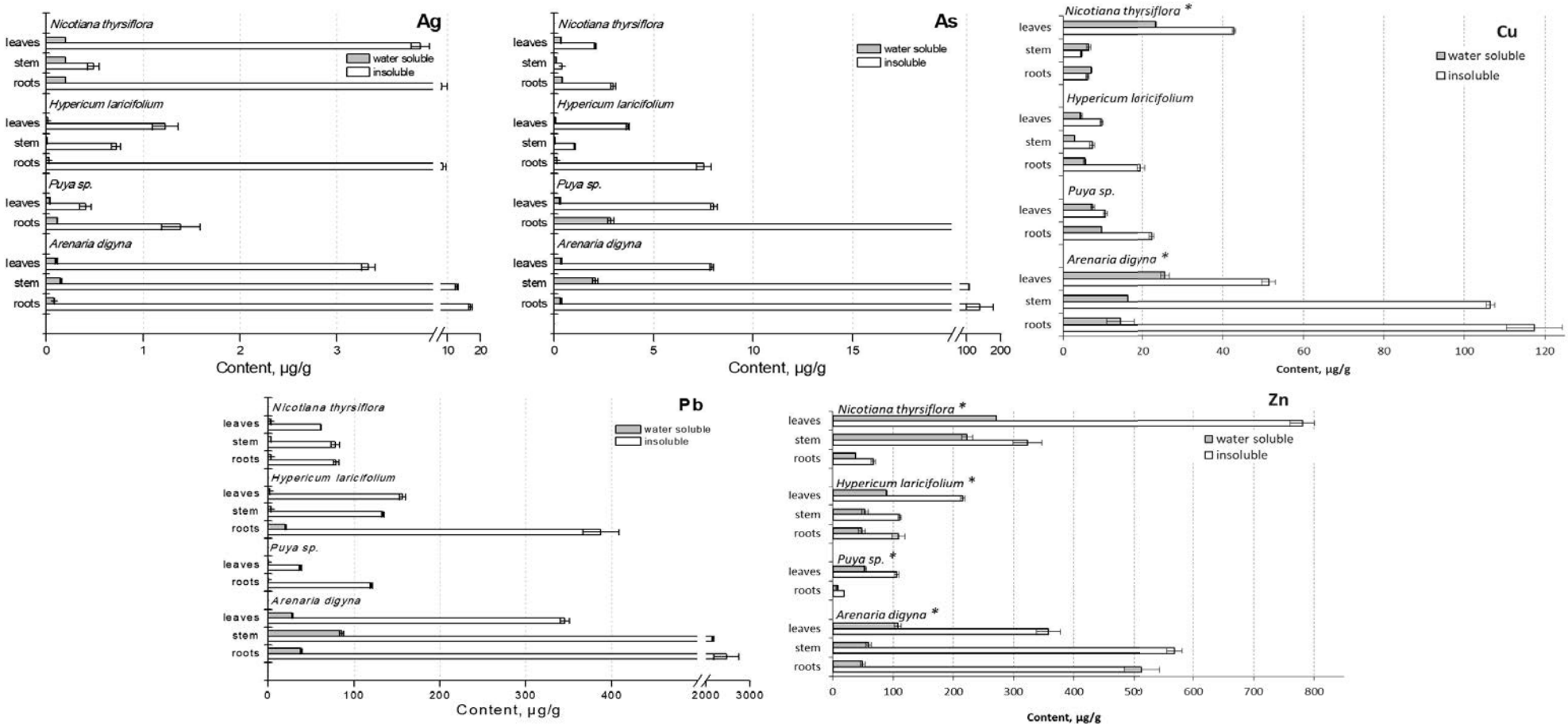

Figure 2. Ag, As, Cu, Pb and Zn fractionation into water soluble and insoluble fraction in individual organs of the studied plants.

The first one, SEC, provides molecular size based fractionation and can be used for a relatively large spectrum of sizes, usually from several tens of thousands to several hundred Da. However, the resolution is low, so single-species peaks are difficult to obtain and labile metal coordination complexes tend to dissociate on-column leading to non-quantitative elution and carry over effects. Moreover, the standard bore chromatographic columns require relatively long time runs and their coupling to ESI is problematic (the eluents have to be adapted by elimination of salts and addition of organic solvents which affects the separation).

The use of HILIC is restricted to LMW hydrophilic complexes, so the information on potentially present HMW water soluble species is lost. On the other hand, upon suitable optimization, the resolution usually allows the separation of individual species and their ESI MS identification. However, HILIC elutions are usually carried out with gradients which results in changing ionization conditions in ICP MS and ESI MS and may affect the datasets obtained (species more or less readily ionized).

Molecular size fractionation by fast size-exclusion chromatography

The SEC separation were carried out using recently introduced fast-SEC technology (in Ultra-High Perfomance Liquid Chromatography (UHPLC) mode) with a stationary phase having the solvent stability and mechanical strength which provided significant improvement in separation efficiency and 3-4-old shortening of the analysis time (Perez-Moral et al., 2018; Uliyanchenko et al., 2011). The chromatographic separation were completed within less than 15 minutes. The chromatograms obtained for Ag, As and Pb water extracts are shown in **Figure 3**. The Ag and Pb peaks eluted close to the exclusion volume of the column proving high MW of the metal complexes. The identification of these species has not been attempted, however, one of strong candidates seems to the complex formed with the dimer of a pectic polysaccharide, rhamnogalacturonan II found in edible plants (*41, 42*). In agreement with the data shown in Figure 2, which demonstrate low contents of water soluble fractions for these three elements, the intensity of the peaks is relatively low with the exception of lead in *Arenaria digyna, Hypericum laricifolium* and *Nicotiana thyrsiflora*. The intensity of the peaks correlated well with the total elements contents determined showing no translocation of the elements from roots towards over ground organs.

a. *Nicotiana thyrsiflora*

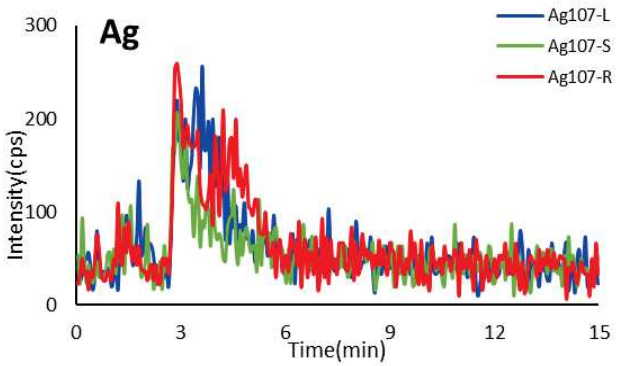

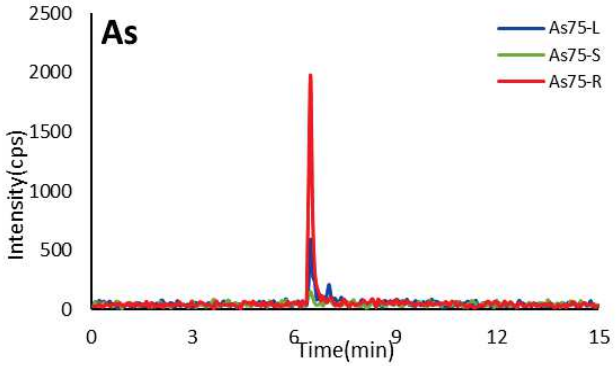

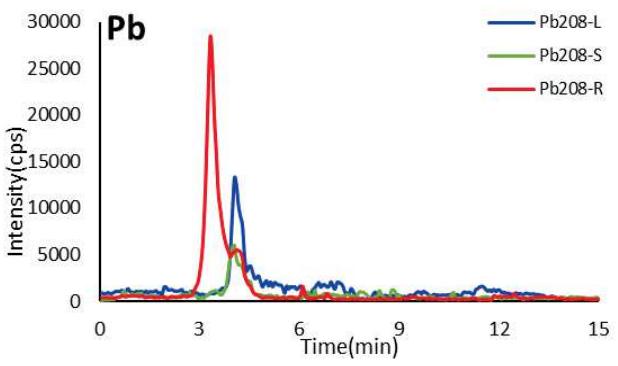

b. *Hypericum laricifolium*

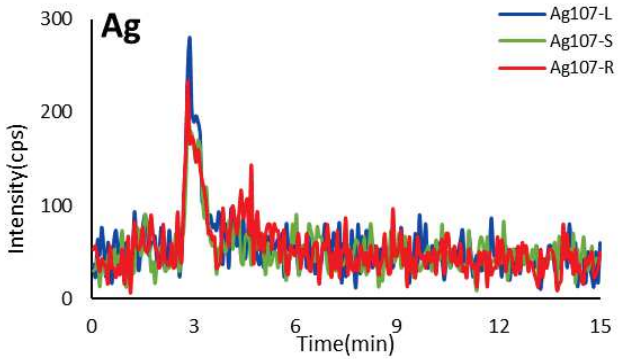

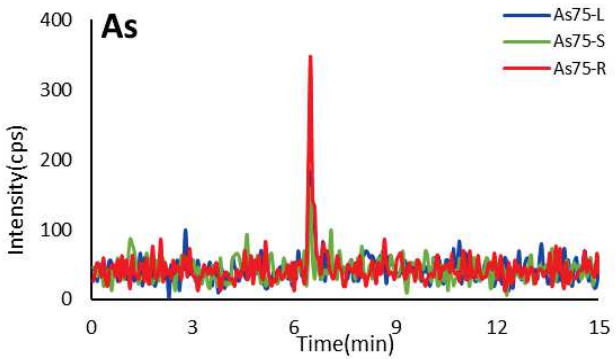

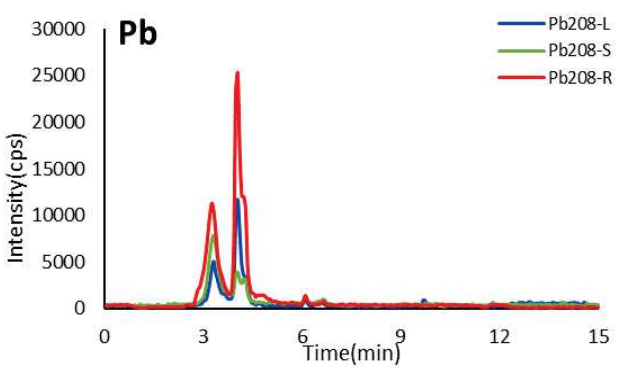

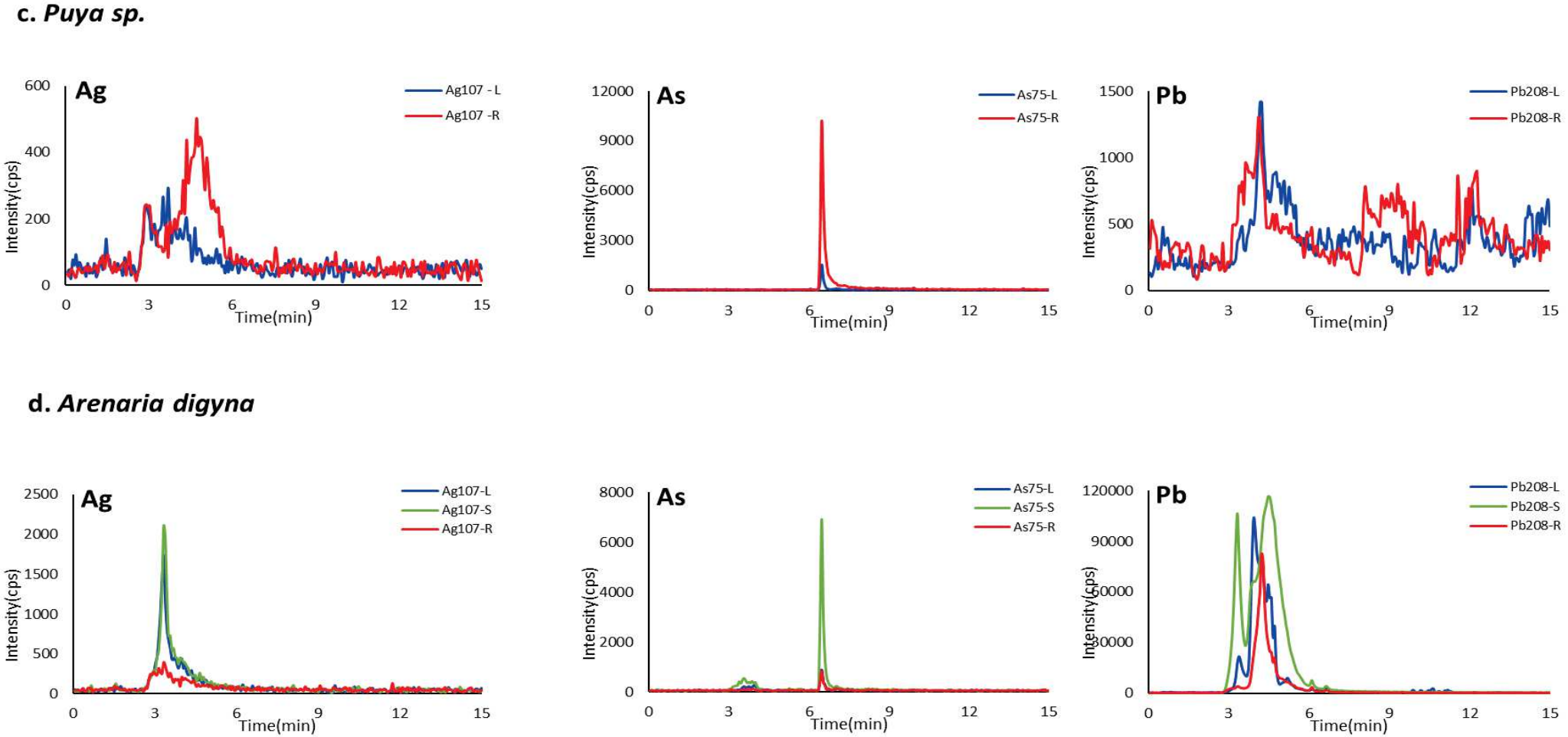

Figure 3. SEC-ICP MS fractionation of the water soluble species of Ag, As, and Pb leaves (blue lines), stems (green lines), and roots (red lines) of *Nicotiana thyrsiflora*, *Hypericum laricifolium*, *Puya sp.*, and *Arenaria digyna*

The molecular weight fractionation of water soluble species of Cu and Zn in the leaves, stems, and roots of *Nicotiana thyrsiflora*, *Hypericum laricifolium, Puya sp., and Arenaria digyna* is shown in **Figure 4.** All the peaks elute in the low molecular (less than 2 kDa) weight range and their intensity correlates well with with the determined total elements contents showing, in most cases, the translocation of the elements from roots towards over ground organs. The identification of the species producing Cu- and Zn-containing peaks was carried out by ESI MS upon post-column addition of the organic solvent necessary to assure efficient ionization. Initially, the identification was carried out using a targeted approach looking for masses of Cu- and Zn-complexes reported in the literature. Then, the non-targeted approach based on the search for elemental isotopic pattern was applied. Both copper and zinc are present in the Nature as a mixture of isotopes; for copper - ^{63}Cu (69.2%) and 65Cu (30.8%) and for Zn - ^{64}Zn (49.2%), ^{66}Zn (27.7%), ^{67}Zn (4.0%), ^{68}Zn (18.5%) and ^{70}Zn (0.6%). The abundance distribution of isotopes is conserved in all the species containing these elements, and this *isotopic pattern* is a means to recognize element species in a mass spectrum. The search is carried out automatically but usually has to be validated by the examination of the candidate molecules found.

In **Figure 4**, the SEC-ICP MS chromatograms are correlated with corresponding ESI MS extracted ion chromatograms (XICs) of the detected species. The list of the species together with their masses is given in **Table 5.**

a. *Nicotiana thyrsiflora*

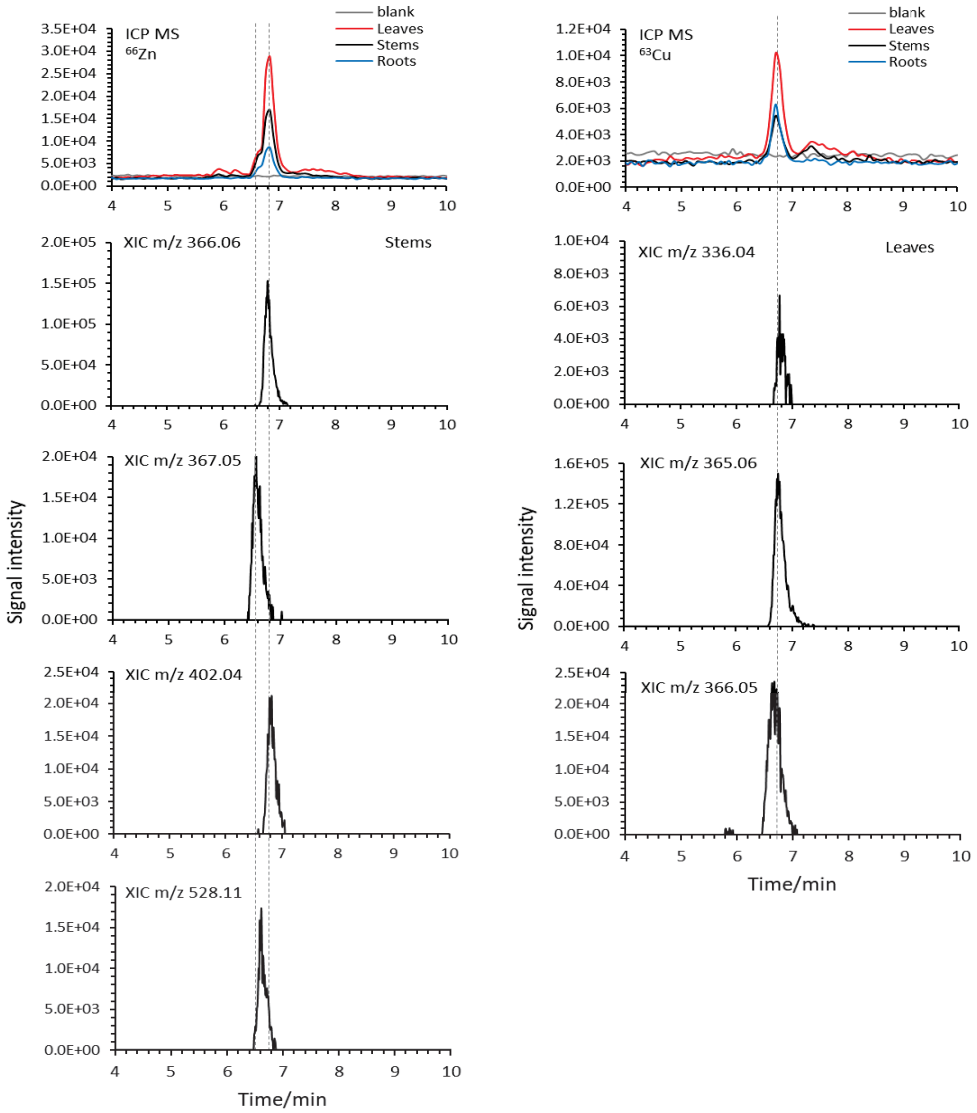

b. *Hypericum laricifolium*

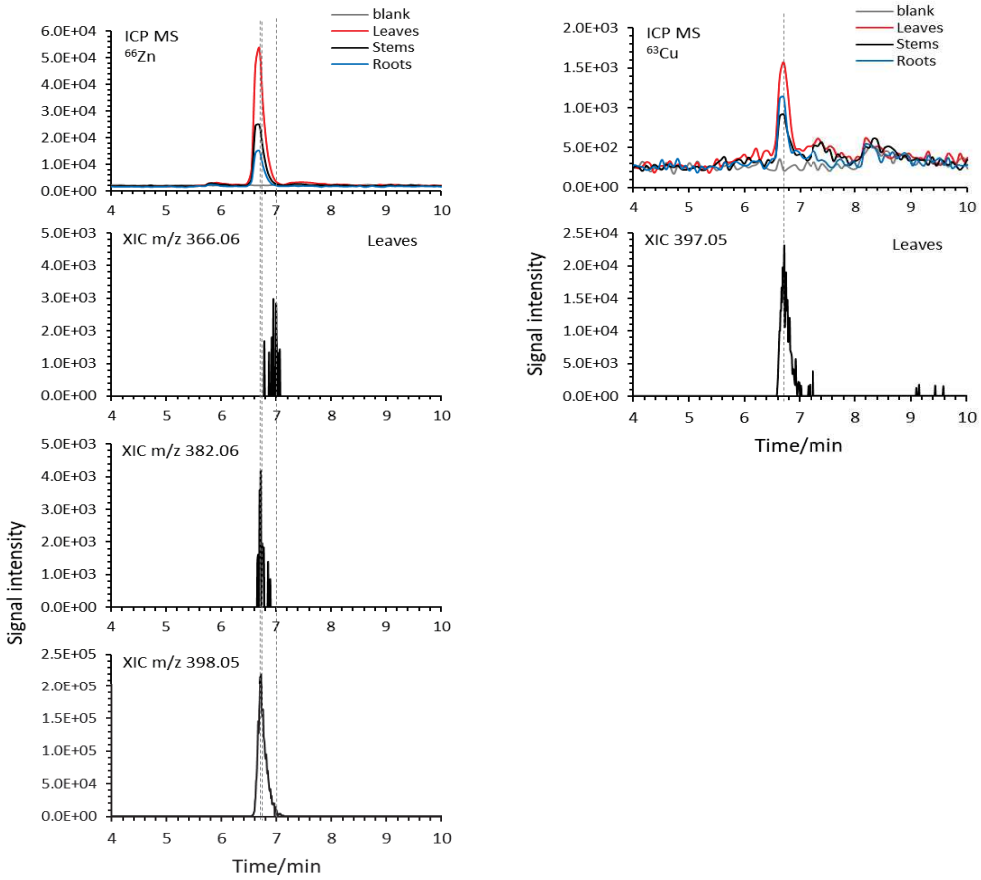

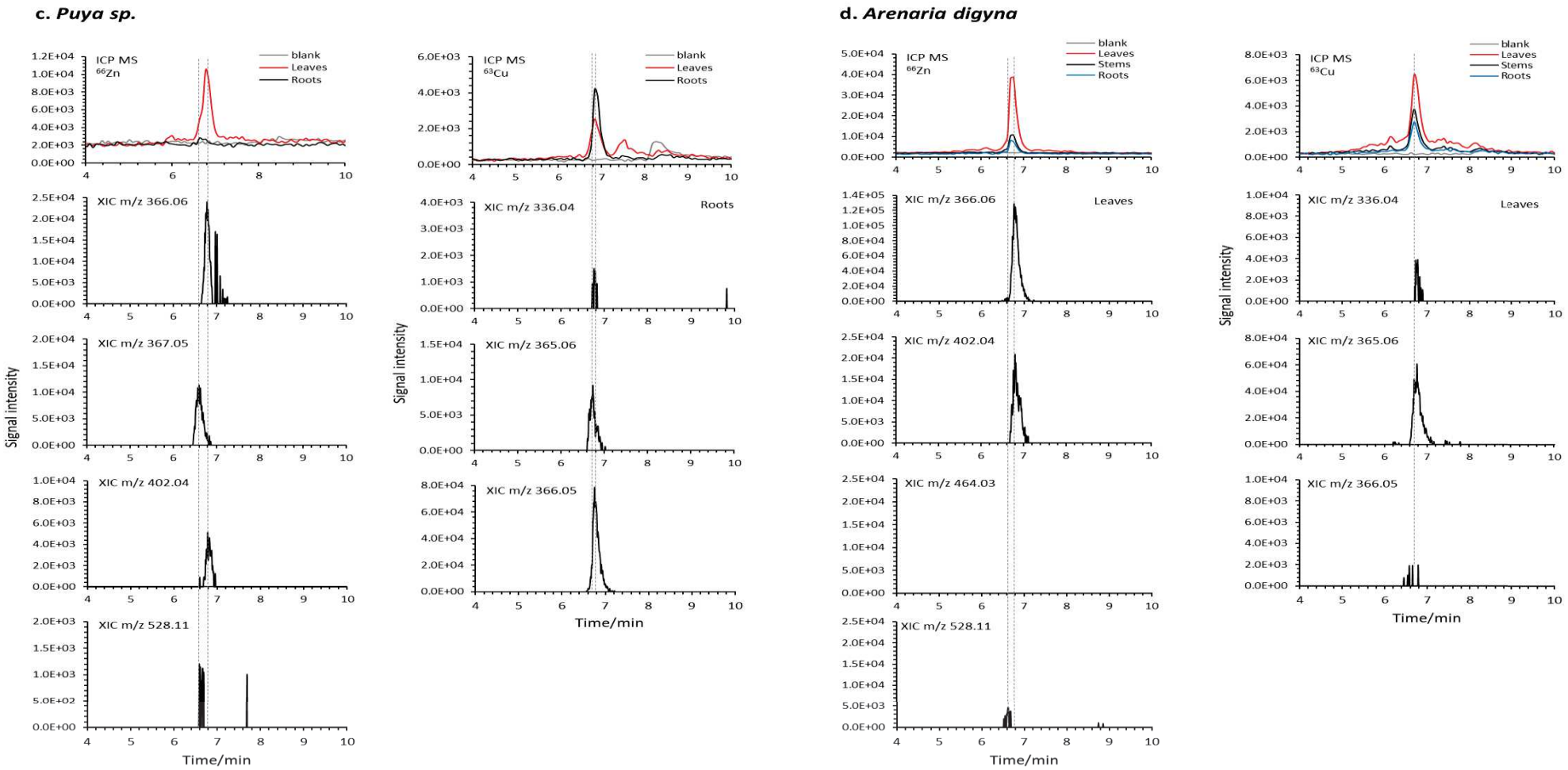

Figure 4. SEC- ICP/ESI MS speciation of water soluble Cu and Zn species in the leaves, stems, and roots extract of *Nicotiana thyrsiflora*, *Hypericum laricifolium, Puya sp. and Arenaria digyna*

Table 5. List of the species together with their masses of Cu and Zn

MW	Monoisotopic mass	FORMULA (neutral form)		m/z
Nicotiana thyrsiflora				
335.8	335.03043	C11 H16 O6 N2 Cu	[M+H]+1	336.03771
			[M+K]+1	373.99360
			[M-H+2K]+1	411.94948
364.84	364.05698	C12 H19 O6 N3 Cu	[M+H]+1	365.06426
			[M+K]+1	403.02014
			[M-H+2K]+1	440.97603
			[M-H]-1	363.04971
365.83	365.04100	C12 H18 O7 N2 Cu	[M+H]+1	366.04828
			[M+K]+1	404.00416
			[M-H+2K]+1	441.96004
			[M-H]-1	364.03373
366.67	365.05653	C12 H19 O6 N3 Zn	[M+H]+1	366.06381
			[M+K]+1	404.01971
			[M-H+2K]+1	441.97568
367.66	366.04054	C12 H18 O7 N2 Zn	[M+H]+1	367.04837
		C12 H20 Cl N3 O6 Zn* C15 H17 O7 N2 Zn *	[M+H]+1	402.04053**
		C18 H29 O11 N3 Zn * C17 H23 O6 N10 Zn *	[M+H]+1	528.11658**
Puya sp.				
335.8	335.03043	C11 H16 O6 N2 Cu	[M+H]+1	336.03771
			[M+K]+1	373.99360
			[M-H+2K]+1	411.94948
364.84	364.05698	C12 H19 O6 N3 Cu	[M+H]+1	365.06426
			[M+K]+1	403.02014
			[M-H+2K]+1	440.97603
			[M-H]-1	363.04971
365.83	365.04100	C12 H18 O7 N2 Cu	[M+H]+1	366.04828
			[M+Na]+1	388.03022
			[M+K]+1	404.00416
			[M-H+2K]+1	441.96004
			[M-H]-1	364.03373
			[M-2H+K]-1	401.98961
366.67	365.05653	C12 H19 O6 N3 Zn	[M+H]+1	366.06381
			[M+K]+1	404.01971
			[M-H+2K]+1	441.97568
367.66	366.04054	C12 H18 O7 N2 Zn	[M+H]+1	367.04837
		C16 H13 O3 N6 Zn * C12 H20 O6 N3 Cl Zn *	[M+H]+1	402.04129**
		C18 H29 O11 N3 Zn * C17 H23 O6 N10 Zn *	[M+H]+1	528.11609**

MW	Monoisotopic mass	FORMULA (neutral form)		m/z
Hypericum laricifolium				
396.84	396.04681	C12 H19 O8 N3 Cu	[M+H]+1	397.05409
			[M+K]+1	435.00997
			[M-H+2K]+1	472.96586
			[M-H]-1	395.03954
			[M-2H+K]-1	432.99542
366.67	365.05653	C12 H19 O6 N3 Zn	[M+H]+1	366.06381
382.67	381.05144	C12 H19 O7 N3 Zn	[M+H]+1	382.05872
398.67	397.04636	C12 H19 N3 O8 Zn	[M+H]+1	398.05364
			[M+Na]+1	420.03558
			[M+K]+1	436.00952
			[M+2K-H]+1	473.96540
			[M-H]-1	396.03908
			[M-2H+K]-1	433.99497
Arenaria digyna				
335.8	335.03043	C11 H16 O6 N2 Cu	[M+H]+1	336.03771
			[M+K]+1	373.99360
			[M-H+2K]+1	411.94948
			[M-H]-1	334.02316
364.84	364.05698	C12 H19 O6 N3 Cu	[M+H]+1	365.06426
			[M+K]+1	403.02014
			[M-H+2K]+1	440.97603
			[M-H]-1	363.04971
365.83	365.04100	C12 H18 O7 N2 Cu	[M+H]+1	366.04828
			[M+K]+1	404.00416
			[M-H+2K]+1	441.96004
			[M-H]-1	364.03373
366.67	365.05653	C12 H19 O6 N3 Zn	[M+H]+1	366.06381
			[M+K]+1	404.01971
			[M-H+2K]+1	441.97568
			[M-H]-1	364.04926
		C15 H17 O7 N2 Zn *	[M+H]+1	402.04001**
		C18 H29 O11 N3 Zn * C17 H23 O6 N10 Zn *	[M+H]+1	528.11627**

* suggested formula
** experimental m/z

Speciation by HILIC ICP/ESI MS

Hydrophilic interactions chromatography is a well accepted method for the speciation of metal complexes with small organic ligands (*15*). **Figure 5** shows HILIC-ICP/ESI MS chromatograms of water extracts of the leaves, stems, and roots of *Nicotiana thyrsiflora, Hypericum laricifolium, Puya sp., and Arenaria digyna;* they present Cu and Zn species detected by ICP MS (on the basis of their metal content) and corresponding ESI MS extracted

ion chromatograms (XICs) of the detected species. The results are in good agreement with the SEC-based findings thus validating them.

Speciation of zinc in water soluble fraction of plant organs

In three out of four investigated plants, namely *Arenaria digyna, Nicotiana thyrsiflora* and *Puya sp.,* Zn-nicotianamine is the most abundant (and in *Arenaria digyna* the only one) Zn species in water soluble fraction. Also uncomplexed (free) NA was observed in these three plants. Zn-DMA was observed in two samples: *Nicotiana thyrsiflora* and *Puya sp.* The contributions of Zn-DMA, which has a lower complex formation (12.7 for Zn(II)-DMA) (*43*) constant than Zn-NA (ca. 15 (*44, 45*)) were much lower although free DMA was present in the samples.

Similar quantities of Zn-DMA were found in roots and leaves of *Puya sp.,* Zn-NA was very high in leaves with only traces present in roots. In *Nicotiana thyrsiflora* the concentration of Zn-NA complex doubles when passing from roots to stems and then from stems to leaves, traces of DMA-Zn can be observed only in stems and leaves. In *Arenaria digyna* similar Zn-NA levels were present in roots and stems and significantly higher (ca. 4 times) in leaves, no Zn-DMA complex could be detected in any of the organs. Additionally, in all three plants traces of m/z 402.041 and m/z 528.117 species showing Zn isotopic pattern were detected. However, their intensity was too low to allow acquiring good quality fragmentation spectra necessary for identification.

The presence of DMA in *Nicotiana thyrsiflora* is interesting because for a long time it has been thought that only graminaceous plants biosynthesize MAs. However, at least two recent LC-TOF-MS studies reported the presence of DMA in non-graminaceous plant species such as peanut (*Arachis hypogaea L.)* (*46*) and olive trees (*Olea europaea L.*) (*47*). For the first one, the authors concluded that peanut's roots absorbed Fe-DMA complex generated by DMA secreted from neighbouring maize plants (*46*). Similarly, the detected presence of Zn-DMA in lettuce was considered to be a contamination in (*48*). However, in the study of Suzuki et al., the intercropping was excluded and DMA complexes detected in both the xylem sap and leaves of olive trees (*47*). The analysis of these two matrices - one analyzed directly (xylem sap) and the other one which required tissue homogenization and extraction (leaves) - provides a mutual validation of these two approached as the results are in agreement for both (*47*). In our case, although in the field sampling the intercropping could not be excluded, the presence of free (apo) DMA in *Nicotiana thyrsiflora* organs confirmes our finding of Zn-DMA (and also Cu-DMA) complexes. A possibility of the contamination during the analytical procedure (and, in particular, chromatographic carryover) has been carefully examined and discarded. The genes for DMA biosynthesis were detected by transcriptome analysis of *Olea europaea L.* and it has been suggested that NAAT and DMAS might have evolutionally loose substrate specificities in olive plants compared with those in graminaceous plants (*47*). Indeed, recent studies stressed several shared components of the metal complexing strategies among plants, questioning the validity of the earlier concept of their mutual exclusivity (*49*).

Nicotianamine (NA) is the most often reported LMW ligand complexing zinc in plants which may be partly due to its stability and ability to survive sample preparation steps. Its zinc-

binding constant (logK) is between 14.7 (*44*) and 15.4 (*45*). Zn-NA complex identification was carried out in both in unprocessed plant liquids (*5*),(*15*),(*50*),(*51*) and in extracts obtained upon the plant tissue homogenization (*52*),(*48*). It was identified by ESI-TOF MS (as the only Zn species) in the phloem sap of rice (*5*), of castor bean plants (*Ricinus communis*) treated with cadmium (*53*), xylem of *Arabidopsis thaliana* (*50*), xylem and embryo sac liquid of *Pisum sativum* (*15*) and in coconut water (*51*). Nicotianamine was also shown to be the major ligand binding zinc in hydroponiccally cultured lettuce leaves; the Zn–NA complex was found to account for more than 70% of the total zinc content extracted by ammonium acetate buffer (*48*). Nicotianamine, glutathione and desGluPC$_2$ ligands were identified in Zn-containing SEC fractions of Tris-NaCl extracts of root and shoot tissues of laboratory grown wild type *Aradidopsis halleri*, but no data for intact complexes were shown (*52*). Other, besides NA, Zn-binding ligands reported included citrate in coconut water (*51*).

Although nicotianamine and deoxymugineic acid are usually discussed in relation with metal defficiency (*54*), studies have shown that NA may have a role in the rice tolerance of Zn excess (*55*). In Zn excess, endogenous NA and DMA and DMA secretion in roots increased, suggesting that NA is responsible for the tolerance of excess Zn, in addition to the being the precursor of DMA. Although the function of DMA in excess Zn conditions is not known, the synthesis of DMA in roots in Zn excess may also be involved in maintaining Zn availability in rice plant (*55*).

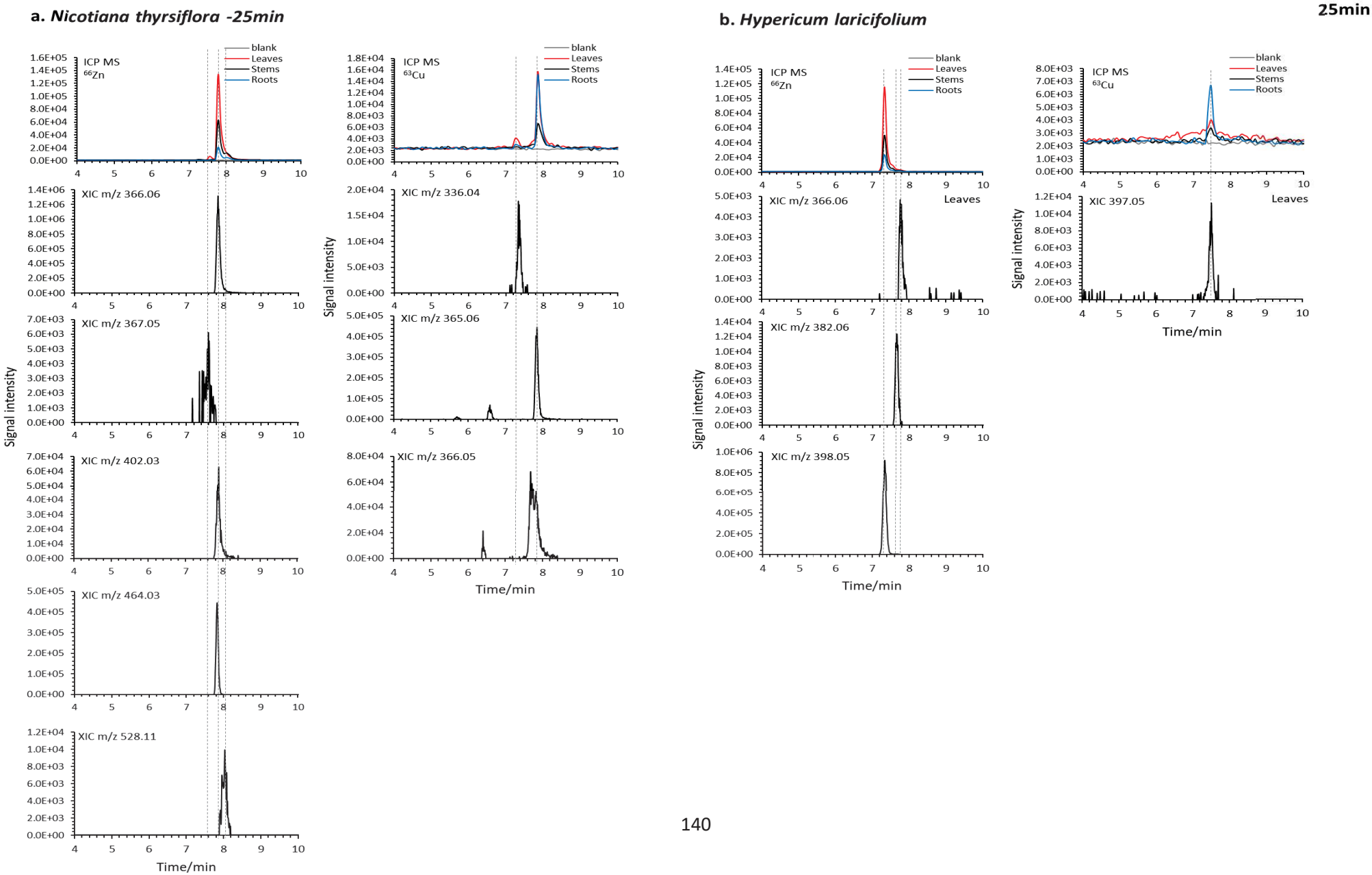
a. Nicotiana thyrsiflora -25min
b. Hypericum laricifolium
25min
ICP MS
66Zn
63Cu
blank
Leaves
Stems
Roots
XIC m/z 366.06
XIC m/z 367.05
XIC m/z 402.03
XIC m/z 464.03
XIC m/z 528.11
XIC m/z 336.04
XIC m/z 365.06
XIC m/z 366.05
XIC m/z 382.06
XIC m/z 398.05
XIC 397.05
Signal intensity
Time/min

c. *Puya sp.*

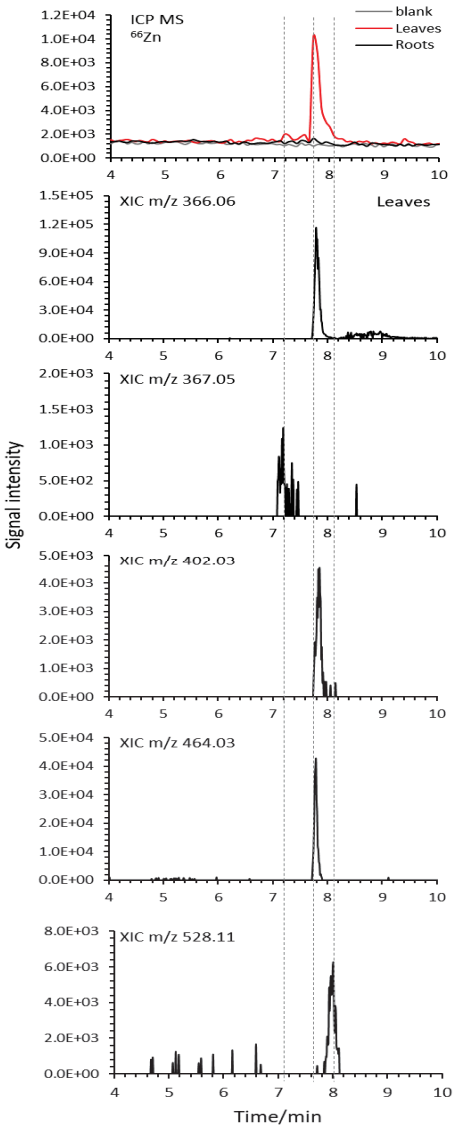

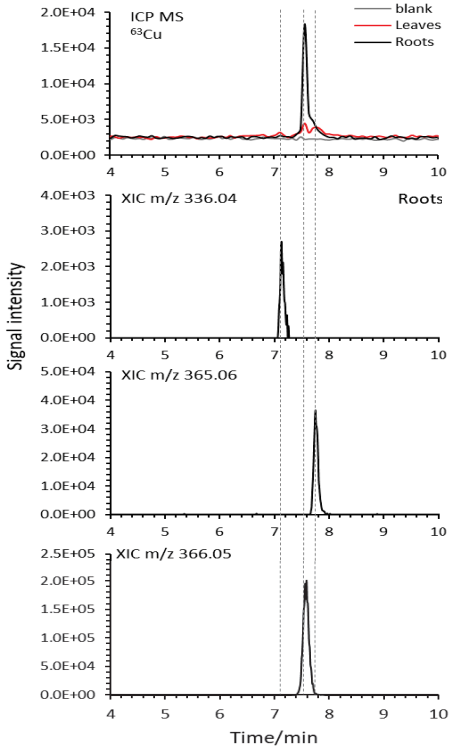

d. *Arenaria digyna*

25min

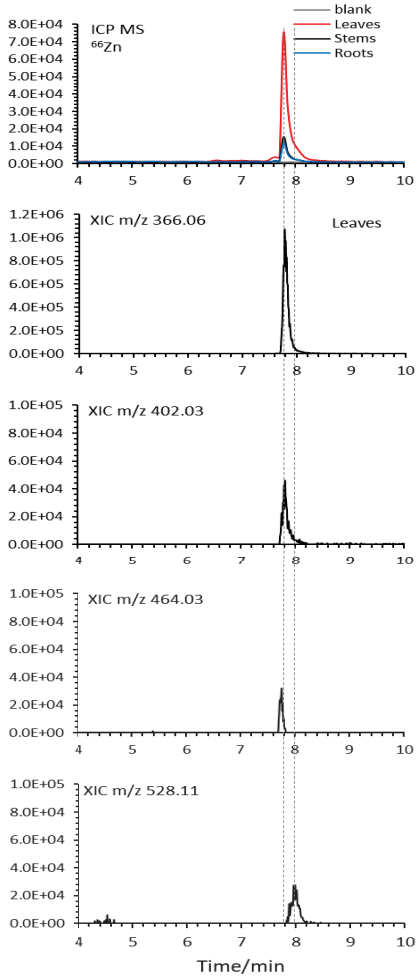

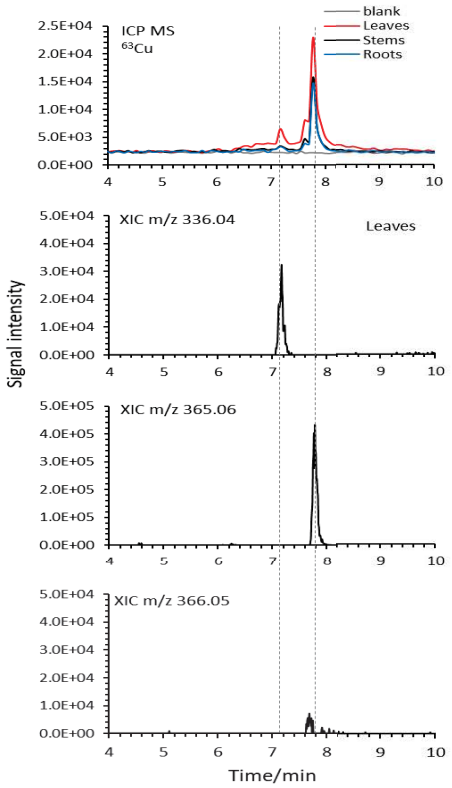

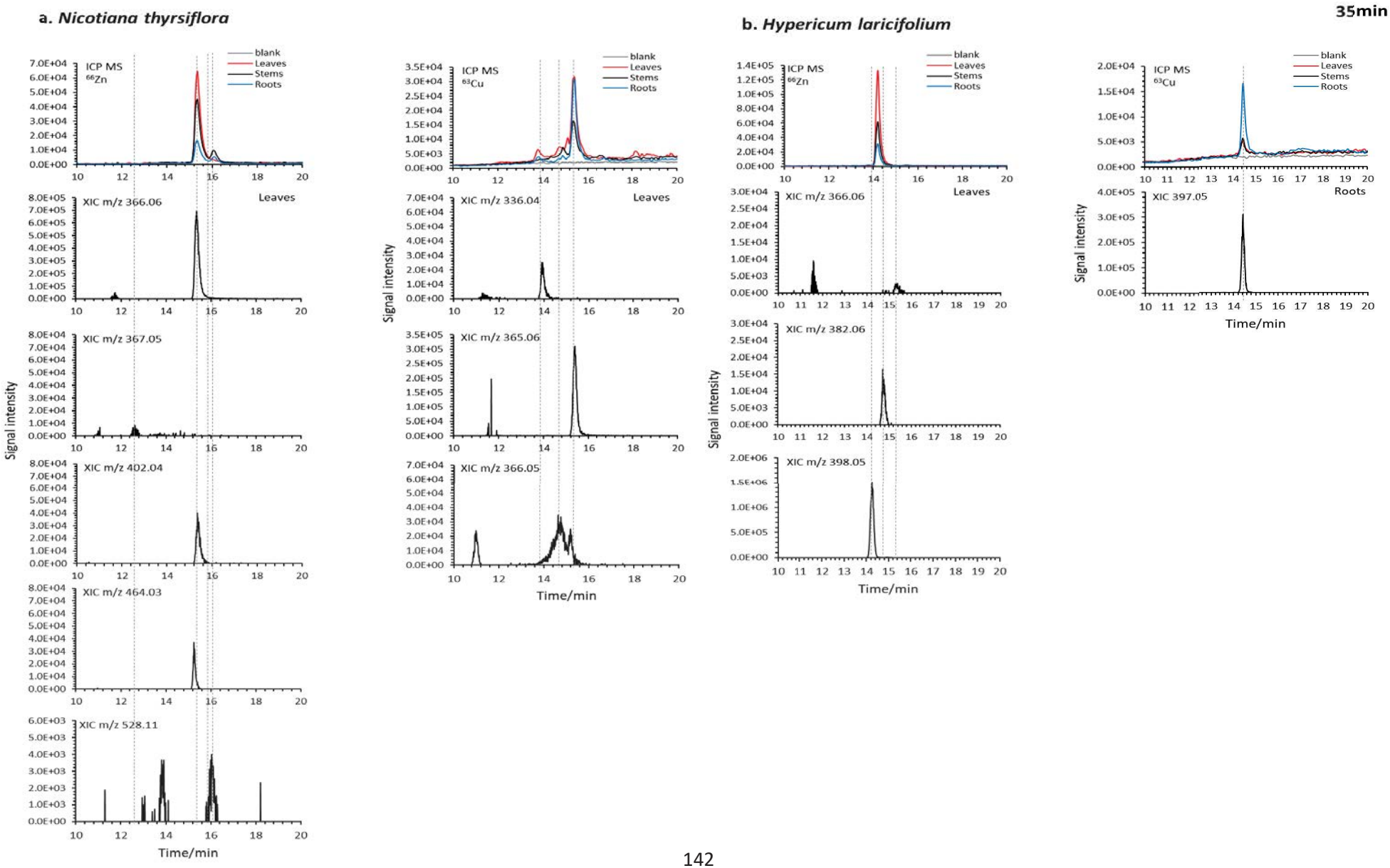
a. Nicotiana thyrsiflora
b. Hypericum laricifolium
35min
ICP MS
66Zn
63Cu
blank
Leaves
Stems
Roots
XIC m/z 366.06
XIC m/z 367.05
XIC m/z 402.04
XIC m/z 464.03
XIC m/z 528.11
XIC m/z 336.04
XIC m/z 365.06
XIC m/z 366.05
XIC m/z 382.06
XIC m/z 398.05
XIC 397.05
Signal intensity
Time/min

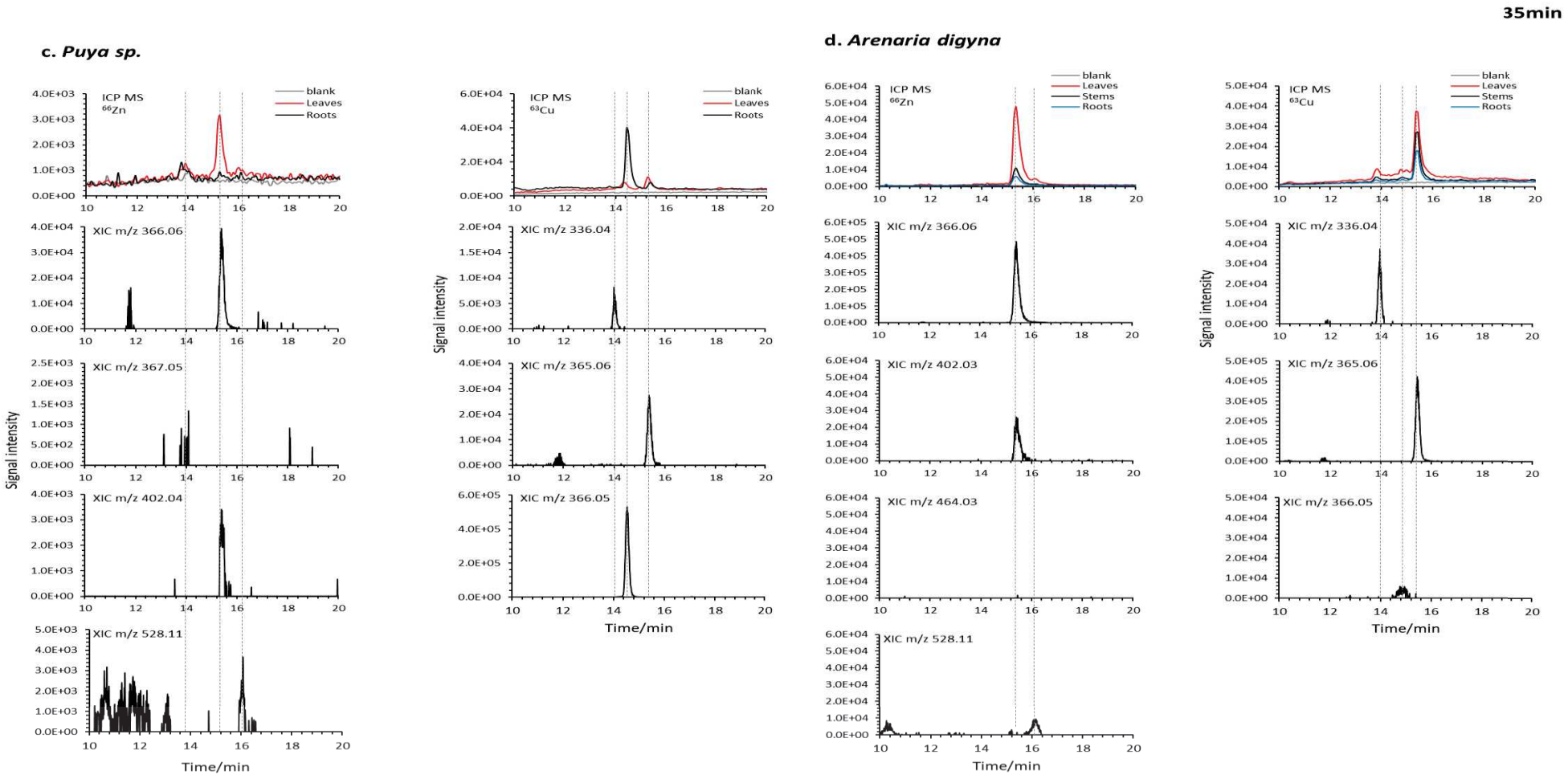

Figure 5. HILIC-ICP/ESI MS speciation of water soluble Cu and Zn species in the leaves, stems, and roots extract of *Nicotiana thyrsiflora*, *Hypericum laricifolium, Puya sp. and Arenaria digyna.*

Hypericum laricifolium presented a distinctive difference in Zn speciation from the other three plants studied. The majority of Zn was present in the form an unknown species with m/z 397.046361 which corresponds to the formula $C_{12}H_{19}N_3O_8Zn$. The structure of this species, presenting a characteristic Zn isotopic pattern, was investigated by ESI MS^n. The hypothesis of the structure of doubly hydroxylated nicotianamine derivative was examined. The obtained fragments were compared with *in silico* fragmentation of isomers dihydroxy-nicotianamine and also nicotianamine, 2'-hydroxy-nicotianamine and 2''-hydroxy-nicotianamine. On the basis of ESI MS^2 data 3 possible isomeric structures could be proposed (**Figure 6**). In addition to the complexed form, free uncomplexed dihydroxy-nicotianamine was detected in *Hypericum laricifolium* and *Nicotiana thyrsiflora*. Another Zn species present in *Hypericum laricifolium* was its complex with 2'-hydroxy-nicotianamine. Monohydroxy-nicotianamines complexes of Cu and Zn were putatively identified in grassland soil based on formula, MS/MS fragmentation spectra, and similarity of metal binding to nicotianamine (*56*). Free monohydroxynicotianamine (but not its metal complexes) was isolated from buckwheat powder, and has also been shown to exist in some polygonaceous plants (*57*).

The distribution of free ligands vs. metal complexes is presented in **Figure 7**, whereas the distribution of individual Zn and Cu species is summarized in **Figure 8**.

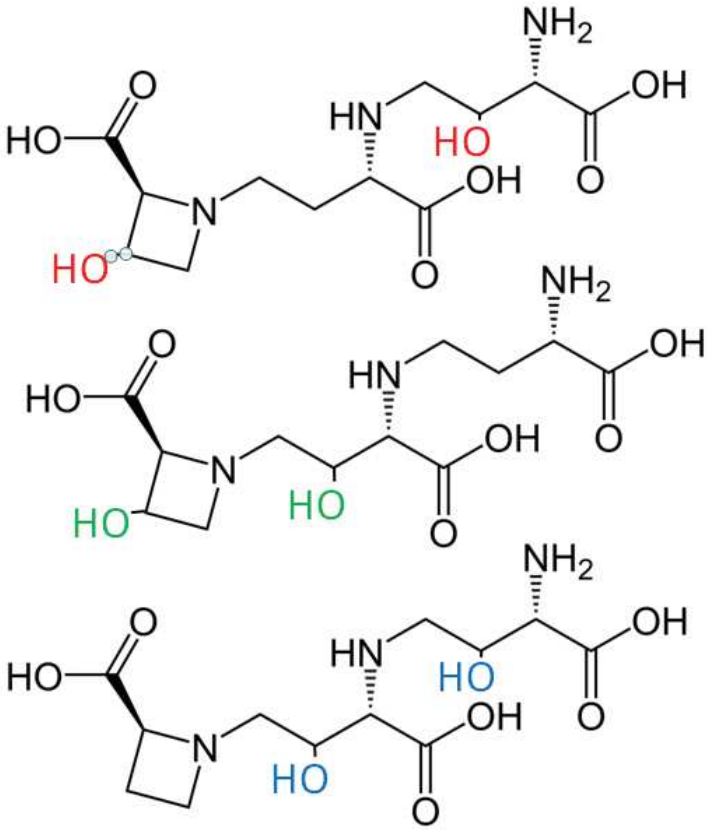

Figure 6. Possible isomeric structures of dihydroxynicotianamine

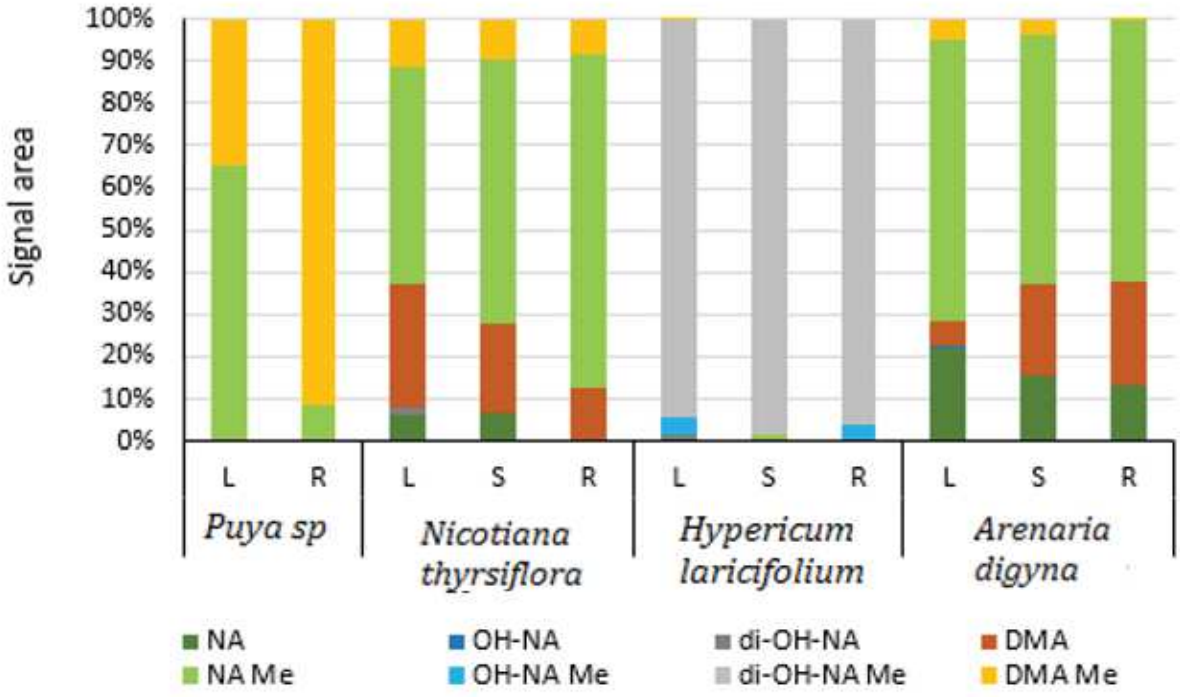

Figure 7. Distribution of free and metal-complexed ligands in water soluble factions of plant organs

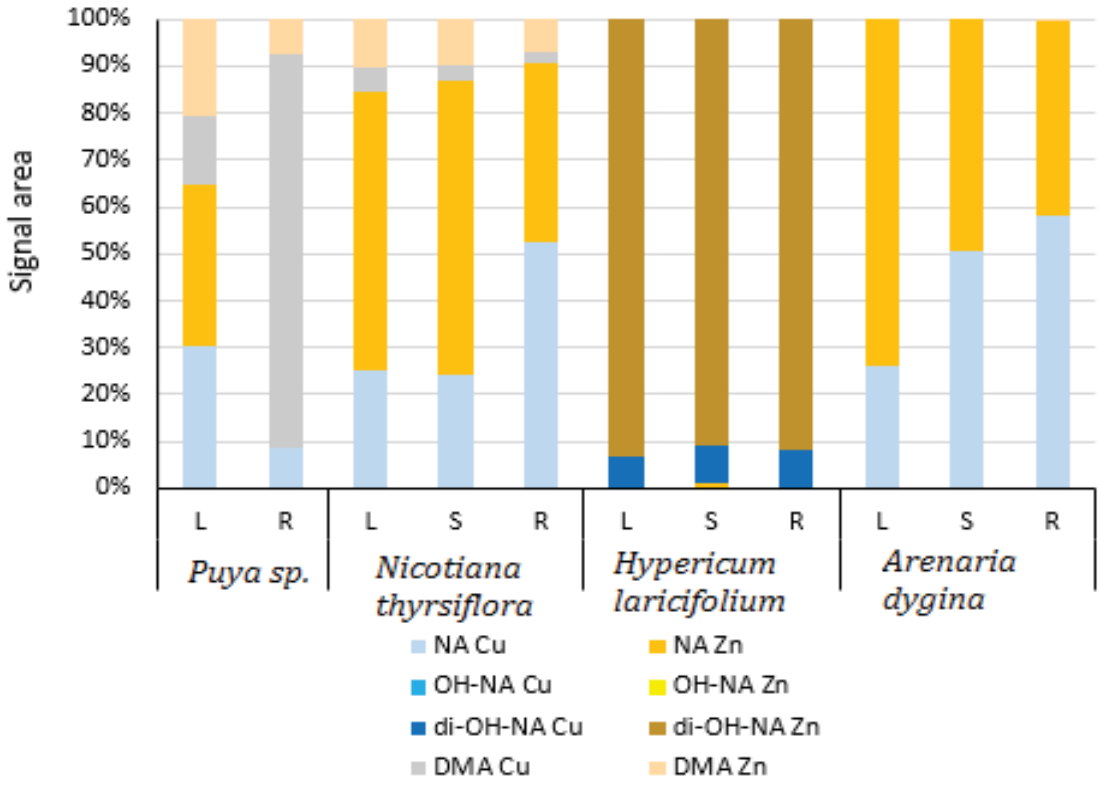

Figure 8. Distribution of copper and zinc species in water soluble factions of plant organs

Speciation of copper in water soluble fraction of plant organs

Similarly to the results obtained for zinc, in three out of four investigated plants, namely *Arenaria digyna, Nicotiana thyrsiflora* and *Puya sp.,* Cu-nicotianamine is the most abundant Cu species in the water soluble fraction with an exception of *Puya sp.* roots where Cu-DMA dominates. In *Nicotiana thyrsiflora* Cu-NA is accompanied by Cu-DMA and traces of a m/z 335 species; similar levels of Cu-NA are present in leaves and roots but lower in stems. In *Arenaria digyna* similar levels Cu-NA are found in in stem and roots and higher in leaves, traces of Cu-DMA (the highest in roots) are also present. The only Cu species detected in *Hypericum laricifolium* is its dihydroxy-NA complex with the highest abundance in roots.

The literature data on Cu speciation is less abundant than for Zn. Extended X-ray absorption fine structure measurements on frozen-hydrated samples suggested that most of Cu absorbed by rice plants is retained in the roots owing to its high binding to the cell wall compounds, thus preventing metal translocation to the aerial parts of the plants. However, no molecular information has been given (*8*). μ-XANES investigation of Cu transport from paddy soil into roots of rice (*10*) showed sequesteration of Cu in the root in the form of complexes with C/N ligands; in the root xylem, thiol-S bound Cu(I) complex was observed (*10*). The dominant chemical form of Cu in *P. australis* was similar to Cu citrate. The results suggest that although Cu can be easily transported into the vascular tissues in roots and stems via Cu citrate, most of the metal absorbed by plants is retained in the roots because if its high binding to the cell wall, thus preventing metal translocation to aerial parts of the plants (*58*). It was postulated that Cu was transported from the root to the aerial part bound to C/N ligands such as histidine, which was observed in the root xylem (*10*). The dominant chemical form of Cu (79.1%) in rice roots was similar to that in the Cu-cell wall compounds (*8*). In a model study on *Brassica carinata,* it was concluded that increased Cu concentrations induced the selective synthesis of certain amino acids in the sap, of which histidine and proline were the most important whereas copper deficiency stimulated synthesis of NA (*59*). Electrospray ionization time-of-flight MS speciation analysis of Cu in phloem and xylem saps from castor bean plants (*Ricinus communis*) treated with of cadmium allowed the identifiaion of Cu-NA (*53*)

Histidine was identified from a Cu-containing fraction of rice (*Oryza sativa*) phloem sap (*60*) Ando et al. (*60*) identified Cu-DMA by electrospray ionization time-of-flight mass spectrometry (ESI-TOF MS) in rice xylem sap and identified Cu-NA in a Cu-containing fraction from rice phloem sap. A single Cu complex with NA peak was found in the phloem sap from castor bean plants (*Ricinus communis*) treated with cadmium; it contained Cu-NA identified by ESI-TOF MS, Cu-His was suspected (no formal identification) but much smaller - Cu-NA was a dominant form in the castor bean phloem sap (*53*). Significantly different speciation was found in the amphibious Cu hyperaccumulator (up to 9,000 ppm in shoots) water plant *Crassula helmsii*. Extended X-ray absorption fine structure measurements on frozen-hydrated samples revealed almost exclusive Cu binding to oxygen ligands, likely organic acids, and not to any sulfur ligand. The analysis did not reveal any nicotianamine contribution and the contribution of His was not significant (*7*). Reductive detoxification ability of Cu(II) to Cu(I) during the transport of Cu in the rootswas suggested on the basis of the observed gradient of Cu(I)-glutathione content (*9*). The observation of Cu-histidine in

root internal cell layers showed another Cu detoxification pathway based on coordinating amino ligands (*9*).

The ability to accumulate phosphorous and nitrogen nutrients in rhizosphere was proposed as an option for in situ phytostabilization of metals in contaminated mining area (*9*). In the root cross-section of *Miscanthus floridulus*, synchrotron-based micro-Xray fluorescence (μ-XRF) microscopy and micro-XANES results indicated that most Cu was sequestered around the root surface/epidermis, primarily forming Cu alginate-like species (*9*).

Conclusions

Speciation of Ag, As, Cu, b and Zn in water soluble fractions of the organs of four native plants growing in Andean post-mining mountain areas: *Arenaria digyna, Puya sp, Hypericum laricifolium* and *Nicotiana thyrsiflora* was examined. The species responsible for Zn and Cu uptake and translocation in the studied plants were identified by HPLC with ICP and ESI MS detection using two separation mechanisms. They belong to the class of siderophores. The presence of copper and zinc complexes with nicotianamine and, much less abundant, deoxymutageneic acid was demonstrated in organs of *Arenaria digyna, Nicotiana thyrsiflora* and *Puya sp.* The major Cu and Zn ligand in *Hypericum laricifolium* was a novel, never reported so far, was identified as dihydroxy-nicotianamine. No complexes with common organic acids present in plant liquids such as, *e.g.,* histidine or citric acid were observed. The findings are in agreement with the general principle formulated by Küpper *et al* and Mijovilovich *et al* stating that the metals are bound by weak ligands in hyperaccumulators but bound by strong ones in non-accumulators (*7, 61*).

References

1. Figueroa, B. E.; Orihuela, R. C.; Calfucura, T. E., Green Accounting and Sustainability of the Peruvian Metal Mining Sector. *Resour. Policy* **2010,** *35*, 156-167.
2. Minas., M. d. E. y., Anuario Minero 2018;. *Oficina de Imagen Institucional y Comunicaciones: Lima, Peru* **2018**.
3. van der Ent, A.; Baker, A. J. M.; Reeves, R. D.; Pollard, A. J.; Schat, H., Hyperaccumulators of metal and metalloid trace elements: Facts and fiction. *Plant and Soil* **2013,** *362*, 319-334.
4. Reeves, R. D.; Baker, A. J. M.; Jaffré, T.; Erskine, P. D.; Echevarria, G.; van der Ent, A., A global database for plants that hyperaccumulate metal and metalloid trace elements. *New Phytol.* **2018,** *218*, 407-411.
5. Nishiyama, R.; Kato, M.; Nagata, S.; Yanagisawa, S.; Yoneyama, T., Identification of Zn-nicotianamine and Fe-2'-deoxymugineic acid in the phloem sap from rice plants (Oryza sativa L.). *Plant and Cell Physiology* **2012,** *53*, 381-390.
6. Aucour, A. M.; Bedell, J. P.; Queyron, M.; Tholé, R.; Lamboux, A.; Sarret, G., Zn Speciation and Stable Isotope Fractionation in a Contaminated Urban Wetland Soil-Typha latifolia System. *Environmental Science and Technology* **2017,** *51*, 8350-8358.
7. Küpper, H.; Gotz, B.; Mijovilovich, A.; Küpper, F. C.; Meyer-Klaucke, W., Complexation and toxicity of copper in higher plants. I. Characterization of copper accumulation, speciation, and toxicity in Crassula helmsii as a new copper accumulator. *Plant Physiology* **2009,** *151*, 702-714.

8. Lu, L.; Xie, R.; Liu, T.; Wang, H.; Hou, D.; Du, Y.; He, Z.; Yang, X.; Sun, H.; Tian, S., Spatial imaging and speciation of Cu in rice (Oryza sativa L.) roots using synchrotron-based X-ray microfluorescence and X-ray absorption spectroscopy. *Chemosphere* **2017,** *175*, 356-364.
9. Cui, J. L.; Zhao, Y. P.; Chan, T. S.; Zhang, L. L.; Tsang, D. C. W.; Li, X. D., Spatial distribution and molecular speciation of copper in indigenous plants from contaminated mine sites: Implication for phytostabilization. *Journal of Hazardous Materials* **2020,** *381*.
10. Cui, J. L.; Zhao, Y. P.; Lu, Y. J.; Chan, T. S.; Zhang, L. L.; Tsang, D. C. W.; Li, X. D., Distribution and speciation of copper in rice (Oryza sativa L.) from mining-impacted paddy soil: Implications for copper uptake mechanisms. *Environment International* **2019,** *126*, 717-726.
11. Schaumlöffel, D.; Ouerdane, L.; Bouyssiere, B.; Łobiński, R., Speciation analysis of nickel in the latex of a hyperaccumulating tree Sebertia acuminata by HPLC and CZE with ICP MS and electrospray MS-MS detection. *Journal of Analytical Atomic Spectrometry* **2003,** *18*, 120-127.
12. Ouerdane, L.; Mari, S.; Czernic, P.; Lebrun, M.; Łobiński, R., Speciation of non-covalent nickel species in plant tissue extracts by electrospray Q-TOFMS/MS after their isolation by 2D size exclusion-hydrophilic interaction LC (SEC-HILIC) monitored by ICP-MS. *Journal of Analytical Atomic Spectrometry* **2006,** *21*, 676-683.
13. Grevenstuk, T.; Flis, P.; Ouerdane, L.; Lobinski, R.; Romano, A., Identification of the tri-Al tricitrate complex in Plantago almogravensis by hydrophilic interaction LC with parallel ICP-MS and electrospray Orbitrap MS/MS detection. *Metallomics* **2013,** *5*, 1285-1293.
14. AlChoubassi, G.; Aszyk, J.; Pisarek, P.; Bierla, K.; Ouerdane, L.; Szpunar, J.; Lobinski, R., Advances in mass spectrometry for iron speciation in plants. *TrAC - Trends in Analytical Chemistry* **2018,** *104*, 77-86.
15. Flis, P.; Ouerdane, L.; Grillet, L.; Curie, C.; Mari, S.; Lobinski, R., Inventory of metal complexes circulating in plant fluids: a reliable method based on HPLC coupled with dual elemental and high-resolution molecular mass spectrometric detection. *New Phytologist* **2016,** *211*, 1129-1141.
16. Cruzado-Tafur, E.; Torró, L., ,; Szpunar, J.; Tauler, E., Geo-ecological evaluation of metal contents in soils and inventory of native flora species growing at Mining Environmental Liabilities in the Peruvian Andes: The Hualgayoc district. *submitted* **2020**.
17. Müller, G.; Müller, G.; Putz, G., Index of geoaccumulation in sediments of the Rhine river. *Geojournal* **1969,** *2*, 108–118
18. Yaroshevsky, A. A., Abundances of chemical elements in the Earth's crust. *Geochem. Int.* **2006,** *44*, 48-55.
19. Santos-Francés, F.; Martinez-Graña, A.; Alonso Rojo, P.; García Sánchez, A., Geochemical Background and Baseline Values Determination and Spatial Distribution of Heavy Metal Pollution in Soils of the Andes Mountain Range (Cajamarca-Huancavelica, Peru). *Int. J. Environ. Res. Public. Health* **2017,** *14*.
20. Okedeyi, O. O.; Dube, S.; Awofolu, O. R.; Nindi, M. M., Assessing the enrichment of heavy metals in surface soil and plant (Digitaria eriantha) around coal-fired power plants in South Africa. *Environ. Sci. Pollut. Res.* . **2014,** *21*, 4686-4696.
21. Cruzado-Tafur, E., Accumulation of As, Ag, Cd, Cu, Pb and Zn by Native Plants Growing in Soils Contaminated by Mining Environmental Li-abilities in the Peruvian Andes. **2021**.
22. Chase, M. V.; Knapp, S.; Cox, A. V.; Clarkson, J. J.; Butsko, Y.; Joseph, J.; Savolainen, V.; Parokonny, A. S., Molecular Systematics, GISH and the Origin of Hybrid Taxa in Nicotiana (Solanaceae). *Annals of Botany* **2003,** *92*, 107-127.
23. Clarkson, J. J.; Knapp, S.; Garcia, V. F.; Olmstead, R. G.; Leitch, A. R.; Chase, M. W., Phylogenetic relationships in Nicotiana (Solanaceae) inferred from multiple plastid DNA regions. *Mol. Phylogenet. Evol.* **2004,** *33*, 75-90.
24. inproyen Study of the propagation of native cloud forest species and high Andean herbaceous and shrub species in the Cajamarca mountain range - Peru. (19 January),

25. Sisson, V. A.; Severson , R. F., Alkaloid Composition of the Nicotiana Species. *Beitrage zur Tabakforschung International* **1990,** *14*, 327-339.
26. Robson, N. K. B., Studies in the genus Hypericum L. (Hypericaceae) 9. Addenda, corrigenda, keys, lists and general discussion. *Phytotaxa* **2012,** *72*, 1-111.
27. Aguilar, Z.; Ulloa, C.; Hidalgo, P., Proyecto de Manejo y Aprovechamiento Sustentable de Alpacas en los Páramos de Zuleta. PPA-EcoCiencia. Quito. *Guía de Plantas Útiles de Los Páramos de Zuleta, Ecuador* **2009**.
28. El-Seedi, H. R.; Ringbom, T.; Torssell, K.; Bohlin, L., Constituents of Hypericum laricifolium and their cyclooxygenase (COX) enzyme activities. *Chemical and Pharmaceutical Bulletin* **2003,** *51*, 1439-1440.
29. Ramírez-González, I.; Amaro-Luis, J. M.; Bahsas, A., Xanthones from aerial parts of Hypericum laricifolium Juss. *Natural Product Communications* **2013,** *8*, 1731-1732.
30. Ccana-Ccapatinta, G. V.; Stolz, E. D.; da Costa, P. F.; Rates, S. M. K.; von Poser, G. L., Acylphloroglucinol Derivatives from Hypericum andinum: Antidepressant-like Activity of Andinin A. *J. Nat. Prod.* **2014,** *77*, 2321–2325.
31. Roja, J.; Buitrago, A.; Rojas, L. B.; Morales, A., Chemical composition of Hypericum laricifolium Juss. Essential oil Collected from Merida—Venezuela *Med. Aromat. Plants* **2013,** *2*, 1-3.
32. Ccana-Ccapatinta, G. V.; von Poser, G. L., Acylphloroglucinol derivatives from Hypericum laricifolium Juss. *Phytochemistry Letters* **2015,** *12*, 63-68.
33. Salinas, L.; Arana; Suni, M., Nectar of Puya species like resource for high Andean hummingbirds of Ancash, Peru. *Revista Peruana de Biologia* **2007,** *14*, 129-134.
34. Hornung-Leoni, C. T.; González-Gómez, P. I.; Troncoso, A. J., Morphology, nectar characteristics and avian pollinators in five Andean Puya species (Bromeliaceae). *Acta Oecologica* **2013,** *51*, 54-61.
35. Wang, Z.; Hwang, S. H.; Guillen Quispe, Y. N.; Gonzales Arce, P. H.; Lim, S. S., Investigation of the antioxidant and aldose reductase inhibitory activities of extracts from Peruvian tea plant infusions. *Food Chemistry* **2017,** *231*, 222-230.
36. Hornung-Leoni, C. T., Bromeliads: traditional plant food in Latin America since prehispanic times. *Polibotánica* **2011**, 219-229.
37. Chandra, S.; Rawat, D. S., Medicinal plants of the family Caryophyllaceae: a review of ethno-medicinal uses and pharmacological properties. *Integrative Medicine Research* **2015,** *4*, 123-131.
38. Valencia, N.; Cano, A.; Delgado, A.; Trinidad, H.; Gonzales, P., Plant composition and coverage of bofedales in an Est-West macrotransect in he Central Peru. In *Monitoring Biodiversity: Lessons from a Trans-Andean Megaproject*, Alonso, A.; Dallmeier, F.; Servat, G. P., Eds. Smithsonian Institution Scholarly Press: Washington (DC), 2013.
39. Kabata-Pendias, A., *Trace Elements in Soils and Plants,*. CRC Press Taylor & Francis Group,: Boca Raton London New York, 2011.
40. Lago-Vila, M.; Arenas-Lago, D.; Rodríguez-Seijo, A.; Andrade, M. L.; Vega, F. A., Ability of Cytisus scoparius for phytoremediation of soils from a Pb/Zn mine: Assessment of metal bioavailability and bioaccumulation. , . *J. Environ. Management.* **2019,** *235*, 152-160.
41. Szpunar, J.; Pellerin, P.; Makarov, A.; Doco, T.; Williams, P.; ŁObińSki, R., Speciation of metal-carbohydrate complexes in fruit and vegetable samples by size-exclusion HPLC-ICP-MS. *Journal of analytical atomic spectrometry* **1999,** *14*, 639-644.
42. Szpunar, J.; Pellerin, P.; Makarov, A.; Doco, T.; Williams, P.; Medina, B.; Łobiński, R., Speciation analysis for biomolecular complexes of lead in wine by size-exclusion high-performance liquid chromatography-inductively coupled plasma mass spectrometry. *Journal of Analytical Atomic Spectrometry* **1998,** *13*, 749-754.

43. Tasuku, M.; Kunio, I.; Minato, H.; Shigeru, K.; Sei-ichi, T., Stabilities of Metal Complexes of Mugineic Acids and Their Specific Affinities for Iron(III). *Chemistry Letters* **1989,** *18*, 2137-2140.
44. Beneš, I.; Schreiber, K.; Ripperger, H.; Kircheiss, A., Metal complex formation by nicotianamine, a possible phytosiderophore. *Experientia* **1983,** *39*, 261-262.
45. Anderegg, G.; Ripperger, H., Correlation between metal complex formation and biological activity of nicotianamine analogues. *Journal of the Chemical Society, Chemical Communications* **1989**, 647-650.
46. Xiong, H.; Kakei, Y.; Kobayashi, T.; Guo, X.; Nakazono, M.; Takahashi, H.; Nakanishi, H.; Shen, H.; Zhang, F.; Nishizawa, N. K.; Zuo, Y., Molecular evidence for phytosiderophore-induced improvement of iron nutrition of peanut intercropped with maize in calcareous soil. *Plant, cell & environment* **2013,** *36*, 1888-902.
47. Suzuki, M.; Nozoye, T.; Nagasaka, S.; Nakanishi, H.; Nishizawa, N. K.; Mori, S., The detection of endogenous 2'-deoxymugineic acid in olives (Olea europaea L.) indicates the biosynthesis of mugineic acid family phytosiderophores in non-graminaceous plants. *Soil Science and Plant Nutrition* **2016,** *62*, 481-488.
48. Wojcieszek, J.; Jimenez-Lamana, J.; Bierla, K.; Asztemborska, A.; Ruzik, L.; Jarosz, M.; Szpunar, J., Elucidation of the fate of zinc in model plants using single particle ICP-MS and ESI tandem MS. *J. Anal. At. Spectrom.* **2019,** *34*, 683.
49. Grillet, L.; Schmidt, W., Iron acquisition strategies in land plants: not so different after all. *New Phytologist* **2019,** *224*, 11-18.
50. Weber, G.; Wir´en, N. v.; Hayen, H., Hydrophilic interaction chromatography of small metal species in plants using sulfobetaine and phosphorylcholine type zwitterionic stationary phases. *J. Sep. Sci.* **2008,** *31*, 1615-1622.
51. Alchoubassi, G.; Kińska, K.; Bierla, K.; Lobinski, R.; Szpunar, J., Speciation of essential nutrient trace elements in coconut water. *Food Chemistry* **2021,** *339*.
52. Deinlein, U.; Weber, M.; Schmidt, H.; Rensch, S.; Trampczynska, A.; Hansen, T. H.; Husted, S.; Schjoerring, J. K.; Talke, I. N.; Krämer, U.; Clemens, S., Elevated Nicotianamine Levels in Arabidopsis halleri Roots Play a Key Role in Zinc Hyperaccumulation. *The Plant Cell* **2012,** *24*, 708-723.
53. Hazama, K.; Nagata, S.; Fujimori, T.; Yanagisawa, S.; Yoneyama, T., Concentrations of metals and potential metal-binding compounds and speciation of Cd, Zn and Cu in phloem and xylem saps from castor bean plants (Ricinus communis) treated with four levels of cadmium. *Physiologia Plantarum* **2015,** *154*, 243-255.
54. Díaz-Benito, P.; Banakar, R.; Rodríguez-Menéndez, S.; Capell, T.; Pereiro, R.; Christou, P.; Abadía, J.; Fernández, B.; Álvarez-Fernández, A., Iron and Zinc in the Embryo and Endosperm of Rice (Oryza sativa L.) Seeds in Contrasting 2'-Deoxymugineic Acid/Nicotianamine Scenarios. *Frontiers in Plant Science* **2018,** *9*.
55. Ishimaru, Y.; Suzuki, M.; Ogo, Y.; Takahashi, M.; Nakanishi, H.; Mori, S.; Nishizawa, N. K., Synthesis of nicotianamine and deoxymugineic acid is regulated by OsIRO2 in Zn excess rice plants. *Soil Science and Plant Nutrition* **2008,** *54*, 417-423.
56. Boiteau, R. M.; Shaw, J. B.; Pasa-Tolic, L.; Koppenaal, D. W.; Jansson, J. K., Micronutrient metal speciation is controlled by competitive organic chelation in grassland soils. *Soil Biology and Biochemistry* **2018,** *120*, 283-291.
57. Aoyagi, Y., An angiotensin-I converting enzyme inhibitor from buckwheat (Fagopyrum esculentum Moench) flour. *Phytochemistry* **2006,** *67*, 618-621.
58. Wu, J.; Wang, L.; Ma, F.; Zhao, L.; Huang, X., The speciation and distribution characteristics of Cu in Phragmites australis (Cav.) Trin ex. Steudel. *Plant Biology* **2019,** *21*, 873-881.

59. Irtelli, B.; Petrucci, W. A.; Navari-Izzo, F., Nicotianamine and histidine/proline are, respectively, the most important copper chelators in xylem sap of Brassica carinata under conditions of copper deficiency and excess. *Journal of Experimental Botany* **2009,** *60*, 269-277.
60. Ando, Y.; Nagata, S.; Yanagisawa, S.; Yoneyama, T., Copper in xylem and phloem saps from rice (Oryza sativa): The effect of moderate copper concentrations in the growth medium on the accumulation of five essential metals and a speciation analysis of copper-containing compounds. *Functional Plant Biology* **2013,** *40*, 89-100.
61. Mijovilovich, A.; Leitenmaier, B.; Meyer-Klaucke, W.; Kroneck, P. M. H.; Götz, B.; Küpper, H., Complexation and Toxicity of Copper in Higher Plants. II. Different Mechanisms for Copper versus Cadmium Detoxification in the Copper-Sensitive Cadmium/Zinc Hyperaccumulator Thlaspi caerulescens (Ganges Ecotype). *Plant Physiology* **2009,** *151*, 715-731.

Table SI-1. Metal abundances in soil at the plants sampling sites

Plants sampled	Ag	As	Cd	Co	Cr	Cu	Mn	Mo	Ni	Pb	Tl	V	W	Zn
Puya sp.	11.3 ± 5.1	296 ± 12.7	1.1 ± 0.1	15 ± 4.2	69.5 ± 34.6	270.7 ± 4.5	1921.5 ± 618.7	4 ± 2.8	4 ± 1.4	2446.5 ± 108.2	2 ± 0.1	62 ± 8.5	10 ± 0.1	289 ± 2.5
Nicotiana thyrsiflora *Hypericum laricifolium* *Arenaria digyna*	24.85 ± 12.1	361 ± 56.6	3.5 ± 1.7	6 ± 1.4	89.5 ± 24.7	329.6 ± 31.5	1978.5 ± 290.6	6.5 ± 3.5	8 ± 1.4	3872 ± 1146.9	2 ± 0.1	90.5 ± 13.4	10 ± 0.1	532.6 ± 231.6

Table SI-2. Metal abundances in the Earth's Crust and geochemical baseline values near at the sampling sites

	Ag	As	Cd	Co	Cr	Cu	Mn	Mo	Ni	Pb	Tl	V	W	Zn
Abundances of Chemical Elements in the Earth's Crust*	0.07	1.7	0.13	18	83	47	1000	1.1	58	16	1	90	1.3	83
Geochemical baseline values in a natural region (La Zanja) at 30 km from the sampling place**	-	27.5	4.36	-	8.26	22.2	-	-	56.97	44.87	-	-	-	47.42

*Santos-Francés, F., Martinez-Graña, A., Alonso Rojo, P. & García Sánchez, A. Geochemical Background and Baseline Values Determination and Spatial Distribution of Heavy Metal Pollution in Soils of the Andes Mountain Range (Cajamarca-Huancavelica, Peru). *Int. J. Environ. Res. Public. Health* **14**, (2017).

Yaroshevsky, A. A. Abundances of chemical elements in the Earth's crust. *Geochem. Int.* **44, 48–55 (2006).

Table SI-3. Approximate concentrations of trace elements in mature leaf tissue generalized for various species

Element	Sufficient or normal concentration in leaf tissue* (mg/kg)
Ag	0.5
As	1-1.7
Cu	5-30
Pb	5-10
Zn	27-150

* Kabata-Pendias, A., 2011. Trace Elements in Soils and Plants, 4th Ed. ed. CRC Press Taylor & Francis Group, Boca Raton London New York.

IV. CONCLUSIONS

IV. CONCLUSIONS

Mining Environmental Liabilities (MEL) in polymetallic districts may possess a high content in potentially toxic metals. Therefore, they represent a potential pollution risk to the surrounding areas and their denizens. The PhD project has allowed for the assessment of soil and native plant species around two mining environmental liabilities in the Hualgayoc district, Cajamarca region, in the Peruvian Andes. The mainconclusions derived from this research include:

- The studied soils presented Andean properties and were classified as Gleyic Cambisols. The samples yielded extremely low pH values (3.50 - 4.19 in site #1 and 2.74 - 4.02 in site #2), absence of carbonates, non-saline yielding, moderate to high organic matter content, low cation exchange (CEC) capacity, and low available P and K content. Soils were very poor in essential nutrients and had low fertility, probably because of the low pH values facilitating metal lixiviation. Their colour was dark reddish brown to brownish yellow (site #1) and brown to dark yellowish brown (site #2), soil particle-size were relatively coarse (sandy clay loam and clay loam) with low clay content directly correlated with decreasing CEC. Their mineralogical composition was dominated by illite, kaolinite, quartz, and jarosite.

- After the analysis of the total concentrations of 34 elements in soils by Inductively coupled plasma emission spectrometer (ICP-OES), high content and potentially toxic concentrations of Pb, Zn, As, Cu, Ag, and Cd were found. These six elements exceeded the maximum allowable values for agricultural soils according to the Peruvian and Canadian regulations.

- The evaluation of the soil environmental quality by the geo-accumulation (Igeo), Nemerow Pollution (NI), Improved Nemerow (INI), and Potential Ecological Risk (RI) indexes indicates high indices of contamination with a high potential to affect surrounding ecosystems and local communities.

- A total of 22 plants of native flora (15 species from site#1, and 12 species from site #2, with 5 species in common in the two sites) belonging to 12 family species and growing up around the studied MEL sites were identified, thus having potential for phytoremediation purposes.

- The mobility and availability of the six elements (sequential extraction of Pb, Zn, Cu, As, Ag, and Cd) in the soils were quantified by ICP mass spectrometry (ICP-MS) and showed no significant

differences between the upper (0–15 cm) and lower (15–30 cm) soil layers. The distribution of metals in the soil showed dominant presence of the fractions with limited metal mobility (F2, F3, and F4), even if the acidic pH was expected to increase the bioavailability of metals.

- The *Pernettya prostrata* and *Gaultheria glomerate* were suitable for Zn phytostabilization, and *Gaultheria glomerata* and *Festuca sp.* Were suitable for Cd phytostabilization. It should be noted that the specie *Gaultheria glomerata* were suitable both for the phytostabilization of Zn and Cd. *Cortaderia bifida* was the most abundant plant found at the two sampling areas.

- *Achyrocline alata*, *Ageratina fastigiate*, *Ageratina glechonophylla*, *Baccharis alnifolia*, *Calceolaria tetragona*, *Arenaria digyna*, *Bejaria sp*., *Pernettya prostrata*, *Hypericum laricifolium*, *Brachyotum radula*, and *Nicotiana thyrsiflora* were suitable for Cd phytoremediation. *Achyrocline alata*, *Ageratina fastigiate*, *Baccharis alnifolia*, *Calceolaria tetragona*, *Arenaria digyna*, *Hypericum laricifolium*, *Brachyotum radula*, and *Nicotiana thyrsiflora were suitable for Zn phytoremediation*. All plant species suitable for Zn phytoremediation could also be used for Cd phytoremediation. None of the studied plants appeared to be suitable for Pb, Cu, As, and Ag phytoremediation.

- For the speciation studies, four native hypertolerant plant species, *Arenaria digyna*, *Puya sp*, *Hypericum laricifolium*, *Nicotiana thyrsiflora* were selected due to high translocation factor of Zn and Cu into over ground plant organs. The analytical strategy based on fastSEC-ICP/ESI-MS and HILIC-ICP/ESI-MS allowed to demonstrate the presence of nicotianamine and deoxymutageneic acid copper and zinc complexes in organs of *Arenaria digyna*, *Nicotiana thyrsiflora* and *Puya sp*. Finally, a novel, never reported so far, dihydroxy-nicotianamine species was identified as the most abundant Cu and Zn ligand in *Hypericum laricifolium*.

ET LUX IN TENEBRIS LUCET
MCMXVII